The Low Load Limit of Gasoline Partially Premixed Combustion (PPC)

Experiments in a Light Duty Diesel Engine

Patrick Borgqvist

LUND
UNIVERSITY

DOCTORAL DISSERTATION
by due permission of the Faculty of Engineering, Lund University, Sweden.

To be defended at M-Building, room M:B. Date 26/4 and time 1000.

Faculty opponent

Professor Hua Zhao, Brunel University

Organization	Document name
LUND UNIVERSITY	DOCTORAL DISSERTATION
	Date of issue
Author Patrick Borgqvist	Sponsoring organization KCFP

Title and subtitle

The Low Load Limit of Gasoline Partially Premixed Combustion – Experiments in a Light Duty Diesel Engine

Abstract

The decreasing oil supply, more stringent pollutant legislations and strong focus on decreasing carbon dioxide emissions drives the research of more efficient and clean combustion engines. One such combustion engine concept is Homogeneous Charge Compression Ignition (HCCI) which potentially achieves high efficiency and low NOx and soot emissions. One practical realization of HCCI in SI engines is to use a variable valve train to trap hot residual gases in order to increase the temperature of the fresh charge to auto-ignite around top dead center. The limited operating region of HCCI and lack of immediate control actuator, which makes feedback control of the combustion difficult, are two contributing reasons to change focus from HCCI to gasoline Partially Premixed Combustion (PPC). The advantage with using gasoline is a longer ignition delay which enhances the mixing of the fuel and air before combustion. But the attainable operating region is limited at low load with high octane number fuels and the main part of the thesis is devoted to extending the low load limit of gasoline PPC. The goal is to extend the operating region of the engine towards low load using the variable valve train system, the glow plug and more advanced injection strategies.

The thesis is based on experimental investigations performed in a single cylinder research engine. During the first part of the thesis, results from a fundamental experimental study on HCCI combustion in comparison with SI combustion using different variable valve timing strategies is presented. Residual gas enhanced HCCI with negative valve overlap (NVO) or rebreathing has higher efficiency compared to SI combustion. To extend the operating range of the NVO HCCI engine, a combustion mode switch from SI combustion to HCCI combustion using NVO, was investigated.

In the first gasoline PPC investigation, a comparison between diesel and two gasoline fuels with different octane numbers was performed. It is shown that the low octane number gasoline (69 RON) can be operated without using a high fraction of trapped hot residual gas down to 1 bar IMEPn. But the operating range of the 87 RON gasoline fuel was limited and could be run down to approximately 2 bar IMEPn using a high fraction of trapped hot residual gas. The rest of the gasoline PPC work is devoted to the 87 RON gasoline fuel. Experimental investigations on the effects of the hot residual gas using NVO and rebreathing, more advanced fuel injection strategies and effects of the glow plug are presented.

In order to minimize fuel consumption while maintaining combustion stability, the suggested gasoline PPC low load operating strategy is to use the NVO valve strategy with a fuel injection during NVO at low engine load up to approximately 2 bar IMEPn and then switch to the rebreathing valve strategy using a split main fuel injection strategy at higher engine load.

Key words
PPC, low temperature combustion, HCCI, negative valve overlap, rebreathing, low load, glow plug

Classification system and/or index terms (if any)

Supplementary bibliographical information

Language
English

ISSN and key title
0282-1990

ISBN
978-91-7473-486-7

Recipient's notes

Number of pages
212

Price

Security classification

Signature Patrick Borgqvist Date _____

The Low Load Limit of Gasoline Partially Premixed Combustion (PPC)

Experiments in a Light Duty Diesel Engine

Patrick Borgqvist

LUND
UNIVERSITY

Division of Combustion Engines
Department of Energy Sciences
Faculty of Engineering
Lund University
P.O. Box 118
SE-22100 Lund

ISBN 978-91-7473-486-7
ISRN LUTMDN/TMHP-13/1091-SE
ISSN 0282-1990

Printed in Sweden by Media-Tryck, Lund University
Lund 2013

List of Papers

Paper 1

Investigation and Comparison of Residual Gas Enhanced HCCI using Trapping (NVO HCCI) or Rebreathing of Residual Gases

Patrick Borgqvist, Per Tunestål, and Bengt Johansson

SAE 2011-01-1772

Paper 2

Investigating Mode Switch from SI to HCCI using Early Intake Valve Closing and Negative Valve Overlap

Anders Widd, Rolf Johansson, Patrick Borgqvist, Per Tunestål, and Bengt Johansson

SAE 2011-01-1775

Paper 3

Gasoline Partially Premixed Combustion in a Light Duty Engine at Low Load and Idle Operating Conditions

Patrick Borgqvist, Per Tunestål, and Bengt Johansson

SAE 2012-01-0687

Paper 4

The Usefulness of Negative Valve Overlap for Gasoline Partially Premixed Combustion, PPC

Patrick Borgqvist, Martin Tuner, Augusto Mello, Per Tunestål, and Bengt Johansson

SAE 2012-01-1578

Paper 5

The Low Load Limit of Gasoline Partially Premixed Combustion Using Negative Valve Overlap

Patrick Borgqvist, Öivind Andersson, Per Tunestål, and Bengt Johansson

ICEF2012-92069

Approved for publication in Journal of Engineering for Gas Turbines and Power

Paper 6

Comparison of Negative Valve Overlap (NVO) and Rebreathing Valve Strategies on a Gasoline PPC Engine at Low Load and Idle Operating Conditions

Patrick Borgqvist, Per Tunestål, and Bengt Johansson

SAE 2013-01-0902

Other Publications

HCCI Heat Release Data for Combustion Simulation, Based on Results from a Turbocharged Multi Cylinder Engine

Thomas Johansson, Patrick Borgqvist, Bengt Johansson, Per Tunestål, and Hans Aulin

SAE 2010-01-1490

Transient Control of Combustion Phasing and Lambda in a 6-Cylinder Port-Injected Natural-Gas Engine

Mehrzad Kaiadi, Magnus Lewander, Patrick Borgqvist, Per Tunestål, and Bengt Johansson

ICES2009-76004

Internal Combustion Engine Mode Switch Control Using LabVIEW Real-Time and FPGA

Patrick Borgqvist

A control system case study presented at NI-Days 2010 in Stockholm, Sweden. Winner of Swedish Graphical System Design Achievement Award 2010.

Abstract

The decreasing oil supply, more stringent pollutant legislations and strong focus on decreasing carbon dioxide emissions drives the research of more efficient and clean combustion engines. One such combustion engine concept is Homogeneous Charge Compression Ignition (HCCI) which potentially achieves high efficiency and low NOx and soot emissions. One practical realization of HCCI in SI engines is to use a variable valve train to trap hot residual gases in order to increase the temperature of the fresh charge to auto-ignite around top dead center. The limited operating region of HCCI and lack of immediate control actuator, which makes feedback control of the combustion difficult, are two contributing reasons to change focus from HCCI to gasoline Partially Premixed Combustion (PPC). The advantage with using gasoline is a longer ignition delay which enhances the mixing of the fuel and air before combustion. But the attainable operating region is limited at low load with high octane number fuels and the main part of the thesis is devoted to extending the low load limit of gasoline PPC. The goal is to extend the operating region of the engine towards low load using the variable valve train system, the glow plug and more advanced injection strategies.

The thesis is based on experimental investigations performed in a single cylinder research engine. During the first part of the thesis, results from a fundamental experimental study on HCCI combustion in comparison with SI combustion using different variable valve timing strategies is presented. Residual gas enhanced HCCI with negative valve overlap (NVO) or rebreathing has higher efficiency compared to SI combustion. To extend the operating range of the NVO HCCI engine, a combustion mode switch from SI combustion to HCCI combustion using NVO, was investigated.

In the first gasoline PPC investigation, a comparison between diesel and two gasoline fuels with different octane numbers was performed. It is shown that the low octane number gasoline (69 RON) can be operated without using a high fraction of trapped hot residual gas down to 1 bar IMEPn. But the operating range of the 87 RON gasoline fuel was limited and could be run down to approximately 2 bar IMEPn using a high fraction of trapped hot residual gas.

The rest of the gasoline PPC work is devoted to the 87 RON gasoline fuel. Experimental investigations on the effects of the hot residual gas using NVO and rebreathing, more advanced fuel injection strategies and effects of the glow plug are presented.

In order to minimize fuel consumption while maintaining combustion stability, the suggested gasoline PPC low load operating strategy is to use the NVO valve strategy with a fuel injection during NVO at low engine load up to approximately 2 bar IMEPn and then switch to the rebreathing valve strategy using a split main fuel injection strategy at higher engine load.

Popular Summary in Swedish

Utökning av arbetsområdet för en motor med partiellt förblandad förbränning

Förbränningsmotorn med inre förbränning har funnits i över hundra år. Förbränningsmotorn har fördel av att det är en tillförlitlig, kompakt och relativt billig kraftkälla. Den finns i många olika utföranden och storlekar och finns i allt ifrån modellflygplan till transportfartyg. Bilindustrin domineras av ottomotorn och dieselmotorn. Ottomotorn i kombination med en trevägskatalysator anses vara en ren motor med låga utsläpp av giftiga förbränningsprodukter som obrända kolväten, kolmonoxid och kväveoxider. Problemet med ottomotorn är att bränsleförbrukningen är relativt hög. Dieselmotorn har lägre bränsleförbrukning jämfört med ottomotorn men problemet är istället utsläppen av giftiga förbränningsprodukter av framförallt partiklar och kväveoxider. En annan viktig aspekt, oavsett motortyp, är koldioxidutsläppen som minskas genom lägre bränsleförbrukning.

I takt med stigande oljepriser ökar efterfrågan på motorer med lägre bränsleförbrukning samtidigt som fordonstillverkarna brottas med allt hårdare lagkrav på rening av förbränningsprodukterna. Rening av förbränningsprodukter kan i stor utsträckning göras i avgasröret men problemet är kostnaden av efterbehandlingssystemen. Ett alternativ är att istället påverka förbränningen inne i motorn så att andelen giftiga avgasprodukter i utsläppen minskar. Utmaningen är att hitta ett förbränningskoncept som ger både låg bränsleförbrukning, låga utsläpp och som täcker hela motorns arbetsområde. Ett koncept som har studerats flitigt i motorforskningssammanhang är HCCI som bygger på kompressionsantändning av förblandat bränsle och luft. Fördelen med HCCI är låg bränsleförbrukning i kombination med låga utsläpp av framförallt sotpartiklar och kväveoxider. En nackdel är att förbränningen är svårare att styra och att arbetsområdet är mer begränsat.

Ett praktiskt sätt att realisera denna typ av koncept är att använda ett system för variabla ventiltider och hålla kvar en stor del av de varma avgaserna inne i cylindern. Värmen från avgaserna höjer temperaturen på bränsle- och luftblandningen till självantändning efter kompression. Oftast används en strategi som heter NVO, eller negativt ventilöverlapp. Ett alternativ till NVO är rebreathing där avgaserna först släpps ut och sen sugs tillbaka igen. Fördelen med denna strategi är att man undviker

att komprimera de varma avgaserna under gasväxlingen vilket ger lägre värmeförluster. Den inledande studien i avhandlingen innehåller en studie och jämförelse mellan olika ventilstyrda HCCI strategier och ottoförbränning. HCCI koncepten ger signifikant lägre bränsleförbrukning även då ottoförbränningen körs utan trottel. Problemet är det begränsade arbetsområdet. För att utöka arbetsområdet mot lägre last kan man köra motorn med ottoförbränning på låga laster och sen växla förbränningskoncept till HCCI på lite högre laster. En studie i avhandlingen är gjord där två olika styrstrategier för förbränningen i HCCI efter strategiväxlingen har studerats. En modellbaserad styrstrategi ger ett något mjukare förlopp jämfört med den enklare PI regulatorn.

Ett annat förbränningskoncept, kring vilket den största delen av den här avhandlingen är uppbyggd, är partiellt förblandad förbränning med bensin, eller bensin PPC (partially premixed combustion). Syftet med det högoktaniga bränslet är att öka tändfördröjningen, det vill säga tiden mellan bränsleinsprutning och antändning. Detta ger mer tid för bränslet och luften att blandas vilket undertrycker bildningen av sotpartiklar. Recirkulerade avgaser, EGR, används för att få ner bildningen av kväveoxider och kan även användas för att få längre tändfördröjning. PPC med diesel använder höga halter av EGR för att få längre tändfördröjning. Ett sätt att skilja mellan PPC-förbränning och traditionell dieselförbränning är att allt bränsle ska vara insprutat innan det antänds. Problemet med bensin PPC är att arbetsområdet är begränsat på låga laster med högoktaniga bränslen. Förbränningsstabiliteten minskar och utsläpp av obrända kolväten och kolmonoxid ökar. Målet med avhandlingen är att utöka motorns arbetsområde på låga varvtal och laster mot tomgång. Undersökningar har gjorts med variabla ventiltider, bränsleinsprutningsstrategier och glödstift. Syftet är att undersöka hur olika strategier påverkar förbränningsstabiliteten och utsläpp av kolväten. Två olika ventilstrategier för att fånga varma avgaser har studerats. Syftet är samma som med HCCI, det vill säga att få upp temperaturen inne i cylindern. Både NVO och rebreathing har använts. Studien visar att det går att utöka arbetsområdet med framförallt de variabla ventiltiderna och bränsleinsprutningsstrategin. Glödstiftet får en mindre påverkan i kombination med ventilsystemet. Beroende på val av ventilstrategi kan en mer optimal bränslestrategi väljas och olika kombinationer ger olika fördelar. På de allra lägsta lasterna ger en ventilstrategi med NVO i kombination med bränsleinsprutning under gasväxlingen bäst förbränningsstabilitet. På lite högre laster är det en fördel att växla till rebreathing för att få lägre bränsleförbrukning.

Acknowledgements

I would like to thank the Centre of Competence for Combustion Processes (KCFP) for financing my project. There are many people who have contributed to this work but unfortunately too little space to mention all. I am grateful to you all.

First, I would like to thank my supervisor Per Tunestål for his support, and many hours of valuable discussions and feedback. Bengt Johansson, who accepted me here as a PhD student and for all the help and feedback. Rolf Johansson, for introducing me to Bengt Johansson and Per Tunestål and made my internship at Toyota in Japan possible before I started as a PhD student. I would like to acknowledge Martin Tuner and Augusto Mello who made the AVL Boost model simulations. Öivind Andersson, for many interesting discussions and help with the experimental planning in the fuel injection strategy investigation.

Special thanks to Bill Cannella from Chevron for supplying the gasoline fuels that were used in the PPC experiments. Urban Carlsson and Anders Höglund at Cargine Engineering, for supplying and helping me with the valve train system. Håkan Persson at Volvo Cars, for engine hardware support. To Pelle Steen at National Instruments for the LabVIEW support.

To all the technicians in the lab during my time at the division, Kjell Jonholm, Mats Bengtsson, Anders Olsson, Tommy Petersen, Bertil Andersson, Tom Hademark, for helping me out with the engine hardware and keeping the engine running. Krister Olsson for his help with computers and for sharing my programming interest. Thomas Johansson, our new lab manager, for his help in the lab and also for being a friend.

I would also like to thank all my colleges during my time at the division. Thanks for all your support.

Last but not least, I would like to thank my wife Jenny for her patience, especially during the last couple of months before printing the thesis. Without her support this would not have been possible. To my daughter Lilly, for reminding me about what is important. To my parents and brothers and sisters, for all your support.

Nomenclature

ATDC	After Top Dead Center
BMEP	Break Mean Effective Pressure
BTDC	Before Top Dead Center
CA10	Crank Angle 10 % burned
CA50	Crank Angle 50 % burned
CA90	Crank Angle 90 % burned
CAD	Crank Angle Degree
CAI	Controlled Auto Ignition
CO	Carbon Monoxide
CO2	Carbon Dioxide
COV	Coefficient of Variation
DOE	Design of Experiments
EGR	Exhaust Gas Recirculation
EIVC	Early Intake Valve Closing
FMEP	Friction Mean Effective Pressure
FSN	Filter Smoke Number
GDCI	Gasoline Direct Injection Compression Ignition
HC	Hydro Carbon emissions
HCCI	Homogeneous Compression Ignition
IMEP	Indicated Mean Effective Pressure
IVC	Intake Valve Closing
LHV	Lower Heating Value
LIVC	Late Intake Valve Closing

LTC	Low Temperature Combustion
MK	Modulated Kinetics
MON	Motor Octane Number
NOx	Nitrogen Oxide
NVO	Negative Valve Overlap
p	Pressure
PM	Particulate Matter
PMEP	Pump Mean Effective Pressure
PPC	Partially Premixed Combustion
r_c	Compression ratio
Reb	Rebreathing
RON	Research Octane Number
RPM	Revolutions Per Minute
SACI	Spark Assisted Compression Ignition
SCR	Selective Catalytic Reduction
SI	Spark Ignition
SOC	Start of Combustion
SOI	Start of Injection
STD	Standard Deviation
T	Temperature
TDC	Top Dead Center
V	Volume
VVT	Variable Valve Timing
λ	Relative air-fuel ratio
γ	Specific heat ratio

Table of Content

1 Introduction

1.1 Background

The internal combustion engine has been used to power vehicles for more than a hundred years. It is a robust and affordable power generator with a high power to weight ratio which makes it very useful for transportation applications. One problem is the increasing price and decreasing supply of oil which drives the demand for more efficient engines. Another problem is the environmental impact from pollutants. Local emissions, such as carbon monoxide (CO), unburned hydrocarbons (HC), nitrogen oxide (NOx), and particulate matter (PM) are harmful for both the environment and the public health. One strategy is to apply some sort of after-treatment such as a three-way catalyst, particulate filter, selective catalytic reduction (SCR) systems or oxidizing catalyst depending on the targeted emissions and demand from the combustion concept. The global carbon dioxide (CO2) emissions are not handled by the after-treatment system and have to be reduced through lower fuel consumption of more fuel efficient engines.

The transportation market is dominated by spark ignition (SI) engines and diesel engines. The conventional spark ignition engine is relatively clean because it is usually operated with a three-way catalyst which simultaneously reduces CO, NOx and HC emissions. But the efficiency is lower compared to diesel. The lower efficiency is partly because the intake air has to be throttled to control load. The diesel engine efficiency is high compared to the SI engine but the problem is instead the NOx and soot emissions. A three-way catalyst cannot be used because it is operated lean. NOx emissions can be reduced by using recycled exhaust gases (EGR) or SCR, or both. Soot can be removed with particulate filters.

After-treatment systems are generally expensive and there is a need for more advanced combustion concepts that simultaneously achieves high efficiency in combination with cleaner combustion. One such combustion concept aimed towards this goal is gasoline partially premixed combustion (PPC).

The European emissions standards are shown in Table 1. Emissions are tested over the NEDC chassis dynamometer procedure. A part of the procedure is an urban driving cycle (ECE), which was devised to represent city driving conditions. It is characterized by low vehicle speed, low engine load, and low exhaust gas temperature [1]. The challenges with the gasoline PPC concept are the auto-ignition problems with higher octane number fuels and HC and CO emissions at low load and engine speed operating conditions. Due to the low exhaust gas temperature at low load, after treatment of HC and CO will be a challenge using a standard oxidizing catalyst alone. Low combustion efficiency itself is a problem because it increases the fuel consumption. Hence there is a need to reduce HC and CO emissions as much as possible before they are emitted into the exhaust pipe.

Table 1. EU emissions standards for passenger cars (Compression Ignition, Diesel) [1]

Stage	Date	CO (g/km)	HC (g/km)	HC+NOx (g/km)	NOx (g/km)	PM (g/km)	PN (#/km)
Euro 4	2005.01	0.5	-	0.3	0.25	0.025	-
Euro 5a	2009.09	0.5	-	0.23	0.18	0.005	-
Euro 5b	2011.09	0.5	-	0.23	0.18	0.005	6.0×10^{11}
Euro 6	2014.09	0.5	-	0.17	0.08	0.005	6.0×10^{11}

1.2 Objective

The research was performed during two different projects. In the beginning of this work, the project was named Spark Assisted Compression Ignition (SACI). The focus of the project changed from SACI to light-duty gasoline PPC in 2010. As part of the SACI project, the goal was to characterize and compare the effects of different variable valve train strategies on HCCI combustion and SI combustion. A SI to HCCI combustion mode switch strategy was designed, implemented and evaluated. The goal was to achieve a smooth transition from SI to HCCI. A focus on low load investigation utilizing the variable valve train was maintained when the project changed from SACI to gasoline PPC. The main work of the thesis was performed as part of the Gasoline PPC Light Duty Project. The goal was to extend the operating range of the engine with high octane number fuels using the variable valve train system, the glow plug and more advanced injection strategies. The engine speed was kept low and the goal was to reach idle operating condition.

1.3 Method

This work is based on experimental measurements on a single cylinder engine. The main source of information is the in-cylinder pressure, which is used to calculate the net and gross indicated mean effective pressures and heat release rate. A control system was developed in National Instruments LabVIEW that permitted control of the main variables, the valve timings and fuel injections, as well as data acquisition of in-cylinder pressure, valve lift curves, and fuel injection command signal, on the same system. A part of this work also used an engine simulation tool, AVL BOOST, to extract information on in-cylinder temperature and residual gas fraction. The post-processing of the data was made with Matlab.

1.4 Contribution

The first part of the thesis includes investigations of residual HCCI using negative valve overlap and rebreathing in comparison to SI combustion at part load operating conditions. It also includes an investigation of HCCI combustion control strategies in connection to combustion mode switching from SI to HCCI. The main part of the thesis is focused on the gasoline PPC combustion concept. Gasoline PPC is a promising combustion concept which has shown great potential for high efficiency and low soot and NOx emissions. While there are advantages at high load operation with high octane number fuel there are problems with ignitability at low load operation. The main contribution of the thesis is that it is more in depth investigation on the extension of low load operation with gasoline PPC. Different parametrical studies on the effects of the variable valve train, injection strategies and glow plug have been performed. It was shown that it is possible to extend the low load operating region using primarily the variable valve train system and more advanced fuel injection strategies. A comparison between two different valve strategies, NVO and rebreathing, has been performed. The result is a suggested low load gasoline PPC operating strategy with different valve and fuel injection strategies depending on engine load.

2 Low Temperature Combustion Concepts (LTC)

Low temperature combustion (LTC) has gained popularity in the last decade because of the possibility to combine high efficiency with low engine-out emissions of NOx and soot. There are many different kinds of LTC and the following sections provide a brief overview of the ones that are relevant for the work in this thesis.

2.1 HCCI

The HCCI combustion concept is based on compression ignition of a pre-mixed charge by using either port fuel injection or early direct injection to obtain a homogeneous mixture of fuel and air. The fuel is auto-ignited after compression from increased pressure and temperature. The charge ignites in several locations simultaneously where the local temperature is higher or where the mixture is richer so that the conditions are more favorable for the chemical reactions to occur [2]. There is no global flame propagation and the combustion rate is fast [3]. The soot formation zones are avoided because the combustion is fairly homogeneous. NOx formation is avoided since the mixture is diluted with either air or EGR which lowers the combustion temperature. A high dilution level also keeps the pressure rise rate at an acceptable level. The efficiency is generally high because of the fast combustion which, by having the combustion phasing close to TDC, increases the expansion ratio. Also because the HCCI engine is operated without a throttle, the pumping losses are reduced in comparison to the SI engine at part load. But there are some drawbacks and limitations with HCCI. The power density is low because of the required dilution level. The emissions of CO and HC increase from incompletely oxidized fuel [4]. The operating range is limited. HCCI combustion is also difficult to control due to lack of an immediate control actuator such as a spark plug which is used in the SI engine. A lot of work has been performed to address the different problems with HCCI. In a work by Christensen et al. [5] supercharging in combination with EGR was used on a single cylinder heavy duty engine fueled with natural gas and isooctane to extend the high load limit of HCCI. Load as high as 16 bar IMEPg was reported. High load

operation up to 16 bar BMEP was reported by Olsson et al. [6] on a dual fuel turbo charged 6-cylinder truck engine. Examples of strategies to control HCCI combustion include heating of the intake temperature [7], variable compression ratio [8], or using dual fuels with different auto ignition properties [9].

There are different ways to realize HCCI combustion and cope with the practical limitations of HCCI. As a result two main branches emerged. The first is usually implemented in SI engines, where HCCI is achieved by reusing the hot residual gases from the previous cycle to auto-ignite the fresh fuel/air charge. This type of combustion is often referred to as CAI (Controlled Auto Ignition) combustion. The second branch is more closely related to the diesel engine and is referred to as partially premixed combustion, PPC. With PPC, the fuel is injected late compared to HCCI and combustion timing is controlled with the fuel injection timing. The charge is however still sufficiently premixed in order to reduce soot emissions and it is usually diluted with EGR to simultaneously reduce NOx emissions.

2.2 Controlled Auto Ignition (CAI)

Using negative valve overlap (NVO) is one way to achieve HCCI combustion. The exhaust valves are closed early and a large fraction of hot residual gas is trapped in the cylinder. The hot residual gas elevates the temperature of the fresh charge to have auto ignition around TDC. The strategy was proposed by Willand et al.[10] in 1998 and the first results were shown by Lavy et al. [11] in 2000. An alternative to using NVO is to rebreathe the exhaust gas during the intake stroke. This can be done in different ways, for example by delaying the exhaust valve closing or reopening the exhaust valves later during the intake stroke [12]. The advantage with rebreathing compared to NVO is that recompression of the exhaust gas is avoided. Recompression of the exhaust gas introduces additional heat losses and thus lowers the efficiency of the engine.

One problem with CAI is the limited operating region. At low engine load, the auto-ignition can be further enhanced by using a spark plug [13] [14]. This is called Spark Assisted Compression Ignition (SACI). The slowly propagating flame increases the temperature and triggers the HCCI combustion. SACI can be useful when performing mode switches from SI to HCCI and back. A combustion mode switch to SI combustion can be used to cover the entire operating region of the engine. A mode switch strategy on a camless port-fuel injected engine was developed by Koopmans et al. [15] on both a single cylinder engine and a multi cylinder engine. The mode transition from SI mode to HCCI mode could be made within one engine cycle. Milovanovic et al. [16] presented a mode switch investigation from SI mode to HCCI mode within one cycle using valve profile switching. Fuel was port-fuel injected. Kakuya et al. [17] developed a mode switch strategy on a multi-cylinder direct

injected engine from SI mode to HCCI mode. Before complete transition to HCCI mode an intermediate step was taken in order to suppress IMEP fluctuations by controlling A/F ratio and EGR rate with assistance from spark and double fuel injection. Kitamura et al. [18] investigated an HCCI ignition timing model and applied it to combustion mode switching from Otto-Atkinson SI mode (intake valve closing timing occurring late during the compression stroke) to HCCI mode on a port fuel injected multi-cylinder engine. Zhang et al. [19] demonstrated a mode switch from SI mode to HCCI mode using spark timing, effective compression ratio and residual gas fraction adjustments for control during the transition. A control oriented model of HCCI mode transition was proposed and evaluated by Shaver et al. in [20].

If a direct injection system is used there are additional degrees of freedom to control the combustion. The low load limit can be extended by injecting a portion of the fuel during the NVO to influence also the main combustion. Fuel injection during NVO was first proposed by Willand et al. [10] and experimental results were reported by Urushihara et al. [21] and Koopmans et al.[22]. Berntsson et al. [23] used a SI stratified charge fuel injection, together with a pilot injection prior to the NVO TDC and a main injection after the NVO TDC, to expand the low load HCCI operational range. Yun et al. [24] extended the HCCI operating range to idle condition, 0.85 bar IMEPn at 800 rpm, using a combination of NVO, multiple injections and two spark ignition events, one during NVO and one during the compression stroke. Johansson et al. [25] extended the operating region of a light duty multi cylinder turbocharged NVO HCCI engine. An operating region from 1 to 6 bar IMEPn between 1000 and 3000 rpm was reported.

In the thesis, a comparison between different residual HCCI strategies using NVO and rebreathing in comparison to SI combustion is presented. Control strategies for HCCI combustion after mode switch from SI are also evaluated.

2.3 Partially Premixed Combustion (PPC)

PPC combustion is a combination of traditional diesel combustion and HCCI. With PPC, the fuel injection is complete before start of combustion to promote mixing of fuel and air but the charge is not homogeneous. Long ignition delays can be achieved by high fractions of cooled EGR and lower compression ratios. This concept was used by Nissan and is called Modulated Kinetics (MK) [26]. The advantage is that soot and NOx emissions are low. Miles et al. [27] depicted a postulated path for late-injection MK-like combustion in a phi-T diagram and this is shown as the black arrows in Figure 1. The white unfilled arrow shows the path for conventional diesel combustion without EGR. The goal is to suppress combustion temperatures to simultaneously avoid soot and NOx formation. Toyota used high EGR rates with an advanced injection to suppress both soot and NOx with the smokeless rich diesel combustion

concept [28]. The term PPC was used to characterize the combustion mode with a combination of high EGR ratio and low compression ratio to achieve low simultaneous soot and NOx emissions up to 15 bar IMEP in a work by Noehre et al. [29]. The problem with diesel PPC is that it is difficult to achieve a premixed charge at high load conditions even with a high level of EGR. EGR levels of over 70% to suppress NOx and soot were reported. A high level of EGR leads to reduced combustion efficiency. If a lower compression ratio is used, this also results in lower efficiency.

Toyota developed a different concept which is called Uniform Bulky Combustion System (UNIBUS) [30]. Instead of using high EGR levels, Toyota used a split injection in the part-load operating region. The first injection is used to start the low temperature reactions and an injection close to TDC is used to control the ignition of the remaining combustion.

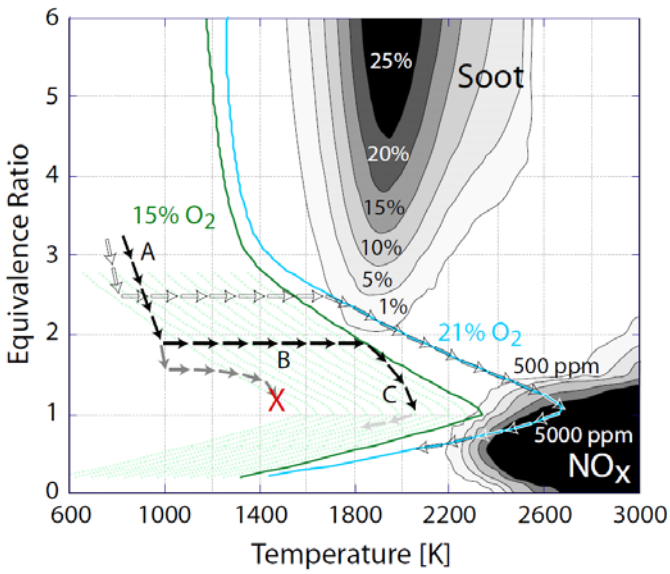

Figure 1. Homogeneous reactor simulation results after 2 ms giving soot and NOx formation zones in a Φ-T map. The solid lines show the adiabatic flame temperatures at 21% and 15% ambient oxygen concentration [27].

2.4 Gasoline PPC

Using gasoline instead of diesel has the potential to extend the high load region without using excessive EGR levels and a lower compression ratio. This combustion concept is referred to as gasoline PPC. Kalghatgi introduced the concept of gasoline partially premixed combustion in 2006 [31]. Experiments were performed in a 2.0 L single cylinder engine with a compression ratio of 14 at an engine speed of 1200 rpm. The gasoline fuel was a commercial gasoline with 94.7 RON and 85.9 MON. The ignition delay was longer for gasoline compared to diesel and much higher IMEP could be attained with gasoline for a given intake pressure and EGR level while maintaining lower NOx and smoke emissions. The highest IMEP that could be reached with gasoline was 14.86 bar with soot level 0.36 FSN and ISNOx level of 1.21 g/kWh. It was also observed that the engine could be run with gasoline in PPC mode at conditions where it could not be run with early injection in HCCI mode either because of failure to auto-ignite or because of excessive pressure rise rates. Different fuel injection strategies were investigated by Kalghatgi et al. in [32]. With gasoline, a pilot injection early during the compression stroke enabled higher IMEP because of a lower maximum heat release rate and enabled retarded combustion phasing with low cyclic variation. 15.95 bar IMEP with soot below 0.07 FSN was reported. To get the same smoke with diesel IMEP had to be below 6.5 bar.

At Lund University, Manente et al. [33] [34] developed a gasoline PPC strategy using a variety of gasoline fuels with different octane numbers in a single cylinder heavy-duty engine. The engine was run with 50 % EGR and was boosted to maintain λ around 1.5. Gross indicated efficiencies up to 57 % with low NOx emissions, soot levels below 0.5 FSN as well as low HC and CO emissions were reported. Light duty experiments were reported in [35]. A triple injection strategy was used with gasoline to control engine load and avoid excessive pressure rise rates. For the load sweep between 6 and 17 bar IMEPg, gross indicated efficiencies above 45 %, NOx between 2 and 17 ppm, and soot below 0.05 FSN was reported. The gross indicated efficiency was 10 % higher with diesel compared to gasoline but the soot level increased up to 9 FSN for diesel while it was always below 0.01 FSN for gasoline. By running the engine with approximately 50 % EGR and λ around 1.5, the combustion temperature stays between 1500 and 2000 K. This is the operating region where emissions of CO, HC and NOx are suppressed simultaneously. More details on the gasoline PPC strategy from Lund can be found in [36].

At Delphi Corporation, Sellnau et al. [37] [38] achieved higher efficiency with 91 RON pump fuel gasoline compared to diesel in a single cylinder light duty Hydra engine with the gasoline direct injection compression ignition (GDCI) strategy. At operating condition 6 bar IMEP at 1500 rpm, using a triple injection strategy, an indicated thermal efficiency of 46.2 %, which was 8 % better compared to the diesel tests, was reported. At low load operating conditions, 2 bar IMEP at 1500 rpm, a

rebreathing valve strategy was used to extend the low load limit. At higher loads, late intake valve closing was used to reduce cylinder pressure and temperature and increase the ignition delay.

One important aspect with gasoline PPC is the auto-ignition properties of the fuel. Hildingsson et al. [39] investigated different gasoline fuels in a light duty engine with 16:1 compression ratio using a single injection strategy at both a low load and engine speed operating condition (4 bar IMEP/1200 rpm) and higher engine load and engine speed operating conditions (10 bar IMEP / 2000 and 3000 rpm). It was argued that the optimum fuel might be in the 75 to 85 RON range for the engine compression ratio in the investigation. Lower octane number fuels loose the ignition delay advantage over diesel at high load while higher octane number fuels will have difficulties to ignite at low load. Lewander et al. [40] showed that it was possible to extend the high load limit with PPC combustion with a multi-cylinder heavy-duty engine using gasoline to cover 50% of the heavy-duty engine nominal operating region.

One alternative strategy to gasoline PPC is the Reactivity Controlled Compression Ignition (RCCI) strategy which was developed at University of Wisconsin – Madison [41] [42]. A blend of gasoline and diesel was used to control combustion phasing and heat release rate. The gasoline fuel was port injected and the diesel fuel was directed injected. The idea is to adjust the auto-ignition properties of the fuel mixture depending on engine speed and load. Olsson et al. also used a dual fuel strategy with HCCI combustion using a mixture of ethanol and n-heptane in [6] and isooctane and n-heptane in [9] to control the combustion timing. The difference in this work is that both fuels were port injected and thus creating a more homogeneous mixture.

One of the problems with gasoline PPC is the combustion stability and combustion efficiency at low load. Solaka et al. [43] could extend the low load limit of a single cylinder light duty engine at 1500 rpm engine speed down to 2 bar IMEPg using boosted inlet air. The absolute inlet pressure at 2 bar IMEPg was approximately 2 bar for the fuels with the highest RON (88.6 and 87.1) with 53 % EGR level. HC and CO emissions were higher with the higher RON value gasoline fuels.

The advantage with higher octane number fuels are seen at high load operating conditions. At low load, the high octane number fuels are difficult to ignite and the emissions of HC and CO are high. The main work of the thesis is devoted to extending the low load limit with gasoline in a single cylinder light duty engine.

3 Combustion Engine Analysis

There are different approaches of experimental combustion engine research depending on the purpose of the research. This work is mainly based on results from a single cylinder engine. Single cylinder engine research is useful to get a basic understanding of the combustion process and effects of individual parameters, for example fuel injection timings on combustion and engine performance. Experimental work on a single cylinder engine is a good starting point before moving on to optical diagnostics or multi-cylinder experiments. Optical engines permit visual access to the combustion chamber and the combustion process can be studied in detail. Multi-cylinder experiments provide a closer representation of actual production type engine results.

The results that are presented in this work are based on in-cylinder pressure measurements. The in-cylinder pressure is used to calculate the net and gross indicated mean effective pressures and heat release rate. This section gives the definitions and short descriptions of the analytical tools (equations) that are used in this work.

3.1 Mean Effective Pressures

To be able to compare engines of different sizes running at different speeds, normalized quantities are used. This is achieved by comparing the performance per cycle normalized with the displacement volume. The result is the mean effective pressures with the unit Pascal, (Pa), which is normally presented as kPa, MPa or bar. Mean effective pressures are used to compare as well as visualize the energy flow through the engine from the supplied fuel to the output power as shown in the Sankey diagram in Figure 2.

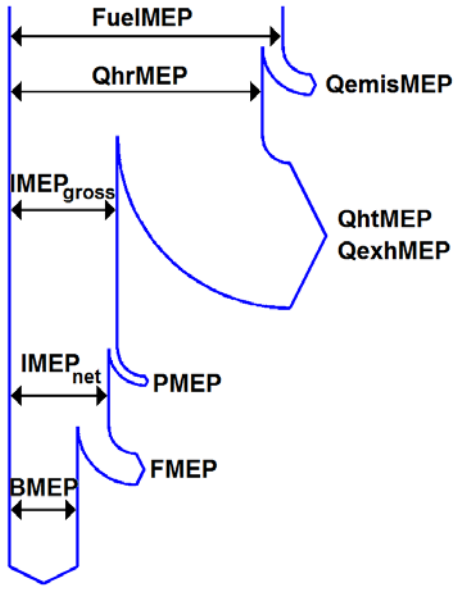

Figure 2. Sankey diagram of mean effective pressures.

The starting point is the supplied fuel energy which gives the fuel mean effective pressure according to:

$$FuelMEP = \frac{m_f \cdot Q_{LHV}}{V_d} \tag{3.1}$$

where m_f is the mass of fuel supplied per cycle, Q_{LHV} is the lower heating value of the fuel, and V_d is the displacement of the engine.

QemisMEP represents the energy loss due to incomplete combustion. The heat released mean effective pressure, *QhrMEP*, is the ratio between Q_{HR} which is the heat released during combustion and the displacement volume.

$$QhrMEP = \frac{Q_{HR}}{V_d} \tag{3.2}$$

Energy from the heat released after combustion that is not converted to work can be separated into two different losses. *QhtMEP* is the energy losses due to heat transfer to cylinder walls and *QexhMEP* is the energy lost with the exhaust flow due to elevated temperature and pressure.

The indicated mean effective pressure, *IMEP*, is the energy that is converted into work on the piston, W_C, divided by the displacement volume according to:

$$IMEP = \frac{W_C}{V_d} = \frac{\oint pdV}{V_d} \tag{3.3}$$

Two different definitions of IMEP are commonly used depending on whether the entire cycle is used or if the gas exchange process is excluded. If the entire cycle is used, *IMEPn* (net IMEP) is obtained, and if the gas exchange process is excluded *IMEPg* (gross IMEP) is obtained. The difference between *IMEPg* and *IMEPn* is called *PMEP*, according to:

$$PMEP = IMEP_g - IMEP_n \tag{3.4}$$

PMEP represents the pumping losses during the gas exchange process.

From engine torque measurements, *T*, the brake mean effective pressure, *BMEP*, can be calculated according to:

$$BMEP = \frac{4\pi T}{V_d} \tag{3.5}$$

The difference between *IMEPn* and *BMEP* is the friction mean effective pressure.

$$FMEP = IMEP_n - BMEP \tag{3.6}$$

3.2 Efficiencies

The efficiencies are calculated as shown in the flow chart, Figure 3, with the mean effective pressures defined in the previous section.

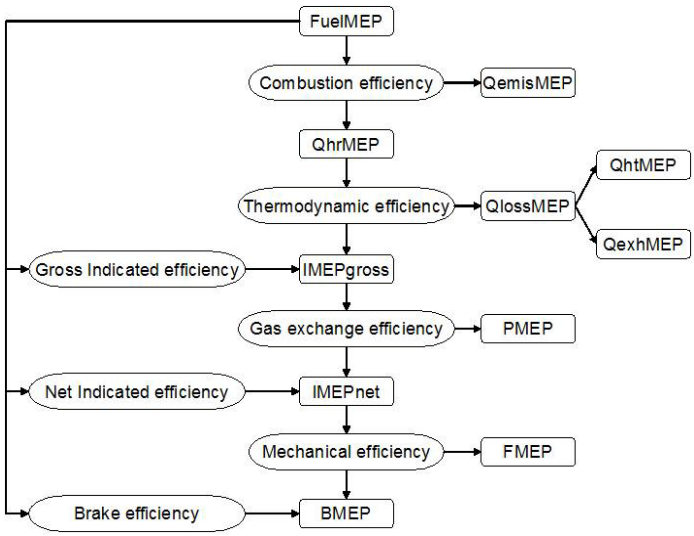

Figure 3. Mean effective pressure and efficiencies flow chart.

The combustion efficiency, η_c, reflects how much of the fuel energy that is converted into heat:

$$\eta_c = \frac{QhrMEP}{FuelMEP} = 1 - \frac{QemisMEP}{FuelMEP} \tag{3.7}$$

The combustion efficiency can be estimated from the incomplete combustion products in the exhaust divided by the supplied fuel heat according to:

$$\eta_c = 1 - \frac{\sum_i m_i \cdot Q_{LHV,i}}{m_f \cdot Q_{LHV,f}} \tag{3.8}$$

where m_i is the mass of the combustion product, $Q_{LHV,i}$ is the lower heating value of the combustion product, m_f is the fuel mass and $Q_{LHV,f}$ is the lower heating value of the fuel.

The thermodynamic efficiency, η_{th}, is the ratio between *IMEPg* and *QhrMEP* and represents the efficiency of converting released heat to indicated work.

$$\eta_{th} = \frac{IMEP_g}{QhrMEP} = 1 - \frac{QhtMEP + QexhMEP}{QhrMEP} \tag{3.9}$$

The gas exchange efficiency, η_{ge}, is defined as the ratio between the indicated work for the entire cycle and the closed cycle without the gas exchange process.

$$\eta_{ge} = \frac{IMEP_n}{IMEP_g} = 1 - \frac{PMEP}{IMEP_g} \tag{3.10}$$

The gross indicated efficiency is defined as:

$$\eta_{i,g} = \frac{IMEP_g}{FuelMEP} \tag{3.11}$$

The net indicated efficiency is defined as:

$$\eta_{i,n} = \frac{IMEP_n}{FuelMEP} \tag{3.12}$$

Finally, the mechanical efficiency accounts for the friction from piston rings, bearings, auxiliary equipment and more.

$$\eta_{mech} = \frac{BMEP}{IMEP_n} = 1 - \frac{FMEP}{IMEP_n} \tag{3.13}$$

3.3 Heat Release

By performing heat release calculations qualitative information on the burn profile and quantitative information such as combustion timing and combustion duration can be calculated.

The heat release analysis in this work is based on a single zone model which utilizes the first law of thermodynamics for a system as shown in (3.14). The thermal energy release from combustion, ∂Q, is given by the sum of the change in internal energy, ∂U, the work done by the system, ∂W, the heat transfer to the cylinder walls, ∂Q_{HT}, and the energy losses due to crevice flows, ∂Q_{cr}.

$$\partial Q = \partial U + \partial W + \partial Q_{HT} + \partial Q_{cr} \tag{3.14}$$

Using the equation of state, assuming the cylinder content to be an ideal gas and that the trapped mass is constant, the thermal energy release per unit crank angle, θ, or heat release rate is given by:

$$\frac{dQ}{d\theta} = \frac{\gamma}{\gamma - 1} p \frac{dV}{d\theta} + \frac{1}{\gamma - 1} V \frac{dp}{d\theta} + \frac{dQ_{HT}}{d\theta} + \frac{dQ_{Crevice}}{d\theta} \tag{3.15}$$

Where V and p are the cylinder volume and pressure, γ is the ratio of specific heats C_p/C_v. The heat transfer to the cylinder walls is estimated with a zero-dimensional model according to (3.16). The temperature of the gas, T_g, is assumed to be homogeneous and the wall surface temperature, T_w, is assumed to be constant. The wall area, A_w, is the sum of the cylinder head, piston crown and exposed cylinder liner area.

$$\frac{dQ_{HT}}{dt} = hA_w(T_g - T_w) \tag{3.16}$$

The heat transfer coefficient, h, is estimated by the relationship introduced by Woschni [44]. This is based on a Nusselt-Reynolds relationship according to:

$$h = CB^{-0.2} p^{0.8} T^{-0.55} w^{0.8} \tag{3.17}$$

C is an engine specific constant, B is the engine bore, p and T are the cylinder pressure and temperature, and w is a characteristic gas velocity, which is defined according to

$$w = C_1 S_p + C_2 \left(\frac{V_d}{V_r}\right)\left(\frac{p - p_{mot}}{p_r}\right) T_r \tag{3.18}$$

C_1 and C_2 are correlation coefficients that must be tuned for the individual engine. S_p is the mean piston speed, V_d is the displacement volume, and V_r, p_r, T_r are the reference volume, pressure and temperature, respectively, reflecting in-cylinder conditions at IVC. The cylinder pressure is p, and p_{mot} is the calculated motored pressure.

From the cumulative heat release it is possible to calculate different parameters. Figure 4, which is from Per Tunestål's doctoral thesis [45], shows the definitions of the most commonly used parameters. The crank angle of 50 % cumulated heat release, CA50, is used as a measure of combustion timing. The combustion duration is calculated as the difference between 90 and 10 % cumulative heat release (CA90 – CA10). The reason is that these parameters are considered more robust and less sensitive to measurement and model uncertainties compared to for example CA1 and CA99.

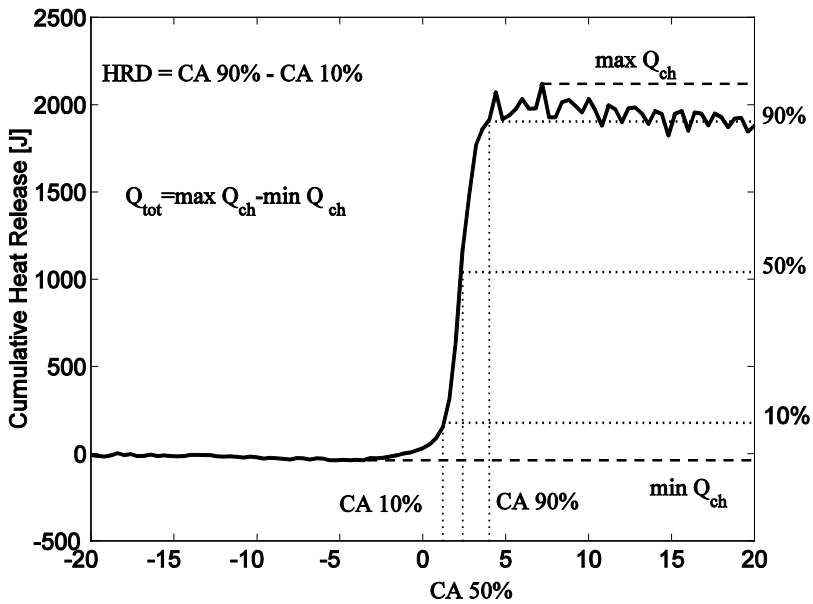

Figure 4. Definitions of some heat release based cycle parameters [45].

3.4 Cycle-to-Cycle Variations

COV of IMEP is a commonly used measure of the cyclic variability between different cycles derived from the pressure trace data [46]. An operating point with high cyclic variability is considered as unstable. COV of IMEP is calculated by dividing the standard deviation of IMEP by the mean IMEP. Similarly to [47] the standard deviation of IMEP is used as a measure of combustion stability instead of COV of IMEP. The reason is that the experiments are performed at low load and engine speed. At low load, COV is generally high due to the division by a low mean IMEP. Also, a change in mean IMEP will have a large influence on COV for the same reason. 500 consecutive cycles have been saved at each operating point to calculate IMEP and the standard deviation of IMEP.

4 Experimental Apparatus

A brief description of the experimental engine, auxiliary equipments and measurement devices, including the engine control system, is given in this section.

4.1 Engine and Auxiliary Equipment

The experimental engine is based on a Volvo D5 light duty diesel engine. The engine specifications can be seen in Table 2. It is run on only one of the five cylinders and is equipped with a fully flexible pneumatic valve train system supplied by Cargine Engineering. The engine speed is controlled with a 30 kW AC motor used as dynamometer to both motor and brake the engine.

Table 2. Engine specifications.

Displacement (one cylinder)	0.48 Liters
Stroke	93.2 mm
Bore	81 mm
Compression ratio	16.5:1
Number of Valves	4
Valve train	Fully flexible

The Cargine valve train system was first demonstrated by Trajkovic et al. [48]. The Cargine system has also been used by Håkan Persson [49]. The actuators are sufficiently small to be fitted directly on top of the valve stem. But to allow space for the fuel injector, the valve actuators were placed on an elevated plate above the fuel injector and were connected to the valve stems with push-rods. Maximum valve lift was set to approximately 5 mm by installing mechanical stoppers (hollow metal cylinders) between the cylinder head and the valve spring retainer. The valve lift profiles are measured using MicroStrain displacement sensors installed below the valve actuator. The displacement sensor measures the horizontal distance to a cone shaped skirt which moves up and down with the valve and gives a varying horizontal distance with valve lift. The Cargine actuators also have a simpler contact sensor

which is used to detect the crank angle of 1 mm valve lift opening. The dynamic range of the sensor (difference in volts between the sensor reading at minimum and maximum valve lift) is different for each sensor. The valve lift profile is calculated by assuming a linear correlation between the maximum and minimum sensor output and the known maximum valve lift. The calculated valve lift profile crank angles at 1 mm valve lift is in good agreement with the output of the simpler contact sensor. The valve lift profile calculation has also been verified by measuring the valve lift from below the cylinder head using a Wenglor YP06MGV80 reflex sensor measuring directly on the valve face. A photograph of the Microstrain displacement sensor and an example of calculated valve lift curves are shown in Figure 5. The lift profiles of the pneumatic valve train is different compared to a more conventional cam shaft controlled system.

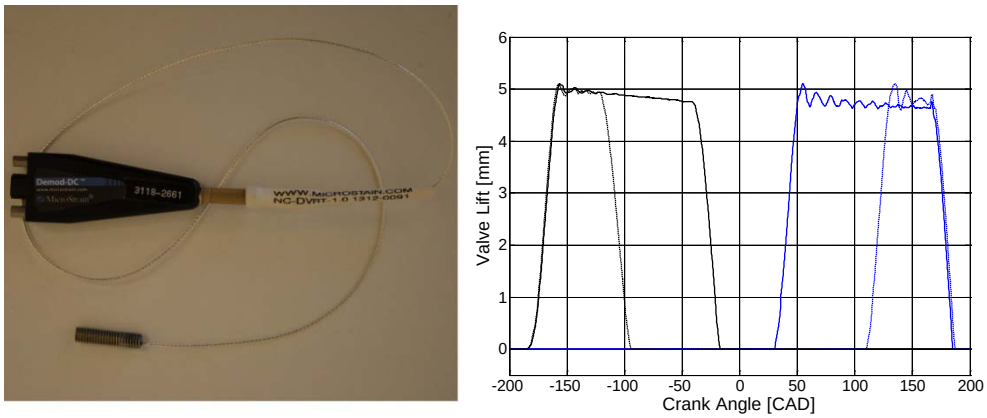

Figure 5. The MicroStrain displacement sensor with signal amplifier (left image) and calculated valve lift curve examples (right image).

The actuators work with pressurized air to lift the valve. The air supply is controlled with two solenoids and a pressurized hydraulic circuit is used to achieve a stable and constant valve lift. The valve timings are controlled by activating the solenoids. This is managed by the engine control system. The performance of the valve system is based on the supplied air pressure and the force of the valve springs, independent of engine speed. The air pressure was kept between 3 and 4 bar gauge (4 and 5 bar absolute) and the hydraulic pressure was kept at 4 bar gauge (5 bar absolute). At 800 rpm the opening and closing ramp of the valve is approximately 20 CAD from 0 to 5 mm valve lift. At increased engine speed the valve lift profile would be closer to a more traditional valve lift curve. The valve lift profile can be changed, but only to a limited extent and not in real-time. The air pressure can be moderated to change the valve opening speed but the valve closing speed is dependent on the spring properties.

Photographs of the experimental engine and the two different piston crowns that were used are shown in Figure 6. The modified piston was machined at the department and mounted on top of a machined Volvo D5 piston with three screws. The purpose of the design was to enable valve clearance at top dead center with the Cargine valve train system. It is not expected that the combustion chamber geometry is optimal for any of the combustion processes investigated in the thesis. The modified piston crown was used in Paper 1 and 2 and in an introductory low NVO setting comparison study in Paper 3. The rest of the presented results, which cover the PPC results of the thesis, have been measured with the standard piston crown. The compression ratio with both pistons is 16.5:1.

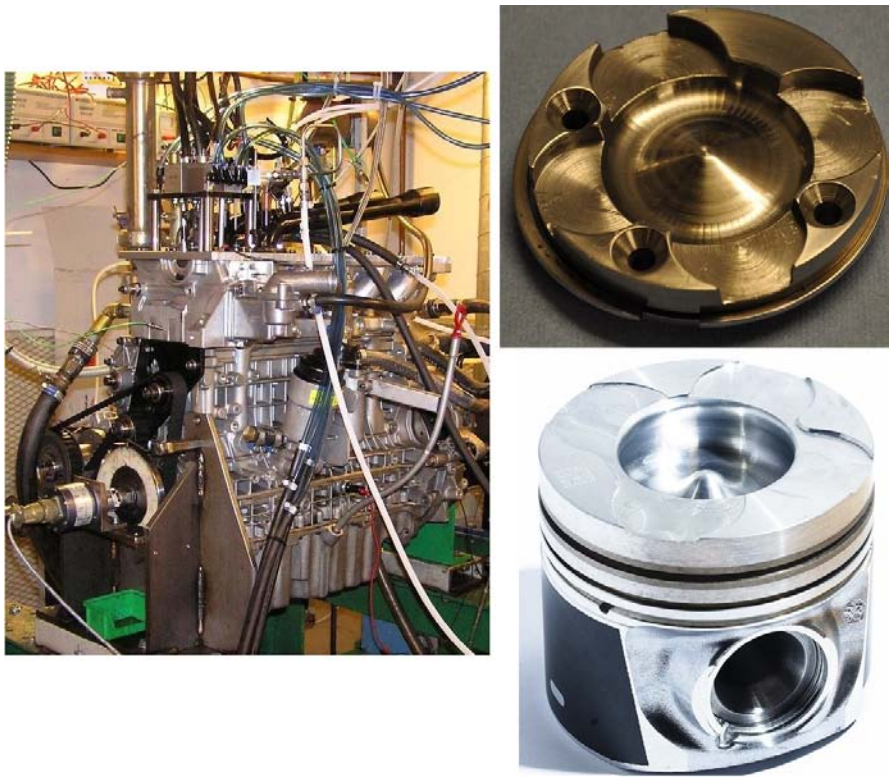

Figure 6. The experimental engine (left image), the modified piston crown (upper right image) and the standard Volvo D5 piston (lower right image).

A minimum NVO setting had to be used with the standard piston crown in order to avoid hitting the piston with the valves. A minimum NVO setting of 60 CAD was selected to also include a small margin. The conclusion from the low NVO setting comparison study in Paper 3 was that the differences between the lower NVO case (10 CAD) and the 60 CAD NVO case were minor.

The engine is equipped with both a port fuel injector and a direct injection system. The direct injection system is a common rail system with a 5 hole nozzle solenoid injector. The umbrella angle is 140 degrees and the nozzle hole diameters are 0.159 mm. For the low engine load and engine speed operating points in the thesis, the common rail pressure was relatively low, 400-500 bar.

During the measurements for Paper 1 and Paper 2, an 8 mm thread NGK ER8EH spark plug was installed in the glow plug hole. The spark plug was fitted and fixated using a custom made insulator. This is the same spark plug configuration that has previously been used by Håkan Persson [49]. The spark plug was replaced by a glow plug when the focus of the project changed from HCCI/SACI to PPC.

The engine was operated at ambient pressure and no boosted air. The inlet temperature was controlled with a heater in the intake manifold. If nothing else is stated, the inlet temperature was kept at 40 °C. External EGR was used only in Paper 3 and was produced by pumping back the exhaust gases from the exhaust manifold to the inlet with a screw type compressor.

An overview of the engine control system hardware components and measurement apparatus is shown in Figure 7. The engine control system consists of two separate computers that are controlled from the same LabVIEW project. The host computer is a standard desktop PC running Windows. The real-time system consist of a National Instrument PXI-8110 (embedded controller with a 2.26 GHz Quad-Core CPU), PXI-7853R (Multifunction reconfigurable I/O (RIO) with Virtex-5 LX85 FPGA), and a PXI-6251 multifunctional data acquisition (DAQ) card. Most of the physical wires are connected to the real-time computer which is situated in the test-cell. The exceptions are the thermocouples, which are connected directly to the Hewlett Packard 34970A DAQ/switch unit (data logger) situated in the control room, and the instruments that use serial port communication (the fuel balance and soot meter).

Thermocouples are used to measure the temperature of the intake, exhaust, fuel, oil, and cooling water. The oil and cooling water temperatures were kept constant at 85 °C and 80 °C respectively. The cylinder pressure is measured with a Kistler6053CC60 piezo-electric pressure transducer fitted through a cooling channel and merged between the intake and exhaust valves. The absolute pressures in the intake and exhaust manifolds are measured with a Keller PAA-23S absolute pressure sensor. Crank angle pulses and a synchronization pulse (one per revolution) are generated by a Leine-Linde crank angle encoder with resolution 5 pulses per crank angle. The air flow is measured with a Bronkhorst F-106AI-AGD-02-V air-flow meter and the fuel flow is calculated by recording the fuel tank mass placed on the Sartorius CP 8201 precision balance. The time difference between each fuel balance reading was recorded by the control system and used to calculate the fuel mass flow. A linear correlation between the fuel injector opening duration and the calculated fuel flow was assumed. This was found to be in close agreement with the measured fuel flows. The

calculated fuel mass flow was used regularly to calibrate the fuel injector. The fuel injector was recalibrated for each fuel injection strategy. At least four measurement points were taken for each calibration. For the PPC measurements, given the low engine speed and load, a total measuring time of at least 8 minutes was used to ensure adequate fuel-flow calculations.

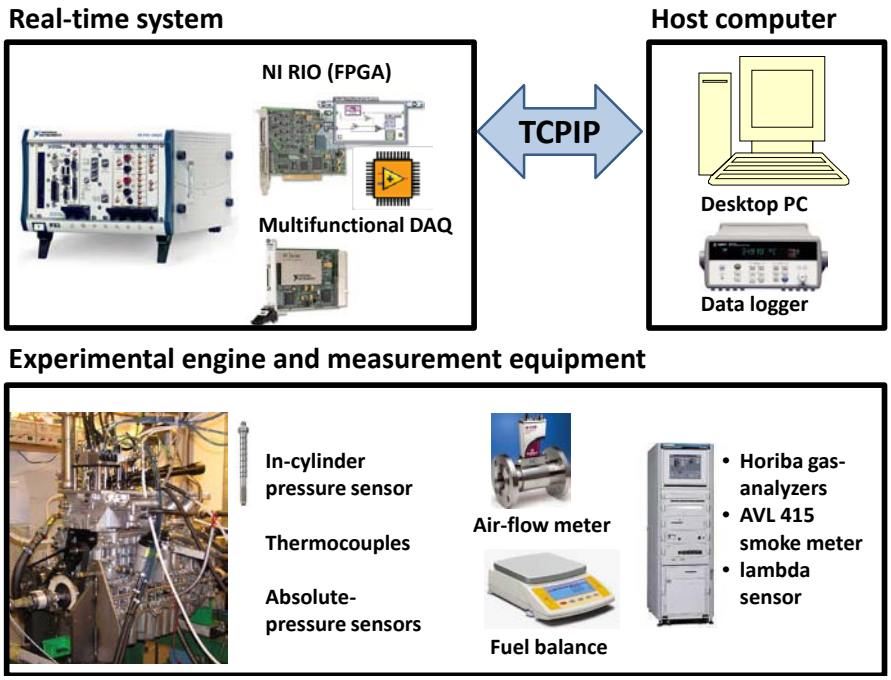

Figure 7. Overview of the engine control system and measurement apparatus.

The HC, CO, CO2 and NOx emissions are measured with a Horiba Mexa 7500 gas analyzer system. Soot is measured with an AVL 415 smoke meter. There is also a lambda sensor with an Etas LA3 module but it is mainly used for complementary monitoring in real-time. In Papers 1-3, the air-fuel ratio and relative air-fuel ratio, λ, were calculated from the measured exhaust gas composition, basically following the same procedure as described in Heywood [46]. After completion of Paper 3, the calculated air- and fuel-flows were used to calculate the air-fuel ratio. In Paper 3, cold/external EGR was used and produced by pumping back exhaust gas from the exhaust manifold to the inlet with a screw type compressor. The EGR ratio is calculated as the inlet CO2 fraction divided by the exhaust CO2 fraction. The inlet CO2 fraction was measured with a Horiba Mexa 554JE system. The exhaust gases were cooled down before reaching the intake manifold.

4.2 Engine Control System

An introduction and brief description of the LabVIEW based engine control system is given in this section. The LabVIEW based engine control system has been used to collect all of the experimental results presented in this thesis. The design and LabVIEW programming of the system was performed by the author. A short presentation of the system was given as part of a case study presented during NIDays 2010 in Stockholm. The case study was awarded with the NIDays Graphical System Design Achievement Award. The main front panel of the engine control system is shown in Figure 8.

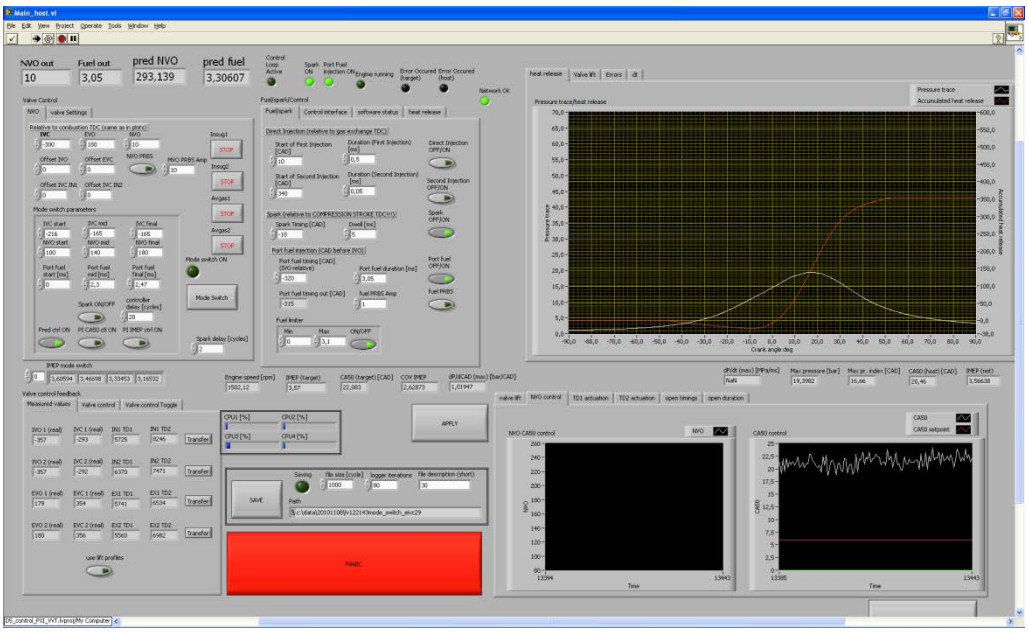

Figure 8. Front panel of the real-time control system.

There were a number of reasons for starting to work with LabVIEW. First, in the early phase of the project, the engine control system was divided amongst different subsystems, and computers, and no communication between them. The in-cylinder pressure traces were recorded at one station, the valves were controlled from a stand-alone system and the data logging of the fuel, emissions and thermocouples were handled with a third, independent, system. In order to be suitable for feedback control, the different subsystems were merged to a single system, with direct access to all of the measured quantities and control actuators. LabVIEW was chosen because it was relatively easy to include all of the subsystems in a single LabVIEW project. Another

reason for choosing LabVIEW was the FPGA (field-programmable gate array) hardware support and that programming of the FPGA can be performed easily in LabVIEW. The FPGA program runs more or less independently within the engine control system which offers many advantages as will be discussed later.

LabVIEW is not the only solution available and used for engine control system applications. MathWorks offers the xPC Target platform, which is a real-time software environment that runs Simulink models and connects them with the real world [50]. Graphical modeling with Simulink is possible also with the dSPACE systems. A dSPACE system was used by Hans Aulin [51] at the same department as the author in Lund. And Petter Strandh, also at the department in Lund, developed a control system in C++ including Simulink generated controllers [52].

LabVIEW (G programming) is a graphical programming language which is programmed by wiring graphical icons. The programming language includes standard programming concepts found in most traditional programming languages, including loops, variables, data types and event handling. The starting point of the program is normally the measured data and the execution of the code progresses through connected wires in a data flow fashion, which is different from more traditional procedural approaches. More information on LabVIEW can be found on National Instrument's web page[1].

Working with LabVIEW is not without difficulties. There are programming tasks that are more easily carried out in text-based programming languages, for example, more advanced operations on String data types. But the opposite is also true, there are programming tasks that are more easily handled in LabVIEW, for example, data acquisition and creating multiple tasks (threads) executing in parallel.

The graphical programming is intuitive to start to work with and it is relatively easy to get a basic data acquisition platform up and running. But a larger control system requires careful planning and it is important to think in advance how the different subtasks interact and communicate. This is generally true for most programming applications. If not, in worst case, you end up with a single virtual instrument (LabVIEW program) covering literally a large area of wires and icons that is impossible to overlook. It is important to split up the control task into different subtasks. This makes the control system easier to overview and performance is potentially improved because it enables different processes to execute in parallel. An example of how this can look is shown in Figure 9, where three different control loops, each handling a specific task, is shown. But even with careful planning and design, it will often be necessary to add a new block into an existing LabVIEW code

[1] www.ni.com

which often means that more program area needs to be made available. This is often cumbersome and the LabVIEW code tends to occupy an increasing amount of code area. In a more traditional programming language, inserting new code is simply achieved by pressing the enter key to create a new line.

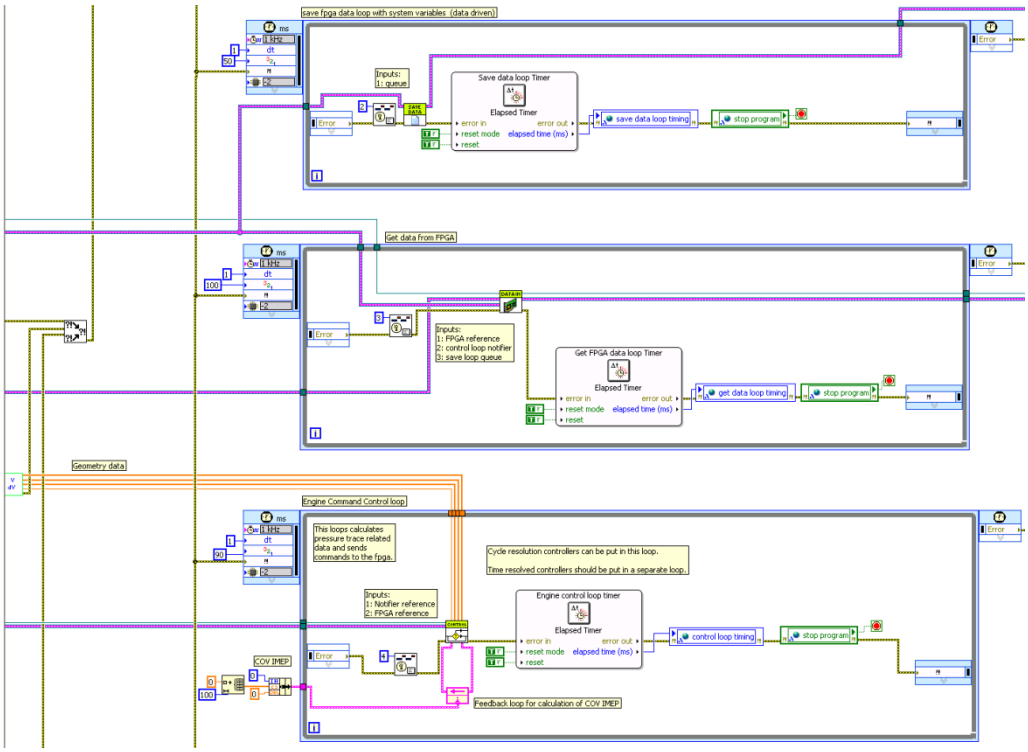

Figure 9. LabVIEW block diagram screenshot of the engine control system.

The LabVIEW engine control system task is split up into different subtasks that execute either on the host computer, the real-time target (PXI computer), or on the FPGA chip. The host computer handles the graphical user interface (GUI) and transmits user inputs to the rest of the system. The real-time target handles communication and data acquisition from the FPGA and the multifunctional DAQ hardware. It also has separate loops for heat release calculation and engine control, common rail pressure control, saving data, and Cargine valve train system control. Some loops of the control system are event driven, meaning that a loop is executed only if it is triggered by an event, for example, at completion of a new engine cycle. And the other loops execute at a predefined rate in time. The real-time target has a dedicated real-time operating system (LabVIEW Real-time). What makes a real-time

operating-system different is that it ensures that programs run with consistent timings according to priorities that are set by the programmer. A separate real-time computer is optional and the control system can easily be modified to run on a single desktop PC depending on the performance requirement of the control system. This has to be decided from case to case.

The FPGA chip is a part of the PXI-7853R hardware module in the real-time target, but the FPGA software runs on the FPGA hardware more or less independently of the rest of control system. Programming of the FPGA software is also made in LabVIEW. An FPGA LabVIEW block diagram example is shown in Figure 10. Unlike processors, FPGAs are truly parallel in nature and are made up of a finite number of predefined resources with programmable interconnects [53]. A more comprehensive description of the FPGA chip is included in Carl Wilhelmsson's doctoral thesis [54]. In the LabVIEW engine control system, the FPGA is used to handle more computationally simple tasks but with high execution rates. The time base of the FPGA control loops is the crank angle encoder which generates 5 pulses per crank angle degree. For the crank angle triggered FPGA software loops, at engine speed 800 rpm, this corresponds to a loop execution rate of 24000 iterations per second. In comparison, the software loops on the real-time target, typically runs at an execution rate of 5-30 iterations per second.

The FPGA is used for many different tasks of the engine control system. The FPGA is used to send digital and analog signals to different engine actuator drivers at predetermined crank angles or with a fixed frequency. Such drivers include the Cargine system valve train driver to the solenoids, the fuel injector driver, and the driver to the high pressure fuel supply pump for the common rail. The FPGA is also used to sample the in-cylinder pressure and valve lift curves at the same sampling rate as the crank angle encoder, 5 samples per crank angle degree. One advantage with a programmable sampling task is that it can be programmed specifically for the engine to automatically recover from measurement errors due to, for example, noise on the crank angle encoder signals. It is also straightforward to include logical signals, for example, whether or not the pulse to the fuel injector driver is high or not, together with the sampled signals to be shown in the GUI or recorded on the hard drive at the same sample rate as the in-cylinder pressure trace. This can be useful in the post-processing of the data and calculation of, for example, the ignition delay. Since the FPGA is run more or less independently of other parts of the control system it can also be used to implement automatic safety features such as automatic shut down of the fuel injection, for example, if communication is lost with the real-time target or if the pressure rise rate is too high.

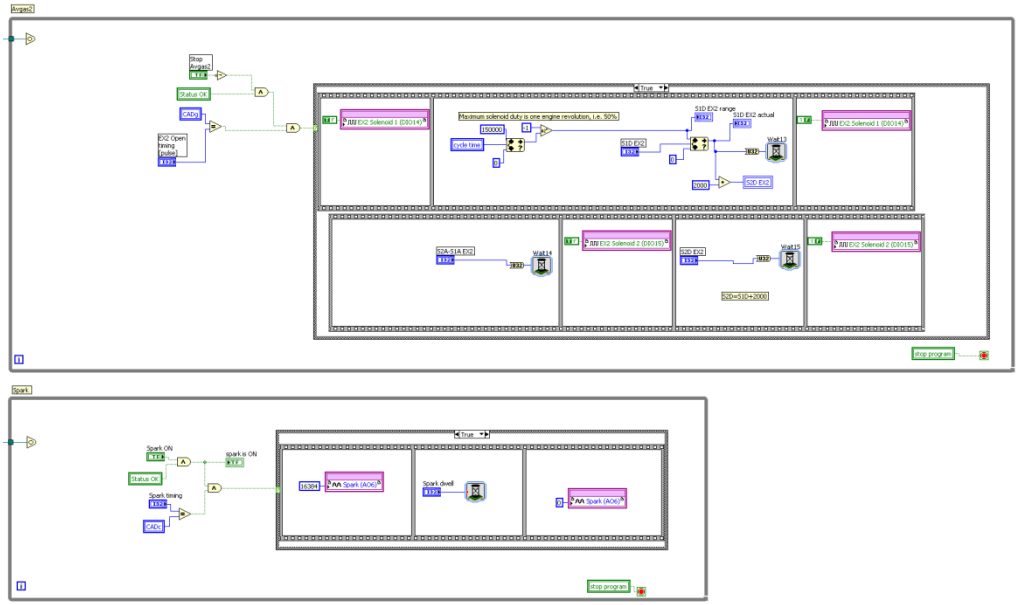

Figure 10. LabVIEW Block diagram of a small part of the FPGA LabVIEW code.

4.3 Post Processing

The post processing of the data is made with Matlab. Engine performance in terms of engine load can be calculated directly from the measured in-cylinder pressure and calculated volume. Since the experiments in this work have been performed on a single cylinder engine, adequate torque measurements for calculation of BMEP were unavailable.

The heat release calculations are dependent on the initial conditions of temperature, pressure and residual gas fraction. For an engine with more conventional valve timings the residual gas fraction can be assumed to be low and the initial charge temperature can be estimated from the inlet temperature. When the engine is operated with a high fraction of trapped residual gases, the initial in-cylinder temperature is increased and the ratio of specific heats, γ, is lower. Accurate estimates of the in-cylinder temperature and residual gas fraction is difficult to obtain and simplifications have to be made.

The method used in this work is a combination of residual gas fraction and temperature estimation and automated heat release calibration by means of parameter tuning. The main tuning parameter is the specific heat ratio. A rough estimation of the

residual gas fraction and in-cylinder temperature at intake valve closing timing can be calculated from the air-flow, exhaust temperature and exhaust gas composition measurements. A simplification can be made by assuming that the fresh charge has the same density in the cylinder as in the intake manifold. The rest of the displaced volume is then assumed to contain trapped residuals with the same temperature as the exhaust temperature. This was used to get a rough estimate of the initial charge temperature at intake valve closing timing.

There are two additional parameters that need to be estimated in order to calculate the heat release rate. This method was inspired by the work by Tunestål [55]. The first parameter is the unknown offset, Δp, between the measured pressure, p_m, and actual in-cylinder pressure, p.

$$p = p_m + \Delta p \tag{4.1}$$

The second parameter is the specific heat ratio, γ. It is assumed that there is a linear relationship between the specific heat ratio and the cylinder temperature, T. The specific heat ratio is approximated with

$$\gamma \cong \kappa_0 + k \cdot (T - T_{ref})/1000 \tag{4.2}$$

The estimated temperature at intake valve closing timing is chosen as reference temperature, T_{ref}. A straight line fit approximation as function of the mean charge temperature was used by Gatowski et al. [56]. This specific heat ratio calculation expression was included in an evaluation by Egnell [57] and also in a work by Ceviz et al. [58].

The parameters κ_0 and Δp are estimated from the measured cylinder pressure and calculated volume using linear least square and (3.15). Note that κ_0 is used instead of γ_0 since the estimated parameter is not necessarily the true thermodynamic specific heat ratio. A background on least-squares estimation is given in for example Johansson [59]. The assumption is that the parameter estimation interval in crank angles is sufficiently short so that the heat transfer term can be omitted and the total rate of heat released is zero. If the energy loss term by crevice flows is also omitted, (3.15) can be simplified to

$$\frac{dQ}{d\theta} = \frac{\kappa_0}{\kappa_0 - 1}(p_m + \Delta p)\frac{dV}{d\theta} + \frac{1}{\kappa_0 - 1}V\frac{dp_m}{d\theta} = 0 \tag{4.3}$$

where the pressure, p, has been replaced with (4.1) and γ with κ_0 from (4.2). This expression can be reformulated to be more suitable for linear least squares estimation of κ_0 and Δp according to

$$\kappa_0 p_m \frac{dV}{d\theta} + \kappa_0 \Delta p \frac{dV}{d\theta} = -V \frac{dp_m}{d\theta} \tag{4.4}$$

Note that the resulting least squares estimates are the parameters κ_0 and $\kappa_0 \Delta p$. The pressure offset Δp is easily obtained by dividing the second estimated parameter $\kappa_0 \Delta p$ with the first κ_0. A suitable estimation interval during the cycle needs to be selected. Selecting a suitable interval length is a trade-off between a sufficiently short interval for the zero rate of heat released assumption to hold but sufficiently long to obtain reasonable statistics for the least squares estimation. The length of the interval was empirically chosen to 40 crank angle degrees. The interval starting point should be set to early during the compression stroke for basically the same reasons. Since the simplification was made to omit the heat transfer term in (4.3), selecting a relatively late starting point will include more of the heat transfer losses in the estimation of κ_0. The starting point of the interval was empirically chosen to -100 CAD ATDC.

The remaining tuning parameter is k from (4.2). During the early stages of the experimental work the parameter k was manually tuned for each measurement point. But this soon turned out to be time consuming and the results were potentially biased with respect to the operator who for each case needs to make a manual decision on the value of the tuning parameter. Instead a cost function was designed to be minimized with respect to the k parameter according to

$$\min_k \left[\sum_{\theta_b} dQ(\theta_b)^2 + \sum_{\theta_a} dQ(\theta_a)^2 \right] \tag{4.5}$$

Two intervals are selected, θ_b and θ_a, before and after combustion, where it can be assumed that the rate of heat release is zero. This is normally true before fuel injection in a direct injection engine and late during the expansion stroke, sufficiently long after the crank angle of maximum accumulated heat released. There are applications where it is assumed that the heat release rates during similar intervals are not zero. A similar cost function was used in a work by Tunestål [60] about TDC estimation from motored cylinder pressure data where a nonzero, constant, heat release rate reference level was used. The difference in this work is that a heat transfer term is included explicitly in the calculation of dQ.

The main purpose of this final step is to have an unbiased estimate of the remaining tuning parameter with respect to the operator. In principle, this is a similar procedure that initially was carried out manually. After completion of the automated heat release calculation, each operating point was manually inspected to make sure that the algorithm produced reasonable results with respect to the overall shape of the heat release curve and maximum value of the accumulated heat released.

The motivation for using this method is that it is a standardized procedure capable of handling the large variations of in-cylinder conditions with respect to residual gas fraction in reasonable time and with a reasonable effort. Some tuning parameters are inevitable due to the many uncertainties and the simplified nature of the model but an effort was made to include also more conventional established methods, such as the Woschni [44] heat transfer coefficient estimation. The main parameters of interest that are extracted from the accumulated heat release curve are the crank angles of 10, 50 and 90% of accumulated heat released. These parameters are relatively robust with respect to calculation errors of peak accumulated heat release.

4.4 Real-Time System Heat Release Calculation

The real-time calculation of the accumulated net heat release was designed with emphasis on real time performance. In real-time applications computation time also needs to be considered. A simpler heat release method was adopted in the real-time system compared to the more complex method that was used in the post processing. In the simplified heat release calculation the inlet pressure was used for pressure trace pegging, the specific heat ratio, γ, was assumed constant the heat loss and crevice loss terms in Eq. (3.15) are omitted. Tunestål [45] derived a preintegrated form of Eq. (3.15) with omitted heat loss and crevice loss terms which has the numerical benefit of not having to calculate and include the pressure derivative. The simplified preintegrated version of Eq. (3.15), Q_s, is shown in Eq. (4.6). Avoiding the pressure derivative calculation can be beneficial because the noise of the pressure input tends to be amplified. The preintegrated heat release equation is used in the control system.

$$Q_s(\theta) = \frac{1}{\gamma - 1}\left[p(\theta)V(\theta) - p(\theta_0)V(\theta_0)\right] + \int_{\theta_0}^{\theta} p(\theta)\frac{dV}{d\theta}\,d\theta \tag{4.6}$$

The parameter of interest in real-time, while operating the engine, is the combustion timing, defined as crank angle of 50 % accumulated heat released. Using a simplified heat-release calculation for CA50 estimation gives almost the same accuracy as using a more complete heat-release calculation [61].

4.5 Calculations of Start of Injection and Ignition Delay

The binary fuel control signal was recorded in the control system simultaneously with the pressure trace and valve lift curves. The signal is connected to a fuel injector driver which in turn is connected to the fuel injector. The problem is that there is an unknown time delay from the rising edge of the fuel control signal from the FPGA to when fuel is actually injected. An attempt was made to estimate the time delay based on heat-release data. The assumption was that fuel is injected just before the rate of heat release curve becomes negative. This is the first indication of fuel vaporization. The injection time delay was pre-determined and was kept constant, 400 μs or approximately 2 CAD at 800 rpm. Values of injection delays in common rail system ranging from 0.30 to 0.75 ms have been reported [62]. The injection time delay was used to adjust the start of injection timing for the ignition delay calculations. The ignition delay is defined as the crank angle difference between 10% accumulated heat release and start of injection. If not stated otherwise, the mentioned start of injection timings in the thesis will refer to the settings that were set in the control system, without the time delay compensation. But the time delay compensation is included in the calculated ignition delays.

5 Results

5.1 HCCI Results

In the beginning of this work, the associated project was named Spark Assisted Compression Ignition (SACI). But after Manente et al. [33] [34] developed the gasoline PPC strategy during 2009-2010, the focus of this project changed from SACI to light-duty gasoline PPC. This section gives a summary of the results that were collected before changing the focus of the project to gasoline PPC.

5.1.1 Publications

The results in this section are based on two articles. The first article (Paper 1) is "Investigation and Comparison of Residual Gas Enhanced HCCI using Trapping (NVO HCCI) or Rebreathing of Residual Gases", which was presented by the author at the SAE International Powertrains, Fuels and Lubricants Meeting, 2011, in Kyoto, Japan. The experiments were planned, carried out and post-processed by the author. The article was written by the author. The work was supervised by Per Tunestål and Bengt Johansson who both provided valuable feedback. The second article (Paper 2) is "Investigating Mode Switch from SI to HCCI using Early Intake Valve Closing and Negative Valve Overlap", which was presented by Anders Widd at the same conference as the first article. Both the author and Anders Widd planned and performed the engine experiments and wrote the paper. Anders Widd was responsible for the controller design and evaluation. The author was responsible for the LabVIEW implementations and post-processing of the data. This work was supervised by Rolf Johansson, Per Tunestål and Bengt Johansson.

The objectives were to get qualitative comparisons of different HCCI and SI combustion strategies with the variable valve train and investigation of SI to HCCI mode switch at low engine load. One of the problems with HCCI is the limited attainable operating region. One example of attainable operating region of an engine running in HCCI mode with trapped residual gases using NVO is shown in Figure 11. This figure is from Håkan Persson's doctoral thesis [49]. Similar operating ranges were reported by Zhao et al. [63] and Allen et al. [64]. Basically, high engine load operation is limited by excessive pressure rise rates and low engine load operation is limited by insufficient temperature for auto ignition. At the low load limit in Figure

11, the engine was operated with spark assistance which enabled a small extension of the low load operating limit. But one drawback with spark assistance is that the typical SI combustion fluctuations are introduced [65]. In order to cover the entire operating range, one strategy is to run the engine in SI mode past the high and low load operating limits of HCCI. A suitable mode switch strategy should be used to ensure a smooth transition between SI and HCCI.

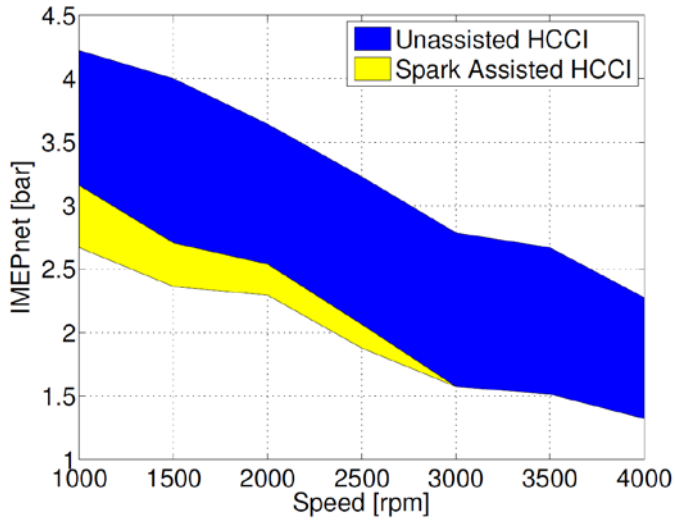

Figure 11. Operating range of NVO HCCI [49].

For the experiments presented in Paper 1 and Paper 2, the single cylinder engine was equipped with a spark plug in place of the glow plug. The fuel used was commercial Swedish gasoline (RON 95) and was port injected. The valve opening rate of the variable valve train system is fast compared to a conventional camshaft system at these relatively low engine speeds (1500 and 2000 rpm), and could not be controlled in real-time. In order to be able to operate the engine with maximum flexibility of the variable valve train system, the original Volvo D5 piston was replaced with a piston crown with 5 mm deep valve pockets. The purpose of the design was to have valve clearance at top dead center. No attempts were made to quantify the flow structures during compression. Also the compression ratio is high (16.5:1) in comparison to what is usually associated with a CAI engine (10-12:1). It is not expected that this combustion chamber geometry is optimal for any of the combustion processes in these investigations. This piston crown was used mainly for these two articles. For the rest of the work, the standard Volvo D5 piston was used.

An advantage with a fully flexible variable valve train system for the SI combustion is that the engine can be operated without the throttle. Engine load can then be controlled

with the valve timings or valve lift or both. This potentially results in higher efficiency compared to when a throttle is used because of the gain in gas-exchange efficiency at low and part-load operating conditions. A second advantage is that the intake and exhaust valves as control actuators are expected to be faster compared to a conventional throttle. This is an advantage for the mode switch strategy which potentially can be made faster and smoother.

5.1.2 Part Load Concepts (Paper 1)

The results that are presented in the first investigation were taken at steady state operating conditions. Any improvements in fuel consumption do not necessarily reflect numbers that would be obtained if it would be possible to drive a complete drive cycle. The load ranges used in this study are based on the attainable operating region for HCCI combustion. Conclusions drawn from the relative improvements of the SI cases are also drawn within this narrow interval and would perhaps have been somewhat different, if the engine load range had been wider.

The valve lift curves for the strategies included in the investigation can be found in Paper 1. The SI throttle case was operated with as close to conventional valve timings as possible and with a throttle to control load with stoichiometric combustion. The SI LIVC and EIVC cases were operated stoichiometric with late and early intake valve closing to control load. The HCCI cases, NVO, Reb1, Reb2 and heater, were operated with lean combustion. The NVO case was run with a negative valve overlap to trap hot residual gas. In the Reb1 case, the exhaust valves were kept open during and after the gas exchange top dead center to reinduct hot exhaust gas. In the Reb2 case, the exhaust valve was opened again later during the intake stroke, around intake valve closing timing, which occurred earlier during the intake stroke. In these cases, the combustion timing was automatically controlled using a PI controller with the exhaust valve timings as the main control actuator. In the HCCI heater case, the more conventional valve timings were used and combustion timing was manually controlled with the inlet temperature. The combustion-, thermodynamic-, gas-exchange- and net indicated efficiencies are shown in Figure 12.

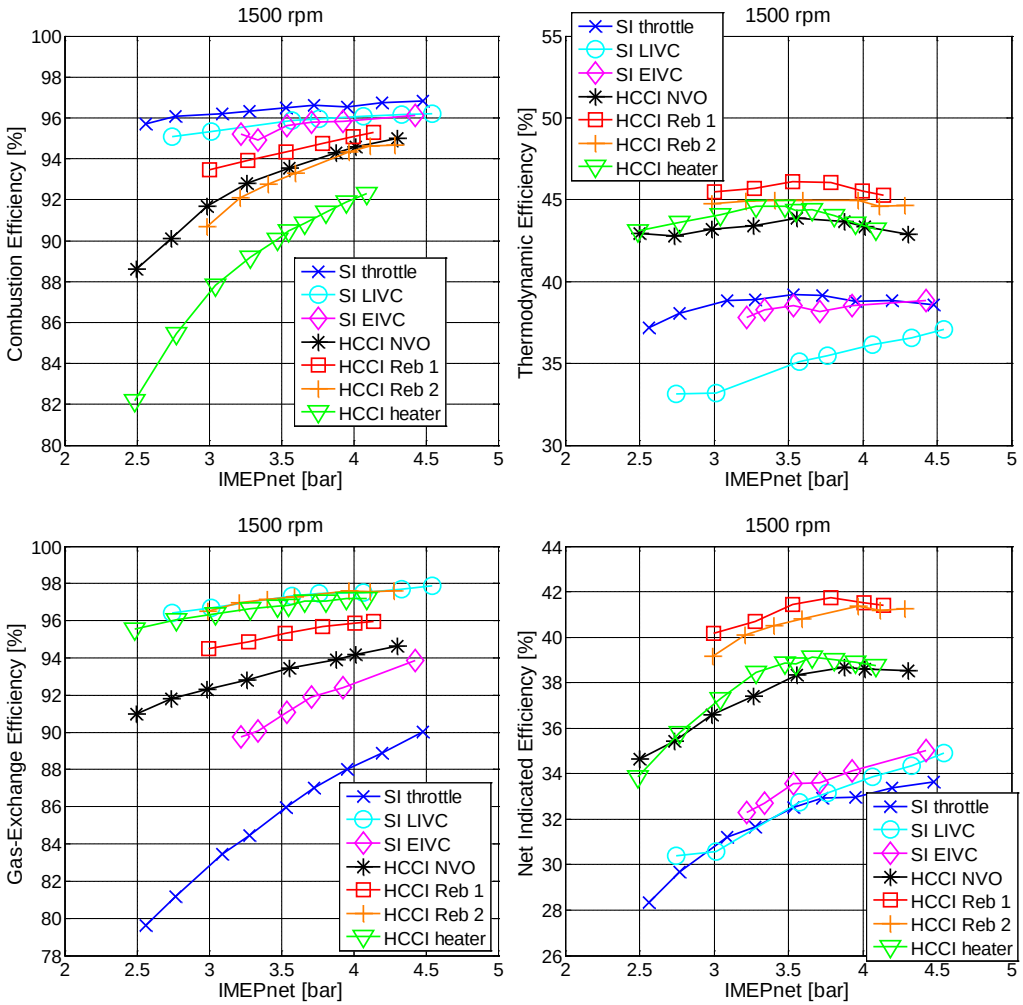

Figure 12. Combustion, thermodynamic, gas-exchange and net indicated efficiencies for the different SI and HCCI cases.

The HCCI cases have higher net indicated efficiency compared to the SI cases. This can mainly be attributed to the higher thermodynamic efficiency explained by the higher expansion ratio. The NVO HCCI case has low gas-exchange efficiency compared to the other HCCI cases. And the HCCI heater case has low combustion efficiency. The HCCI cases with the highest net indicated efficiency are the rebreathing cases. At engine speed 1500 rpm, there is only a small improvement with the EIVC SI strategy compared to the throttled case. Results from only one engine speed are shown here. More results and discussions are found in the article. In short

summary, for the higher engine speed case, 2000 rpm, the differences between the LIVC and EIVC SI cases net indicated efficiencies were found to be larger. The LIVC SI strategy resulted in higher net indicated efficiency compared to the throttled case and the EIVC SI case had lower efficiency compared to the throttled case for which the net indicated efficiency did not change with increasing engine speed. The relatively high compression ratio is expected to give higher thermodynamic efficiencies but lower combustion efficiencies due to increased fuel mass in crevices. An HCCI displacement study by Hyvönen et al. [66], also included a comparison between two SI cases, run on the same base engine with 0.5 dm^3 cylinder displacement, with high (18:1) and standard (9.5:1) compression ratio. The high compression ratio SI case had highest net indicated efficiency due to higher thermodynamic efficiency. The net indicated efficiency was 28-32 % at 2-4 bar BMEP for the high compression ratio case in the study, which is in agreement with the SI cases results from Paper 1.

The steep pressure rise rates on the high load limit of the HCCI cases are clearly seen in Figure 13. Steep pressure rise rates result in acoustic noise and can also potentially cause damage to the engine hardware. The pressure rise rate increase with engine load is relatively fast, especially if compared to the SI cases. At the high load limit of the residual gas enhanced HCCI cases, the residual gas fraction temperature is higher and a lower fraction of residual gas is needed to initiate auto-ignition at the desired combustion phasing. A lower fraction of trapped residual gas means less dilution and steeper pressure rise rates. Low engine load operation with the residual gas enhanced HCCI cases is limited by insufficient residual gas temperature. At the low load limit of the residual gas enhanced HCCI strategies the combustion efficiency, Figure 12, decreases with decreasing engine load which results in increasing HC and CO emissions. COV of IMEP, Figure 13, is a measure of combustion instability and increases with decreasing engine load with the residual gas enhanced HCCI cases. There is also a significant increase of COV of IMEP with the EIVC SI strategy. The reason is most likely that the combustion chamber is not optimal for this strategy. The combustion duration was the longest in comparison to the other cases which indicates low in-cylinder turbulence, hence slow flame propagation [67].

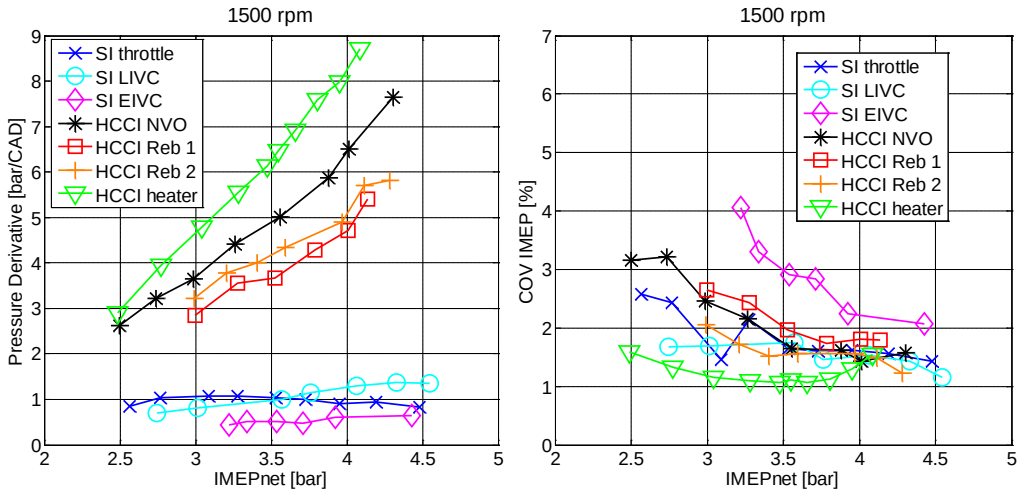

Figure 13. Pressure derivative (measure of pressure rise rate) and COV of IMEP for the different HCCI and SI cases.

5.1.3 Mode Switching from SI to HCCI (Paper 2)

Mode switching from SI to HCCI was investigated in Paper 2. Following the nomenclature of Paper 1, the investigation was made with a combustion mode transition from SI EIVC to HCCI NVO. The transition could be made within a few cycles before the engine load and combustion timing controllers were activated. The rate of heat released curves during a combustion mode transition is shown in Figure 14. Two different control strategies were compared. The first strategy was to use two PI controllers, one for engine load and one for combustion timing (CA50). The second strategy was a model based state feedback controller governing both NVO and fuel injection duration to control combustion timing and engine load. The details can be found in Paper 2.

Since the engine was operated port fuel injected, the first problem was to burn off the residual fuel in the inlet manifold. Since the efficiency with the HCCI combustion strategy is significantly higher, less fuel is needed for the same engine load after the transition. And the amount of fuel remaining in the inlet alone was sufficient to sustain combustion for one cycle. Also the residual gas temperature from SI combustion is significantly higher compared to HCCI operation at the same operating point. An initial mode switch sequence was investigated by testing different intake valve closing timings and NVO combinations in order to avoid misfiring and excessive pressure rise rates during the transition.

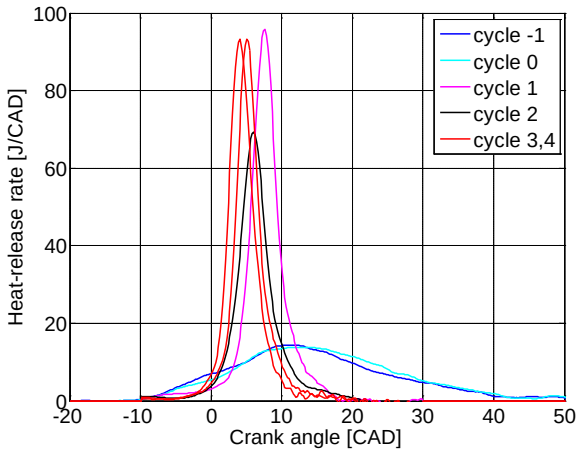

Figure 14. Rate of heat-released curves during a combustion mode transition from SI to HCCI combustion.

After the transition, the engine load and combustion timing controllers were activated as soon as possible. The engine load and combustion timing, starting in SI mode in open loop, and then switching to HCCI for the two different HCCI control strategies are shown in and Figure 15 and Figure 16. The model-based approach provided a smoother transient and could be activated one cycle earlier compared to the PI controllers. The PI controllers generated ringing in both outputs following the mode switch, particularly in engine load (IMEPnet). The main benefit of the model state feedback controller is that the interference between the control objectives can be avoided. Looking more closely at the NVO signal of the PI controller, Figure 15, compared to the state feedback controller in Figure 16, there is a longer oscillating behavior on the NVO signal which is a response to the effects originating from the load controller.

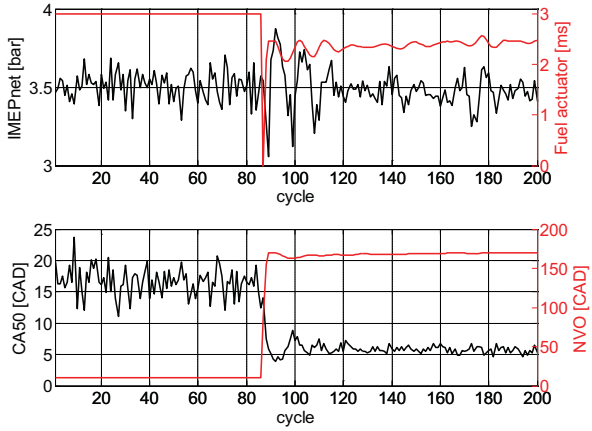

Figure 15. Engine load (IMEPnet) and combustion timing (CA50) starting in SI mode and then switching to HCCI with the PI controllers.

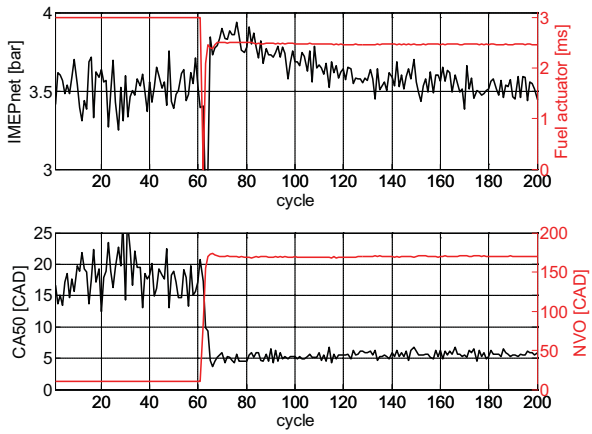

Figure 16. Engine load (IMEPnet) and combustion timing (CA50) starting in SI mode and then switching to HCCI with the model-based controller.

One limitation of this work was the port fuel injection. With a direct injection system, the intermediate step during the transition to burn off the residual fuel from the intake manifold would be avoided. And it is expected that the response time from fuel injection to engine load is faster since intake manifold wall wetting is avoided. The model would be improved further by monitoring the states from the SI combustion mode. This information could be used by an intermediate model-based controller that would determine proper valve and fuel injection parameters during the transition.

5.1.4 Summary

Combustion mode switch is a challenge and there is a strong motivation for extending the attainable HCCI region as much as possible. The limited operating region of HCCI and lack of immediate control actuator, which makes feedback control of the combustion difficult, are two contributing reasons to change focus from spark assisted HCCI to gasoline PPC. However, running a diesel engine on gasoline is not without challenges. The problem with low load engine operation remains and the rest of this work is devoted to extending the low load limit of gasoline PPC.

5.2 Low Load Gasoline PPC Results

5.2.1 Introduction

One way to characterize PPC combustion is that the fuel injection event is complete before start of combustion giving a positive mixing period [40]. Using gasoline, this is achieved through the inherent resistance to auto-ignition, the higher the RON the longer the ignition delay [43]. The attainable operating region plotted against fuel octane number (RON) is shown in Figure 17. The experiments were performed by Manente et al. [34] in a heavy duty engine. The minimum attainable load clearly increases as a function of fuel octane number (RON).

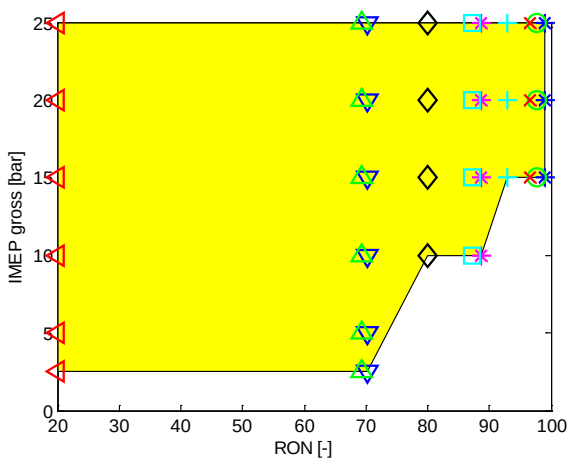

Figure 17. PPC operating region from heavy duty experiments [34].

One of the major problems with gasoline in comparison to diesel at low load operating conditions is the higher emission levels of HC and CO [31] [39]. A low load investigation with different gasoline fuels was performed by Solaka et al. [43] in a similar light duty single cylinder engine configuration as used in this thesis. One of the main differences was that a conventional camshaft was used and that the engine was heavily boosted. It was shown also by Solaka et al. that higher RON value fuels gave higher levels of CO and HC. The CO and HC yield predicted by homogeneous reactor simulations at constant temperature and pressure for various equivalence ratios and temperatures are shown in Figure 18. The figure is from a work by Kim et al. [68]. Since most of the experiments in the thesis were taken at low load operating conditions with a higher octane number gasoline, the region of interest for the results is dominantly on the lean side at relatively low temperatures. With a long ignition delay of the fuel, the local mixture strength approaches the global mixture strength, which is lean. In Figure 18, lean regions resulting in a high CO yield can be seen for temperatures between approximately 800 and 1400 K. The HC yield is also high at lean conditions with temperatures below approximately 1200 K. Below 800 K the fuel does not ignite which results in 100 % HC. At temperatures between approximately 1200 and 1400 K, on the lean side, HC oxidation is almost complete but there is still a high CO yield which is explained by the slow kinetics of CO oxidation compared to the HC oxidation [68].

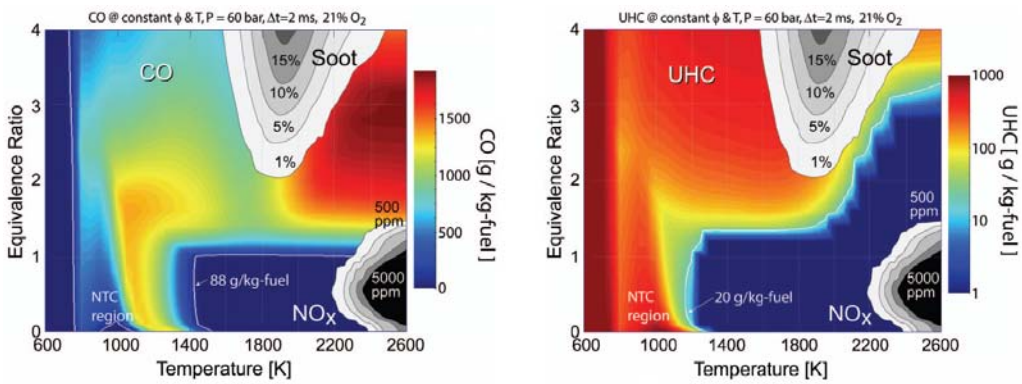

Figure 18. CO and HC yield at 2.0 ms as a function of equivalence ratio and temperature obtained from a homogeneous reactor simulation of an n-heptane-air mixture [68].

The main focus of the thesis is to improve the combustion efficiency and stability in the previously unattainable low load operating region with high octane number fuels. The experimental data was collected at a low engine speed, 800 rpm, with the goal to reach idle engine load operating conditions. The potential of a variable valve train system in combination with different fuel injection strategies and the effect of the

glow plug are investigated. The variable valve train system is used to trap hot residual gas which elevates the temperature of the subsequent cycle. Another effect of an increased residual gas fraction is increased levels of stratification of temperature and internal EGR distribution [69] which is also influenced by the valve strategy, for example NVO or rebreathing [12]. But the global air-fuel ratio becomes lower with an increased residual gas fraction which means that the available oxygen concentration is reduced. The temperature increase furthermore depends on the residual gas temperature which is relatively low at low load operating conditions. Also, the potential temperature increase at time of combustion, given by an elevated initial charge temperature, is reduced by an increased heat capacity of the cylinder charge. The effects of recycled burned gases on CAI combustion have been summarized in a work by Zhao et al. [70].

Using VVT to trap hot residual gases is usually associated with CAI combustion concepts and has been reported by several authors. The question is if similar strategies can be used on a diesel engine operated with gasoline in order to extend the attainable operating region. The context of this work is gasoline PPC which is operated with a higher compression ratio compared to more conventional CAI configurations. Most of the fuel is injected late during the compression stroke to achieve a less homogeneous mixture compared to HCCI. There is a glow plug instead of a spark plug. A more stratified mixture is essential for combustion to occur as demonstrated by Kalghatgi et al. [31] and Hildingsson et al. [39]. It was demonstrated that if the same amount of gasoline fuel was injected early at the same conditions with fully premixed, HCCI conditions, ignition might not occur at all. A similar result was reported in a work by Weall et al. [71] in a light duty multi cylinder engine. Auto-ignition of the European 95 RON gasoline did not occur with HCCI combustion using an advanced injection earlier than 50 CAD BTDC despite using 0.95 bar boost and 95 °C inlet temperature.

5.2.2 Fuel Comparisons (Paper 3)

The results in this section are taken from Paper 3, “Gasoline Partially Premixed Combustion in a Light Duty Engine at Low Load and Idle Operating Conditions”, which was presented by the author at the SAE World Congress, 2012, in Detroit. The experiments were planned, carried out and post-processed by the author. The article was written by the author. The work was supervised by Per Tunestål and Bengt Johansson who both provided valuable feedback. Complementary data analysis has been performed to provide additional insights and clarifications of the results.

This was the first low load gasoline PPC investigation. The objective of this investigation was to compare different fuels, with different RON values, at low engine load and engine speed operating conditions. The goal is to reach idle operating conditions. The selected fuels were diesel, 69 RON gasoline and 87 RON gasoline.

Some of the fuel properties are listed in Table 3. The gasoline fuels were supplied by Chevron Corporation and were taken from different streams of an oil refinery.

Table 3. Fuel properties.

Fuel	RON	MON	LHV [MJ/kg]	A/F stoich
Diesel MK1	n.a.	20	43.15	14.9
Gasoline 69 RON	69	66	43.80	14.68
Gasoline 87 RON	87	81	43.50	14.60

Two separate investigations, with different experimental conditions, have been performed. The first investigation is with varying engine load and the second investigation is with varying NVO. The EGR level was set differently in the two investigations. In the varying engine load investigation, EGR was set for each engine load to suppress NOx emissions to 20 ppm which corresponds to a NOx emission index of approximately 1 g/kg fuel. This limit is a compromise between NOx suppression and combustion efficiency. The EGR settings for the varying engine load cases are shown in the left diagram in Figure 19. A single fuel injection strategy was used for all cases. The common rail pressure was constant at 500 bar for all measurements. For the diesel and 69 RON gasoline cases combustion timing, CA50, was kept constant around 5 CAD. For the 87 RON gasoline case this was not achievable given the long ignition delay. Instead the fuel injection timing was kept constant at -22 CAD. It could not be set earlier because of a significant increase in HC emissions from fuel trapped in squish and crevice volumes. As a result, CA50 was retarded from 6 CAD ATDC at 1.8 bar IMEPn to 8 CAD ATDC at 2.8 bar IMEPn.

In the varying NVO investigation, the EGR level was determined at the minimum NVO operating conditions (60 CAD) for the diesel and 69 RON gasoline cases. The EGR level was then decreased as NVO increased to maintain a constant lambda. In the case of the 87 RON gasoline, EGR was set to match the settings of the diesel and gasoline cases. The EGR settings for the varying NVO cases are shown in the right diagram in Figure 19. The fuel injection strategies for the different cases were the same as with the varying load cases. The engine load was set to 2 bar IMEPg at the 60 CAD NVO case and the injected fuel amount was then kept constant.

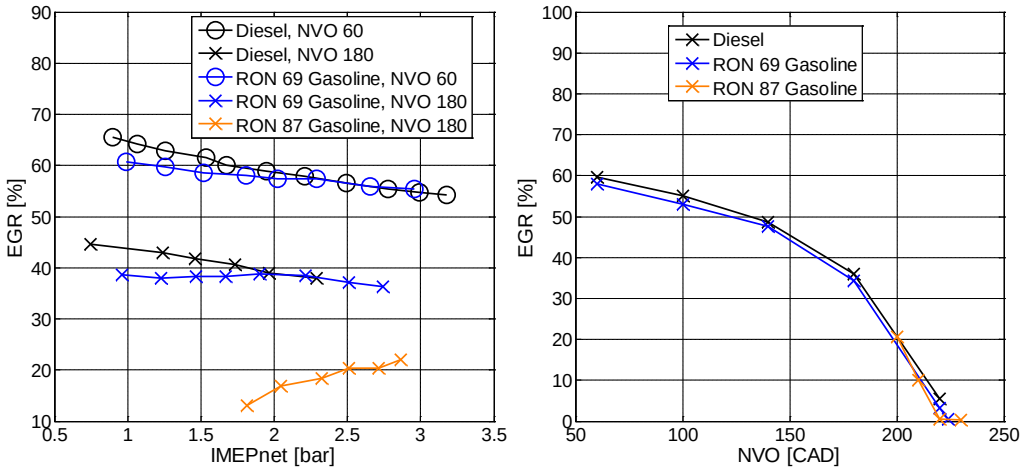

Figure 19. settings used for the different fuels with varying engine load (left) and NVO (right).

After the article was published, it was discovered that CO instrument readings above a certain value were unreliable. Further analysis showed that the gas-analyzer measurement computer kept sending out values above the actual saturation limit. The real saturation limit is 10000 ppm but the system would report values up to 20000 ppm, which the author at the time mistakenly interpreted as the saturation limit of the instrument. In the paper, this will affect the calculations of the combustion efficiency, thermodynamic efficiency and lambda calculations of the gasoline results. Both combustion efficiency and lambda calculations of the gasoline results are affected because these are based on the exhaust gas composition. The thermodynamic efficiency is affected because it is calculated from the gross indicated efficiency and the combustion efficiency using the expressions: $\eta_{th} = \eta_{i,g}/\eta_c$. After this discovery was made, an air-flow meter was installed and used together with the fuel-flow calculations to calculate lambda. Additionally, CO readings above 10000 ppm were corrected in the post-processing to 10000 ppm. Operating points with saturated CO readings are clearly indicated in Papers 4-6. The combustion efficiency and lambda calculations that are presented in this section have been recalculated using the correct saturation limit of the CO instrument.

The lambda values are shown in Figure 20. Both the original values, from Paper 3, and the recalculated values using the correct saturation limit of the CO measurement instrument, are shown. In the diesel cases, the CO instrument was not saturated and did not have to be recalculated. Note that the recalculated lambda values do not show the actual correct lambda values. They have only been modified to show how the calculations would have looked if the correct saturation limit of the CO instrument would have been applied. In the varying fuel cases, EGR, and not lambda, was the

main control parameter used to suppress NOx. In the varying NVO cases, the goal was to keep a constant lambda with varying NVO by decreasing EGR with NVO. After updating the lambda calculations, it now appears as if there is a small decrease in lambda with NVO. But again, it should be stressed that the correct lambda is unknown. The same EGR settings were used for all fuels at the different NVO settings which implies that the assumption that lambda was kept constant is not unreasonable.

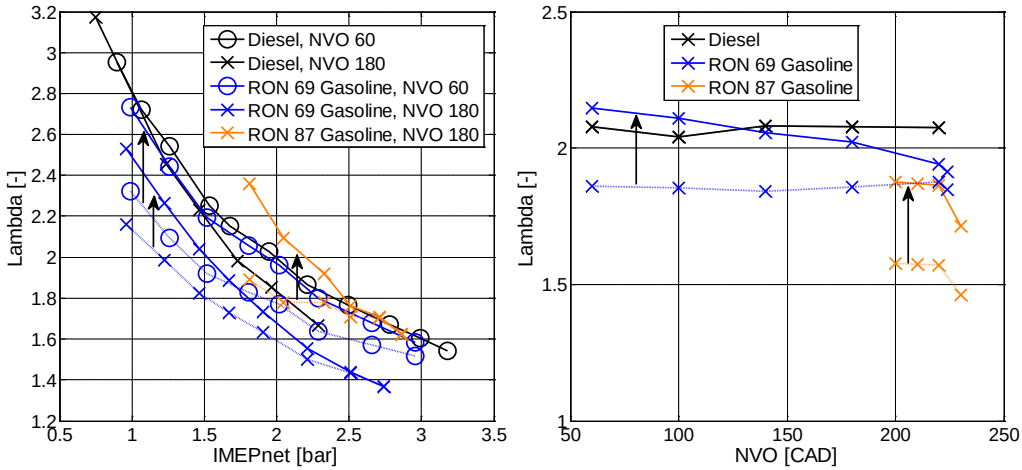

Figure 20. Recalculated (solid) and original (dashed) lambda values with varying engine load (left) and NVO (right).

The ignition delay with varying engine load and NVO for the different fuels is shown in Figure 21. The ignition delay increases with fuel RON. The effect of NVO on ignition delay in these cases was found to be relatively small. There is a small decrease of the ignition delay as EGR is gradually replaced with trapped hot residual gases which can be explained by an increased temperature.

The ignition delay becomes longer with increasing engine load which was an unexpected result. The effect is more clearly seen with the gasoline fuels. In the 87 RON fuel case, fuel injection timing was constant and the longer ignition delay can be explained by that the EGR fraction was increased. EGR was adjusted for each measurement point, for all fuels and NVO settings, to suppress NOx to 20 ppm. A higher EGR fraction reduces the available oxygen concentration and increases the heat capacity which increases the ignition delay [72]. For the diesel and 69 RON gasoline cases there is a small decrease of EGR to suppress NOx with increasing load which was unexpected. The collected data alone does not provide sufficient information to explain these trends. Instead, two different suggestions to explain these trends are given.

As load is increased the ignition delay becomes shorter due to an increased charge temperature at injection timing from increased residual gas and wall temperatures [46]. But there are also competing factors that could contribute to a longer ignition delay. First, CA50 was constant and the fuel injection timing was advanced (not retarded as stated in Paper 3) by 2.6 CAD for the 69 RON gasoline cases and 1.6 CAD for the NVO 60 CAD diesel case, from 1 bar IMEPn to 3 bar IMEPn. The 180 CAD NVO diesel case was only measured up to 2.3 bar IMEPn but the trend was the same as the NVO 60 CAD case. The in-cylinder pressure and temperature is lower when fuel is injected earlier which results in a longer ignition delay [43]. But the difference in injection timing is small in these cases. The second contributing factor could be a decreased temperature from increased vaporization of a larger amount of injected fuel. This explanation was suggested in paper 3 as the more reasonable explanation.

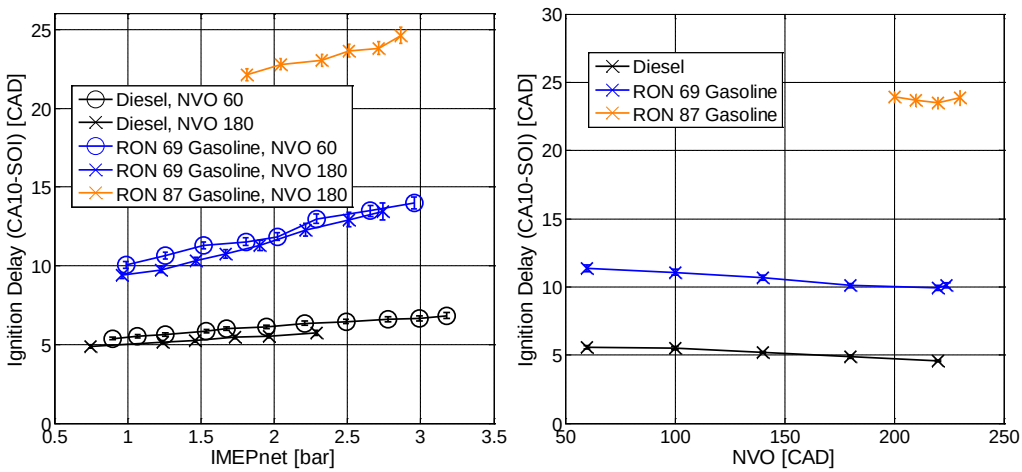

Figure 21. Ignition delay at varying engine load (left) and NVO (right) for the different fuels.

The NOx emissions are shown in Figure 22. In the varying load cases (left diagram), NOx was suppressed using EGR. In the varying NVO cases (right diagram), there is an increase in NOx when EGR is replaced with hot internal EGR due to increased temperature. The NOx sensitivity to temperature is well established and understood from the Zeldovich mechanism [46]. The soot emissions, Figure 23, are high for diesel compared to gasoline which is explained by the short ignition delay. A short ignition delay gives less time for fuel and air to mix prior to combustion which results in more fuel rich zones. There is also a significant difference between the NVO 60 CAD and NVO 180 CAD cases for the diesel fuel. This can be explained by the lower lambda for the 180 CAD NVO case which indicates that the amount of available oxygen is lower. Since the trapped hot residual gas fraction is higher, the total EGR fraction would have to be increased in order to suppress NOx emissions. It should again be

noted that the EGR level was set differently for the varying NVO and varying load investigations. This is the reason why the trends in soot emissions are different between the two investigations.

When the article was written, the reason for the soot and NOx emissions behavior of the 87 RON gasoline case with varying NVO was not completely understood. The recalculation of the lambda values showed that the lambda calculations were unreliable. The recalculated lambda values of the 87 RON gasoline became higher as a result of the new imposed saturation limit. But in reality, the lambda values are probably much lower, and possibly also lower than the previously calculated values. The low NOx values and higher soot emissions of the 87 RON gasoline case with varying NVO are then explained by a lower temperature and global air-fuel ratio because of the combination of EGR and a high residual gas fraction.

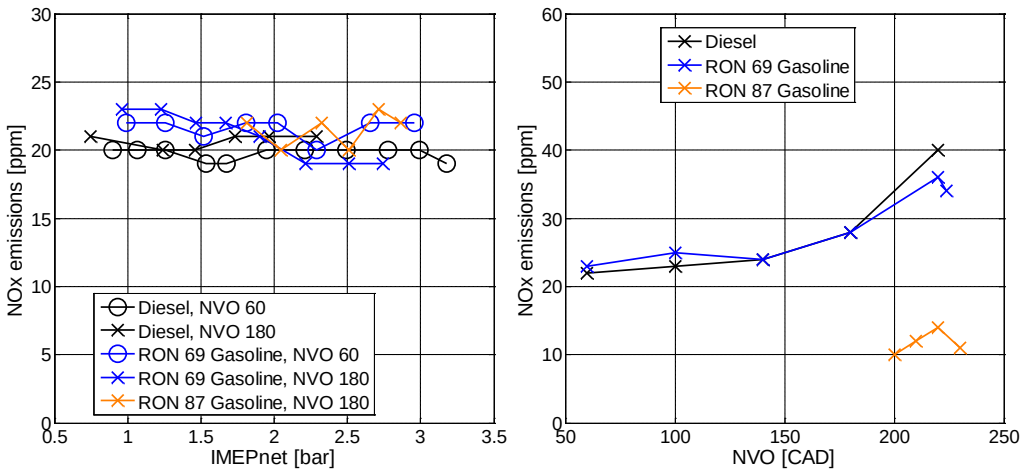

Figure 22. NOx emissions at varying engine load (left) and NVO (right) for the different fuels.

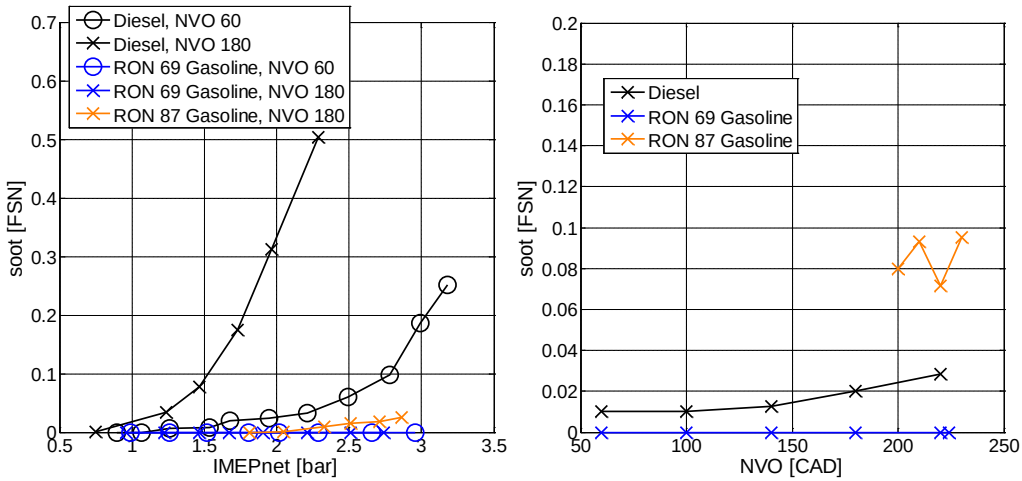

Figure 23. Soot emissions at varying engine load (left) and NVO (right) for the different fuels.

The standard deviation of IMEPn, Figure 24, is used as a measure of combustion instability. It is seen that the standard deviation of IMEPn is higher with gasoline compared to diesel at low load. Since CA50 was the same for diesel and the 69 RON gasoline cases, one possible explanation is the difference in ignition delay. A longer premixing period before combustion occurs increases the sensitivity to the local in-cylinder conditions and variations.

The change of standard deviation in IMEPn with NVO is minor for the diesel and 69 RON gasoline cases. A more significant effect is seen with the 87 RON gasoline case. In this case, fuel injection timing and not CA50 is constant. The standard deviation in IMEPn follows the trend in CA50 in this case, as seen in Figure 25.

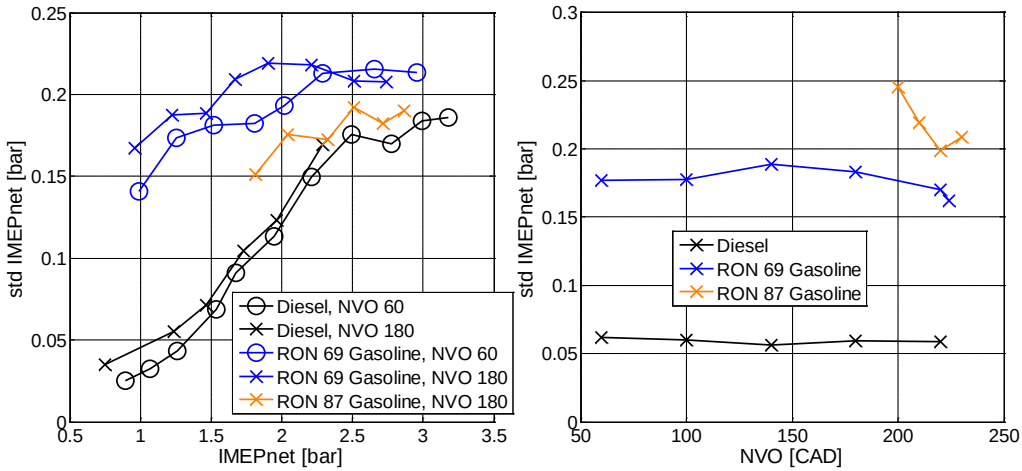

Figure 24. Standard deviation of IMEPn at varying engine load (left) and NVO (right) for the different fuels.

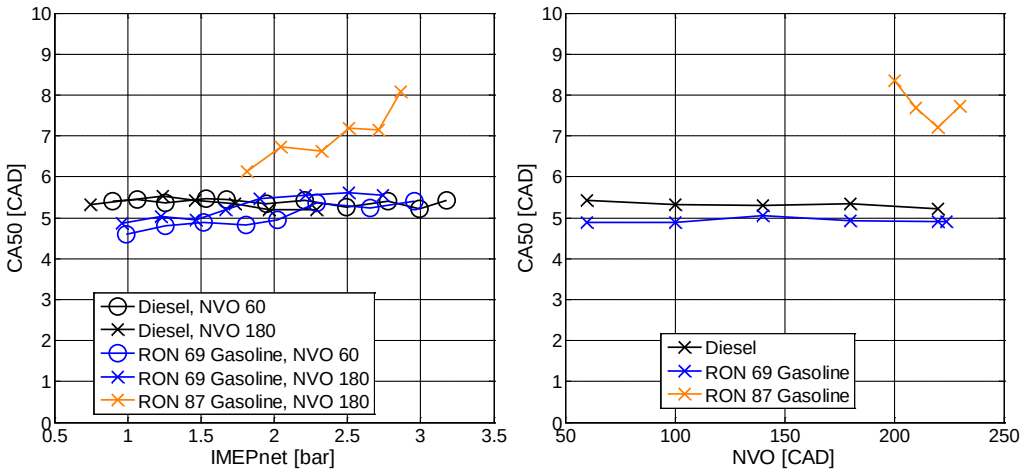

Figure 25. CA50 at varying engine load (left) and NVO (right) for the different fuels.

The combustion efficiency is shown in Figure 26. The exact magnitudes of the combustion efficiency of the CO-saturated gasoline cases remain unknown. The variations that are still seen on the combustion efficiency on the recalculated combustion efficiencies are from the HC emissions. It is still clearly seen that the combustion efficiency is significantly lower with gasoline compared to diesel.

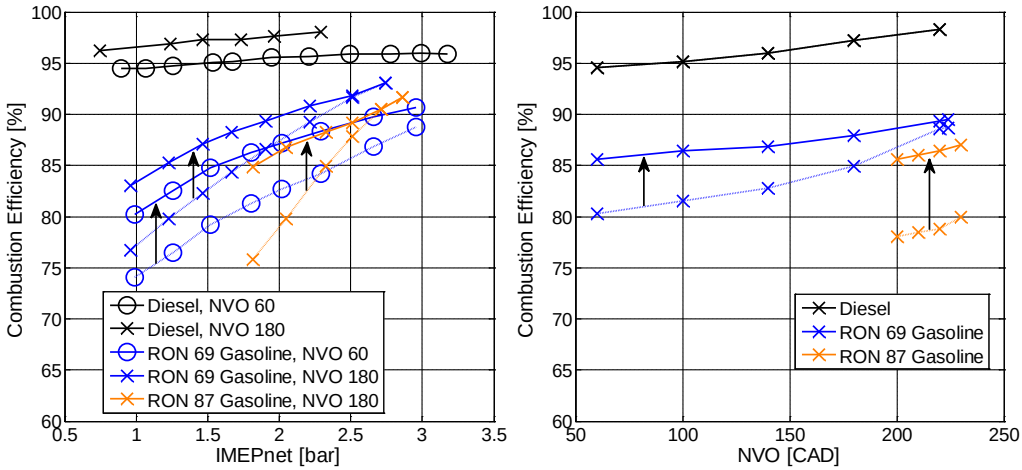

Figure 26. Combustion efficiency at varying engine load (left) and NVO (right).

The thermodynamic efficiency, Figure 27, reflects the efficiency to convert the released heat to indicated work (not mechanical work as was stated in Paper 3). The fraction of heat which is not converted to indicated work is lost either as heat losses through cylinder walls or through the exhaust. It is shown here to give the updated thermodynamic efficiency calculation as a complement to the other selected results.

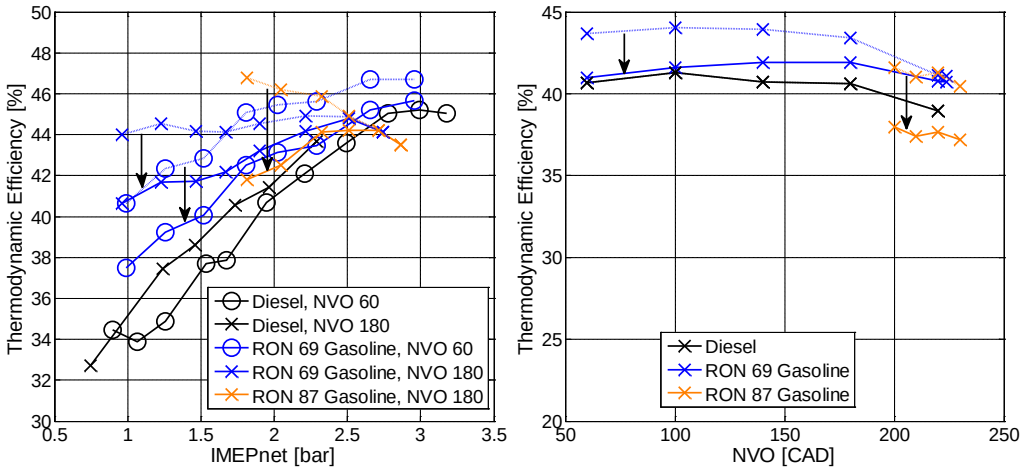

Figure 27. Thermodynamic efficiency at varying engine load (left) and NVO (right).

The main result from this first low load gasoline PPC investigation was that the 69 RON gasoline fuel could be run down to 1 bar IMEPn engine load without trapped hot residual gases. The minimum attainable load with the 87 RON gasoline fuel was approximately 1.8 bar IMEPn (or 2 bar IMEPg) with a significant fraction of trapped hot residual gases. The effect of NVO on combustion stability (standard deviation in IMEPn) was found to be the most positive with the 87 RON gasoline fuel because CA50 was advanced in response to the decreasing EGR and increasing NVO.

After this initial investigation, it was decided to focus on the 87 RON gasoline fuel and try to extend the low load limit as far as possible using the variable valve train system, more advanced injection strategies and the glow plug. EGR will not be used because NOx emissions are not the main problem at low load operating conditions. The main problem is the ignitability, combustion stability and combustion efficiency.

5.2.3 Hot Residual Gas (Papers 4 and 6)

The results in this section are taken from Papers 4 and 6. Paper 4, “The Usefulness of Negative Valve Overlap for Gasoline Partially Premixed Combustion, PPC”, which was presented by the author at the SAE 2012 International Powertrains, Fuels & Lubricants Meeting, 2012, in Malmö. The experiments were planned, carried out and post-processed by the author. The article was written by the author. Martin Tuner and Augusto Mello did the AVL Boost engine simulations. The work was supervised by Per Tunestål and Bengt Johansson who both provided valuable feedback. Paper 6, “Comparison of Negative Valve Overlap (NVO) and Rebreathing Valve Strategies on a Gasoline PPC Engine at Low Load and Idle Operating Conditions”, has been submitted and approved for publication at the SAE World Congress, 2013, in Detroit. The experiments were planned, carried out and post-processed by the author. The article was written by the author. Per Tunestål and Bengt Johansson supervised the work. Complementary data analysis has been performed to provide additional insights and clarifications of the results.

The objective was to investigate potential benefits using hot residual gas and the glow plug with the 87 RON gasoline fuel in more detail. Two different valve strategies have been evaluated and compared. A NVO valve strategy has been used more extensively; a rebreathing valve strategy has been used for comparison. The question is if similar improvements can be seen with the rebreathing valve strategy compared to the NVO valve strategy. The motivation is that a rebreathing valve strategy potentially has higher efficiency compared to NVO since it avoids recompression of the trapped residual gases. The recompression of the residual gas results in lower gas-exchange efficiency. This can be understood from the definition of the gas-exchange efficiency, given in (3.10). The recompression of the residual gas results in a lower IMEPn due to

heat losses which in turn lowers the gas-exchange efficiency. The potential drawback with rebreathing is that the elevated temperature at intake valve closing timing could be lower with rebreathing compared to NVO due to additional cooling in the exhaust manifold of the residual gas [12]. However, recompression of the residual gas during NVO results in heat losses which reduce the in-cylinder temperature also for the NVO case.

If not stated otherwise, the glow plug was continuously on in these investigations. The motivation is that this is an investigation at low engine loads with the goal to extend the low load limit as much as possible with the available tools. Had the glow plug not been used, the remaining question would have been about the additional benefits from the glow plug. These are now included in the results. The effects from the glow plug in relation to the trapped residual gases on combustion stability and efficiency are shown and discussed in the Glow Plug section.

The combustion timing, CA50, is one of the most important parameters regarding engine performance in terms of efficiency, stability and emissions. The problem with the long ignition delay of the 87 RON gasoline fuel was that CA50 could not be set sufficiently early using the fuel injection timing as control actuator alone. Therefore, the ignition delay is considered as one of the more important parameters. A limit was set on the earliest possible main fuel injection timing in order to avoid excessive HC emissions from trapped fuel in squish and crevice volumes. The consequence was that the fuel injection timing was kept constant, with few exceptions, at 22 CAD BTDC. The exceptions were at the highest measured engine load operating conditions, at NVO 120-200 CAD and rebreathing 50-70 CAD, and with the glow plug on. In these cases the fuel injection was set later to 18-15 CAD BTDC in order to have combustion timing after TDC. The common rail pressure was constant at 500 bar for all measurements.

The valve lift curves of the NVO and rebreathing valve strategies are shown in Figure 28. With the rebreathing valve strategy, residual gas is reinducted during the intake stroke. The exhaust valves are reopened at 30 CAD ATDC. A minimum NVO of 60 CAD had to be used in order to avoid hitting the piston. This had to be used also for the rebreathing strategy. The consequence is that the 0 CAD rebreathing setting is the same as the 60 CAD NVO setting. With the control system setup that was used, there was also a limit on the shortest possible valve open duration to ensure stable operation of the valves. The lowest rebreathing setting that could be used was 50 CAD. The maximum NVO setting that was used is 220 CAD and the maximum rebreathing that was used is 110 CAD. By comparing the measured air flows it was observed that the rebreathing setting of 110 CAD does not decrease the amount of inducted air to the same extent as NVO 220 CAD. If it is assumed that the measured air flow is directly connected to the residual gas fraction, the residual gas fraction that is obtained with 110 CAD rebreathing corresponds to a setting of approximately 205 CAD NVO.

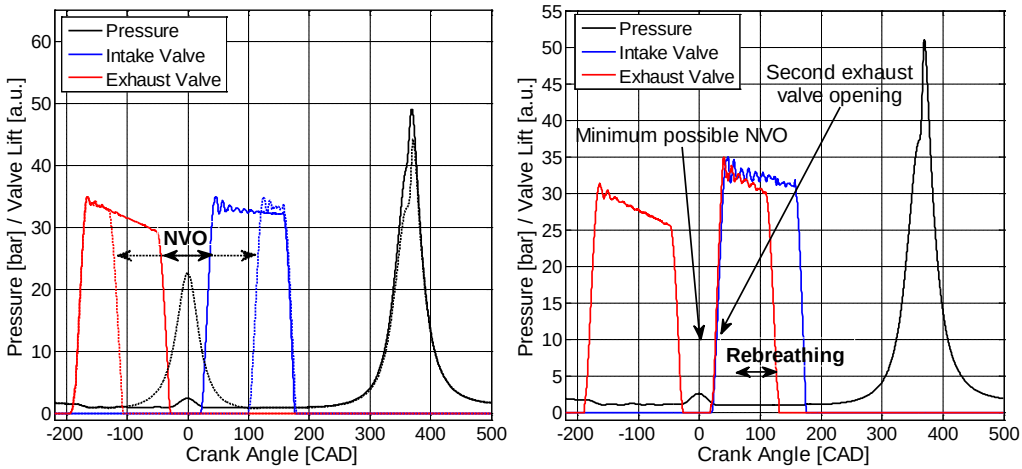

Figure 28. NVO (left) and rebreathing (right) valve strategies valve lift curves.

The results will be presented in contour plots against engine load and variable valve timing settings. Contour plots were preferred because it easy to see the overall trends and variations with the two investigated parameters. The disadvantage with contour plots is that it is more difficult to extract the exact numbers at specific operating points. The contour plots were generated in Matlab with the commands *contourf* and *TriScatteredInterp* using linear interpolation. The magenta colored circles show the measurement points.

A 1-D engine simulation tool, AVL Boost, was used to determine the residual gas fractions and in-cylinder temperatures with the NVO valve strategy at different NVO and engine load operating conditions. The AVL Boost model implementation details are given in Paper 4. The simulated residual gas mass fraction results and in-cylinder temperature at intake valve closing timing are shown in Figure 29. It is seen that the residual gas mass fraction is increased from approximately 10 to 50 % and the IVC temperature is increased by approximately 50 K from the lowest to the highest NVO settings.

The ignition delay, defined as the difference in crank angle between the crank angle of 10% accumulated heat release and the start of injection is shown in Figure 30. It is shown for both the NVO (left diagram) and the rebreathing (right diagram) valve strategies. The observation from the comparison between the valve strategies is that similar trends are seen regardless of valve strategy. Three operating regions are identified as follows. At relatively high engine loads, from approximately 3 bar IMEPg, there is an intermediate setting of NVO, 120 to 200 CAD, and 50 to 70 CAD rebreathing, where the ignition delay is the shortest. The ignition delay is significantly

shorter in this region compared to the lower engine load operating conditions. The ignition delay is relatively independent of the increased residual gas fraction at engine loads below 3 bar IMEPg and moderate NVO/rebreathing. The ignition delay is long with both the highest setting of NVO and rebreathing.

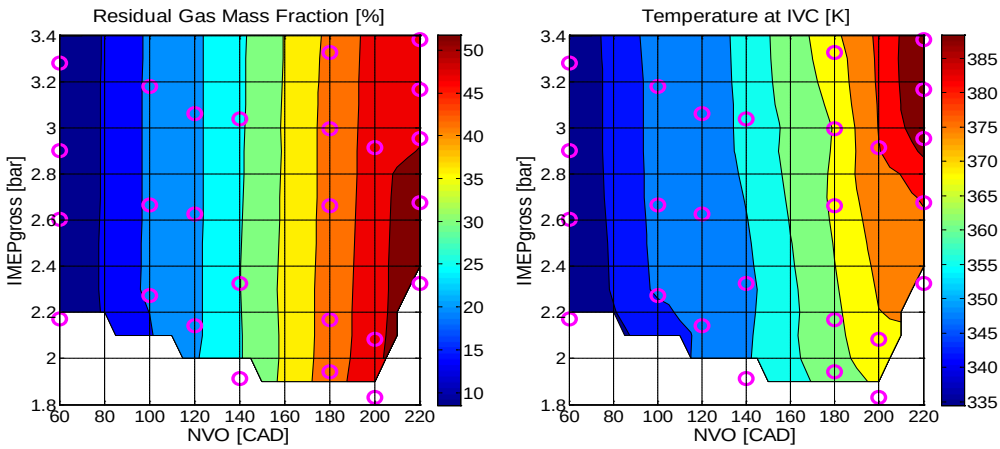

Figure 29. AVL Boost model results of the residual gas mass fraction and in-cylinder temperature at intake valve closing timing.

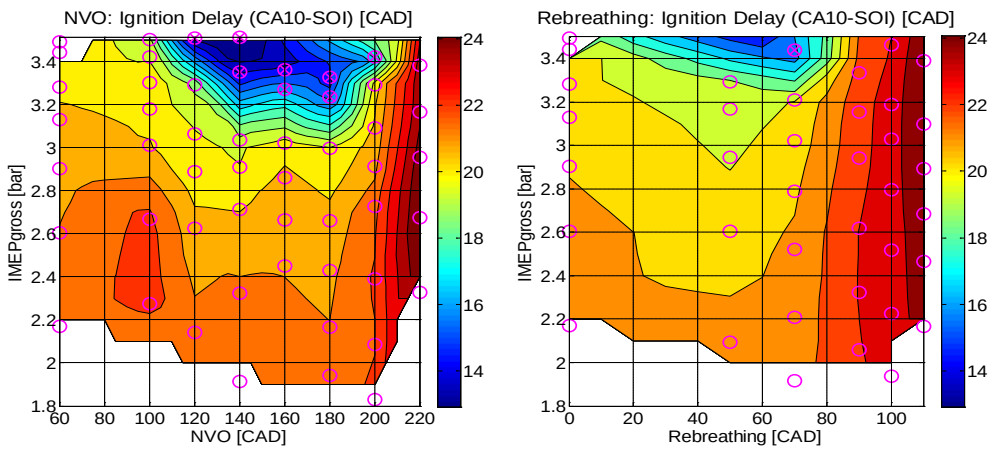

Figure 30. Ignition delay with the NVO (left) and rebreathing valve strategies (right).

The significant change of the ignition delay at the high engine load operating conditions can be explained by the difference in fuel injection timings and the glow plug. As mentioned before, the fuel injection timings were adjusted at the highest measured engine load operating conditions, at NVO 120-200 CAD, from 22 CAD BTDC to 18-15 CAD BTDC. These operating conditions are indicated in Figure 30 with enclosed 'x' in the magenta colored circles. The reason was to have combustion timing no earlier than 2 CAD ATDC. This had to be done only for the cases when the glow plug was turned on. When the glow plug was turned off, Figure 31, combustion timing, CA50, was close to 2 CAD ATDC at the corresponding high load operating conditions, but it was never earlier than 2 CAD ATDC.

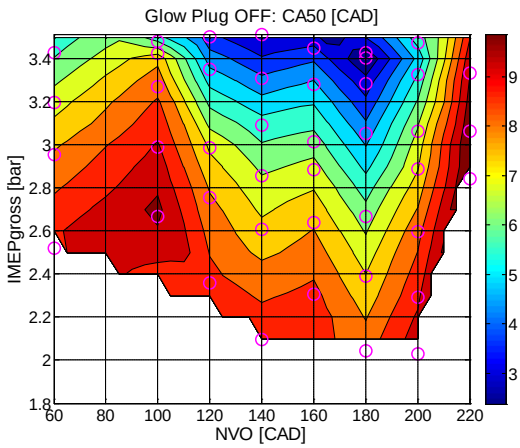

Figure 31. Combustion timing, CA50, with the NVO valve strategy and the glow plug turned off.

The ignition delay, using the NVO valve strategy, and with the glow plug turned off, is shown in the left diagram of Figure 32. The right diagram shows the calculated difference of the ignition delay between the cases with the glow plug turned off and the cases with the glow plug turned on. The same overall trend as in the left diagram in Figure 30 is also seen when the glow plug is turned off. The difference at low load operating conditions is relatively small, 1-2 CAD. But above 3 bar IMEPg, there is a region with a large difference between when the ignition delay is turned off compared to when it is turned on. This can now be explained by the fuel injection timing retard when the glow plug was on. The effect of fuel-injection timing on combustion phasing is complicated when the ignition delay is long. The direct connection between the fuel injection timing and CA50 is weaker and the combustion is closer to HCCI combustion than PPC. Figure 33 shows an operating point without the glow plug, at 3 bar IMEPg and 180 CAD NVO, where the fuel-injection timing has to be retarded

beyond -18 CAD ATDC before the combustion phasing becomes retarded. It would have been interesting to also include the fuel injection timing as a variable in the experiments but the number of variables in the experiments had to be reduced to save time and it was decided to keep the fuel injection timing constant. Additional analysis of the ignition delay is presented in a separate Ignition Delay Model section.

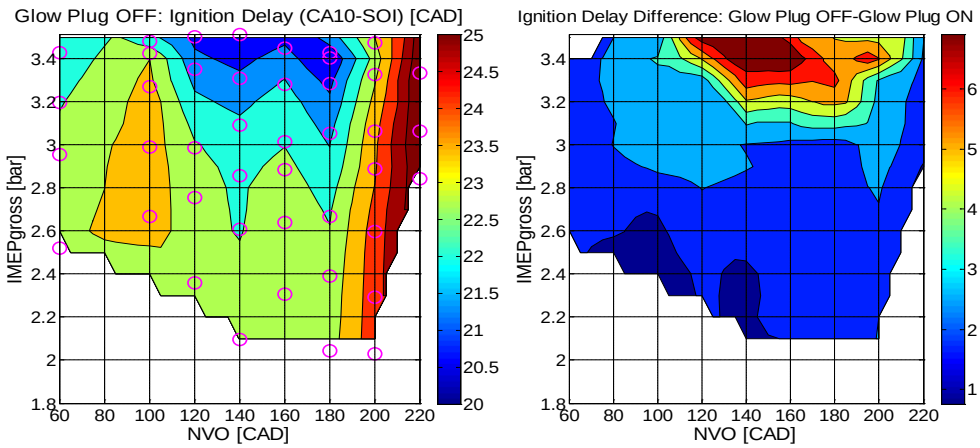

Figure 32. Ignition delay with the NVO valve strategy and the glow plug turned off (left) and the ignition delay difference between cases with the glow plug off and the cases with the glow plug turned on (right).

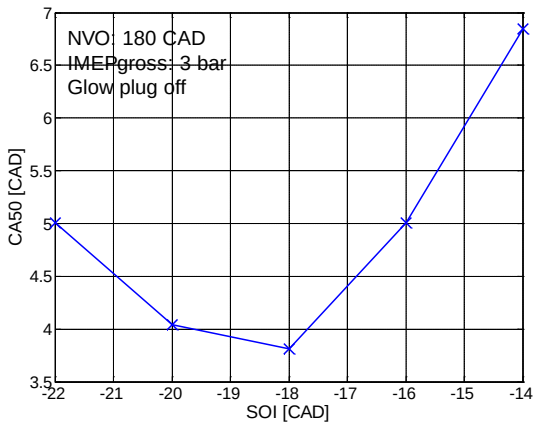

Figure 33. Effect of fuel injection timing on CA50.

The combustion instability, measured as the standard deviation in IMEPn for both the NVO and rebreathing valve strategies are shown in Figure 34. Unburned hydrocarbon emissions and CO emissions are shown in Figure 35 and Figure 36. The saturated CO emissions values, 10000 ppm, have been colored grey in the figures. The optimal NVO and rebreathing settings, with respect to combustion stability, HC and CO emissions, were found to be around 180 and 70 CAD respectively. For a given engine load, this is where the combustion timing, Figure 37, is the most advanced. Since the fuel injection timing is constant, a longer ignition delay results in more retarded combustion timing. But the resulting CA50 is not explained by the ignition delay alone. It is the ignition delays in combination with the combustion duration, Figure 38, that result in the combustion timing that are seen in Figure 37.

The effects of hot residual gases on CAI combustion was summarized in a work by Zhao et al. [70]. The effects of increasing trapped residual gas can explain the observed trends on the combustion duration. The combustion duration becomes shorter with increased residual gas fraction because of increased temperature. The combustion duration is extended because of increased heat capacity and reduced oxygen concentration at very high residual gas fraction levels. With moderate residual fractions the temperature effect is dominant and the combustion duration is decreased. At the highest settings of NVO and rebreathing the heat capacity and reduced oxygen effects become more apparent and the combustion duration becomes longer. Shortest combustion durations are seen around NVO 180 CAD and rebreathing 70 CAD.

If the standard deviation of IMEPn is limted to 0.2 bar, the extension of the low load limit using hot residual gas can be quantified. With the lowest settings of NVO and rebreathing, the low load limit would be reached already at approximately 3.2-3.3 bar IMEPg. With the optimum settings of NVO and rebreathing, the low load limit can be extended down to approximately 2.2 bar IMEPg. The temperature increase, according to the AVL Boost model, with the NVO strategy from 60 to 180 CAD NVO is approximately 30-40 K.

The HC and CO emissions correlate with the combustion timing. At later combustion timings there is less time to fully oxidize the fuel. Also, the peak combustion temperature is lower. Both time and temperature is needed to fully oxidize the fuel and intermediate species, for example CO. High amounts of CO are produced because of insufficient temperature and time to be fully converted to CO2. This is in agreement with the opening discussions on sources of HC and CO emissions in the introduction to the PPC Results. The CO measurement instrument was saturated from approximately 3.2 bar IMEPg with the lowest NVO and rebreathing settings and from approximately 2.5-2.6 bar IMEPg with higher NVO and rebreathing settings.

Note that the unit of the unburned hydrocarbon emissions in Figure 35 is ppm, which was calculated from the gas-analyzer by dividing the measured quantity, with unit $ppmC_1$, by the number of carbon atoms in the fuel molecules, 7.2. The measured

quantities from the gas-analyzer are easily obtained by multiplying the numbers of the color bar by 7.2. This can also be used for the unburned hydrocarbon emissions in Paper 5 and Paper 6 to obtain the corresponding ppmC_1 quantities.

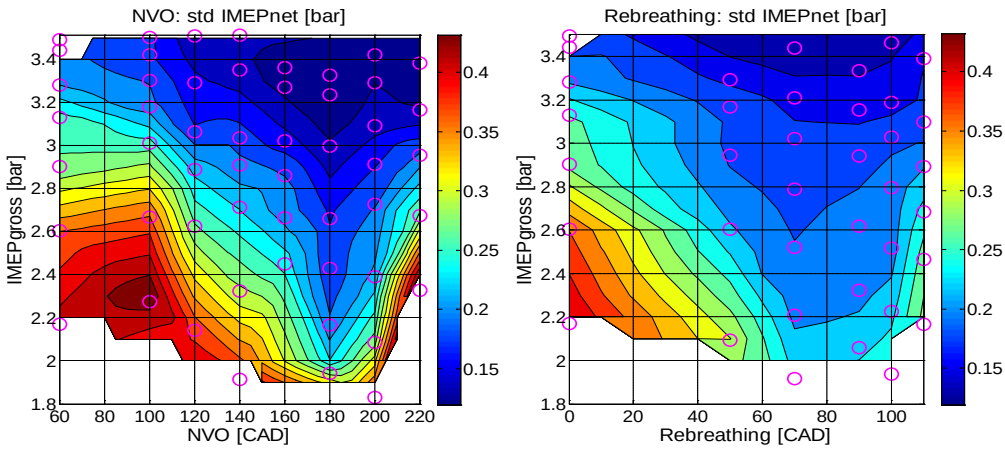

Figure 34. Combustion instability, measured as standard deviation of IMEPn, with the NVO (left) and rebreathing (right) valve strategies.

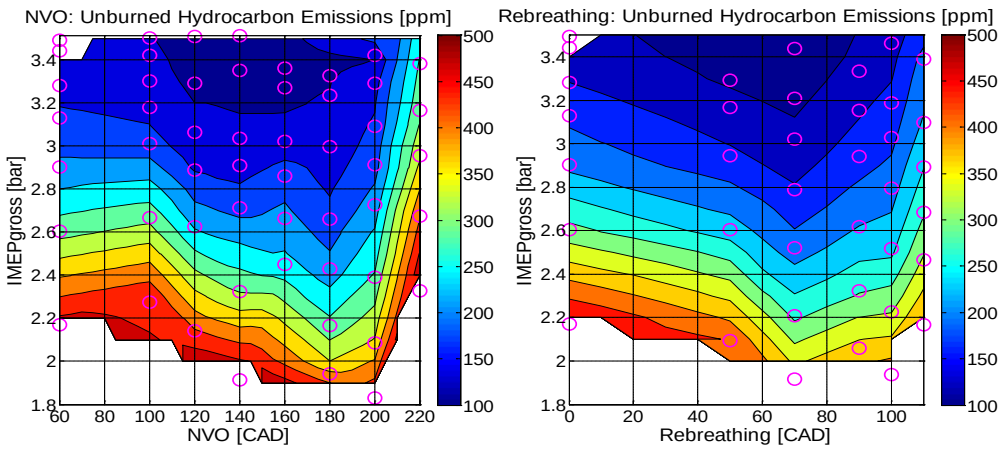

Figure 35. Unburned hydrocarbon emissions with the NVO (left) and rebreathing (right) valve strategies. If multiplied by number of carbon atoms in the fuel molecules, 7.2, the corresponding quantities with the unit ppmC_1 are obtained.

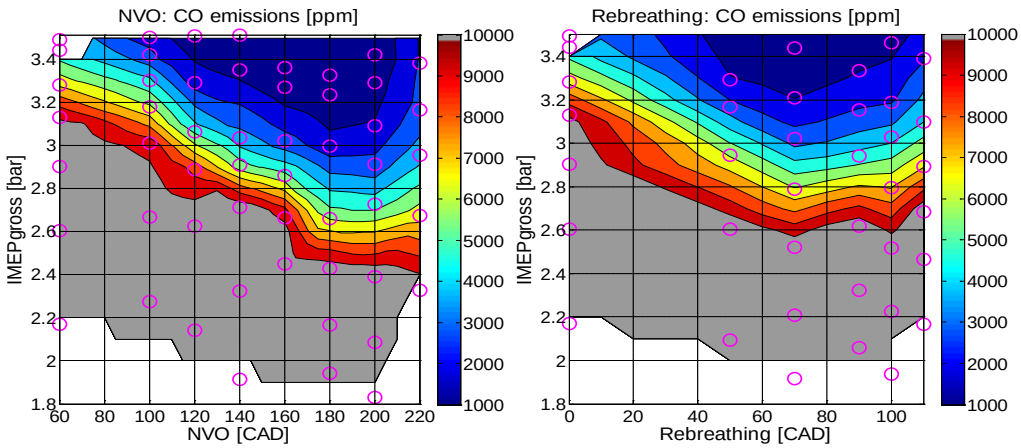

Figure 36. CO emissions with the NVO (left) and rebreathing (right) valve strategies.

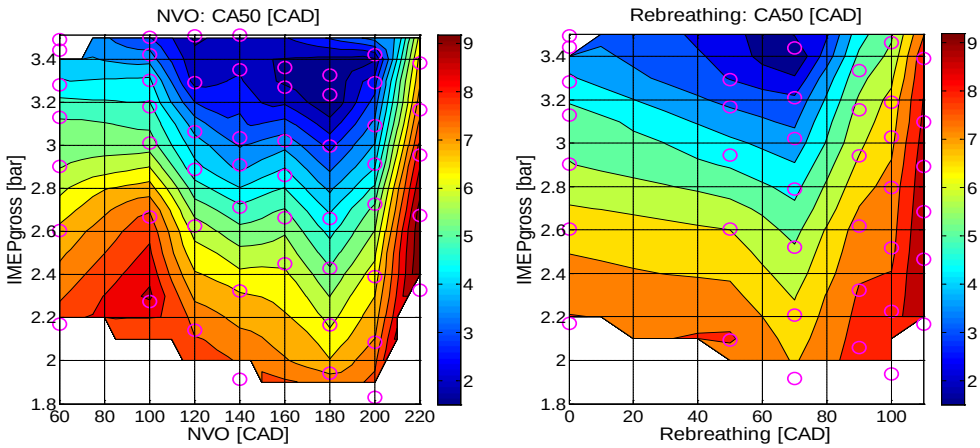

Figure 37. Combustion timing, CA50, with the NVO (left) and the rebreathing (right) valve strategies.

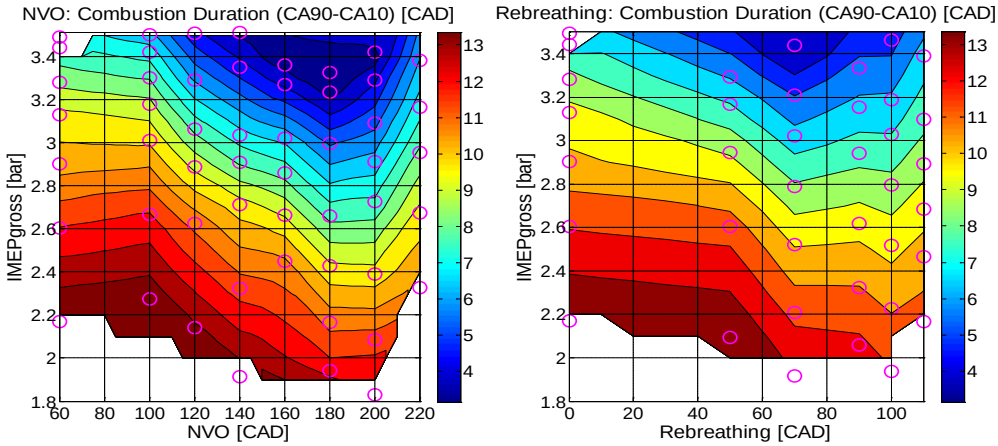

Figure 38. Combustion duration, with the NVO (left) and the rebreathing (right) valve strategies.

The conclusion is that the rebreathing valve strategy has similar improving effects as the NVO valve strategy at low load. The same overall trends in improvements of combustion stability, HC and CO emissions are seen with rebreathing as with NVO. Based on the air flow measurements, the optimal rebreathing setting 70 CAD gives the same reduced air flow as the NVO 160 CAD. The optimal NVO setting 180 CAD would match a rebreathing setting of 80 CAD which unfortunately was not measured. But the implication is that similar levels of trapped residual gas give approximately the same improving effects of the combustion. It can then be assumed that the temperature increase is approximately the same for both strategies.

Unfortunately time did not permit to simulate also the rebreathing results. An adequately tuned engine simulation model could be useful to extract residual gas fraction and temperature data also for the rebreathing cases. This is left as future work. It could also be interesting to investigate and see if there are any differences in in-cylinder temperature and internal EGR distribution between the valve strategies using optical diagnostics or CFD modeling. A modeling approach was used for HCCI combustion in a work by Babajimopoulos et al. [73] and it was concluded that a rebreathing strategy yields a more homogeneous composition compared to using negative valve overlap at high residual gas fraction levels.

The gas-exchange efficiency is shown in Figure 39, and the net indicated efficiency is shown in Figure 40. As expected, the gas-exchange efficiency is higher with the rebreathing strategy compared to the NVO strategy. The net-indicated efficiency is shown versus IMEPn rather than IMEPg because it more clearly shows the effect of the gas-exchange efficiency with varying NVO. The net indicated efficiency is generally higher with rebreathing compared to NVO. This is due to the higher gas-exchange efficiency with the rebreathing strategy. But the net-indicated efficiency

with the NVO strategy is not completely dominated by the decrease in gas-exchange efficiency. With increasing NVO there is also an increase in combustion efficiency, as indicated by the decrease of unburned hydrocarbon and CO emissions. With the rebreathing strategy, the highest efficiency is found at the optimum rebreathing setting. This is where the combustion phasing is the most advanced, the combustion stability is the highest and HC emissions are the lowest.

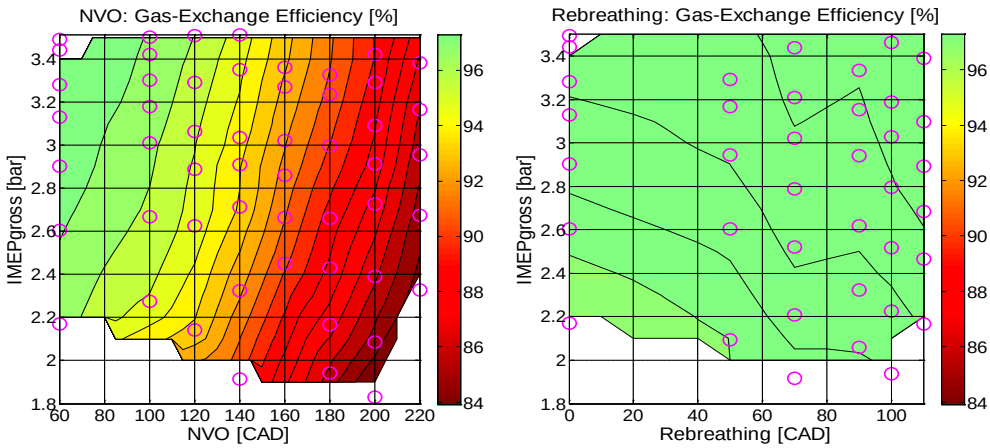

Figure 39. Gas-exchange efficiency with the NVO (left) and the rebreathing (right) valve strategies.

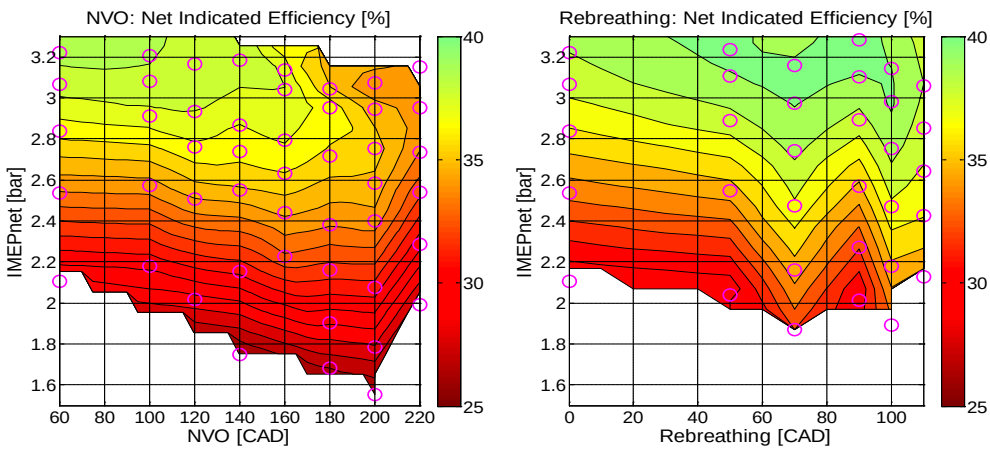

Figure 40. Net-indicated efficiency with the NVO (left) and the rebreathing (right) valve strategies.

Ignition Delay Model

An attempt is made to model the ignition delay to see how well the trends are captured by the model and to get a quantitative estimate of the contribution of each factor in the model. According to literature [74], the ignition delay can often be correlated to temperature, equivalence ratio, and pressure according to

$$\tau_{id} = C_e \cdot \left(\frac{P}{P_0}\right)^a \cdot \phi^b \cdot e^{E_a/R\overline{T_a}} \tag{5.1}$$

The unit of the ignition delay, τ_{id}, is milliseconds, but it is easily converted to crank angles. C_e, a and b are empirically determined constants. P is the ambient pressure and P_0 is a reference pressure. ϕ is the equivalence ratio. $\overline{T_a}$ is the estimated average temperature and E_a/R is an apparent activation energy where R is the universal gas constant. In a work by Kook et al. [72], the ignition delay was found to be effectively predicted with

$$\tau_{id} = A \cdot \bar{p}^{-n} \cdot X_{O_2}^{-m} \cdot e^{E_a/R\overline{T_a}}, \qquad E_a/R = 3242.4\ K \tag{5.2}$$

where A, n and m are constants dependent on fuel and airflow characteristics, p is the ambient pressure, X_{O_2} is the oxygen concentration. The ignition delay model in (5.1) was preferred in this work because the available in-cylinder oxygen concentration is unknown. The main trends are assumed to be captured also with the measured equivalence ratio. The expected behavior is that the ignition delay becomes longer when the equivalence ratio is increased in response to the reduced available oxygen concentration and increased heat capacity from increased NVO. The model is fitted to the ignition delay data without the glow plug. The temperature, $\overline{T_a}$, is estimated by fitting a second order regression model from the AVL Boost simulation model temperature at start of fuel injection timing according to

$$\overline{T_a} = k_1 \cdot NVO^2 + k_2 \cdot NVO + k_3 \cdot IMEP_g{}^2 + k_4 \cdot IMEP_g + k_5 \tag{5.3}$$

The reason is that a corresponding engine simulations data set with the glow plug off is unavailable. It is assumed that the temperature data at crank angle of start of fuel injection is valid also for the entire data set without the glow plug. The pressure, P, is extracted from the measured in-cylinder pressure at start of fuel injection. The equivalence ratio is calculated from the measured air- and fuel-flows. Selecting reasonable values for the empirical constants a and b in (5.1) was done after some considerations. Reasonable model agreement with the measured data could be achieved over a wide interval of empirical constants, a and b. But the estimated influence of the individual model factors would change depending on how the

parameters were selected. It was instead decided to set the parameter a to -1. This value was used in the work by Kook et al. [72] with the motivation that this constant is typically close to -1. This is the n parameter in (5.2). The remaining empirical constants, C_e and b are selected based on the best model fit to the measured ignition delays.

The apparent activation energy, E_a/R, is estimated by taking the logarithm of (5.1) and rewriting the equation according to

$$log\left(\tau_{id} \cdot \left(\frac{P}{P_0}\right)^{-a} \cdot \phi^{-b}\right) = E_a/R \cdot \frac{1}{\overline{T_a}} + log\, C_e \tag{5.4}$$

Figure 41 shows the left side of (5.4) plotted against $1/\overline{T_a}$. The estimated slope of a line fitted to the data is taken as the apparent activation energy estimate. A value of 2457.9 K was found. The result can be seen in Figure 42. The corresponding measured ignition delays are shown in Figure 32. It can be seen that there is a reasonable agreement between the model and the measured ignition delay and that the overall trends are captured by the ignition delay model, (5.1). There is an intermediate NVO setting where the ignition delay is the shortest and the ignition delay is long at the highest NVO settings.

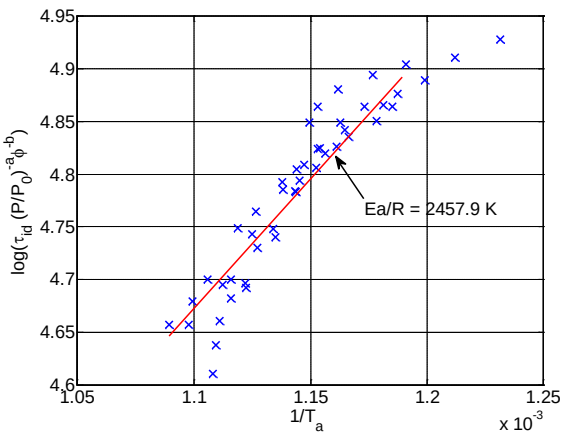

Figure 41. Correlation of ignition delay with average pressure, temperature and equivalence ratio.

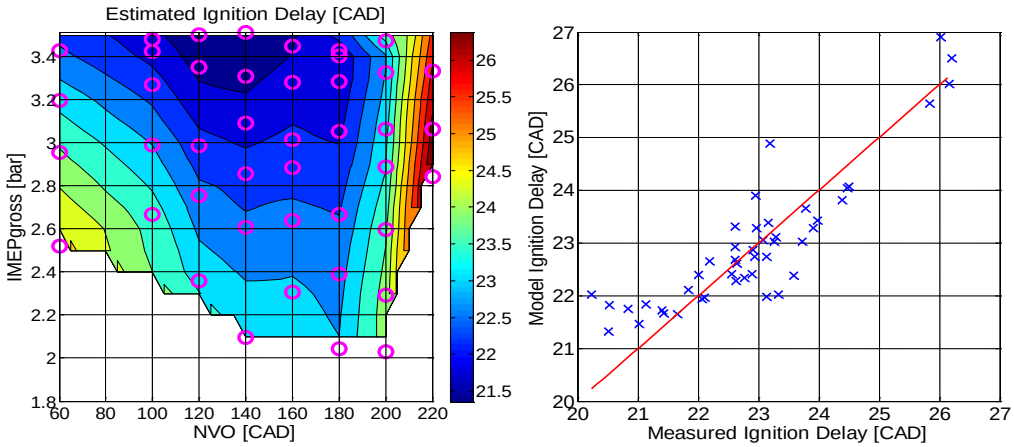

Figure 42. The estimated ignition delay (left) and the measured ignition delays plotted against the model ignition delay (right).

The individual factors from (5.1) are shown in Figure 43. The idea is to get a quantitative estimate of the contribution of each factor in the model. The plots have been normalized with the lowest value of each factor to show the contribution, of each factor, on how much longer the ignition delay becomes, in percent, at varying NVO and engine load. The datum point, 0%, is where the factors are the lowest. Moving away from the datum point results in an increase of the ignition delay and this is shown in the figures. Note that these are dependent on how the empirical constants are selected. The results that are shown here are with the empirical constant a set to -1, with b=0.20 and C_e=7.2. It is seen that the contributions from the factors containing the temperature and equivalence ratio have the largest influence with 35% and 25% difference, respectively, from shortest to longest ignition delays. The pressure factor results in a 14% increase of the ignition delay from the lowest NVO setting to the highest. The ignition delay becomes longer as the temperature is decreased as a result of decreasing NVO. A significant effect from temperature on ignition delay is expected [74]. The ignition delay becomes longer with increasing equivalence ratio because air is replaced with trapped residual gases which lowers the oxygen concentration and increases the heat capacity of the ambient gas. Increasing NVO also lowers the specific heat ratio, which results in a lower pressure after compression which can be understood from the well-known relation of isentropic compression: $p_{comp} = p_{IVC} \cdot r_c^{\gamma}$.

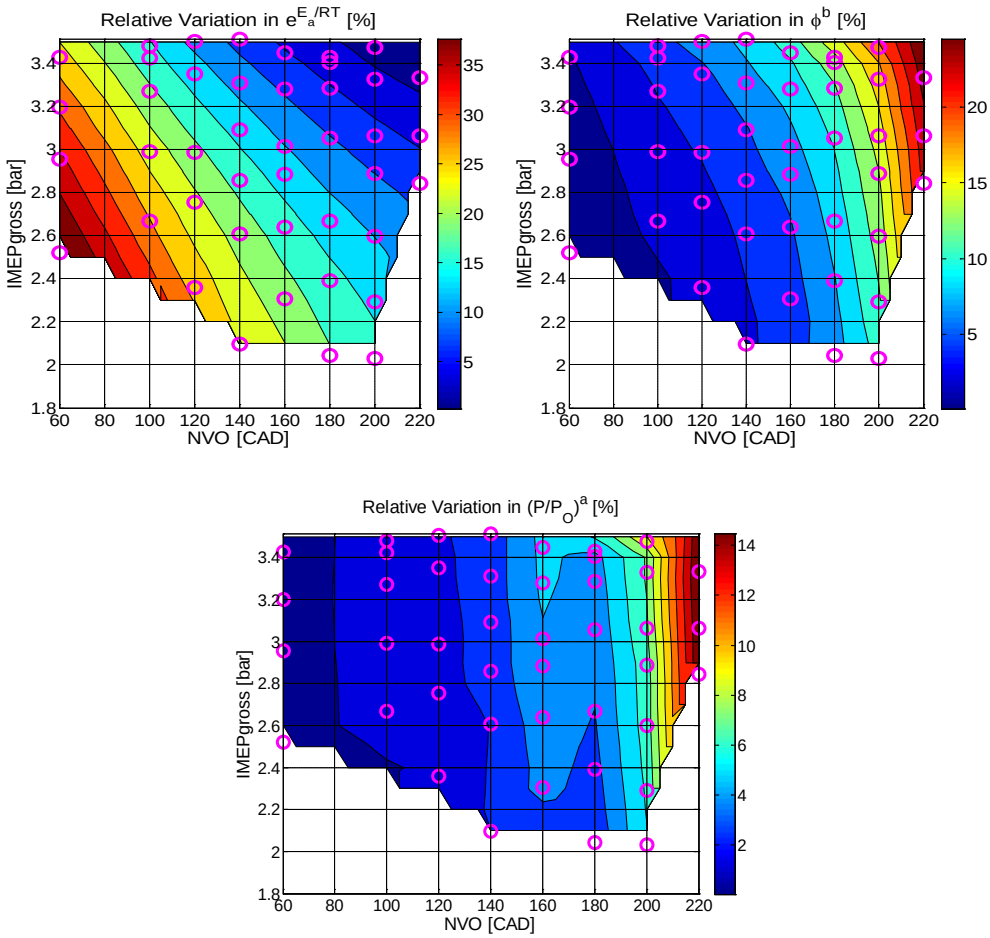

Figure 43. Relative variation of the factors in (5.1). The contour plots show the contribution from each factor on how much longer the ignition delay becomes with varying NVO and engine load.

An attempt has been made to capture the overall trends with varying NVO and engine load using a relatively simple but established ignition delay model. It was used to show that the overall trends on the ignition delay can be explained by the changes in temperature, pressure and equivalence ratio from varying NVO and engine load. The estimation procedure is not perfect and it is influenced by how the empirical constants are selected. A suggested improvement is to use a different data set to calibrate the model with known reference conditions. This can be achieved by, for example, using external EGR, instead of trapped residuals, and to control the inlet temperature with the air heater. More accurate temperature data can be obtained by performing complementary engine simulations in AVL Boost instead of using a regression model. A potential practical application for this relatively simple ignition delay model is as

part of an engine control system. If the model parameters are adequately tuned over the different engine operating regions, alternatively using variable parameters, the model might be used to predict the ignition delay at varying fuel injection timings. Lewander et al. [75] designed a model predictive control strategy for a heavy duty engine operated in PPC mode. One of the model constraints was that the ignition delay has to be sufficiently long to ensure a positive mixing period. The model in Lewander's work was a black box model with model parameters derived from system identification. It shows a potential application for an ignition delay model.

5.2.4 Fuel Injection Strategies (Papers 5 and 6)

The results in this section are taken from Papers 5 and 6. Paper 5, "The Low Load Limit of Gasoline Partially Premixed Combustion Using Negative Valve Overlap", was presented by the author at the ASME 2012 Internal Combustion Engine Division Fall Technical Conference, in Vancouver. The experiments were planned, carried out and post-processed by the author. The article was written by the author. Öivind Andersson supervised the experimental planning of the split main fuel injection strategy optimization using Design of Experiments and provided valuable feedback. The work was also supervised by Per Tunestål and Bengt Johansson who both provided valuable feedback. The NVO fuel injection strategy results are taken from Paper 6.

In the previous section, results using a rebreathing valve strategy were presented as an alternative to the NVO valve strategy. The motivation is that the net indicated efficiency is higher with rebreathing compared to NVO. In the first part of this section, more advanced fuel injection strategies are evaluated and compared. The intention is to see if NVO can be substituted with a more advanced fuel injection strategy. In the second part, an opportunity that is available with NVO is to add a fuel injection during NVO to see if the low load limit can be extended further.

As in the previous section, no external EGR is used, the fuel is the 87 RON gasoline and the glow plug is kept on. The different fuel injection strategies from Paper 5 are shown in Figure 44. A single fuel injection strategy is used as reference. The subjects of investigation are a split main fuel injection strategy, with optimized fuel injection timings and duration. And the other two fuel injection strategies are the single and split main fuel injection strategies with a pilot injection during the compression stroke. The common rail pressure was constant 400 bar for all measurements. Up until this point, no investigations had been performed on the effects of the common rail pressure. The reason for lowering the rail pressure from 500 bar to 400 bar was that a pre-investigation on the effect of the rail pressure showed a small improvement on unburned hydrocarbon emissions with the lower common rail pressure. Benefits in combustion stability and lower HC and CO emissions with a lower injection pressure with gasoline were also reported by Hildingsson et al. in [76].

The optimization of the split main fuel injection strategy was done using Design of Experiments (DoE). A central composite design based on a two-level full factorial design with superimposed axial and center points was chosen for the experiments. A more detailed description of this design and properties can be found in [77]. The experimental factors were NVO, the fuel mass ratio between the two injections and the fuel injection separation in crank angles. The standard deviation of IMEPn and combustion efficiency was chosen as output variables and fitted to separate second order regression models. The details are given in Paper 5. From the analysis of the regression models the following conclusions were made: 1) a large fraction of the fuel should be injected with the first fuel injection. 2) A high NVO setting results in improved combustion efficiency but the lowest standard deviation of IMEPn was found for approximately 160 CAD NVO. 3) A too short or a too long separation between the fuel injections should be avoided.

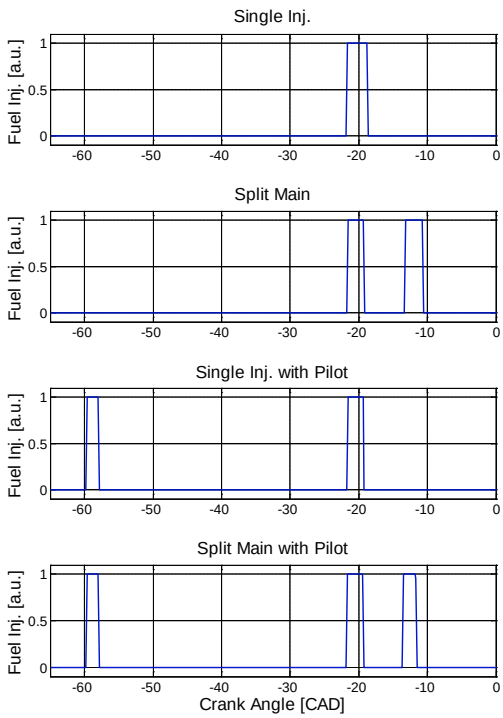

Figure 44. The fuel injection signal from the engine control system for the different injection strategies.

The different fuel injection strategies were used at decreasing engine loads. The fuel injection strategies were evaluated with both a low (60 CAD) and a high (200 CAD)

setting of NVO. A 200 CAD NVO setting was preferred over the 160 CAD NVO setting given the additional improvement in combustion efficiency. The standard deviation and combustion efficiency for the single injection strategy compared to the split main injection strategy are shown in Figure 45. And the corresponding figures in comparison with the single injection with pilot strategy are shown in Figure 46. It is seen that the combustion stability and combustion efficiency are significantly improved with a split main injection strategy compared to a single injection strategy when NVO is low. In the cases with high NVO setting, no significant improvements are observed with the split main fuel injection strategy. And the high NVO cases, regardless of fuel injection strategy, have lower standard deviation in IMEPn and higher combustion efficiency compared to the low NVO cases.

In the case with a pilot injection compared to the single injection strategy, a significant improvement in combustion stability with the low NVO case is observed. The improvement is better also compared to the split main fuel injection strategy. Also the combustion efficiency is improved in the low NVO case. But no significant improvements are observed with the high NVO cases. The combustion efficiency is lower with the high NVO cases when a pilot injection is added. This is most likely because of trapped fuel in crevice volumes. No additional improvements or findings were observed when a pilot injection is added to the split main injection strategy compared to the single injection strategies. The details are found in Paper 5. The conclusions are that a single injection with a pilot strategy has comparably low standard deviation in IMEPn without using a large fraction of trapped hot residual gas over an extended operating region compared to a single injection strategy. The combustion efficiency is significantly improved with a large fraction of trapped hot residual gases and could not be substituted for a more advanced fuel injection strategy.

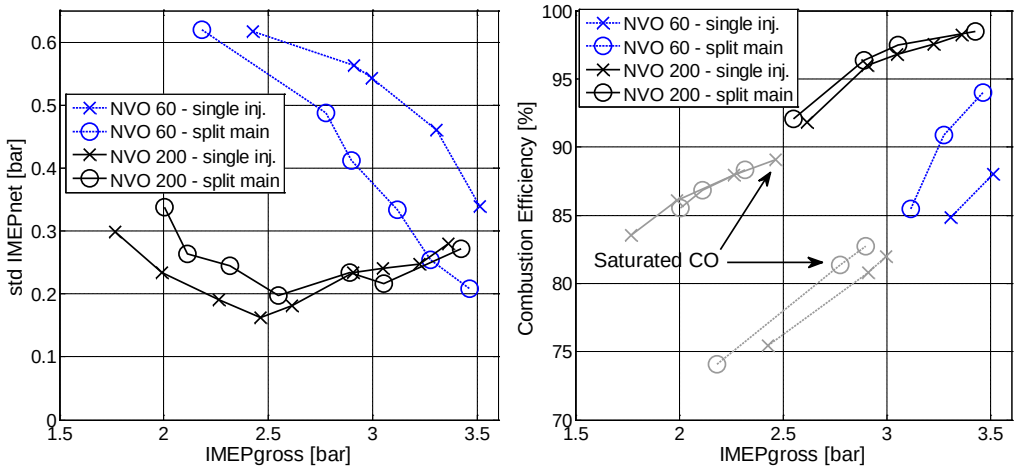

Figure 45. Standard deviation of IMEPn and combustion efficiency of the single injection strategy in comparison with the split main fuel injection strategy.

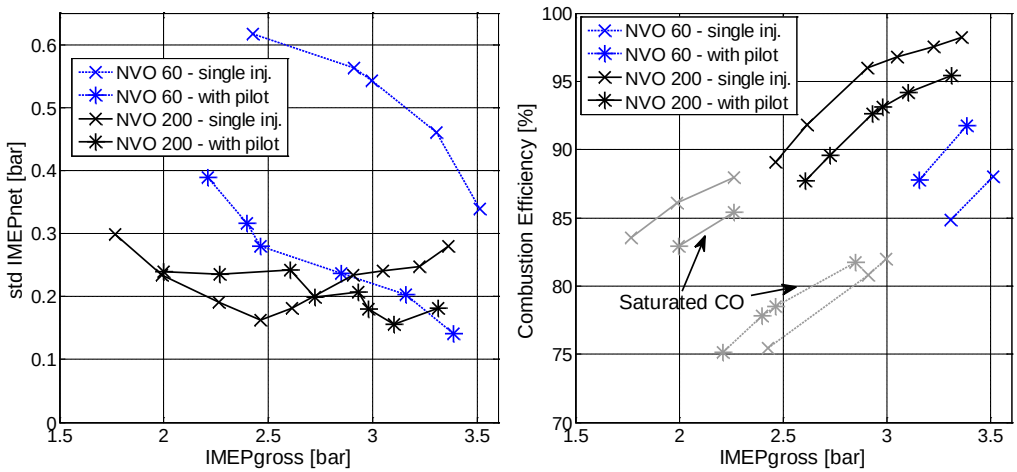

Figure 46. Standard deviation of IMEPn and combustion efficiency of the single injection strategy in comparison with the single injection with a pilot strategy.

When comparing the NVO 60 results of this section to the NVO 60 data from the hot residual gas section, an unexpected result was that the standard deviation in IMEPn became lower with a lower rail pressure of 400 bar. This is shown in Figure 47 for two different NVO cases with a single injection strategy. It is seen that the unburned hydrocarbon emissions and standard deviation are in fact lower at low engine load, but

only for the high NVO cases. One reason could be that the lower rail pressure results in poor atomization of the fuel when the in-cylinder temperature is low which results in a longer ignition delay and retarded CA50 due to over-mixed fuel. With increased NVO, the in-cylinder temperature is increased and vaporization of the fuel is enhanced. No experiments that can better explain this behavior have been performed since it is outside the scope of this thesis. The consequence, for the low NVO cases, is that a more detailed investigation on the effect of the common rail pressure in combination with more advanced injection strategy is needed. This is left as future work. The main results of the thesis are focused on using high settings of NVO or rebreathing, and a positive effect of a lower rail pressure has been observed in these cases at low load.

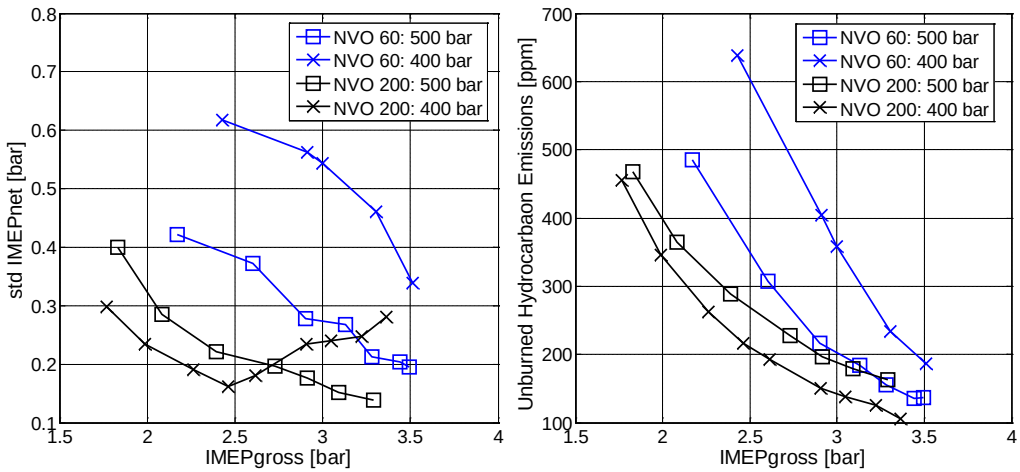

Figure 47. Effects of common rail pressure and NVO on standard deviation in IMEPn and unburned hydrocarbon emissions. If the unburned hydrocarbon emissions are multiplied by number of carbon atoms in the fuel molecules, 7.2, the corresponding quantities with the unit ppmC_1 are obtained.

In the second investigation, fuel is injected during the NVO to try to extend the low load limit further. This strategy has been used by several authors and is usually associated with the CAI concept. The main differences compared to the investigation in the thesis, as mentioned in the introduction, are the higher compression ratio, common rail direct injection system with late injection timings and the glow plug.

Urushihara et al. [21] showed that it was possible to extend the lean limit of HCCI by injecting a portion of the fuel in the NVO. The idea was to change the chemical composition of the fuel injected into the NVO, which was referred to as fuel reformation. Koopmans et al. [22] investigated the effects of lambda and injected fuel amount during NVO. Provided that the auto-ignition temperature is reached,

combustion in the gas-exchange results in an elevated temperature of the sub-sequent main combustion event. The heat release during NVO depends on both the oxygen level and injected fuel mass. An optimal lambda could be found that gave the most advanced combustion phasing. A too lean mixture leads to a lower temperature at the main combustion event due to cooling from excess air and a too rich mixture limits the NVO heat release and consequently lowers the temperature for the main combustion. Waldman et al. [78] investigated the effect of NVO injection timing and fraction of fuel injected into the NVO. Both parameters were found to affect the main combustion timing, emissions and combustion stability. An optimum, load dependent, NVO fuel ratio and timing with respect to fuel consumption and emissions was found. In a work by Aroonsrisopon et al. [79], a multizone, 2D CFD simulation with chemistry, was performed, during the NVO, with varying NVO injection fuel amount and timing. It was shown that both the thermal effect (temperature increase from the NVO heat-release) and the chemical effect (fuel reformation) can be used to promote the main combustion. For conditions where there was no significant heat release during NVO, the chemical effect still had an impact on the main combustion timing. Cao et al. [80] used a multi-cycle 3D engine simulation program to study the thermal and chemical effects of the injection timings of a single injection strategy, and split injection ratios using a double injection strategy. For the single injection strategy, the thermal effect associated with injection during the negative valve overlap was found to have a dominating effect on advancing the start of main combustion. The chemical effect is secondary and it was found to promote the first stage ignition during the compression stroke. For the split injection strategy the best engine performance was obtained with a 50/50 split injection ratio. Berntsson et al. [81] investigated the effects of NVO and main fuel injection ratios in both a multi-cylinder and an optical engine. The changes in combustion phasing were attributed to the heat generated during NVO which increases the compression temperature. Fitzgerald et al. [82] observed that the chemical effects are the most prominent for NVO fuel injections later than 30 CAD BTDC. This was attributed to piston wetting followed by rich combustion from pool fires which can be expected to have an impact on the chemical composition.

The NVO fuel injection strategy used in the thesis is shown in Figure 48. A split injection strategy is used with a constant fuel amount during the NVO at a constant timing -5 CAD ATDC. For the limited load range that is investigated, the proportions between the two fuel injections are on average approximately 50/50. The estimated variation in fuel distribution is from approximately 60/40 at the lowest engine load to approximately 40/60 at the highest engine load. The main fuel injection timing was kept constant at 22 CAD BTDC when possible. The exception was with the higher setting of NVO, 200 and 220 CAD, where the fuel injection was set later to 13-14 CAD BTDC in order to have combustion timing after TDC. The NVO injection timing was optimized with respect to unburned hydrocarbon emissions, combustion stability and net indicated efficiency. The details can be found in Paper 6.

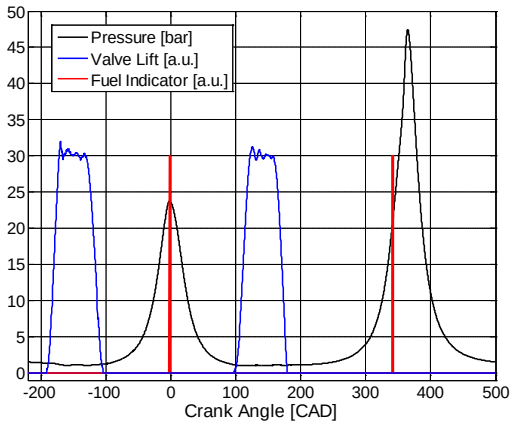

Figure 48. The NVO fuel injection strategy.

The temperature and pressure during NVO are shown in Figure 49. The data was extracted from the NVO data set in the Hot Residual Gas section. Even though the NVO fuel injection was not used in the simulated cases, it is assumed that the figures are still representative of the high pressures and temperatures that are obtained during the gas-exchange also when the NVO fuel injection strategy is applied. The temperatures are the maximum temperature during NVO from the Boost simulation model and the pressure is taken as the maximum measured pressure during NVO. The temperature at start of combustion, from the Boost simulations, and the relative air fuel ratio, lambda, which was calculated from measured air- and fuel-flow, are shown in Figure 50. The auto-ignition temperature (temperature at start of combustion) varies with NVO from 840 K to 910 K, from 60 CAD to 220 CAD NVO. From 180 CAD NVO, the NVO temperature becomes higher than auto-ignition temperature. At the high NVO settings, from approximately 200 CAD and above, the temperature and pressure are sufficiently high for the rate of heat release during NVO to become detectable, as seen in Figure 51. This is an indication that there will be a temperature increase (thermal effect) for the subsequent main combustion event. Changing NVO affects both the temperature, and oxygen availability. The air-fuel ratio is on the lean side but is close to stoichiometric at the highest NVO setting, 220 CAD. This means that the potential temperature increase could be limited by the oxygen supply. Reducing NVO will increase the amount of available oxygen but will decrease the temperature and pressure during NVO. The chemical effects of the NVO injection could also be of importance. It is however difficult to distinguish between chemical and thermal effects without using a more detailed simulation code and this is outside the scope of the thesis.

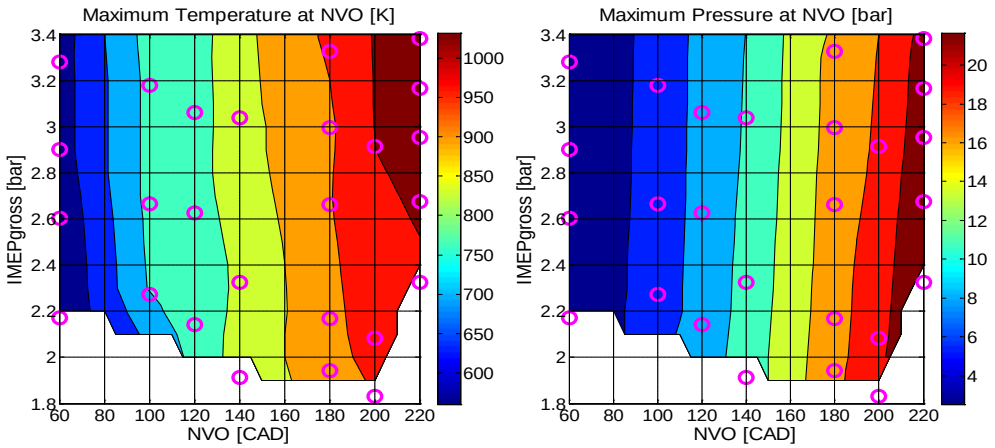

Figure 49. Maximum temperature during NVO from the Boost model simulations, without the NVO injection (left) and measured maximum pressure during NVO from the same data set (right).

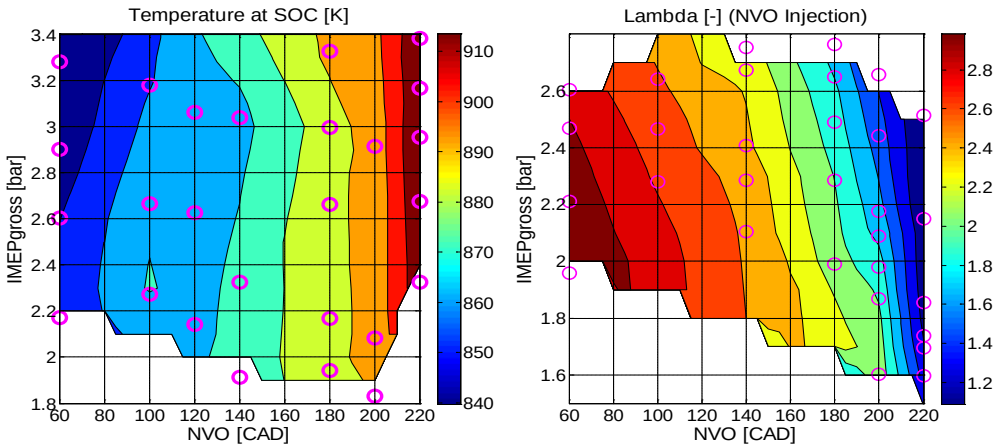

Figure 50. Temperature at start of combustion from the Boost model simulations, without the NVO injection (left) and the relative air fuel ratio with the NVO injection strategy (right).

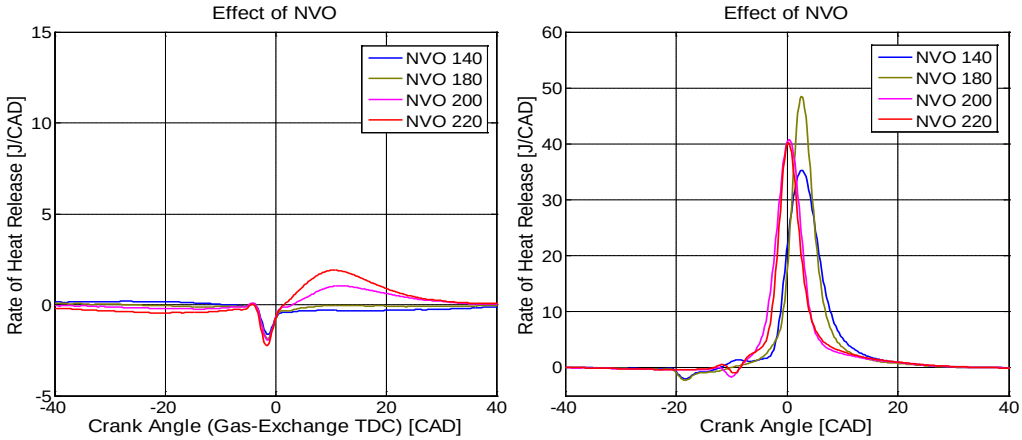

Figure 51. Rate of heat release during NVO (left) and subsequent main combustion (right) with varying settings of NVO.

The resulting ignition delay, combustion duration, CA50, combustion instability, unburned hydrocarbon emissions, soot emissions, and net indicated efficiency, for the NVO injection strategy, are shown from Figure 52 to Figure 55. There is a significant impact of the NVO injection on the ignition delay above 180 CAD NVO. This is explained by the thermal and chemical effects of the NVO injection, as discussed previously. The shortest combustion durations are observed at 180-200 CAD NVO settings. The combustion duration does not show similar trends as the ignition delay. The combustion duration becomes shorter with NVO as a result of the increased temperature but becomes longer due to increased heat capacity and reduced oxygen concentration at the high NVO settings [70]. The resulting combustion timing, CA50, is dominated by the effect of the shorter ignition delay and the combustion stability is significantly improved at the highest NVO settings. Also the unburned hydrocarbon emissions are improved. The unburned hydrocarbon emissions are generally high which can be explained by trapped fuel in crevice and squish volumes from the NVO injection. Soot emissions are high with the highest NVO setting. This is where the ignition delay is short and the air fuel ratio is low. If the oxygen concentration becomes too low during the negative valve overlap it can be assumed that large quantities of soot are formed during the NVO.

The net indicated efficiency is low at the high NVO settings. One explanation is that, even though combustion stability is improved and unburned hydrocarbon emissions become lower, the gas-exchange efficiency is significantly reduced with NVO. Another contribution could be from increased heat losses during NVO due to the elevated temperature from the heat release also during NVO.

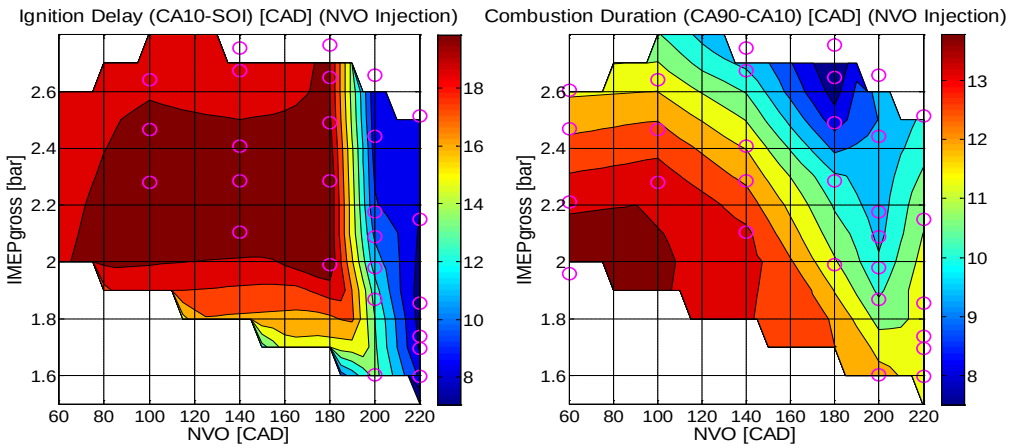

Figure 52. Ignition delay (left) and combustion duration (right) with the NVO Injection strategy.

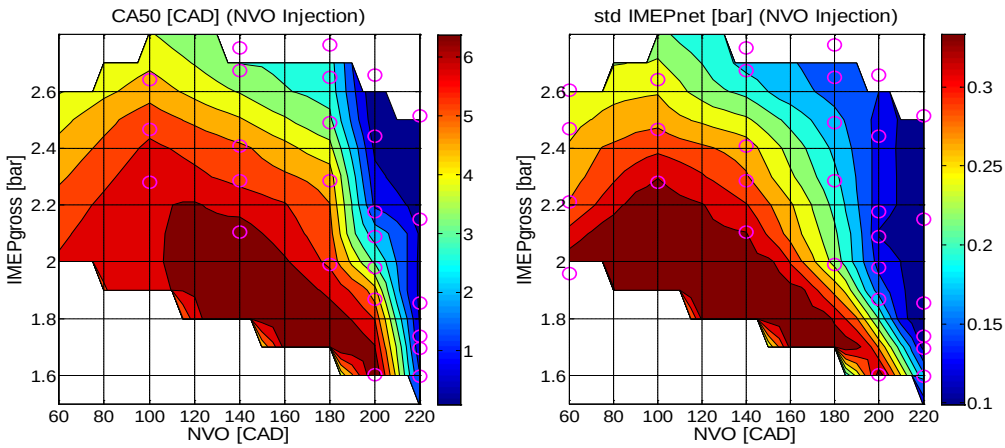

Figure 53. Combustion timing, CA50, (left) and combustion instability, measured as standard deviation in IMEPn (right), with the NVO injection strategy.

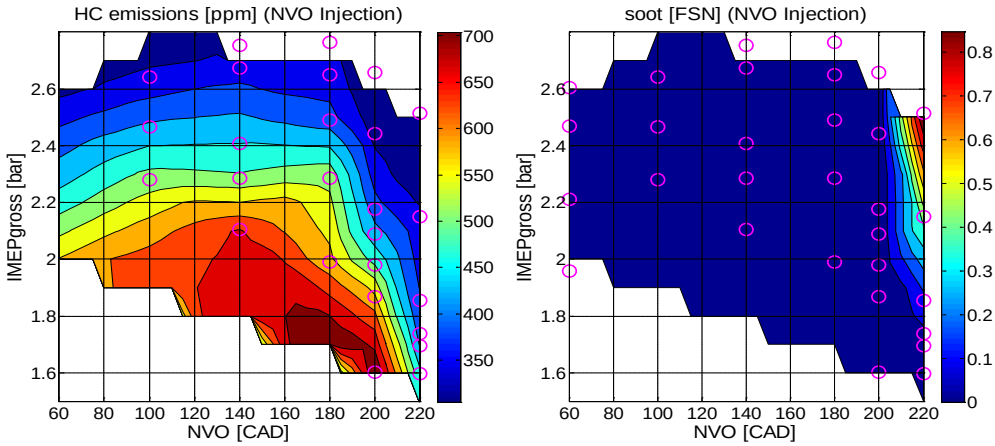

Figure 54. . Unburned hydrocarbon (left) and soot emissions (right) with the NVO injection strategy. If the ppm numbers of the unburned hydrocarbon emissions are multiplied with the number of carbons in the fuel, 7.2, the corresponding quantities with the unit ppmC_1 are obtained.

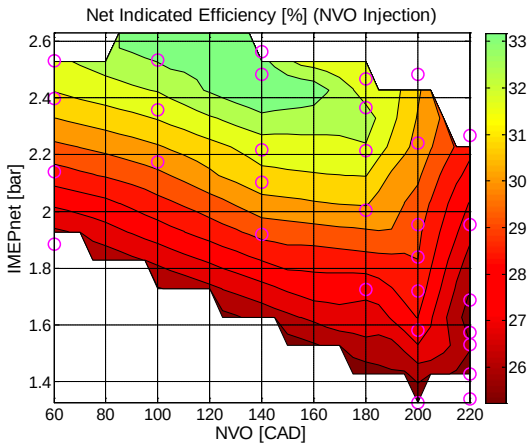

Figure 55. Net indicated efficiency with the NVO injection strategy.

The effect of the NVO injection timing and main injection timing on ignition delay, combustion timing, and soot are shown in Figure 56. The operating point is at NVO 220 CAD with approximately 50/50 split injection fuel ratio between the NVO injection and the main injection. When the NVO injection timing was varied, the main injection timing remained constant at -22 CAD ATDC. And when the main injection timing was varied, the NVO injection timing was constant at -5 CAD ATDC. The numbers in the figures show the soot emissions. The combustion timing, CA50, is significantly affected by the NVO injection timing from -10 CAD ATDC. At later

NVO injection timings the NVO heat release is lower which reduces the temperature of the main combustion. Only a small quantity of soot was detected with the earliest NVO injection timings. The main injection timing has a significant effect on the soot emissions. Retarding the main injection timing reduces the mixing time of the main injection fuel before start of combustion which is seen from the decreasing ignition delay in the right diagram in Figure 56. At the latest main injection timing, the NVO injection fuel is already ignited and the calculated ignition delay becomes negative because it is calculated from the main fuel injection timing. Soot is increased as the ignition delay becomes shorter and the mixing time of the main injection fuel is decreased. This shows that the main injection timing can be used to control also the soot emissions. If the main injection timing is advanced there is a potential for soot reduction.

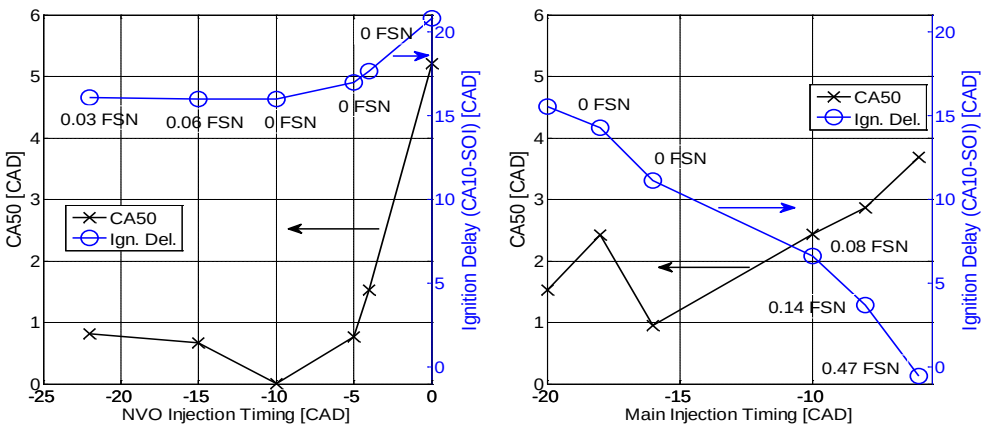

Figure 56. Effect of NVO injection timing (left) and main injection timing (right) at a 220 CAD NVO operating point with 50/50 split injection fuel ratio. The numbers show the soot emissions.

Finally, the effect of a reduction of the amount of fuel in the NVO injection is investigated. The operating point is 220 CAD NVO and two cases with different fuel ratios between the two injections are investigated. The first case is the same as has been shown previously, with a constant amount of fuel injected in the NVO. The fuel distribution is on average approximately 50/50 percent between the two injections. The estimated variation in fuel distribution is from approximately 60/40 at the lowest engine load to approximately 40/60 at the highest engine load. The second case is with a reduced amount of fuel in the NVO injection. The amount of injected fuel in NVO is constant also in the second case. The fuel distribution is on average approximately 30/70 between the two injections. The resulting fuel distribution variation of the second case is from approximately 35/65 at the lowest load to approximately 25/75 at the highest load. The ignition delay and combustion timing of the two different cases

at varying engine load are shown in Figure 57. The ignition delay becomes significantly longer and the combustion phasing is retarded when the amount of fuel in the NVO injection is reduced. One explanation is the lower temperature from the NVO heat release. Since a lower amount of fuel is injected it can be expected that the potential temperature increase is reduced.

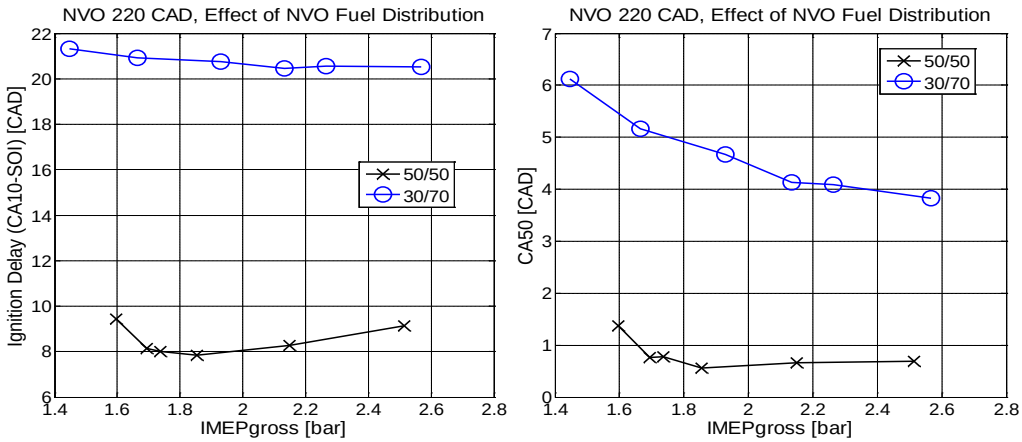

Figure 57. Effect of fuel distribution between the NVO and main fuel injections on ignition delay and combustion timing. The legend shows the approximate fuel distributions in percent between the two injections. The amount of fuel in the NVO was constant and the amount of fuel in the main injection was used to control engine load.

The combustion instability and unburned hydrocarbon emissions are shown in Figure 58 and the soot emissions are shown in Figure 59. The combustion is more stable with the higher NVO injection ratio but the difference becomes smaller with increasing engine load. The advantage with a lower fraction of NVO injection is that the unburned hydrocarbon emissions are reduced because a lower amount of fuel is trapped in squish and crevice volumes. And the soot emissions are significantly reduced. This investigation shows that also the fuel distribution can be used to reduce the soot emissions while maintaining a similar level of combustion stability, especially as load is increased.

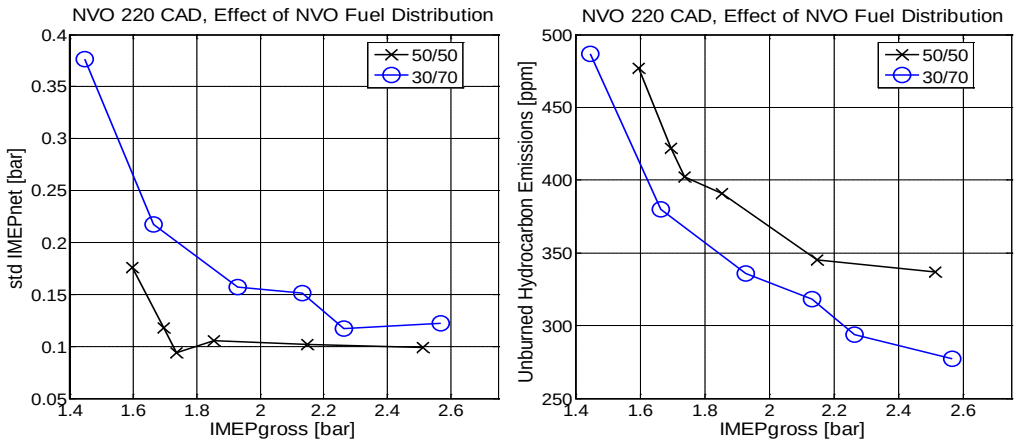

Figure 58. Effect of fuel distribution between the NVO and main fuel injections on standard deviation of IMEPn and unburned hydrocarbon emissions. The legend shows the approximate fuel distributions in percent between the two injections. The amount of fuel in the NVO was constant and the amount of fuel in the main injection was used to control engine load.

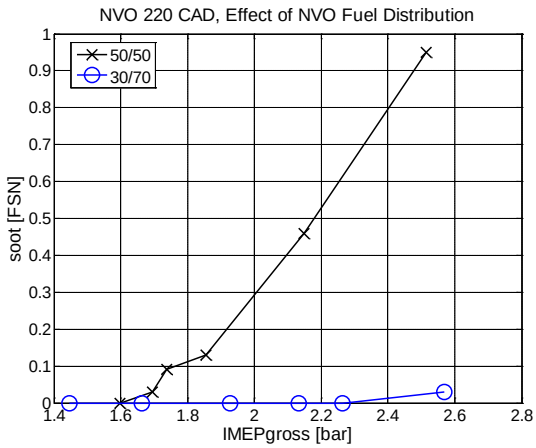

Figure 59. Effect of fuel distribution between the NVO and main fuel injections on soot. The legend shows the approximate fuel distributions in percent between the two injections. The amount of fuel in the NVO was constant and the amount of fuel in the main injection was used to control engine load.

5.2.5 Glow Plug (Paper 4)

The next topic is on the effect of the glow plug. Since the glow plug was kept on in the previous investigations with the 87 RON gasoline fuel in the Hot Residual Gas and Fuel Injection Strategies sections, the question is what would be the difference if the glow plug had been turned off. The combustion instability and combustion efficiency for two cases, with and without the glow plug, are shown in Figure 60. The observation was that the glow plug has an improving effect on both combustion stability and combustion efficiency. But as NVO is increased, the additional improvement from the glow plug becomes less significant and the differences can be expected to be small.

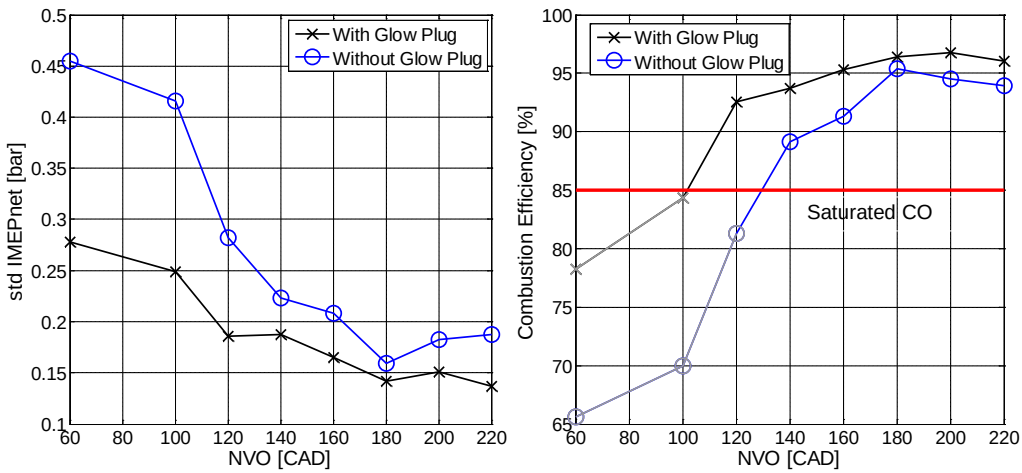

Figure 60. Effect of glow plug on combustion instability (left) and combustion efficiency with varying NVO.

5.2.6 Putting it all Together (Paper 6)

As a summary of what have been shown and discussed up to this point, the different valve and fuel injection strategies are put together and compared in terms of efficiency and emissions. The most optimum settings in terms of valve timings and fuel injection settings have been selected. The effects of the individual parameters have been discussed in previous sections. This is similar to what was shown in Paper 6. The results from Paper 6 are complemented with results using the split main fuel injection strategy for the NVO case and also for the rebreathing case. A separate split main fuel injection strategy optimization, similar to what was used with NVO in Paper 5, has been performed also with the rebreathing valve strategy. The optimum fuel injection

timings did not change significantly with rebreathing compared to NVO. In papers 4 and 6, there was a clear indication that an optimum NVO and rebreathing setting existed. The split main injection strategy with NVO was run again but with the optimum settings of NVO. Also, the NVO fuel injection strategy is complemented with the results showing the effect of a lower fraction of the fuel injected in the NVO. A more detailed summary of the different strategy settings are shown in Table 4.

Table 4. A summary of the different valve and fuel injection strategies.

Name	**Injection Strategy**	**rail pressure [bar]**	**Valve strategy setting**
NVO sing. inj.	Single injection	500	NVO 180 CAD
NVO split main	Split main injection	400	NVO 180 CAD
NVO inj. 220 NVO (50/50)	NVO injection, 50/50 approximate fuel distribution	400	NVO 220 CAD
NVO inj. 220 NVO (30/70)	NVO injection, 30/70 approximate fuel distribution	400	NVO 220 CAD
NVO inj. 200 NVO (50/50)	NVO injection, 50/50 approximate fuel distribution	400	NVO 200 CAD
Reb. sing. inj.	Single injection	500	Rebreathing 70 CAD
Reb. split main	Split main injection	400	Rebreathing 70 CAD

The result is shown here against IMEPn instead of IMEPg. The reason is that this is closer to BMEP which measures the actual work output of the engine. The results plotted against IMEPg are shown in Paper 6. The reason for generally having favored IMEPg is that this shows the results with focus on the main combustion event which makes the comparison between the NVO and rebreathing strategy clearer. This is because there is a significant difference in gas-exchange efficiency, with a high setting of NVO, which results in a lower IMEPn for NVO compared to rebreathing.

The combustion instability and unburned hydrocarbon emissions are shown in Figure 61. It is seen that there is a significant improvement at low load with the NVO injection strategy compared to the other strategies. At higher engine load, from approximately 2.2 bar IMEPn, the split main fuel injection strategy in combination with either rebreathing or NVO has the best combustion stability. There is a clear increase of unburned hydrocarbon emissions with decreased engine load regardless of valve and fuel injection strategy. The CO emissions remained saturated at 10000 ppm for all strategies up to approximately 2 to 2.5 bar IMEPn depending on strategy as shown in Figure 62.

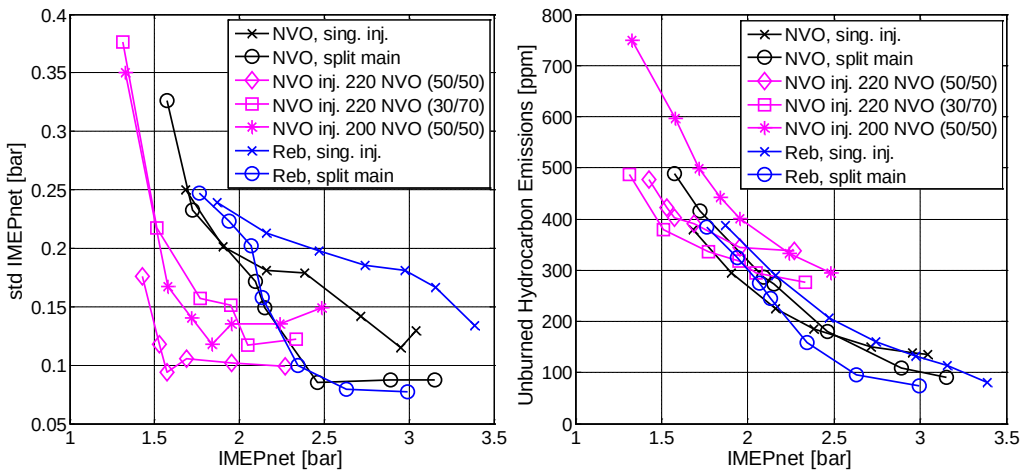

Figure 61. A compilation of the combustion instability and unburned hydrocarbon emissions for the different valve and fuel injection strategies. The approximate NVO injection fuel distribution between the NVO and main injections are indicated in the parentheses.

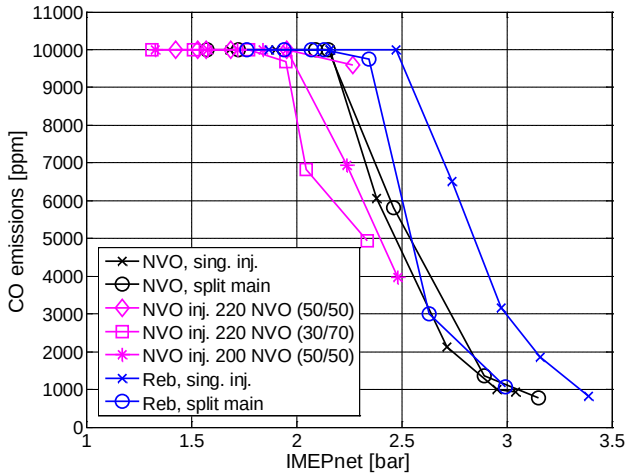

Figure 62. The CO emissions for the different valve and fuel injection strategies. The approximate NVO injection fuel distribution between the NVO and main injections are indicated in the parentheses.

The NOx and soot emissions are shown in Figure 63. The NOx emissions are low when the engine load is sufficiently low. No external EGR has been used in this investigation but it is expected to be required at the higher engine load operating conditions. The soot emissions are high when the NVO injection strategy is used with the highest NVO setting of 220 CAD and a 50/50 percent fuel distribution between the NVO and main fuel injection. As shown previously, there are different means to reduce soot emissions, for example, changing the main injection timing and reduce the amount of fuel injected in NVO. In Figure 63, also selecting a lower NVO is shown to reduce the soot emissions. This was seen also in Figure 54.

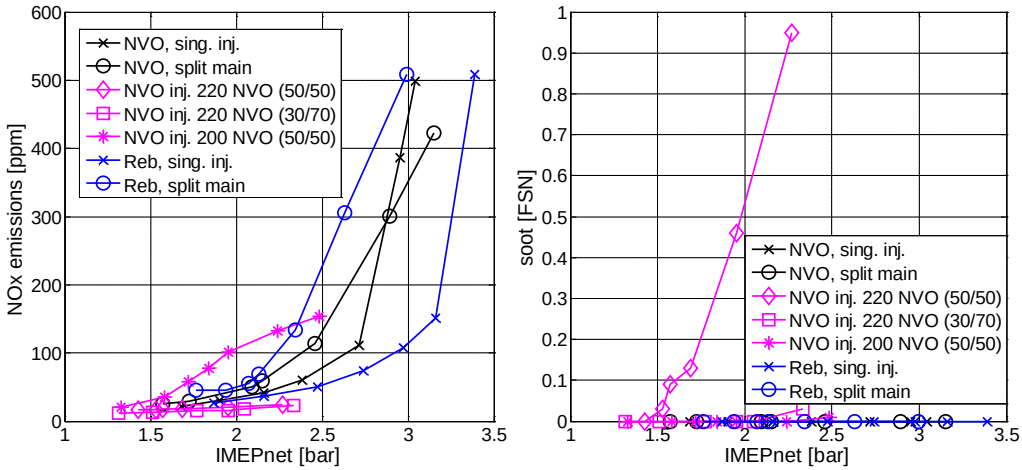

Figure 63. The NOx and soot emissions for the different valve and fuel injection strategies. The approximate NVO injection fuel distribution between the NVO and main injections are indicated in the parentheses.

Finally, the net indicated efficiency is shown in Figure 64. As previously shown, the rebreathing strategy has the highest net indicated efficiency compared to the NVO strategies. There is a significant decrease in efficiency with decreasing engine load which is attributed mainly to the decrease in combustion efficiency, which is indicated by an increase in HC and CO emissions.

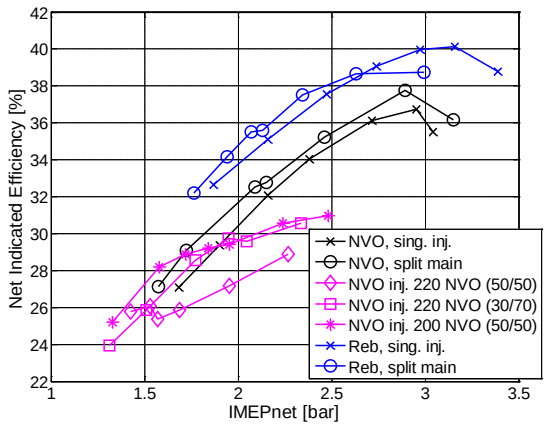

Figure 64. The net indicated efficiency for the different valve and fuel injection strategies. The approximate NVO injection fuel distribution between the NVO and main injections are indicated in the parentheses.

From these results it can be seen that there is not a single valve and fuel injection strategy that is optimal for combustion stability, emissions and efficiency. One suggestion is to operate the engine with the rebreathing strategy, with split main fuel injection, at the higher engine loads, from approximately 2 bar IMEPn and higher, and use NVO with the NVO injection strategy at low engine load. The NVO strategy could be used as an intermediate strategy so that the residual gases are gradually replaced from being re-inducted to becoming trapped. The NVO injection is turned on once a sufficiently high NVO setting has been reached.

At higher engine loads, the variable valve train system will be less useful. The amount of hot residual gas should be decreased, as load is increased, and be replaced with cooled EGR to suppress NOx emissions.

The challenge for the engine control system is to manage the transition between NVO and rebreathing. And another control challenge is to optimize the NVO fuel injection parameters in order to reduce soot emissions and maximize combustion stability. Design, implementation and evaluation of a suitable low load gasoline PPC control strategy is left as future work.

6 Summary

During the first part of the thesis, a fundamental experimental study on HCCI combustion in comparison with SI combustion using different variable valve timing strategies was performed. Residual gas enhanced HCCI with NVO or rebreathing has higher efficiency compared SI combustion. A rebreathing strategy gave the best net indicated efficiency of all strategies over the limited operating region in the investigation. To extend the operating range of the NVO HCCI engine, one alternative is to operate the engine in SI mode at low and high engine load. A combustion mode switch from SI to NVO HCCI was demonstrated. Two different HCCI combustion controllers, which were activated after the mode switch, have been compared. A model-based controller gave a smoother transient and could be activated one cycle earlier compared to the simpler PI controllers.

The limited operating region of HCCI and lack of immediate control actuator, which makes feedback control of the combustion difficult, are two contributing reasons to change focus from HCCI to gasoline PPC. The PPC combustion concept is associated with diesel engines. The ignition delay is longer compared to conventional diesel combustion which enhances the mixing of the fuel and air prior to combustion. The fuel and air becomes partially premixed but is not homogeneous. A longer ignition delay can be obtained by using a high fraction of EGR or a high octane number fuel, for example gasoline. One advantage with PPC compared to conventional diesel combustion is reduced soot emissions. One advantage over HCCI combustion is that the fuel injection timing can be used to control the combustion phasing. And an additional advantage is that the high load operating range is covered.

Running a diesel engine on gasoline is not without challenges. The attainable operating region is limited at low load and the main part of the thesis was devoted to extending the low load limit of gasoline PPC. The goal was to extend the operating region of the engine with high octane number fuels using the variable valve train system, the glow plug and more advanced injection strategies. The engine speed was kept low and the goal was to reach idle operating condition.

In the first gasoline PPC experimental study, a comparison between diesel and two gasoline fuels with different octane numbers were performed. The combustion efficiency and combustion stability was lower for gasoline compared to diesel. The low octane number gasoline (69 RON) could be operated with the minimum NVO setting down to 1 bar IMEPn. But the operating range of the 87 RON gasoline fuel

was limited and could be run down to approximately 2 bar IMEPn using a high fraction of trapped hot residual gas.

The rest of the work was devoted to the 87 RON gasoline fuel. The problem with the long ignition delay of the 87 RON gasoline fuel was that the combustion timing, CA50, could not be set sufficiently early using the fuel injection timing as control actuator alone. The late CA50 results in high emissions of unburned hydrocarbons and low combustion stability. The low load limit could be extended using either NVO or rebreathing from approximately 3.2-3.3 bar IMEPg down to approximately 2.2 bar IMEPg with the optimum settings of NVO and rebreathing. The rebreathing valve strategy has similar improving effects as the NVO valve strategy at low load. The advantage with the rebreathing valve strategy compared to the NVO strategy is improved efficiency because recompression of the hot residual gas is avoided.

The measured ignition delays with the 87 RON gasoline fuel were fitted to a simple empirical ignition delay model. It was found that the overall trends from changes of temperature, pressure and equivalence ratio could be captured by the simple model. A suggested potential practical application is as part of an engine control system.

More advanced fuel injection strategies were investigated. The objective of the first investigation was to see if the dependency on NVO could be reduced using a more advanced fuel injection strategy. The conclusions were that a single injection with a pilot during the compression stroke has comparably low standard deviation in IMEPn without using a large fraction of trapped hot residual gas over an extended operating region compared to a single injection strategy. The combustion efficiency is significantly improved with a large fraction of trapped hot residual gases and could not be substituted for a more advanced fuel injection strategy. It was also observed that the lower common rail pressure, 400 bar, had a deteriorating effect on combustion stability with the low NVO setting in contrast to the result with high NVO setting at low engine load. In the second investigation a portion of the fuel was injected during NVO. The combustion stability was significantly improved when NVO was sufficiently high. The penalty was a significant increase in soot emissions. The soot emissions could be reduced by advancing the main injection timing or reducing the amount of fuel injected in the NVO.

The effect of the glow plug was found to be relatively small compared to the trapped hot residual gases. The observation was that the glow plug had an improving effect on both combustion stability and combustion efficiency but the effect was more apparent at low NVO settings.

The suggested gasoline PPC low load operating strategy is to use NVO with a NVO injection strategy at low engine load up to approximately 2 bar IMEPn and then switch to the rebreathing valve strategy using a split main fuel injection strategy at higher engine load.

7 Future Work

A number of parameters have been evaluated in the experiments for the different strategies in the thesis. There is room for additional improvements that could be made regarding the optimization of the different parameters that were used, for example, fuel injection timing, common rail pressure and NVO injection fuel distribution. There are additional parameters that have not been used in this investigation, for example, inlet air pressure and temperature, which might provide additional benefits if applicable at low engine load operating conditions.

It could also be interesting to investigate the effect of an increased inlet temperature alone, without using the residual gas. One practical application is to use the exhaust heat to raise the temperature of the inlet directly similarly to a fast thermal management system [83].

A low load gasoline PPC strategy has been suggested. The next step is to develop and implement suitable controllers that automatically switch between valve and fuel injection strategy depending on engine load.

An engine simulation tool, AVL Boost, was used to extract temperature and residual gas fractions of the NVO strategy. In order to compare the two strategies in more detail, engine simulations of the rebreathing data could also be made.

To get a deeper understanding of the combustion processes and effects of the different parameters, it would be useful to perform optical diagnostics and CFD simulations. From such investigations it would be possible to quantify the effects of local variations of, for example, fuel and residual gas distribution, from varying residual gas fractions, valve strategy and fuel injection timings.

To extend the low load further, it could be interesting to also investigate the effect of a spark plug, similar to what was shown in work by Yun et al. [24].

8 References

[1] “Emission Standards – European Union – Cars and Light Trucks”, www.dieselnet.com/standards/eu/ld.php

[2] Richter, M., Engström, J., Franke, A., Aldén, M. et al., "The Influence of Charge Inhomogeneity on the HCCI Combustion Process," SAE Technical Paper 2000-01-2868, 2000, doi:10.4271/2000-01-2868

[3] Hultqvist, A., Christensen, M., Johansson, B., Richter, M. et al., "The HCCI Combustion Process in a Single Cycle - Speed Fuel Tracer LIF and Chemiluminescence Imaging," SAE Technical Paper 2002-01-0424, 2002, doi:10.4271/2002-01-0424

[4] Christensen, M., Einewall, P., and Johansson, B., “Homogeneous Charge Compression Ignition (HCCI) using Iso-octane, Ethanol and Natural Gas – A Comparison with Spark Ignition”, SAE Technical Paper 972874

[5] Christensen, M. and Johansson, B., "Supercharged Homogeneous Charge Compression Ignition (HCCI) with Exhaust Gas Recirculation and Pilot Fuel," SAE Technical Paper 2000-01-1835, 2000, doi:10.4271/2000-01-1835

[6] Olsson, J., Tunestål, P., Haraldsson, G., and Johansson, B., "A Turbo Charged Dual Fuel HCCI Engine," SAE Technical Paper 2001-01-1896, 2001, doi:10.4271/2001-01-1896

[7] Martinez-Frias, J., Aceves, S., Flowers, D., Smith, J. et al., "HCCI Engine Control by Thermal Management," SAE Technical Paper 2000-01-2869, 2000, doi:10.4271/2000-01-2869

[8] Haraldsson, G., Tunestål, P., Johansson, B., and Hyvönen, J., "HCCI Combustion Phasing in a Multi Cylinder Engine Using Variable Compression Ratio," SAE Technical Paper 2002-01-2858, 2002, doi:10.4271/2002-01-2858

[9] Olsson, J., Tunestål, P., and Johansson, B., "Closed-Loop Control of an HCCI Engine," SAE Technical Paper 2001-01-1031, 2001, doi:10.4271/2001-01-1031

[10] Willand, J., Nieberding, R., Vent, G., and Enderle, C., "The Knocking Syndrome - Its Cure and Its Potential," SAE Technical Paper 982483, 1998, doi:10.4271/982483

[11] Lavy, J., Dabadie, J., Angelberger, C., Duret, P. et al., "Innovative Ultra-low NOx Controlled Auto-Ignition Combustion Process for Gasoline Engines: the 4-SPACE Project," SAE Technical Paper 2000-01-1837, 2000, doi:10.4271/2000-01-1837

[12] Lang, O., Salber, W., Hahn, J., Pischinger, S. et al., "Thermodynamical and Mechanical Approach Towards a Variable Valve Train for the Controlled Auto Ignition Combustion Process," SAE Technical Paper 2005-01-0762, 2005, doi:10.4271/2005-01-0762

[13] Koopmans, L. and Denbratt, I., "A Four Stroke Camless Engine, Operated in Homogeneous Charge Compression Ignition Mode with Commercial Gasoline," SAE Technical Paper 2001-01-3610, 2001, doi:10.4271/2001-01-3610

[14] Persson, H., Hultqvist, A., Johansson, B., and Remón, A., "Investigation of the Early Flame Development in Spark Assisted HCCI Combustion Using High Speed Chemiluminescence Imaging," SAE Technical Paper 2007-01-0212, 2007, doi:10.4271/2007-01-0212

[15] Koopmans, L., Ström, H., Lundgren, S., Backlund, O. et al., "Demonstrating a SI-HCCI-SI Mode Change on a Volvo 5-Cylinder Electronic Valve Control Engine," SAE Technical Paper 2003-01-0753, 2003, doi:10.4271/2003-01-0753

[16] Milovanovic, N., Blundell, D., Gedge, S., and Turner, J., "SI-HCCI-SI Mode Transition at Different Engine Operating Conditions," SAE Technical Paper 2005-01-0156, 2005, doi:10.4271/2005-01-0156

[17] Kakuya, H., Yamaoka, S., Kumano, K., and Sato, S., "Investigation of a SI-HCCI Combustion Switching Control Method in a Multi-Cylinder Gasoline Engine," SAE Technical Paper 2008-01-0792, 2008, doi:10.4271/2008-01-0792

[18] Kitamura, T., Takanashi, J., Urata, Y., and Ogawa, K., "A Study on Ignition Timing and Combustion Switching Control of Gasoline HCCI Engine," SAE Technical Paper 2009-01-1128, 2009, doi:10.4271/2009-01-1128

[19] Zhang, Y., Xie, H., Zhao, H., "Investigation of SI-HCCI Hybrid Combustion and Control Strategies for Combustion Mode Switching in a Four-Stroke Gasoline Engine," Combustion Science and Technology, 2009, 181:5, 782-799

[20] Shaver, G. M., Roelle, M. J., Gerdes, J. C., "Modeling cycle-to-cycle dynamics and mode transition in HCCI engines with variable valve actuation," Control Engineering Practice, Volume 14, Issue 3, March 2006, Pages 213-222, ISSN 0967-0661, 10.1016/j.conengprac.2005.04.009

[21] Urushihara, T., Hiraya, K., Kakuhou, A., and Itoh, T., "Expansion of HCCI Operating Region by the Combination of Direct Fuel Injection, Negative Valve Overlap and Internal Fuel Reformation," SAE Technical Paper 2003-01-0749, 2003, doi:10.4271/2003-01-0749

[22] Koopmans, L., Ogink, R., and Denbratt, I., "Direct Gasoline Injection in the Negative Valve Overlap of a Homogeneous Charge Compression Ignition Engine," SAE Technical Paper 2003-01-1854, 2003, doi:10.4271/2003-01-1854

[23] Berntsson, A. and Denbratt, I., "Optical study of HCCI Combustion using NVO and an SI Stratified Charge", 2007, doi:10.4271/2007-24-0012

[24] Yun, H., Wermuth, N., and Najt, P., "Development of Robust Gasoline HCCI Idle Operation Using Multiple Injection and Multiple Ignition (MIMI) Strategy," SAE Technical Paper 2009-01-0499, 2009, doi:10.4271/2009-01-0499

[25] Johansson, T., Johansson, B., Tunestål, P., and Aulin, H., "Turbocharging to Extend HCCI Operating Range in a Multi Cylinder Engine- Benefits and Limitations," FISITA2010/F2010A037

[26] Kimura, S., Aoki, O., Ogawa, H., Muranaka, S. et al., "New Combustion Concept for Ultra-Clean and High-Efficiency Small DI Diesel Engines," SAE Technical Paper 1999-01-3681, 1999, doi:10.4271/1999-01-3681

[27] Miles, P. C., Choi, D., Pickett, L. M., Singh, I. P., Henein, N., Rempelewert, B. H., Yun, H., and Reitz, R. D., “Rate-Limiting Processes in Late-Injection, Low Temperature Diesel Combustion Regimes”, Thisel, Valencia, Spain 2004

[28] Akihama, K., Takatori, Y., Inagaki, K., Sasaki, S. et al., "Mechanism of the Smokeless Rich Diesel Combustion by Reducing Temperature," SAE Technical Paper 2001-01-0655, 2001, doi:10.4271/2001-01-0655

[29] Noehre, C., Andersson, M., Johansson, B., and Hultqvist, A., "Characterization of Partially Premixed Combustion," SAE Technical Paper 2006-01-3412, 2006, doi:10.4271/2006-01-3412

[30] Hasegawa, R. and Yanagihara, H., "HCCI Combustion in DI Diesel Engine ," SAE Technical Paper 2003-01-0745, 2003, doi:10.4271/2003-01-0745

[31] Kalghatgi, G., Risberg, P., and Ångström, H., "Advantages of Fuels with High Resistance to Auto-ignition in Late-injection, Low-temperature, Compression Ignition Combustion," SAE Technical Paper 2006-01-3385, 2006, doi:10.4271/2006-01-3385

[32] Kalghatgi, G., Risberg, P., and Ångström, H., "Partially Pre-Mixed Auto-Ignition of Gasoline to Attain Low Smoke and Low NOx at High Load in a Compression Ignition Engine and Comparison with a Diesel Fuel," SAE Technical Paper 2007-01-0006, 2007, doi:10.4271/2007-01-0006

[33] Manente, V., Johansson, B., Tunestal, P., and Cannella, W., “Effects of Different Type of Gasoline Fuels on Heavy Duty Partially Premixed Combustion,” *SAE Int. J. Engines* 2(2):71-88, 2010, doi:10.4271/2009-01-2668

[34] Manente, V., Zander, C., Johansson, B., Tunestal, P. et al., “An Advanced Internal Combustion Engine Concept for Low Emissions and High Efficiency from Idle to Max Load Using Gasoline Partially Premixed Combustion,” SAE Technical Paper 2010-01-2198, 2010, doi:10.4271/2010-01-2198

[35] Manente, V., Johansson, B., Tunestal, P., Sonder, M., Serra, S., ”Gasoline Partially Premixed Combustion: High Efficiency, Low NOx and Low Soot by using an Advanced Combustion Strategy and a Compression Ignition Engine”, FCE09, Istanbul, Turkey, 2009

[36] Manente, V., “Gasoline Partially Premixed Combustion – An Advanced Internal Combustion Engine Concept Aimed to High Efficiency, Low Emissions and Low Acoustic Noise in the Whole Load Range”, Doctoral Thesis, Lund, 2010, ISBN 978-91-628-8144-3

[37] Sellnau, M., Sinnamon, J., Hoyer, K., and Husted, H., "Gasoline Direct Injection Compression Ignition (GDCI) - Diesel-like Efficiency with Low CO2 Emissions," *SAE Int. J. Engines* 4(1):2010-2022, 2011, doi:10.4271/2011-01-1386

[38] Sellnau, M., Sinnamon, J., Hoyer, K., and Husted, H., "Full-Time Gasoline Direct-Injection Compression Ignition (GDCI) for High Efficiency and Low NOx and PM," *SAE Int. J. Engines* 5(2):300-314, 2012, doi:10.4271/2012-01-0384

[39] Hildingsson, L., Kalghatgi, G., Tait, N., Johansson, B. et al., "Fuel Octane Effects in the Partially Premixed Combustion Regime in Compression Ignition Engines," SAE Technical Paper 2009-01-2648, 2009, doi:10.4271/2009-01-2648

[40] Lewander, M., , “Characterization and Control of Multi-Cylinder Partially Premixed Combustion”, Doctoral Thesis, Lund, 2011, ISBN 978-91-7473-148-4

[41] Kokjohn, S., Hanson, R., Splitter, D., and Reitz, R., "Experiments and Modeling of Dual-Fuel HCCI and PCCI Combustion Using In-Cylinder Fuel Blending," *SAE Int. J. Engines* 2(2):24-39, 2010, doi:10.4271/2009-01-2647

[42] Hanson, R., Kokjohn, S., Splitter, D., and Reitz, R., "An Experimental Investigation of Fuel Reactivity Controlled PCCI Combustion in a Heavy-Duty Engine," *SAE Int. J. Engines* 3(1):700-716, 2010, doi:10.4271/2010-01-0864

[43] Solaka, H., Aronsson, U., Tuner, M., and Johansson, B., "Investigation of Partially Premixed Combustion Characteristics in Low Load Range with Regards to Fuel Octane Number in a Light-Duty Diesel Engine," SAE Technical Paper 2012-01-0684, 2012, doi:10.4271/2012-01-0684

[44] Woschni, G., “A Universally Applicable Equation for the Instantaneous Heat Transfer Coefficient in the Internal Combustion Engine”, SAE Trans. 76, SAE Technical Paper 670931, 1967

[45] Tunestål, P., “Estimation of the In-Cylinder Air/Fuel Ratio of an Internal Combustion Engine by the Use of Pressure Sensors”, ”, Doctoral Thesis, Lund University, Faculty of Engineering, 2001

[46] Heywood, J., “Internal Combustion Engine Fundamentals”, MacGraw-Hill, ISBN 0-07-100499-8, 1988

[47] Johansson, T., “Turbocharged HCCI Engine – Improving Efficiency and Operating Range”, Doctoral Thesis, Lund, 2010, ISBN 978-91-7473-061-6

[48] Trajkovic, S., Milosavljevic, A., Tunestål, P., and Johansson, B., "FPGA Controlled Pneumatic Variable Valve Actuation," SAE Technical Paper 2006-01-0041, 2006, doi:10.4271/2006-01-0041

[49] Persson, H., “Spark Assisted Compression Ignition SACI”, Doctoral Thesis, Lund, 2008, ISBN 978-91-628-7578-7

[50] “xPC Target - Perform hardware-in-the-loop simulation and real-time rapid control prototyping”, viewed 2013-01-08, http://www.mathworks.se/products/xpctarget/

[51] Aulin, H., “Turbo Charged Low Temperature Combustion – Experiments, Modeling and Control”, Doctoral Thesis, Lund, 2011, ISSN 0282-1990, ISRN LUMDN/TMHP--11/1078—SE

[52] Strandh, P., “HCCI Operation – Closed loop combustion control using VVA or dual fuel”, Doctoral Thesis, Lund, 2006, ISBN 978-91-628-6845-1

[53] “FPGA Fundamentals”, viewed 2013-01-08, http://www.ni.com/white-paper/6983/en

[54] Wilhelmsson, C., “Embedded Systems and FPGAs for Implementation of Control Oriented Models – Applied to Combustion Engines”, Doctoral Thesis, Lund, 2009, ISBN 978-91-628-7957-0

[55] Tunestål, P., “Self-tuning gross heat release computation for internal combustion engines”, Control Engineering Practice, 1(17), Nov, pp. 518-524, 2009

[56] Gatowski, J., Balles, E., Chun, K., Nelson, F. et al., “Heat Release Analysis of Engine Pressure Data,” SAE Technical Paper 841359, 1984, doi:10.4271/841359

[57] Egnell, R., “Combustion Diagnostics by Means of Multizone Heat Release Analysis and NO Calculation”, SAE Technical Paper 981424, 1998

[58] Ceviz, M.A., Kaymaz, İ., “Temperature and air–fuel ratio dependent specific heat ratio functions for lean burned and unburned mixture,” Energy Conversion and Management, Volume 46, Issues 15–16, September 2005, Pages 2387-2404, ISSN 0196-8904, 10.1016/j.enconman.2004.12.009

[59] Johansson, R., “System Modeling and Identification”, Prentice Hall, Englewood Cliffs, New Jersey, 1993

[60] Tunestål, P., “Model Based TDC Offset Estimation from Motored Cylinder Pressure Data,” 2009 IFAC Workshop on Engine and Powertrain Control, 2009

[61] Bengtsson, J., Strandh, P., Johansson, R., Tunestål, P. and Johansson, B., “Closed-loop combustion control of homogeneous charge compression ignition (HCCI) engine dynamics,” Int. J. Adapt. Control Signal Process., 18: 167–179, 2004, doi: 10.1002/acs.788

[62] Khair, M. K., Jääskeläinen, H., ”Combustion in Diesel Engines”, www.DieselNet.com

[63] Zhao, H., Li, J., Ma, T., and Ladommatos, N., “Performance and Analysis of a 4-Stroke Multi-Cylinder Gasoline Engine with CAI Combustion,” SAE Technical Paper 2002-01-0420, 2002, doi:10.4271/2002-01-0420

[64] Allen, J. and Law, D., “Variable Valve Actuated Controlled Auto-Ignition: Speed Load Maps and Strategic Regimes of Operation,” SAE Technical Paper 2002-01-0422, 2002, doi:10.4271/2002-01-0422

[65] Hyvönen, J., Haraldsson, G., and Johansson, B., "Operating Conditions Using Spark Assisted HCCI Combustion During Combustion Mode Transfer to SI in a Multi-Cylinder VCR-HCCI Engine," SAE Technical Paper 2005-01-0109, 2005, doi:10.4271/2005-01-0109

[66] Hyvönen, J., Wilhelmsson, C., and Johansson, B., “The Effect of Displacement on Air-Diluted Multi-Cylinder HCCI Engine Performance,” SAE Technical Paper 2006-01-0205, 2006, doi:10.4271/2006-01-0205

[67] Johansson, B. and Olsson, K., “Combustion Chambers for Natural Gas SI Engines Part I: Fluid Flow and Combustion,” SAE Technical Paper 950469, 1995, doi:10.4271/950469

[68] Kim, D., Ekoto, I., Colban, W., and Miles, P., "In-cylinder CO and UHC Imaging in a Light-Duty Diesel Engine during PPCI Low-Temperature Combustion," *SAE Int. J. Fuels Lubr.* 1(1):933-956, 2009, doi:10.4271/2008-01-1602

[69] Rothamer, D., Snyder, J., Hanson, R., Steeper, R., Fitzgerald, R., "Simultaneous imaging of exhaust gas residuals and temperature during HCCI combustion," Proceedings of the Combustion Institute, Volume 32, Issue 2, 2009, Pages 2869-2876, ISSN 1540-7489, 10.1016/j.proci.2008.07.018

[70] Zhao, H., Peng, Z., Williams, J., and Ladommatos, N., "Understanding the Effects of Recycled Burnt Gases on the Controlled Autoignition (CAI) Combustion in Four-Stroke Gasoline Engines", SAE Technical Paper 2001-01-3607, 2001, doi:10.4271/2001-01-3607

[71] Weall, A. and Collings, N., "Gasoline Fuelled Partially Premixed Compression Ignition in a Light Duty Multi Cylinder Engine: A Study of Low Load and Low Speed Operation," *SAE Int. J. Engines* 2(1):1574-1586, 2009, doi:10.4271/2009-01-1791

[72] Kook, S., Bae, C., Miles, P., Choi, D. et al., "The Influence of Charge Dilution and Injection Timing on Low-Temperature Diesel Combustion and Emissions," SAE Technical Paper 2005-01-3837, 2005, doi:10.4271/2005-01-3837

[73] Babajimopoulos, A., Lavoie, G., and Assanis, D., "Modeling HCCI Combustion With High Levels of Residual Gas Fraction - A Comparison of Two VVA Strategies," SAE Technical Paper 2003-01-3220, 2003, doi:10.4271/2003-01-3220

[74] McAllister, S., Chen, J., Fernandez-Pello, A. C., ”Fundamentals of Combustion Processes”, Springer, ISBN 978-1-4419-7942-1, 2011

[75] Lewander, M., Johansson, B., Tunestål, P., Keeler, N., Milovanovic, N., Bergstrand, P., ”Closed Loop Control of a Partially Premixed Combustion Engine using Model Predictive Control Strategies”, AVEC’08 Proceeding 006

[76] Hildingsson, L., Johansson, B., Kalghatgi, G., and Harrison, A., "Some Effects of Fuel Autoignition Quality and Volatility in Premixed Compression Ignition Engines," *SAE Int. J. Engines* 3(1):440-460, 2010, doi:10.4271/2010-01-0607

[77] Box, G., E. P., Hunter, J. S., Hunter, W., G., “Statistics for Experimenters: Design, Innovation, and Discovery”, Second Edition, Wiley-Interscience, ISBN-13: 978-0471718130, 2005

[78] Waldman, J., Nitz, D., Aroonsrisopon, T., Foster, D. et al., "Experimental Investigation into the Effects of Direct Fuel Injection During the Negative Valve Overlap Period in an Gasoline Fueled HCCI Engine", SAE Technical Paper 2007-01-0219, 2007, doi:10.4271/2007-01-0219

[79] Aroonsrisopon, T., Nitz, D., Waldman, J., Foster, D. et al., "A Computational Analysis of Direct Fuel Injection During the Negative Valve Overlap Period in an Iso-Octane Fueled HCCI Engine", SAE Technical Paper 2007-01-0227, 2007, doi:10.4271/2007-01-0227

[80] Cao, L., Zhao, H., and Jiang, X., "Investigation into Controlled Auto-Ignition Combustion in a GDI Engine with Single and Split Fuel Injections", SAE Technical Paper 2007-01-0211, 2007, doi:10.4271/2007-01-0211

[81] Berntsson, A., Andersson, M., Dahl, D., and Denbratt, I., "A LIF-study of OH in the Negative Valve Overlap of a Spark-assisted HCCI Combustion Engine", SAE Technical Paper 2008-01-0037, 2008, doi:10.4271/2008-01-0037

[82] Fitzgerald, R. and Steeper, R., "Thermal and Chemical Effects of NVO Fuel Injection on HCCI Combustion", *SAE Int. J. Engines* 3(1):46-64, 2010, doi:10.4271/2010-01-0164

[83] Haraldsson, G., Tunestål, P., Johansson, B., and Hyvönen, J., "HCCI Closed-Loop Combustion Control Using Fast Thermal Management," SAE Technical Paper 2004-01-0943, 2004, doi:10.4271/2004-01-0943

9 Summary of Papers

Paper 1

Investigation and Comparison of Residual Gas Enhanced HCCI using Trapping (NVO HCCI) or Rebreathing of Residual Gases

Patrick Borgqvist, Per Tunestål, and Bengt Johansson

SAE 2011-01-1772, presented by the author at the SAE International Powertrains, Fuels and Lubricants Meeting, 2011, in Kyoto, Japan.

The objectives were to get qualitative comparisons of different HCCI and SI combustion strategies with the variable valve train in terms of efficiencies. The load range was selected based on the attainable operating region for HCCI combustion which was narrow.

The author planned and performed the engine experiments, post-processed the data and wrote the article. The work was supervised by Per Tunestål and Bengt Johansson who both provided valuable feedback.

Paper 2

Investigating Mode Switch from SI to HCCI using Early Intake Valve Closing and Negative Valve Overlap

Anders Widd, Rolf Johansson, Patrick Borgqvist, Per Tunestål, and Bengt Johansson

SAE 2011-01-1775, presented by Anders Widd at the SAE International Powertrains, Fuels and Lubricants Meeting, 2011, in Kyoto, Japan.

A mode switch strategy from SI to HCCI combustion was demonstrated at low engine load. Combustion mode switch is used to be able to operate the engine beyond the limited operating region of HCCI combustion. Two different control strategies for the HCCI combustion, activated after the mode switch, were compared.

Both the author and Anders Widd planned and performed the engine experiments and wrote the paper. Anders Widd was responsible for the controller design and

evaluation. The author was responsible for the LabVIEW implementations and post-processing of the data. This work was supervised by Rolf Johansson, Per Tunestål and Bengt Johansson.

Paper 3

Gasoline Partially Premixed Combustion in a Light Duty Engine at Low Load and Idle Operating Conditions

Patrick Borgqvist, Per Tunestål, and Bengt Johansson

SAE 2012-01-0687, presented by the author at the SAE World Congress, 2012, in Detroit.

This was the first low load gasoline PPC investigation. The objective of this investigation was to compare different fuels, with different RON values, at low engine load and engine speed operating conditions. The goal is to reach idle operating conditions. It was possible to operate the engine at the lowest load with the 69 RON gasoline fuel but the attainable low load operating region of the 87 RON gasoline fuel was limited.

The author planned and performed the engine experiments, post-processed the data and wrote the article. The work was supervised by Per Tunestål and Bengt Johansson who both provided valuable feedback.

Paper 4

The Usefulness of Negative Valve Overlap for Gasoline Partially Premixed Combustion, PPC

Patrick Borgqvist, Martin Tuner, Augusto Mello, Per Tunestål, and Bengt Johansson

SAE 2012-01-1578, presented by the author at the SAE 2012 International Powertrains, Fuels & Lubricants Meeting, 2012, in Malmö

After Paper 3, the focus of the investigations shifted towards extending the attainable low load operating of the 87 RON gasoline fuel. In this investigation the effects of negative valve overlap and the glow plug was investigated. An engine simulation model was used to retrieve information about the residual gas fraction and in-cylinder temperature. The low load limit with the 87 RON gasoline fuel could be extended using NVO. The glow plug was found to have only a small effect in combination with the variable valve train system.

The author planned and performed the engine experiments, post-processed the data and wrote the article. Martin Tuner and Augusto Mello did the AVL Boost engine simulations. The work was supervised by Per Tunestål and Bengt Johansson who both provided valuable feedback.

Paper 5

The Low Load Limit of Gasoline Partially Premixed Combustion Using Negative Valve Overlap

Patrick Borgqvist, Öivind Andersson, Per Tunestål, and Bengt Johansson

ICEF2012-92069, presented by the author at the ASME 2012 Internal Combustion Engine Division Fall Technical Conference, in Vancouver.

The objective of this study was to evaluate more advanced fuel injection strategies in combination with NVO towards the low load limit of gasoline PPC using the 87 RON gasoline fuel. The objective was to see if the NVO requirement could be reduced with a more advanced fuel injection strategy. It was found that the combustion stability could be improved with a single injection with a pilot strategy with a low NVO setting compared to the high NVO setting. But the combustion efficiency remained low compared to the high NVO cases.

The author performed the engine experiments, post-processed the data and wrote the article. Öivind Andersson supervised the experimental planning of the split main fuel injection strategy optimization and provided valuable feedback. The work was also supervised by Per Tunestål and Bengt Johansson who both provided valuable feedback.

Paper 6

Comparison of Negative Valve Overlap (NVO) and Rebreathing Valve Strategies on a Gasoline PPC Engine at Low Load and Idle Operating Conditions

Patrick Borgqvist, Per Tunestål, and Bengt Johansson

SAE 2013-01-0902, the article was submitted and approved for publication at the SAE World Congress, 2013, in Detroit.

A comparison with a rebreathing valve strategy compared to NVO was performed and it was found that similar improvements on combustion stability and unburned hydrocarbon emissions could be achieved towards low load when the same fuel

injection strategy is used. The motivation for using a rebreathing strategy is that the engine efficiency becomes higher. A NVO fuel injection strategy was also evaluated to further extend the low load limit of gasoline PPC. A comparison of the different valve and fuel injection strategies towards low load was given. And it was concluded that the optimal gasoline PPC fuel injection strategy at low load would be to operate the engine with NVO and a NVO fuel injection at the lowest load and switch to the rebreathing strategy when possible to improve the efficiency of the engine.

The author planned and performed the engine experiments, post-processed the data and wrote the article. The work was supervised by Per Tunestål and Bengt Johansson who both provided valuable feedback.

Publication Errata

In Paper 1, Appendix C, the unit of the HC emissions is shown as ppm. The correct unit of the HC emissions here is $ppmC_1$.

In Paper 4, page 14, the injection timing was advanced to keep combustion timing constant, not retarded as stated in the paper.

In Paper 3, page 16, the thermodynamic efficiency is the fraction of the heat released having resulted in indicated work, not mechanical work as stated in the paper.

In Paper 5, page 3, right column, the fuel injection timing of the first fuel injection event is constant -22 CAD ATDC, not BTDC.

In Paper 5, page 5, left column, the pilot injection timing is -60 CAD ATDC, not BTDC.

JSAE 20119058
SAE 2011-01-1772

Investigation and Comparison of Residual Gas Enhanced HCCI using Trapping (NVO HCCI) or Rebreathing of Residual Gases

Patrick Borgqvist, Per Tunestål, Bengt Johansson
Lund University

ABSTRACT

A comparison between throttled and unthrottled spark ignition combustion with residual enhanced HCCI combustion is made. Early intake valve closing and late intake valve closing valve strategies for unthrottled spark ignition combustion are evaluated and compared. Approximately 3-6 percent relative improvement in net indicated efficiency is seen when comparing unthrottled spark ignition combustion with throttled spark ignition combustion depending on valve strategy and engine speed. The relative improvement in efficiency from spark ignition combustion to HCCI combustion is approximately 20 percent for the conditions presented in this study. The rebreathing strategies have the highest efficiency of the cases in this study.

INTRODUCTION

Homogeneous charge compression ignition (HCCI) has been extensively investigated during the past decade due to the potential of achieving high efficiency in combination with low NOx and soot emissions. It was applied to two-stroke engines by Onishi et al. [1] in 1979 and in a four-stroke engine by Najt and Foster [2] in 1983.

For spark ignition (SI) engines, HCCI combustion can be achieved through trapping of hot residual gases. One way, first suggested by Willand et al. [3], is to trap hot residual gases using negative valve overlap (NVO). The first results with NVO HCCI were presented by Lavy et al [4]. This combustion process was named Controlled Auto Ignition (CAI). The alternative to trapping the residuals is to re-induct the residual gases through the exhaust port after the exhaust stroke. This is referred to as rebreathing. For compression ignition engines, the HCCI hybrid concept is known as partially premixed combustion (PPC) [5].

One of the main problems associated with traditional port fuel injected HCCI is the lack of an immediate combustion control actuator. The conditions for the subsequent combustion event are set at intake valve close timing. In addition, the power density is low and high load operation is difficult to achieve without penalty in high acoustic noise. Using either trapped or re-inducted residual gases, combustion is controlled with the valve timings. A method to achieve some additional control actuation and stabilizing effect is to apply spark assistance and was first reported by Koopmans et al. [6]. For PPC combustion the fuel injection timing is the main control actuator.

Hyvönen et al. [7] did a comparison with three multi-cylinder HCCI engines run on U.S. unleaded regular gasoline with different displacements and heated inlet air to control combustion phasing. All the HCCI cases, independent of engine size had about 40 % net indicated efficiency at 2 bar BMEP.

An improvement of fuel consumption up to 21.5 % comparing residual enhanced HCCI with conventional spark-ignited combustion was reported by Kulzer et. al [8]. A fuel consumption reduction of approximately 15-22% running in HCCI mode compared to stoichiometric SI mode was reported by Dahl et al. [9].

The focus of this study is on the residual gas enhanced port fuel injected HCCI combustion in comparison with spark ignited combustion. The spark ignited combustion cases are run both with and without a throttle. In the cases when the engine is run unthrottled, intake valve close timing is used to control air fuel ratio. The compression ratio of the experimental engine is 16.5. This compression ratio is high compared to what is usually seen with CAI combustion engines, which operate with compression ratios between 10:1 and 12:1 [10, 11, 12, 13, 14].

The questions addressed in this study are: What are the relative differences in fuel consumption and emissions between SI and HCCI? What are the relative differences between throttled and unthrottled SI? And what are the relative differences between different valve strategies for residual gas enhanced HCCI combustion cases?

EXPERIMENTAL APPARATUS

ENGINE SETUP

The experimental engine is a Volvo D5 light duty engine. The engine is operating on only one of the five cylinders. The engine is equipped with a fully flexible pneumatic valve train system supplied by Cargine Engineering. The applicability of the Cargine valve train system was first demonstrated by Trajkovic et al. [15]. The valve actuators are placed on an elevated plate above the original diesel fuel injector (not used in this study) and are connected to the valve stems with push-rods. A spark plug is installed in the glow plug hole. The gasoline fuel (RON95) is port fuel injected. The fuel is Swedish commercial gasoline. The engine is run naturally aspirated without cooled external EGR. More engine specifications are listed in Table 1.

Table 1. Engine specifications

Displacement (one cylinder)	0.48 Liters
Bore	81 mm
Stroke	93.2 mm
Compression ratio	16.5:1
Combustion chamber	Pancake cylinder head, modified piston crown
Valve timings	Fully flexible
Maximum valve lift	5 mm
Fuel	Gasoline (RON95), port-fuel injected

The valve lift curves are measured with a MicroStrain displacement sensor fitted below each valve actuator. The valve lift is calculated from the measured valve lift sensor voltage output using linear interpolation between two known reference points.

The valve lift profile is different compared to a standard camshaft valve lift profile. The valve lift open and close rates are faster and cannot be easily controlled in real-time. The maximum vavle lift has been limited to 5 mm. To be able to operate the engine with fully flexible valve strategies, the combustion chamber is modified to have valve clearance at top dead centre enabling full flexibility of the valve timing settings.

The completed piston crown is shown in Figure 1. The piston crown design was inspired by a design presented by Tomoda et al. [16]. The design is made so that the new piston crown can be attached on top of a machined Volvo D5 piston using three screw holes as seen in the photograph.

No simulations or optical measurements have been acquired to quantify the disturbances on flow structure during compression. It is not expected that the combustion chamber geometry is optimal for the combustion processes in this investigation. Conclusions of engine performance parameters, such as emissions and efficiency, are based on relative magnitudes, not absolute.

Figure 1. Installed piston crown

ENGINE CONTROL AND MEASUREMENT SYSTEM

The engine control system is programmed with LabVIEW 2009. LabVIEW is a graphical programming environment developed by National Instruments.

The engine and valve control software is executed on the target PC, which is a dedicated real-time system, NI PXI-8110, running LabVIEW real-time operating system. The PXI system is equipped with an R series multifunction data acquisition card, NI PXI-7853R, with FPGA hardware. The user interface is run on a separate host PC with Windows XP operating system. The host PC communicates with the target PC over TCP/IP.

Pressure trace and valve lift curves are measured crank angle resolved with 0.2 crank angle degrees (CAD) per sample resolution. The cycle resolved data sampling is implemented on the FPGA hardware.

Inlet and exhaust pressures and lambda sensor are sampled at 1 kHz. The 1 kHz samples are measured with an M-series data acquisition card, NI PXI-6251. Temperatures (inlet, exhaust, cooling water, oil) are sampled at a rate of approximately 1 Hz by a Hewlett Packard 34970A data acquisition/switch unit.

Soot is measured with an AVL 415 smoke meter. HC, CO, CO2 and NOx emissions are measured with Horiba Mexa 7500 analyzer system. Soot measurement equipment did not become available until late into the measurement campaign and soot was therefore only measured at selected operating points as HCCI and SI combustion are expected to give low soot levels.

VALVE STRATEGIES

The valve lift curves are measured every cycle simultaneously with the pressure trace. The valve lift curves for the different SI and HCCI cases are seen in Figures 2-7.

The engine is run spark ignited and with HCCI combustion without spark assistance. The spark ignited cases have been run both with conventional valve timings (Figure 2) with a throttle and with wide open throttle with late (Figure 3) or early (Figure 4) intake valve closings, controlling load with IVC. For the cases where either load or combustion phasing is controlled with valve timings, valve curves for both the minimum and maximum load operating points are shown in the same figure. From these figures, it can also be distinguished which valve parameters that have been variable between measurement points and which parameters have been constant.

For the spark ignited cases, combustion is stoichiometric. Combustion timing is controlled with spark timing and load is controlled with either the throttle or intake valve closing timing.

The valve timing calibration factors are, in most cases, automatically controlled and tuned in real-time by the engine control system. The calibration is based on a contact sensor in the valve actuator indicating valve lift after 1 mm displacement. The automatic calibration controller is not used when the EIVC SI valve strategy is applied. When the valve durations are too short the control strategy would have to be adapted to also include the valve lift actuator. This is not supported in the current version of the control system.

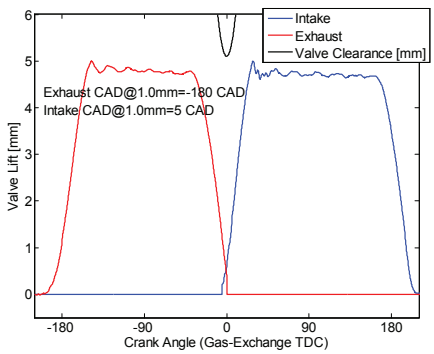

Figure 2. Valve lift curves with standard timings

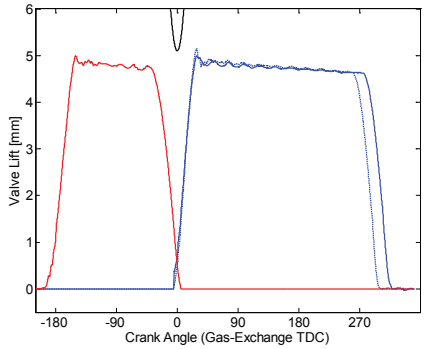

Figure 3. SI LIVC valve lift curves

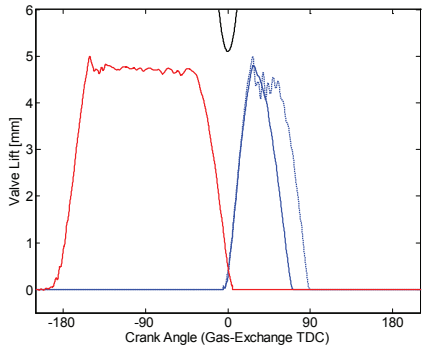

Figure 4. SI EIVC valve lift curves

Different HCCI cases are evaluated and compared; trapping of residual gases using negative valve overlap (NVO), Figure 5, rebreathing of residual gases using late closing of the exhaust valves, Figure 6, or a second exhaust valve opening event during the intake stroke, Figure 7, and finally using an inlet air heater, again, with conventional valve timings. The rebreathing strategy with late exhaust valve closing will be referred to as rebreathing strategy 1 (Reb1). The rebreathing strategy with a second exhaust valve open event will be referred to as rebreathing strategy 2 (Reb2).

For all HCCI cases, combustion is lean. For the negative valve overlap case, combustion timing is controlled with the exhaust valve closing timing. Intake valve open timing is set symmetrically with the exhaust valve closing timing. The Reb1 combustion timing is also controlled with the exhaust valve close timing. The intake valve opening timing is relative to the exhaust valve closing timing. The Reb2 combustion timing is controlled with the exhaust valve opening timing. Intake valve closing timing is relative to exhaust valve opening timing. Combustion timing of the above HCCI cases are automatically controlled with a PI controller with set point 6 CAD ATDC. The combustion timing of the pre-heated air HCCI is manually controlled by adjusting the inlet temperature.

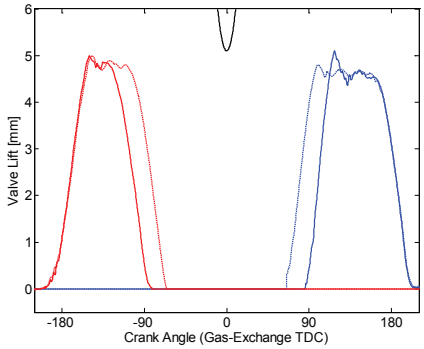

Figure 5. HCCI NVO valve lift curves

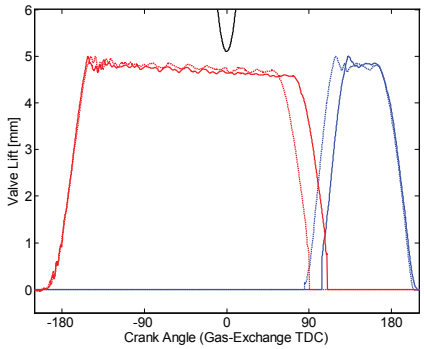

Figure 6. HCCI rebreathing strategy 1 valve lift curves

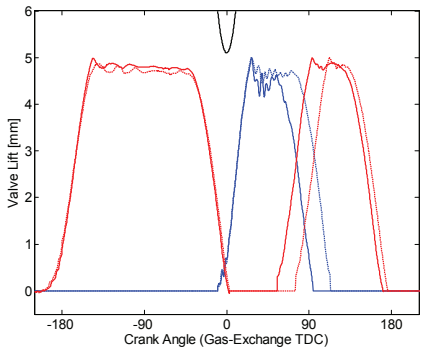

Figure 7. HCCI rebreathing strategy 2 valve lift curves

MEASUREMENT PROCEDURE

The engine is operated at 1500 rpm and 2000 rpm at attainable load conditions for HCCI combustion. Each operating point is sampled at stationary conditions waiting at least five minutes between measurement points after changing either a fuel or valve parameter. At least 500 cycles are recorded for each measurement point. Fuel consumption is measured for at least 6 minutes at a minimum of four operating points for each strategy. In this way the fuel injectors are recalibrated continuously. Engine load is varied in random order.

Valve timing parameters that are not actively used by the control system were optimized and fixed at operating point 1500 rpm 3.5 bar IMEPnet for each valve strategy. For the HCCI cases, measurement sweeps have been performed with varying combustion timings (CA50) but only the optimum in terms of indicated efficiency is presented. The SI combustion timings are set by manually advancing the spark timing until knock is clearly seen on the pressure trace. The spark timing is then retarded and set close to the detected knock limit. This procedure is repeated for all SI measurement points.

At 2000 rpm Reb2 is not included. At this engine speed, the second exhaust valve opening event would be too short to get a stable opening event with the current control system configuration, as explained previously.

RESULTS

PRESSURE TRACE AND HEAT-RELEASE ANALYSIS

Results based on measured cylinder pressure trace analysis are presented here. First, rate of heat release is presented, followed by combustion timing, combustion duration, COV of IMEPnet and finally pressure derivative.

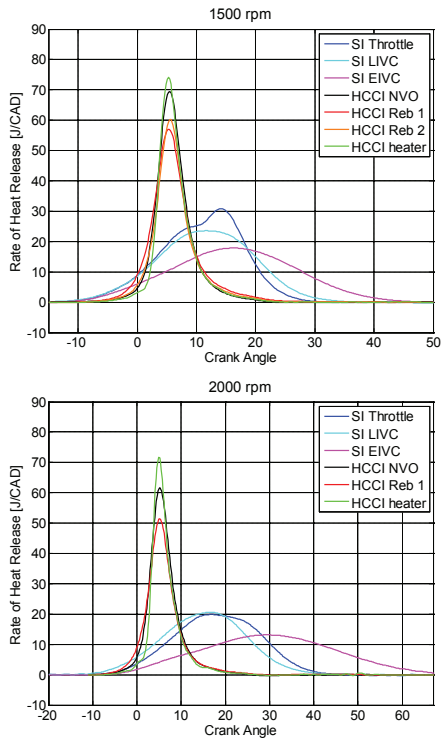

Figure 8. Collected rate of heat-release curves

The rate of heat-release is calculated from measured pressure trace data. The rate of heat-release curves, seen in Figure 8, are the average curves of 500 consecutive cycles from the operating conditions 3.5 bar IMEPnet 1500 rpm and 2000 rpm. The x-axis crank angle interval of the 2000 rpm rate of heat-release figure have been set to have the same interval in time, starting from crank angle 0, as the 1500 rpm rate of heat-release figure.

The burn durations of the SI cases are significantly longer compared to the HCCI cases. Longer burn duration results in lower expansion ratio. The burn duration of the EIVC SI case is the longest, indicating low in-cylinder turbulence, hence slow flame propagation [17]. The shape of the 1500 rpm throttled SI case rate of heat-release curve is different compared to the EIVC and LIVC SI cases. This is because there are more knocking cycles. This is a consequence of insufficient spark timing retardation from the knock limit.

The characteristic rapid combustion of the HCCI cases is clearly seen in the same figure. The peak rate of heat-release is the highest, 74/72 J/CAD, for the pre-heated air HCCI cases, and the lowest for the Reb1 cases, 57/51 J/CAD for 1500 and 2000 rpm operating conditions, respectively.

The rate of heat-release does not change significantly from 1500 rpm to 2000 rpm for the HCCI cases. However, the longer burn duration in crank angle degrees, of the EIVC SI case in particular, result in an even lower expansion ratio.

The combustion timing is seen in Figure 9. Combustion timing is defined as crank angle of 50% accumulated heat released (CA50). The CA50 timings of the spark ignited cases occur significantly later compared to the HCCI combustion timings. The combustion timing of the EIVC SI case has the most retarded combustion timing with CA50 at average 17 CAD ATDC at 1500 rpm and between 20 and 35 CAD at 2000 rpm. The combustion timings of the HCCI cases are stable with low standard deviation at all operating conditions. The standard deviations of CA50 of the spark ignited cases are higher compared to the HCCI cases indicating larger cycle-to-cycle variations.

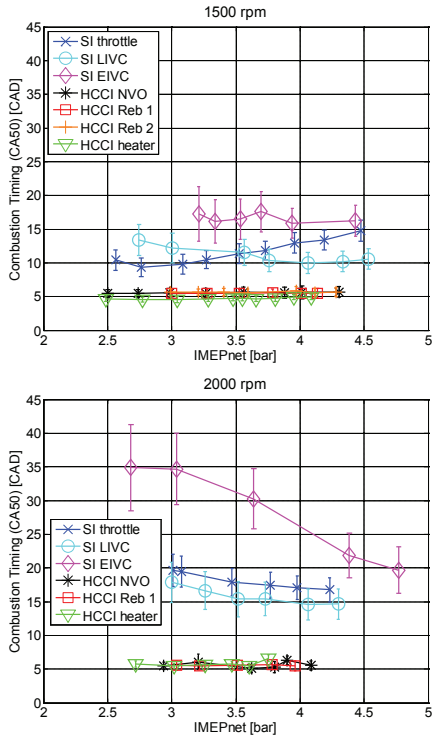

Figure 9. Combustion timing (CA50) with error bars showing plus minus one standard deviation

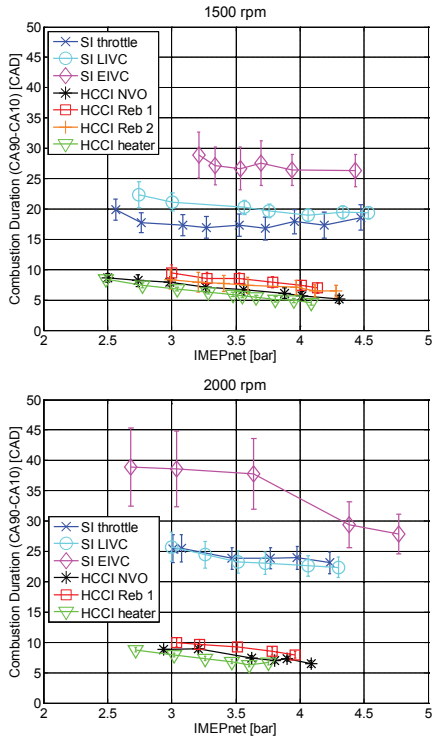

Figure 10. Combustion duration (CA90-CA10) with error bars (plus minus one standard deviation)

The combustion duration is seen in Figure 10. The combustion duration is calculated from CA10 to CA90. The combustion duration of the spark ignited cases using a throttle and late intake valve closing are on average 18 and 20 CAD respectively. The combustion duration of the spark ignited case with early intake valve closing has the longest combustion duration with an average of 27 CAD at 1500 rpm and up to almost 40 CAD at 2000 rpm. The combustion duration of the HCCI cases are short in comparison with durations from 5 to 10 CAD.

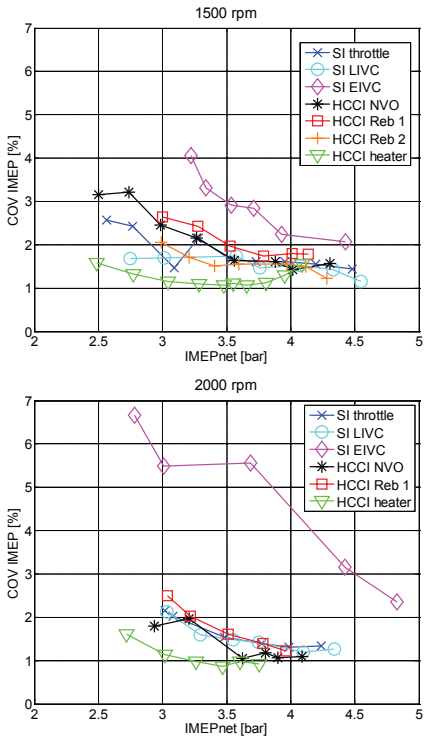

Figure 11. COV IMEPnet

The coefficient of variation of IMEPnet is seen in Figure 11. The COV of IMEPnet is highest for the EIVC spark ignited case and lowest for the pre-heated air HCCI case. Reasons for the high COV of IMEPnet for the EIVC SI case could be the long burn duration (low turbulence) and cycle-to-cycle variations of inducted fresh charge mass due to small variations of the intake valve close timings. Uneven distribution of fuel in the cylinder due to low turbulence leads to variations of equivalence ratio in the vicinity of the spark plug. Conditions in the vicinity of the spark plug, such as turbulent velocity fluctuations and length scales in the flow and equivalence ratio will influence the initial stages of the flame propagation process [18]. From the measured valve lift curves at a single operating point it is seen that the intake valve close timing varies ±2 CAD from cycle-to-cycle. There is then a variation in inducted air fuel mass which affects amount of heat released which in turn affect IMEPnet. Because of the short valve open durations, 65 CAD at 1500 rpm 3.2 bar IMEPnet and 71 CAD at 1500 rpm 4.4 bar IMEPnet, the IVC variations were more apparent for the EIVC SI case compared to the other cases.

For the pre-heated air HCCI case the COV of IMEPnet decreases up to 3.5 bar IMEPnet and then increases. With higher IMEPnet and a more rich air fuel mixture, the pressure rise rate becomes higher and in-cylinder pressure oscillations are apparent. It has been suggested that the pressure oscillations break the thermal boundary layer which increases heat losses. Cycle-to-cycle variations in pressure oscillations cause cycle-to-cycle variations in heat losses which affects IMEPnet [19]. The higher COV of IMEPnet of the residual gas dependent HCCI cases is inherent from the coupling of the combustion from previous cycle due to either trapping or re-induction of residual gases. At lower IMEPnet the residual gas temperature decreases which is compensated with a higher residual gas fraction which in turn leads to higher COV of IMEPnet. The COV of IMEPnet of the residual gas enhanced HCCI cases is close to the COV of the throttle and LIVC SI cases.

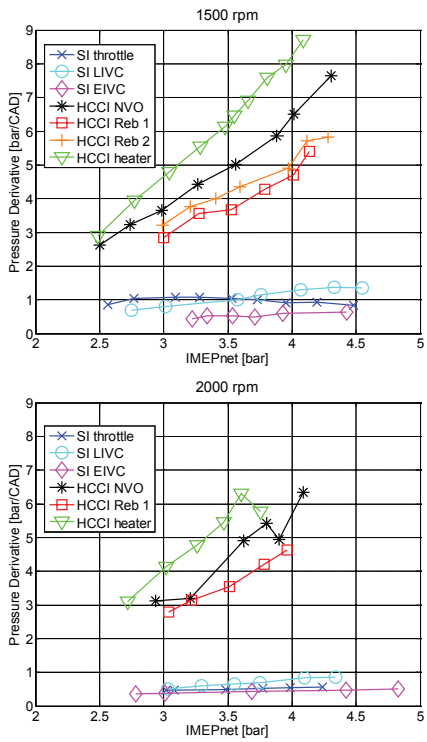

Figure 12. Pressure derivative

For the pressure derivative, Figure 12, there is a clear distinction between HCCI cases and SI cases. There is a small increase with load of the pressure derivative for the EIVC and LIVC SI cases. Depending on valve strategy, if the intake valves are closed either later or earlier to increase the load, the effective compression

ratio is increased which leads to higher in-cylinder peak pressures. The intake air heater controlled HCCI case, with only air to dilute the fuel mixture, has the highest pressure derivative.

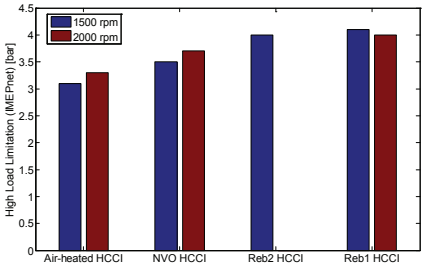

Figure 13. High load limitations of the HCCI cases

If the pressure derivative is used to define the high load limitation, the differences in HCCI operating region for the HCCI strategies can be seen in the same figure. If the limit is set to 5 bar/CAD the operating regions are up to 1500 rpm 3.1 bar IMEPnet and 2000 rpm 3.3 bar IMEPnet for the intake air heater controlled HCCI, 1500 rpm 2.5–3.5 bar IMEPnet and 2000 rpm 2.9-3.7 bar IMEPnet for the NVO HCCI case, 1500 rpm 3.0–4.0 bar IMEPnet for the Reb2 HCCI and case, finally, 1500 rpm 3.0–4.1 bar IMEPnet and 2000 rpm 3.0-4.0 IMEPnet for the Reb1 HCCI case. The high load limitations for the different HCCI cases are seen in Figure 13.

EMISSIONS

Results based on analysis of measured emissions, lambda and exhaust temperature is presented here.

Lambda values are seen in Figure 14. The target lambda of the SI cases is 1.0 (stoichiometric). With lambda 1.0, HC, CO and NOx emissions can be reduced with a three-way-catalyst. The SI cases were run with a small margin on the lean side so that the CO measurement instrument would not saturate. Lambda is the highest for the intake-air heated HCCI case because it is run air-diluted. The NOx reduction of the three-way-catalyst is not necessary because NOx emissions are low for the HCCI cases. High lambda values can then be tolerated for HCCI cases.

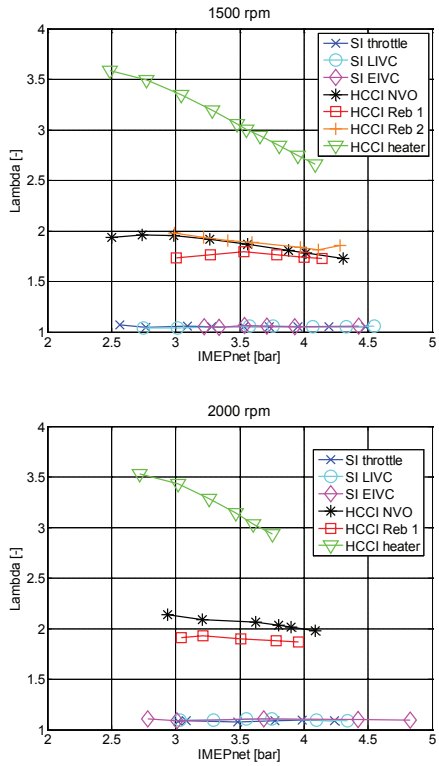

Figure 14. Lambda

For the residual gas enhanced HCCI cases (NVO, Reb1 and Reb2) a fraction of the residual gases are either trapped or re-inducted during the intake stroke. The amount of inducted fresh air per cycle is then reduced which is reflected in the lambda value. No estimation of residual gas fraction has been made but it is expected to be as high as 70-80% for low load operating conditions with low residual gas temperatures. Lambda does not decrease with load as fast for the residual gas enhanced HCCI cases compared to the air-heated HCCI case. The reason is that the residual gas temperature increases with load and the residual gas fraction is then decreased to keep combustion phasing constant. Amount of inducted air is then simultaneously increased as fuel amount (load) is increased which results in lower lambda decrease compared to the air-heated HCCI case.

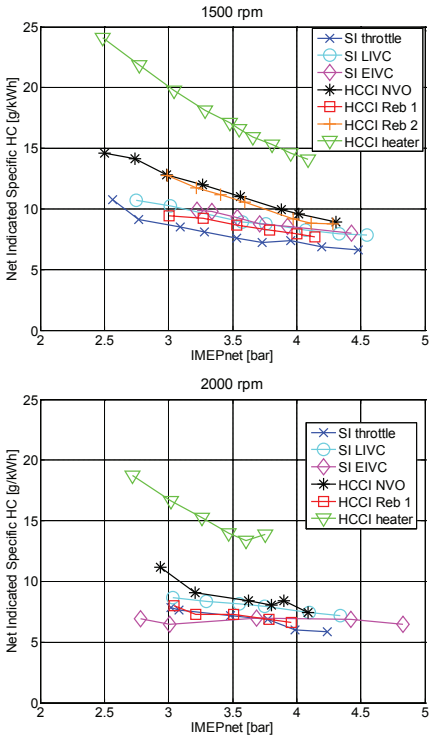

Figure 15. Net indicated specific HC

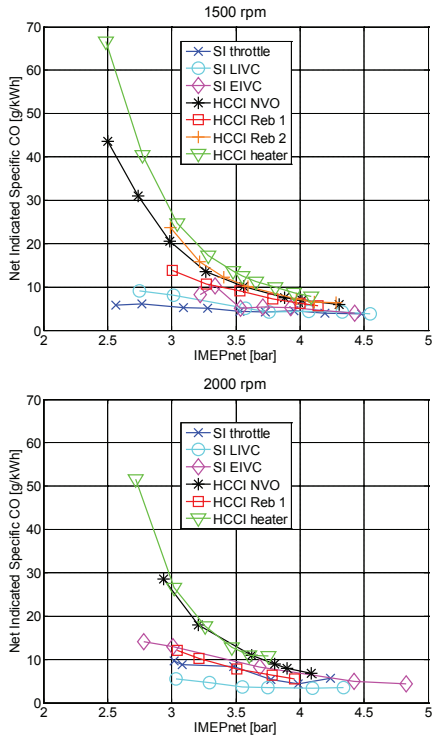

Figure 16. Net indicated specific CO

The net indicated specific HC and CO emissions are seen in Figure 15 and Figure 16 respectively. There is a linear decrease of net indicated specific HC with engine load for all cases and an exponential decrease of net indicated specific CO for the HCCI cases. Generally, for all cases, since the fuel is port fuel injected the major source of HC emissions is from crevices. The contribution of HC due to the screw holes also falls into this category. The combustion chamber is uneven due to the valve pockets which contribute to HC emissions for both the SI and HCCI cases due to wall quenching. Net indicated HC of the air-heated HCCI case is significantly higher compared to the other cases. Looking at the definition of net indicated specific emissions (see Appendix A) one explanation is the high lambda of the air-heated HCCI case. Also, for the residual gas enhanced HCCI cases, a fraction of the unburned gas is used again in the next cycle, having a second chance to combust. This is not the case for the air-heated HCCI case.

CO emissions are a consequence of incomplete oxidation of the fuel to CO_2. For SI combustion, the major source of CO is the air fuel ratio. Insufficient oxygen leads to high levels of CO. For the HCCI cases, CO emissions are formed due to insufficient temperature for complete oxidation to CO_2. The exponential decrease of CO emissions with load for the HCCI cases is explained by the increased temperature with load.

The HC and CO emissions are lowest for the SI cases followed by the residual gas enhanced HCCI (with exception for the Reb1 HCCI case) and the air-heated HCCI case has the highest HC and CO emissions levels. HC and CO emissions will be discussed further in the Efficiencies subsection when discussing the combustion efficiency.

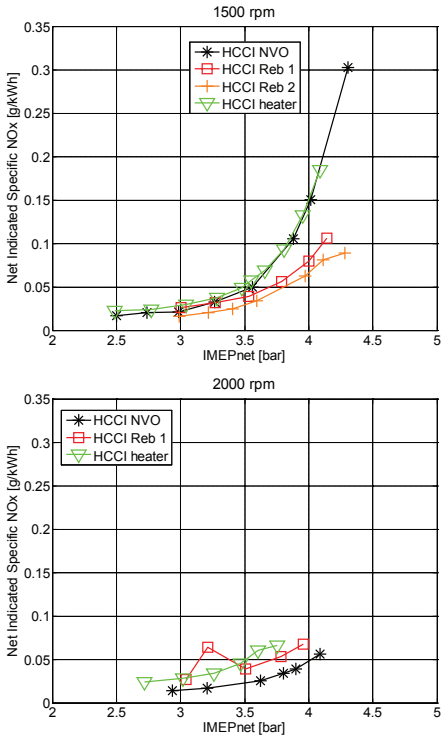

Figure 17. NOx concentration

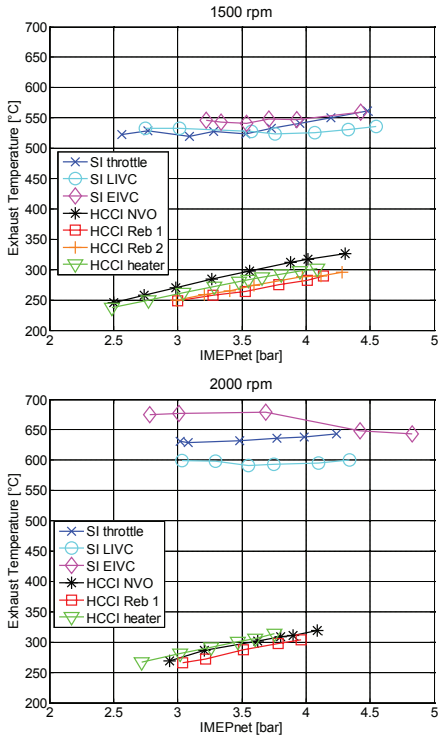

Figure 18. Exhaust temperature

The net indicated specific NOx are shown only for the HCCI cases due to saturation of the measurement instrument when running the SI cases. The limitation of the measurement instrument is approximately 1430 ppm. NOx formation rate is governed by high temperatures and high oxygen concentration [18]. The NOx emissions of the HCCI cases are low, as seen in Figure 17.

NOx emissions increase exponentially with load due to increased temperature. The NVO HCCI case suffers from pumping losses due to recompression of the hot residual gases (will be shown in the Efficiencies subsection). In order to give the same IMEPnet as the other HCCI cases more fuel has to be injected and hence the combustion temperature will be higher for the NVO HCCI case under the same IMEPnet as the other HCCI cases. NOx mole fraction is shown in Appendix B, both against IMEPnet and IMEPgross to illustrate the difference when pumping losses are excluded. The net indicated specific NOx calculation also takes differences in lambda and net specific fuel consumption into account (see definition in Appendix A). The actual mole fraction differences are small if plotted against IMEPgross.

The exhaust temperatures (Figure 18) of the SI cases are approximately doubled compared to the HCCI cases. The burn durations of the SI cases are longer which gives lower expansion ratio and higher exhaust gas temperatures. The SI cases are less diluted compared to the HCCI cases and the adiabatic flame temperature is thus higher. Also, the pumping losses are higher for the throttle and EIVC SI cases (will be shown in the Efficiencies subsection) which means that more fuel is needed for the same IMEPnet as the LIVC SI case.

Soot measurements were taken at 3.5 bar IMEPnet operating point for SI and NVO HCCI cases only. The soot levels were too low to be detected by the measurement system.

EFFICIENCIES

In this subsection, the combustion efficiency, thermodynamic efficiency, gas-exchange efficiency, gross indicated efficiency, net indicated efficiency and the net specific fuel consumption results will be presented and discussed. Definitions of the efficiencies are given in Appendix A.

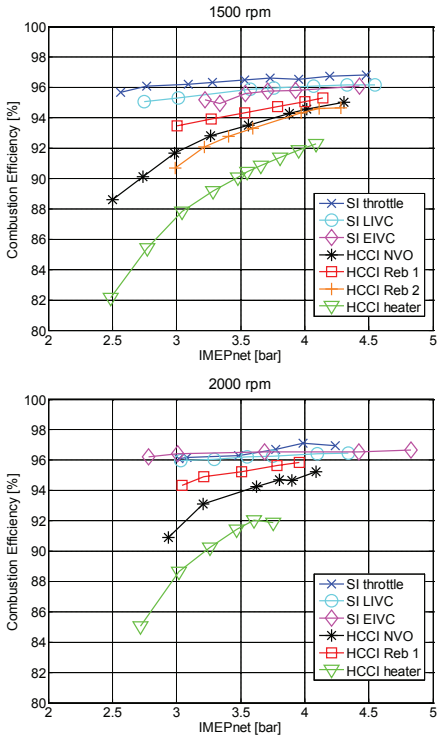

Figure 19. Combustion efficiency

The combustion efficiency is shown in Figure 19. The combustion efficiency of the SI cases, run stoichiometric, is relatively unchanged with load. At 1500 rpm LIVC and EIVC SI have lower efficiency compared to the throttled SI case. At 2000 rpm the difference between SI cases are even lower. The Reb1 HCCI case combustion efficiency is higher than the NVO HCCI case and the Reb2 HCCI case has the lowest combustion efficiency of the residual gas enhanced HCCI cases. The air-heated HCCI case has the lowest combustion efficiency of all cases.

First, looking at the 1500 rpm SI cases, one explanation for the lower combustion efficiency of the EIVC SI case is partial burning due slow combustion. The burn duration and cycle-to-cycle variation figures were shown in Figure 10 and Figure 11. Comparing the HC and CO mole fractions (see Appendix C), it is seen that the HC emissions of the EIVC SI case are the highest followed by the LIVC SI case and then the throttled SI case. Another explanation is the reduced HC oxidation due to lower expansion stroke temperature. In an article by Cleary et al. [20] it was concluded that HC emission levels were 25 % higher for the unthrottled case with EIVC VVA strategy due to lower internal residual mass and lower expansion stroke temperature. Looking at the HC mole fraction at 1500 rpm, it is seen that the HC emissions of the EIVC and LIVC SI cases are approximately 20 % higher compared to the throttled SI case. If the HC mole fraction is plotted against IMEPgross it is seen that the differences between EIVC and LIVC SI are more apparent. This is because the pumping losses of the EIVC SI case are higher which is compensated by injecting more fuel and thus increases the in-cylinder temperature for the same IMEPnet. The EIVC SI case would then have the lowest expansion temperature followed by the LIVC SI case and then the throttled SI case.

Another explanation is the peak cylinder pressure which affects the amount of fuel mass storage within crevice volumes [20]. The in-cylinder peak pressure level is reflected by the burn duration, a longer burn duration results in a lower peak pressure. The burn duration was shown in Figure 10. It is seen that EIVC SI has the longest burn duration, followed by LIVC SI and then throttled SI, in agreement with the HC mole fraction levels. At 2000 rpm the differences in combustion efficiency between the SI cases are even lower. The HC and CO emissions are lower at 2000 rpm compared to 1500 rpm. Looking at the EIVC SI case the burn duration is longer and COV IMEPnet is higher. The lower HC and CO emissions at 2000 rpm are then not explained by reduction of partially burned cycles. In agreement with the discussion above, the in-cylinder temperature could be higher during the expansion stroke, and the burn durations are longer which results in lower peak pressures and reduced amount of fuel in crevices.

Next, comparing the combustion efficiency of the residual gas enhanced HCCI cases, the mole fractions of HC and CO emissions are the highest for the Reb2 HCCI case followed by the NVO HCCI case. For the residual gas enhanced HCCI the composition stratification near TDC can vary significantly [21]. The air-fuel ratio and temperature distribution is expected to vary depending on whether air or residual gas is used to dilute the mixture. It also varies depending on valve strategy. According to Lang et al. [22] the NVO HCCI case has the most stratified charge mixture and highest global in cylinder charge temperature followed by the Reb 1 HCCI case and then the Reb 2 HCCI case, of the residual gas enhanced HCCI cases evaluated in this study. Reb1 HCCI case has the highest combustion efficiency because HC and CO mole fractions and lambda are lower compared to the NVO and Reb2 cases.

At higher IMEPnet the differences in combustion efficiency become less apparent due to reduction of residual gas fraction. The Reb1 HCCI case has the highest residual gas fraction for a given IMEPnet. This is supported by lower lambda (Figure 14), lower pressure derivative (Figure 12) and longer burn duration (Figure 10). One possible explanation for the low HC and CO emissions of the Reb1 HCCI case is then the higher, but more homogeneous, residual gas fraction. The NVO case and Reb2 case have almost the same lambda but the pressure derivative is lower and the burn duration is longer for the Reb2 HCCI case.

The pumping losses are higher for the NVO HCCI case compared to the rebreathing cases. Looking at the HC and CO mole fractions plotted against IMEPgross it is seen that the differences between

NVO and Reb2 HCCI cases are small. The higher combustion efficiency of NVO HCCI compared to Reb2 HCCI is then explained by the difference in additional fuel needed for the NVO HCCI case to give the same IMEPnet. One explanation for the higher HC emissions of the Reb2 HCCI case could be leakage of fuel during the second exhaust valve open event.

The low combustion efficiency of the air-heated HCCI case is explained by the high lambda values.

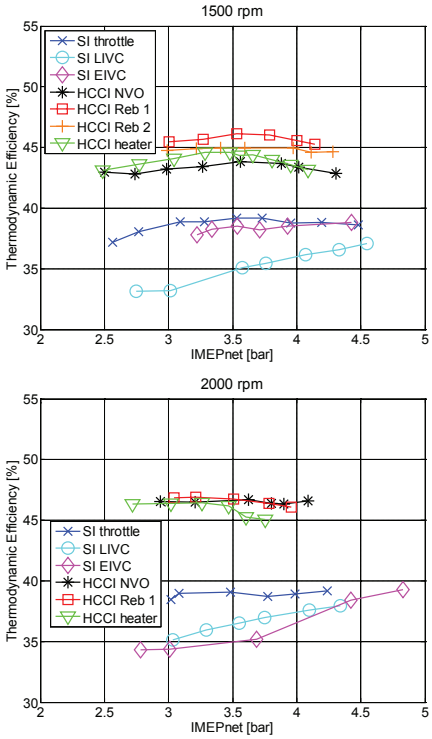

Figure 20. Thermodynamic efficiency

The thermodynamic efficiency is shown in Figure 20. The HCCI cases have higher thermodynamic efficiency explained by the higher expansion ratio compared to the SI cases. At 1500 rpm the thermodynamic efficiency is the highest for the rebreathing HCCI cases followed by the air-heated HCCI case and then the NVO HCCI case. Variations in thermodynamic efficiency can partly be explained by variations of the specific heat ratio from the different residual gas fractions [23]. A higher residual gas fraction leads to a lower specific heat ratio and lower thermodynamic efficiency.

Too short burn duration leads to heat losses due to increased pressure oscillations from steep pressure rise rates and long burn duration leads to a decrease in expansion ratio. For the air-heated HCCI case the specific heat ratio is the highest of the HCCI cases but the problem is with heat losses due to steep pressure rise rates. For the residual gas enhanced HCCI cases the differences in thermodynamic efficiencies can be explained by both variations in residual gas fraction (specific heat ratio) and burn duration. At 1500 rpm the differences in thermodynamic efficiency correlates with the differences in burn duration but this is not the case for the 2000 rpm cases.

Comparing the 1500 rpm SI cases, the LIVC SI case has the lowest thermodynamic efficiency. This is because the air fuel mixture is pushed back into the intake manifold during a part of the compression stroke which results in cooling of the cylinder wall and then increased heat losses. There is a small increase in thermodynamic efficiency for the LIVC SI case at 2000 rpm compared to 1500 rpm explained by less cooling of the cylinder wall. The effect of engine speed on the throttled SI case thermodynamic efficiency is small in comparison. The EIVC SI case thermodynamic efficiency is lower at 1500 rpm compared to 2000 rpm. This is explained by the lower expansion ratio at 2000 rpm. The relative increase of the thermodynamic efficiency with load is higher for the EIVC and LIVC SI cases. A change of intake valve close timing towards higher loads results in an increase in the effective compression ratio. No estimations of the effective compression ratio against IVC have been made.

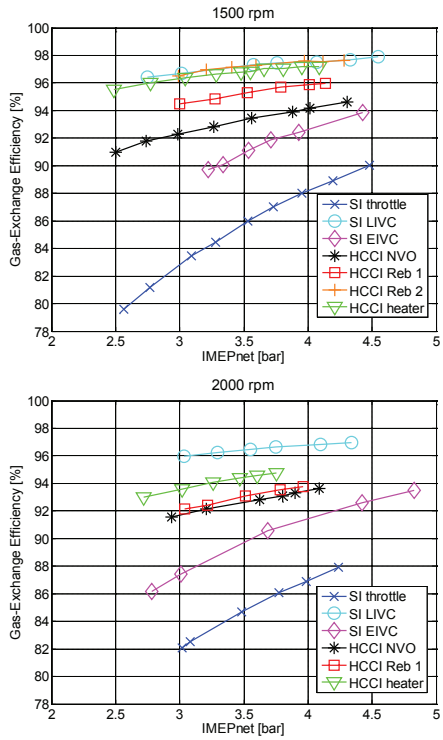

Figure 21. Gas-exchange efficiency

The gas-exchange efficiency is shown in Figure 21. It is defined as the ratio between net and gross indicated work during the complete cycle. Operating conditions with high pumping work result in a low gas-exchange efficiency.

Looking at the 1500 rpm gas-exchange efficiency, the throttled spark ignited case has the lowest gas-exchange efficiency followed by the EIVC spark ignition case. The throttled SI case obviously suffers from throttling losses over the throttle and the EIVC SI case from throttling losses because of the short valve open durations. The gas-exchange efficiency of the LIVC SI case is the highest of all cases at both 1500 rpm and 2000 rpm.

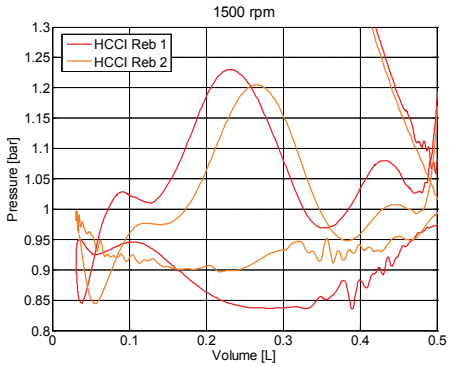

Figure 22. PV diagrams of the gas-exchange stroke from operating condition 3.5 bar IMEPnet

The HCCI case with the lowest gas-exchange efficiency is the NVO case due to recompression of the residual gas resulting in significant heat losses. This will affect the gas-exchange efficiency because the area in the PV-diagram during the residual gas recompression and expansion would ideally be zero in absence of heat losses. But in reality, it becomes negative and lowers the net indicated work, which is the numerator in the definition of the gas-exchange efficiency (see Appendix A).

Reb1 HCCI case has lower gas-exchange efficiency compared to Reb2 HCCI case. Looking at PV-diagrams from 1500 rpm 3.5 bar IMEPnet operating condition (Figure 22) it is seen that the pressure levels during the exhaust stroke have similar trends for both rebreathing strategies but the intake stroke pressure level of the Reb1 HCCI case is lower which results in a larger enclosed negative area in the PV-diagram. The gas-exchange efficiency of the air-heated HCCI case is as high as the Reb2 HCCI case and LIVC SI case gas-exchange efficiencies at 1500 rpm and is lower compared to the LIVC SI case at 2000 rpm.

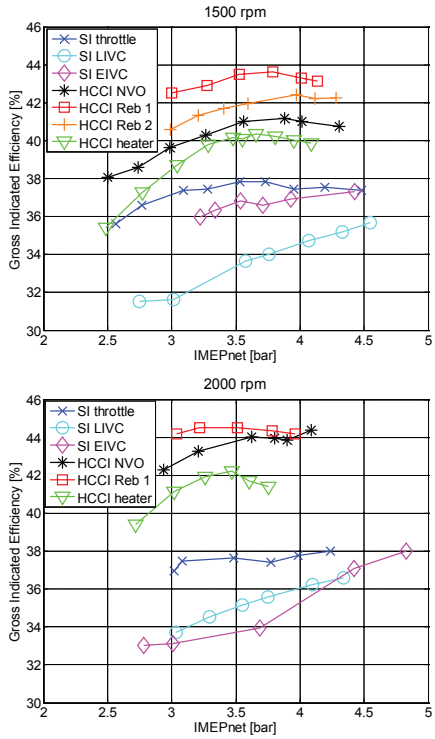

Figure 23. Gross indicated efficiency

Gross indicated efficiency is the product of combustion efficiency and thermodynamic efficiency according to: $\eta_{gross} = \eta_{combustion} \cdot \eta_{therm}$

The gross indicated efficiency is seen in Figure 23. Looking at the SI cases, the gross indicated efficiency is the highest for the throttled SI case. At 1500 rpm the EIVC SI case has higher efficiency than the LIVC and it is the opposite at 2000 rpm. This is explained by the differences in thermodynamic efficiency.

Looking at the residual gas enhanced HCCI cases; the gross indicated efficiency is the highest for the Reb1 HCCI case explained by both the higher combustion efficiency and thermodynamic efficiency. The combustion efficiency of the Reb2 HCCI case was the lowest of the residual gas enhanced HCCI cases but the thermodynamic efficiency was higher than the NVO HCCI case. The NVO HCCI case has the lowest gross indicated efficiency of the residual gas enhanced HCCI cases. The air-heated HCCI case has the lowest gross indicated efficiency which is explained by the low combustion efficiency.

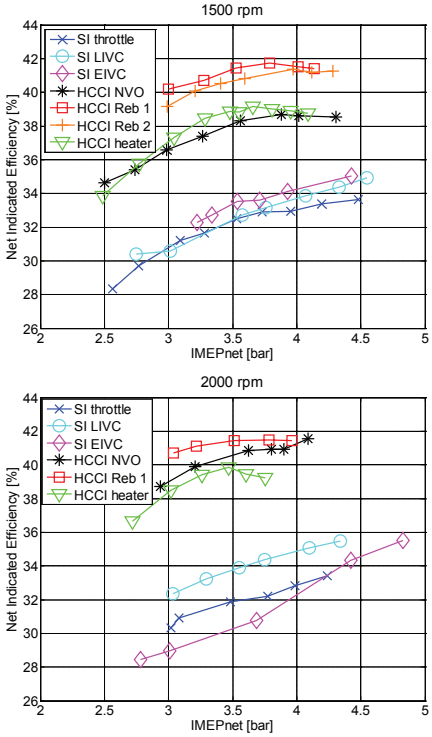

Figure 24. Net indicated efficiency

Figure 24 shows the net indicated efficiency which also takes the gas-exchange efficiency into account according to: $\eta_{net} = \eta_{combustion} \cdot \eta_{therm} \cdot \eta_{ge}$

For the SI cases, when the gas-exchange efficiencies of the throttled SI case and EIVC SI cases are taken into account, the differences in net efficiency compared to gross efficiency become low at 1500 rpm. The EIVC SI case has the highest efficiency, with approximately 3 percent relative improvement over the throttled SI case. At 2000 rpm, the thermodynamic efficiency of the EIVC SI case is the lowest of all SI cases (up to approximately 4.4 bar IMEPnet). Also the gas-exchange efficiency is low compared to the LIVC SI case. As a result, the net indicated efficiency of the EIVC SI case is the lowest of the SI cases at 2000 rpm. At 2000 rpm, the LIVC SI case has the highest net indicated efficiency with approximately 5 percent relative improvement over the throttled SI case.

The net indicated efficiency of Reb1 HCCI case is the highest of all cases evaluated in this study. This is explained by the thermodynamic efficiency, which also was the highest of all cases, in combination with the highest combustion efficiency of the HCCI cases. The gas-exchange efficiency was lower than the Reb2 HCCI case but higher than the NVO HCCI case.

Reb2 HCCI case net indicated efficiency is lower than the Reb1 net indicated efficiency but higher than the NVO HCCI case. Compared to the Reb1 HCCI case, the differences in net indicated efficiency are lower than the gross indicated efficiencies because the Reb2 gas-exchange efficiency is higher. Correspondingly, compared to the NVO HCCI case, the differences in net indicated efficiency are higher than the gross indicated efficiencies because the NVO gas-exchange efficiency is lower.

The net indicated efficiency of the air-heated HCCI case is higher than the NVO HCCI case at 1500 rpm but is lower at 2000 rpm because of the differences in gas-exchange efficiency.

The relative improvement of the Reb1 HCCI case is up to approximately 2 percent compared to the Reb2 HCCI case and approximately 8 and 2 percent compared to the NVO HCCI case at 1500 rpm and 2000 rpm respectively. The relative improvement of the Reb2 HCCI case is approximately 6 percent compared to the NVO HCCI case.

The air-heated HCCI case net indicated efficiency becomes higher than the NVO HCCI case at 1500 rpm because of the lower gas-exchange efficiency of the NVO HCCI case. At 2000 rpm the gas-exchange efficiency of the air-heated HCCI case is lower than at 1500 rpm. The result is that net indicated efficiency of the air heated HCCI case has the lowest net indicated efficiency of all the HCCI cases at 2000 rpm.

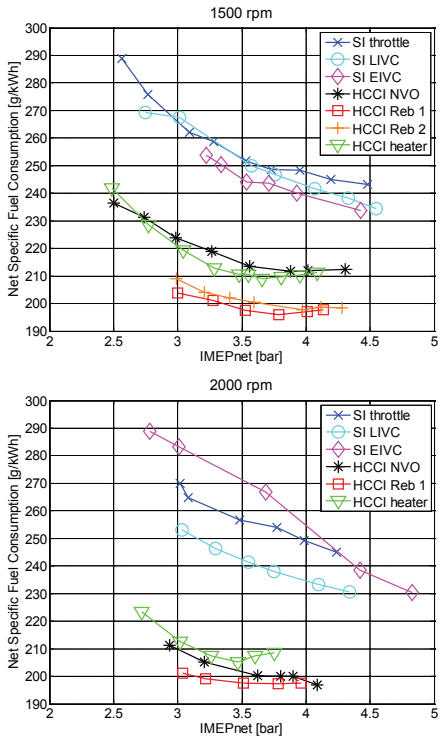

Figure 25. NSFC

The net specific fuel consumption is seen in Figure 25. The net specific fuel consumption of the rebreathing HCCI cases get below 200 g/kWh at 1500 rpm. At 2000 rpm also the net specific fuel consumption of the NVO HCCI case is close to 200 g/kWh.

DISCUSSION

The compression ratio of the experimental engine used in this study is high compared to conventional SI engines and CAI engines. The higher compression ratio is expected to give higher thermodynamic efficiencies but lower combustion efficiencies due to increased fuel mass in crevices. The HCCI displacement study by Hyvönen et al. [7], also included a comparison between two SI cases, run on the same base engine with 0.5 dm^3 cylinder displacement, with high (18:1) and standard (9.5:1) compression ratio. The high compression ratio SI case had highest net indicated efficiency due to higher thermodynamic efficiency. The net indicated efficiency was between 28-32 % at 2-4 bar BMEP for the high compression ratio case in the study, which is in agreement with the SI cases from the present study.

It is important to note that the measurements presented in this study were taken at steady state operating conditions. Any improvements in fuel consumption do not necessarily reflect numbers obtained if it would be possible to drive a complete drive cycle.

The load ranges used in this study are based on the attainable operating region for HCCI combustion. Conclusions drawn from the relative improvements of the SI cases are also drawn within this narrow interval and would perhaps have been somewhat different, if the load range had been wider.

CONCLUSIONS

Comparisons between SI and HCCI combustion using different valve strategies have been made. The combustion chamber had to be modified to get valve clearance around TDC and is not optimal for either SI or HCCI combustion. In addition, the compression ratio was high compared to conventional SI and CAI engines. Conclusions are drawn from relative magnitudes rather than absolute.

- Reb1 HCCI has the highest net indicated efficiency explained by the highest thermodynamic efficiency of all cases and the highest combustion efficiency of the HCCI cases.

- The EIVC SI case has the highest net indicated efficiency of the SI cases at 1500 rpm and the LIVC SI case has the highest efficiency at 2000 rpm. The lower EIVC SI case efficiency at 2000 rpm can be explained by lower thermodynamic and gas-exchange efficiencies.

- The relative improvement in efficiency from EIVC SI to Reb1 HCCI at 1500 rpm is approximately 20 percent and approximately 20 percent from LIVC SI to Reb1 HCCI at 2000 rpm.

- The relative improvement in net indicated efficiency of the EIVC SI case compared to the throttled SI case is approximately 3 percent at 1500 rpm. And the relative improvement of the 2000 rpm LIVC SI case compared to the throttled SI case is approximately 6 percent within the load range evaluated in this study.

- Reb2 HCCI case net indicated efficiency is lower than the Reb1 indicated efficiency but higher than the NVO HCCI case. The relative improvement of the Reb1 HCCI efficiency is up to approximately 2 percent compared to the Reb2 HCCI case and approximately 8 and 2 percent compared to the NVO HCCI case at 1500 rpm and 2000 rpm respectively. The relative improvement of the Reb2 HCCI case is approximately 6 percent compared to the NVO HCCI case.

- The air-heated HCCI case suffers from low combustion efficiency and has the lowest net indicated efficiency of the HCCI cases at 2000 rpm. At 1500 rpm the NVO HCCI case has the lowest efficiency because of low gas-exchange efficiency.

- The HC and CO emissions are lowest for the SI cases followed by the residual gas enhanced HCCI cases. The air-heated HCCI case has the highest HC and CO emissions levels. NOx levels are low for the HCCI cases.

ACKNOWLEDGMENTS

The authors wish to show their appreciation to the Competence Centre Combustion Processes (KCFP), Swedish Energy Agency Grant number 22485-2, for their financial support. The authors would also like to acknowledge Cargine Engineering for supplying and helping with the valve train system. Special thanks are directed to a former colleague at the department, Dr. Thomas Johansson, for valuable discussions regarding the experiments, and the technicians at the department for valuable assistance in the lab.

REFERENCES

1. Onishi S., Jo S. H., Shoda K., Jo P. D., Kato S., “Active Thermo-Atmosphere Combustion (ATAC) – A new Combustion Process for Internal Combustion Engines”, SAE 790501
2. Najt P., Foster D. E., ”Compression-Ignited Homogeneous Charge Combustion”, SAE 830264
3. J. Willand, R-G. Nieberding, G. Vent, C. Enderle, “The knocking Syndrome – Its Cure and its Potential”, SAE Paper 982483

4. J. Lavy, J-C. Dabadie, C. Angelberger, P. Duret, J. Willand, A. Juretzka, J. Schäflein, T. Ma, Y. Lendresse, A. Satre, C. Schultz, H. Krämer, H. Zhao, L. Damiano: “Innovative Ultra-low NOx Controlled Auto-Ignition Combustion Process for Gasoline Engines: the 4-Space Project”, SAE 2000-01-1837
5. V. Manente, B. Johansson, P. Tunestål: “Half Load Partially Premixed Combustion, PPC, with High Octane Number Fuels. Gasoline and Ethanol Compared with Diesel”, SIAT 2009 295
6. L. Koopmans, I. Denbratt, “A Four Stroke Camless Engine, Operated in Homogeneous Charge Compression Ignition Mode with Commercial Gasoline”, SAE 2001-01-3610
7. J. Hyvönen, C. Wilhelmsson, B. Johansson, “The effect of displacement on air-diluted multi cylinder HCCI engine performance “, SAE 2006-01-0205
8. A. Kulzer, W. Fischer, R. Karrelmeyer, C. Sauer, T. Wintrich, K. Benninger, “Homogeneous Charge Compression Ignition on Gasoline Engines - The Potential of CO2 Reduction”, MTZ (worldwide edition) Volume 70, 2009-01
9. D. Dahl, I. Denbratt, L. Koopmans, ”An Evaluation of Different Combustion Strategies for SI Engines in a Multi-Mode Combustion Engine”, SAE 2008-01-0426
10. D. Law, D. Kemp, J. Allen, G. Kirkpatrick, T. Copland: “Controlled Combustion in an IC-Engine with a Fully Variable Valve Train”, SAE 2000-01-0251
11. H. Zhao, J. Li, T. Ma, N. Ladommatos: ”Performance and Analysis of a 4-Stroke Multi-Cylinder Gasoline Engine with CAI Combustion”, SAE 2002-01-0420
12. P. Wolters, W. Salber, J. Geiger, M. Duesmann: “Controlled Auto Ignition Combustion Process with an Electromechanical Valve Train”, SAE 2003-01-0032
13. A. Fuerhapter, W. F. Piock, G. K. Fraidl: “CSI – Controlled Auto Ignition – the Best Solution for the Fuel Consumption – Versus Emission Trade-Off?”, SAE 2003-01-0754
14. L. Cao, H. Zhao, X. Jiang, N. Kalian: ”Effects of Intake Valve Timing on Premixed Gasoline Engine with CAI Combustion”, SAE 2004-01-2953
15. S. Trajkovic, A. Milosavljevic, P. Tunestål, B. Johansson: “FPGA Controlled Pneumatic Variable Valve Actuation”, SAE 2006-01-0041
16. T. Tomoda, T. Ogawa, H. Ohki, T. Kogo, Dr. K. Nakatani, E. Hashimoto, “Improvement of Diesel Engine Performance by Variable Valve Train System”, 30. Internationales Wiener Motorensymposium 2009
17. B. Johansson, K. Olsson, “Combustion Chambers for Natural Gas SI Engines Part I: Fluid Flow and Combustion”, SAE 950469
18. J. Heywood, “Internal Combustion Engine Fundamentals”, page 575, 423, MacGraw-Hill ISBN 0-07-100499-8, 1988
19. T. Tsurushima, Y. Asaumi, Y. Aoyagi: “The effect of Knock on Heat Loss in a Homogeneous Charge Compression Ignition Engine”, SAE 2002-01-108
20. D. Cleary, G. Silvas: “Unthrottled Engine Operation with Variable Intake Valve Lift, Duration, and Timing”, SAE 2007-01-1282
21. A. Babajimopoulos, G. A. Lavoie, D. N. Assanis: “Modeling HCCI Combustion With High Levels of Residual Gas Fraction – A Comparison of Two VVA Strategies”, SAE 2003-01-3220
22. O. Lang, W. Salber, J. Hahn, S. Pischinger, K. Hortmann, C. Bücker, ”Thermodynamical and Mechanical Approach Towards a Variable Valve Train for the Controlled Auto Ignition Combustion Process”, SAE 2005-01-0762
23. J. Olsson, P. Tunestål, J. Ulfvik, B. Johansson: ”The Effect of Cooled EGR on Emissions and Performance of a Turbocharged HCCI Engine”, SAE 2003-01-0743

CONTACT

Corresponding author:
Patrick Borgqvist

Address
Lund University
Dept. of Energy Sciences
Div. of Combustion Engines
P.O. Box 118
221 00 Lund
Sweden

E-mail

patrick.borgqvist@energy.lth.se

DEFINITIONS, ACRONYMS, ABBREVIATIONS

ATDC	After Top Dead Center
BMEP	Break Mean Effective Pressure
CAD	Crank Angle Degree
CAI	Controlled Auto Ignition
CO	Carbon Monoxide
CO2	Carbon Dioxide
COV	Coefficient Of Variation
EIVC	Early Intake Valve Closing
HC	Hydro Carbons
HCCI	Homogeneous Charge Compression Ignition
IMEP	Indicated Mean Effective Pressure
IVC	Intake Valve Closing
LIVC	Late Intake Valve Closing
NOx	Nitrogen Oxides (NO and NO2)
NVO	Negative Valve Overlap
Reb1	Rebreathing with retarded closing of the exhaust valves
Reb2	Rebreathing with a second opening event of the exhaust valves
RON	Research Octane Number
SI	Spark Ignition
VVA	Variable Valve Actuation

APPENDIX A

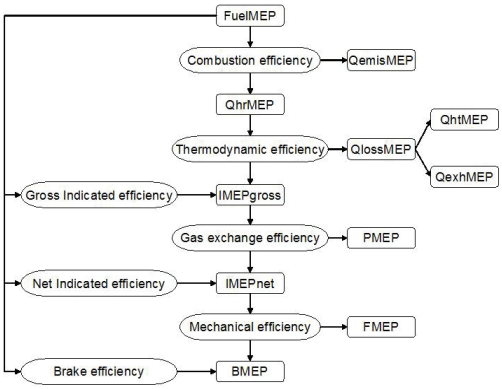

Figure 26. Mean effective pressure flow chart

The definitions of the efficiencies used in this article are given in this section. The efficiencies are calculated with the mean effective pressures, seen in Figure 26.

The *fuel mean effective pressure* is defined as:

$$FuelMEP = \frac{m_f \cdot Q_{LHV}}{V_d}$$

where m_f [kg] is the mass of fuel supplied per cycle, Q_{LHV} [J/kg] is the lower heating value of the fuel, and V_d is the displacement of the engine.

The gross indicated mean effective pressure is defined as:

$$IMEPgross = \frac{\int_{-180}^{180} p \cdot dV}{V_d}$$

The *net indicated mean effective pressure* is defined as:

$$IMEPnet = \frac{\int_{-360}^{360} p \cdot dV}{V_d}$$

where the indicated work per cycle is integrated from the pressure-volume diagram over the entire four-stroke cycle.

The *heat release mean effective pressure* is defined as:

$$QhrMEP = \frac{Q_{HR}}{V_d}$$

where QHR [J] is the heat release during one cycle.

The *combustion efficiency* is defined as:

$$\eta_{combustion} = \frac{QhrMEP}{FuelMEP}$$

but it is calculated from the incomplete combustion products in the exhaust divided with the supplied fuel heat according to:

$$\eta_{combustion} = \frac{\sum_i m_i \cdot Q_{LHV,i}}{m_f \cdot Q_{LHV,fuel}}$$

where m_i [kg] is the mass of the combustion product and $Q_{LHV,i}$ is the lower heating value of the combustion product.

QhrMEP can then be calculated according to:

$$QhrMEP = \eta_{combustion} \cdot FuelMEP$$

The *thermodynamic efficiency* is defined as:

$$\eta_{therm} = \frac{IMEPgross}{QhrMEP}$$

The *gas exchange efficiency* is defined as:

$$\eta_{ge} = \frac{IMEPnet}{IMEPgross}$$

The *gross indicated efficiency* is defined as:

$$\eta_{gross} = \frac{IMEPgross}{FuelMEP}$$

The *net indicated efficiency* is defined as:

$$\eta_{net} = \frac{IMEPnet}{FuelMEP}$$

The *net indicated specific HC, CO and NOx emissions* are defined as:

$$sEM = \left(1 + \lambda\left(\frac{A}{F}\right)_S\right) x_{EM} \frac{M_{EM}}{M_P} \cdot nsfc$$

where *EM* stands for either HC, CO or NOx emissions, x_{EM} is the molar fraction of *EM*, M_P and M_{EM} are the total molar mass and molar mass of *EM* and *nsfc* is the net specific fuel consumption.

APPENDIX B

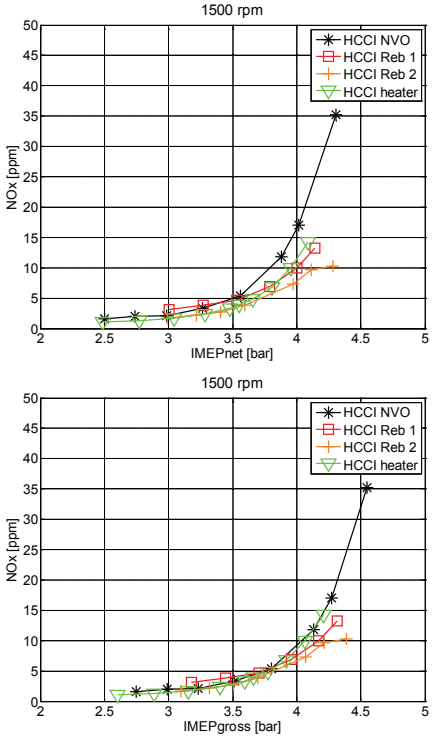

Figure 27. NOx emissions shown against IMEPnet compared with IMEPgross

Figure 27 shows the NOx mole fraction against IMEPnet and IMEPgross. Looking at the NOx mole fraction against IMEPgross it seen that the differences between the HCCI cases are small.

NOx emissions are plotted against IMEPnet in all figures in the Results section to make comparisons between all parameters easier. But, whether the results are presented against IMEPgross or IMEPnet can be of significance for certain parameters.

APPENDIX C

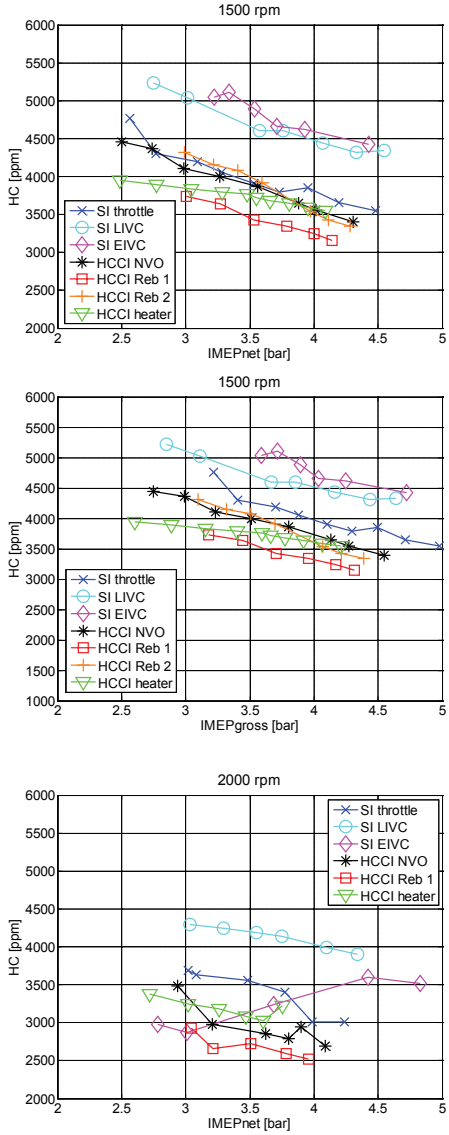

Figure 28. HC mole fraction

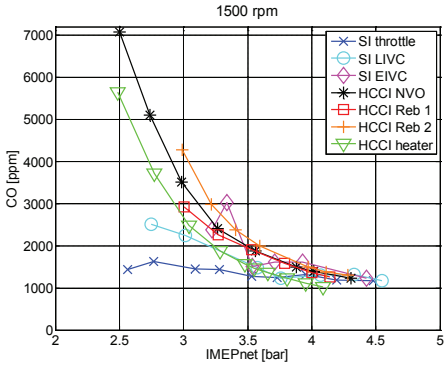

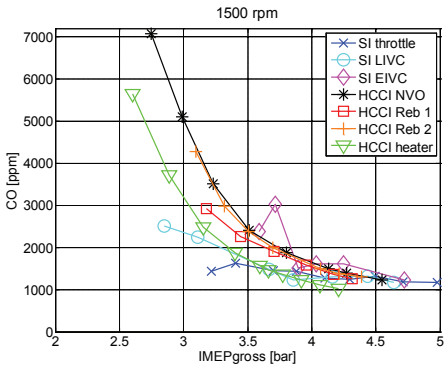

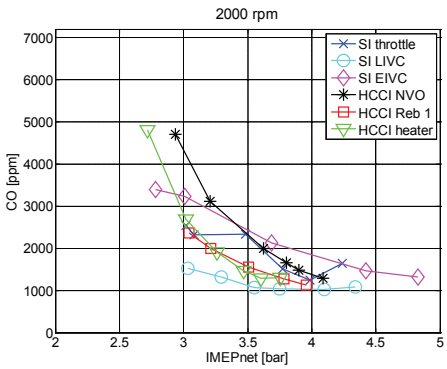

Figure 29. CO mole fraction

2

JSAE 20110923
SAE 2011-01-1775

Investigating Mode Switch from SI to HCCI using Early Intake Valve Closing and Negative Valve Overlap

Anders Widd, Rolf Johansson
Department of Automatic Control, Lund University

Patrick Borgqvist, Per Tunestål, Bengt Johansson
Department of Energy Sciences, Lund University

ABSTRACT

This study investigates mode switching from spark ignited operation with early intake valve closing to residual gas enhanced HCCI using negative valve overlap on a port-fuel injected light-duty diesel engine.

A mode switch is demonstrated at 3.5 bar IMEPnet and 1500 rpm. Valve timings and fuel amount have to be selected carefully prior to the mode switch. During mode transition, IMEPnet deviates by up to 0.5 bar from the set point. The time required to return to the set point as well as the transient behavior of the engine load varies depending on which control structure that is used. Both a model-based controller and a PI control approach were implemented and evaluated in experiments. The controllers were active in HCCI mode. The model-based controller achieved a smoother transition and while using it, the transition could be accomplished within three engine cycles.

The initial deviation in load is unacceptable but can most likely be improved with a predictive mode transition model compared to empirically selected mode transition parameters. Changing the fuel injection method to direct injection instead of port injection is another possible improvement.

INTRODUCTION

Homogeneous charge compression ignition (HCCI) has been extensively investigated during the past decade due to the potential of achieving high efficiency in combination with low NOx and soot emissions [13,14]. For spark ignition (SI) engines, HCCI combustion can be achieved through trapping of hot residual gases. One way, first suggested by Willand et al. [1], is to trap hot residual gases using negative valve overlap (NVO). These types of HCCI hybrids with SI engines are often referred to as controlled auto ignition (CAI) combustion.

One of the main problems associated with traditional port fuel injected HCCI is the lack of an immediate combustion control actuator. The conditions for the subsequent combustion event are set at intake valve close timing. An additional problem is the limited operating range. Low-load operation is limited by insufficient burned gas temperature for auto-ignition in the subsequent cycle. One alternative is to operate the engine in HCCI mode at attainable operating conditions and perform a mode switch to, for example, spark ignited combustion at low-load and high-load operating conditions.

A mode switch strategy on camless port-fuel injected engines was developed by Koopmans et al. [2] on both a single cylinder engine and multi cylinder engine. The mode transition from SI mode to HCCI mode could be made within one engine cycle. Milovanovic et al. [3] presented a mode switch investigation from SI mode to HCCI mode within one cycle using valve profile switching. Fuel was port-fuel injected. Kakuya et al. [4] developed a mode switch strategy on a multi-cylinder direct injected engine from SI mode to HCCI mode. Before complete transition to HCCI mode an intermediate step was taken in order to suppress IMEP fluctuations by controlling A/F ratio and EGR rate with assistance of spark and double fuel injection. Kitamura et al. [5] investigated a HCCI ignition timing model and applied it to combustion mode switching from Otto-Atkinson SI mode (intake valve closing timing occurring late during the compression stroke) to HCCI mode on a port fuel injected multi-cylinder engine. Zhang et al. [8] demonstrated a mode switch from SI mode to HCCI mode by using spark timing, effective compression ratio and residual gas fraction adjustments for control during the transition. A physical model of mode switch was proposed in [12] and evaluated in simulations.

This study investigates mode switching from spark ignited operation with early intake valve closing to residual gas enhanced HCCI using negative valve

overlap on a port-fuel injected light duty diesel engine. The objectives of this study are demonstration of the mode switch principle and evaluation of controllers for combustion timing and load. During combustion mode switch transition, NVO, injected fuel amount and intake valve closing timings were changed over three engine cycles. The valve and fuel parameters during the combustion mode transitions were set prior to mode switching and carried out in open loop. The objective is for the combustion timing and engine load controller to take command as quickly and smoothly as possible after mode switching has been initiated.

The compression ratio of the experimental engine was 16.5:1 which is high compared to what is usually seen for CAI engines, they are usually operated with compression ratios between 10:1 and 12:1 [15, 16, 17, 18, 19]. The complications associated with mode-switching in terms of choosing valve timings and fuel settings during the transition and controller evaluation should still be of interest regardless of the compression ratio.

EXPERIMENTAL APPARATUS

ENGINE SETUP

The experimental engine was a Volvo D5 light duty engine (same setup as in [6]). The engine was run with combustion in only one of the five cylinders. The engine was equipped with a fully flexible pneumatic valve train system supplied by Cargine Engineering [7]. The valve actuators were placed on an elevated plate above the original fuel injector (not used in this study) and connected to the valve stems with push-rods. A spark plug was installed in the glow plug hole. The gasoline fuel (RON95) used was port-fuel injected Swedish commercial gasoline. The engine was run naturally aspirated without cooled external EGR. Additional engine specifications are listed in Table 1.

Displacement (one cylinder)	0.48 Liters
Bore	81 mm
Stroke	93.2 mm
Compression ratio	16.5:1
Combustion chamber	Pancake cylinder head, modified piston crown
Valve timings	Fully flexible
Maximum valve lift	5 mm
Fuel	Gasoline (RON95), port-fuel injected

Table 1. Engine specifications

The valve lift curves were measured with a MicroStrain displacement sensor fitted below each valve actuator. The valve lift was calculated from the measured valve lift sensor voltage output using linear interpolation between two known reference points.

The valve lift profile is different compared to a standard camshaft valve lift profile. The valve lift open and close rates are faster and cannot be easily controlled in real-time. The maximum valve lift was limited to 5 mm. To be able to operate the engine with different valve strategies, the combustion chamber was modified to have valve clearance around top dead center, enabling maximum flexibility of the valve timing settings. This was achieved with a modified piston crown with 5 mm deep valve pockets, as seen in Figure 1. Inspiration for the piston crown design was found in an article by Tomoda et al. [10].

Figure 1. Installed piston crown.

ENGINE CONTROL AND MEASUREMENT SYSTEM

The engine control system was programmed with LabVIEW™ 2009. LabVIEW™ is a graphical programming environment developed by National Instruments.

The engine control software was executed on the target PC, which is a dedicated real-time system, NI PXI-8110, running LabVIEW™ real-time operating system. The PXI system was equipped with an R series multifunction data acquisition card, NI PXI-7853R, with FPGA hardware. The user interface was run on a separate host PC with Windows XP operating system. The host PC communicated with the target PC over TCP/IP. Cylinder pressure trace and valve lift curves were measured crank angle resolved with 0.2 CAD/sample resolution. The cycle resolved data sampling was implemented on the FPGA hardware.

Inlet manifold and exhaust pressures and lambda sensor were sampled at 1 kHz. The 1 kHz samples were measured with an M-series data acquisition card, NI PXI-6251. Temperatures (inlet manifold, exhaust, cooling water, oil) were sampled at a rate of approximately 1 Hz from a logger device manufactured by Hewlett Packard. No emissions were measured during the experiments presented in this article.

MODE SWITCH VALVE STRATEGIES

The engine was run spark ignited (SI) and with HCCI combustion without spark assistance. The spark ignited combustion was run with wide open throttle with early intake valve closing (EIVC). The HCCI combustion was run with negative valve overlap (NVO) to trap hot residuals and control combustion timing. The valve lift curves for both profiles are seen in Figure 2.

For the spark ignited case, combustion was stoichiometric and air fuel ratio was controlled with intake valve close timing. Combustion timing was controlled with spark timing. Due to the high compression ratio, spark timing had to be set to prevent knock rather than maximizing efficiency. For the HCCI case, combustion is lean and combustion timing was controlled with NVO. A higher NVO means earlier closing of the exhaust valve which traps more hot residual gases. The intake valve was opened symmetrically around top dead center.

The valve timings calibration factors were automatically controlled and tuned in real-time by the engine control system in the beginning of each experiment session. The calibration was based on a contact sensor in the valve actuator indicating valve lift after 1 mm displacement. The automatic calibration controller was not continuously used, even though it is possible, when the EIVC SI strategy is used. When the valve durations were too short the control strategy would have to be adapted to also include the valve lift actuator. This is not supported in the current version of the control system.

ENGINE CONTROL AND MEASUREMENT SYSTEM

Cylinder pressure trace and valve lift curves were measured crank-angle resolved with 0.2 CAD/sample resolution. The cycle resolved data sampling was implemented on the FPGA hardware. This enabled increased control of the cycle resolved sampling event and removed problems with cycle drift due to noise acting on the base clock, making the sampling event less sensitive to disturbances. The sampling event was re-synchronized with the TDC pulse every cycle. The FPGA also generated output signals to engine actuators and drivers, such as valve actuators, spark and fuel injectors.

Having the data sampling task and actuator control on the same chip enabled monitoring and automatic shut-down of safety-critical systems, such as fuel injection. For example, if the valves fail to open, the fuel supply could be instantly shut down. Advanced FPGA programming tasks were easily programmed in LabVIEW without any knowledge of other programming languages such as C or VHDL. The data-flow programming paradigm of LabVIEW made FPGA programming intuitive.

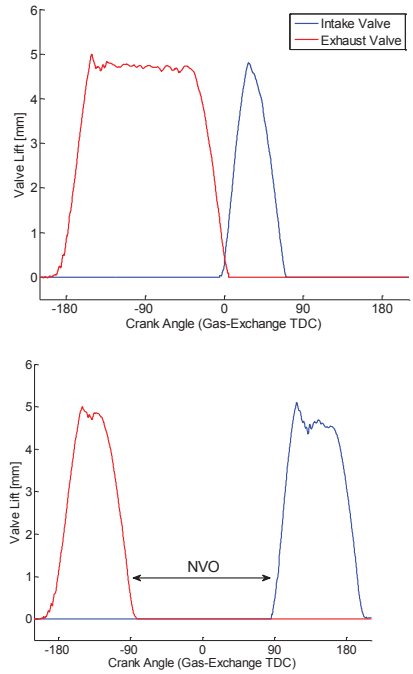

Figure 2. EIVC SI and NVO HCCI valve lift curves.

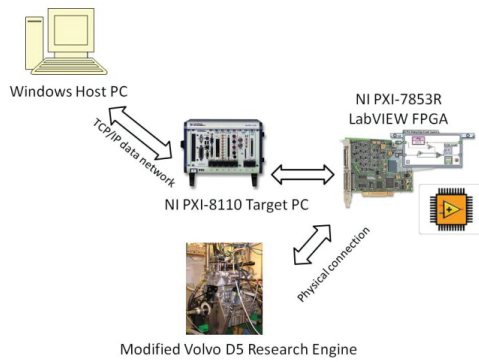

Figure 3. Control system hardware overview.

The medium-speed sampling was carried out by the DAQ hardware, in this case, an M-series card. Moreover, the slow-speed sampling was read from a logger device manufactured by Hewlett Packard.

The engine control software was executed on the target-PC with a dedicated real-time system, PXI-8110, running LabVIEW real-time operating system. The engine control task was divided into several timed loops. By using timed loops it was possible to specify both priority and CPU core. The loop timing interval of each loop was determined either from the data flow or set to fixed timing intervals.

The user interface was run on a separate host computer. The host PC communicated with the dedicated real-time PC over TCP/IP, using network variables. In the control system, the network-transfers were collected in a separate process (timed- loop). In this way, time critical tasks were prevented from being blocked by any overheads associated with network communications.

The front panel of the control system is shown in Appendix A.

In this article, only transitions from EIVC SI to NVO HCCI are presented. Initial experiments were also performed with transitions from late intake valve closing (LIVC) spark ignited combustion, but this was not investigated further.

CONTROLLER DESCRIPTION

Two different control structures were evaluated in experiments: PI control and state-feedback control based on a mathematical model obtained using system identification. The controllers were tuned in the lab to optimize steady-state performance around the nominal steady-state set point of combustion phasing 6 degrees after top dead center and an IMEP of 3.5 bar.

PI CONTROL

Two PI controllers were implemented, one governing IMEP using the fuel injection duration as control signal, and one governing the combustion phasing using NVO as control signal. The controllers were implemented as the discrete-time version of the standard form

$$u = K_{PI}\left(1 + \frac{1}{sT_i}\right)$$

where u is the manipulated variable and K_{PI} and T_i are control design parameters. A block diagram of the control strategy is shown in Fig. 4.

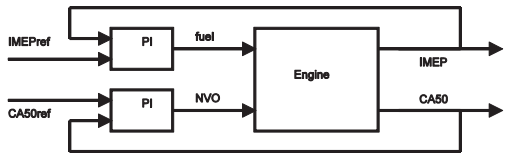

Figure 4. PI Control strategy.

MODEL IDENTIFICATION AND STATE FEEDBACK CONTROL

To enable state feedback control, system identification [11] was used to obtain a model with the fuel injection duration and NVO as inputs and combustion phasing and IMEP as outputs. During the experiments, Pseudorandom Binary Sequence (PRBS) signals were used as inputs covering up to 1.0 bar IMEP and 10 degrees NVO variations. Nine data sets of 1000 cycles were collected and used for cross-validation of the resulting models. The identification was done using the Matlab routine 'pem', a prediction error method, generating state-space models on the form

$$x(k+1) = Ax(k) + Bu(k) + Kw(k)$$
$$y(k) = Cx(k) + w(k)$$

by minimizing the prediction error

$$V(A,B,C,K) = \sum_{k=1}^{N}\left(y(k) - \hat{y}(k|k-1)\right)^2$$

where $\hat{y}(k|k-1)$ is the predicted output at cycle k given a measurement of the previous cycle. The vector of manipulated variables at engine cycle k is denoted u(k), w(k) is uncorrelated white noise, and x(k) is the state vector. The output vector is y(k) and the matrices A, B, C, and K describe the system dynamics and noise properties. For evaluating the models, VAF (variance accounted for) score was used, using the following expression where *var* denotes variance.

$$VAF = 100\left(1 - \frac{var(y - \hat{y})}{var(y)}\right)$$

Table 2 shows the VAF score of 3rd-order and 4th-order order models in cross-validation tests. Overall, the benefit of selecting a fourth-order model was more noticeable in IMEP than in CA50.

Fig. 5 shows a typical cross-validation result with one step ahead prediction using a fourth-order model.

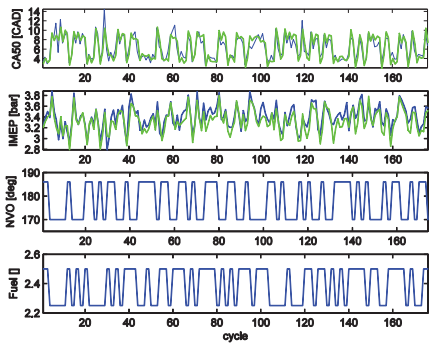

Figure 5: Identification results showing combustion phasing and IMEP as predicted by the model (green) and measured (blue) as well as the control signals NVO and fuel injection duration.

A state feedback controller governing both NVO and fuel injection was designed and implemented in LabVIEW. Reference tracking was introduced using feedforward from the reference signal and the controller did not include integral action. The controller was on the form

$$\hat{x}(k+1) = A\hat{x}(k) + Bu(k) + K\big(y(k) - C\hat{x}(k)\big)$$
$$u(k) = -L\hat{x}(k) + Mr(k) \quad (1)$$

where the second equation constitutes a linear estimator for the state x. The feedback gain L was determined by minimizing

$$J(u) = \sum_{j=0}^{\infty} \left\| Q_y y(j) \right\|_2 + \| Q_u u(j) \|_2$$

where Q_y and Q_u are weighting matrices. The feed forward gain M was chosen so that unit steady state gain was obtained from the reference signal to the outputs. A diagram of the control strategy is shown in Fig. 6. An implementation of the controller where the latest measurement is used to refine the state estimate [20] is given by the following equations.

$$\hat{x}(k+1|k) = A\hat{x}(k|k) + Bu(k)$$
$$\hat{x}(k|k) = \hat{x}(k|k-1) + N\big(y(k) - C\hat{x}(k|k-1)\big)$$
$$u(k) = -L\hat{x}(k|k) + Mr \quad (2)$$

Data set	CA50	IMEP
1	73.64/77.13	70.67/81.76
2	74.77/77.16	71.38/80.72
3	73.37/73.42	69.44/78.01
4	80.12/81.89	69.69/77.19

Table 2: VAF score for 3rd/4th order models.

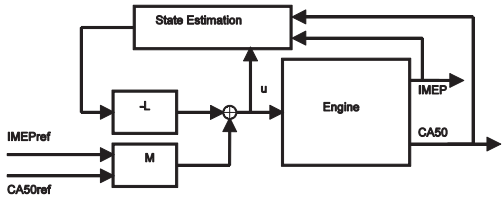

Figure 6. State-feedback control strategy using feedback from estimated state.

RESULTS

OPEN LOOP MODE SWITCH EXPERIMENTS

The initial problem was to burn off the residual fuel in the inlet originating from the port fuel injection system. The amount of residual fuel was sufficient for combustion during one cycle at operating point 3.5 bar IMEP net. The difficulty was to avoid misfire and too steep pressure rise rates. Different NVO and IVC valve settings were tested. All IVC and NVO combinations and the resulting IMEP net from the cycle burning residual fuel were collected and summarized in Figure 7. The black circles show the actual measurement points.

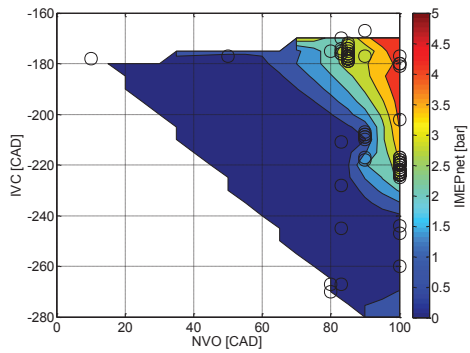

Figure 7. Map of IMEP net from cycle running with residual fuel only as a function of IVC and NVO.

Mode switch sequences are shown in Appendix B and C. The switch is initiated in the engine cycle denoted cycle 0 by disabling the fuel injection and adjusting the exhaust valve to trap hot exhausts. This generates a temperature increase in the charge in cycle 1 where the fuel trapped in the intake port is burned. To avoid misfire and obtain a reasonable pressure rise rate, the inlet valve closing timing must also be selected carefully. After combustion in cycle 1, the fuel injection is activated again and operation proceeds in HCCI mode. As shown in Appendix B and C, NVO and IVC were adjusted gradually to the approximate operating values of 170 and -180 crank angle degrees. The map

in Fig. 4 was used to determine suitable values for these variables.

Figure 8 shows the rate of heat release during a mode switch. The cycle where the trapped fuel was burned exhibited a comparatively high rate of heat release and the combustion then transitions into HCCI.

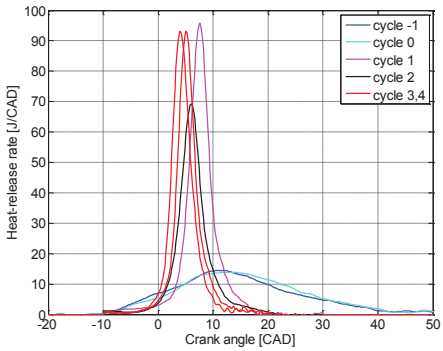

Figure 8. Collected heat-release rate curves during mode switch from SI to HCCI. The cycle numbering corresponds to that in Appendix B and C.

CLOSED LOOP MODE SWITCH EXPERIMENTS

Both control strategies were tested experimentally with varying mode switch sequences. The PI controllers could be activated following a switching sequence of 4 engine cycles while the state feedback controller could be activated after 3 engine cycles.

Figures 9 and 10 show IMEP and CA50 while using state feedback control during a mode switch. The experimental settings were identical in both experiments. In both cases, the control action is fairly smooth after the brief deactivation of the fuel injection during cycle 1 one of the mode switch. Combustion phasing is controlled at its set point within a few cycles and IMEP is within 5% of its set point after just under 60 engine cycles.

Figures 11 and 12 show the corresponding results when using the PI controllers. Both experiments exhibited oscillations in both outputs, particularly in IMEP. There were some variations in the intensity of the oscillations but the general behavior was the same.

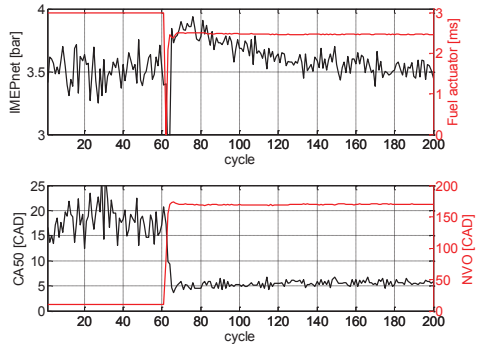

Figure 9. Mode switch using the model-based controller. The top plot shows IMEP in black against the left axis and fuel injection duration in red against the right axis. The bottom plot shows CA50 in black against the left axis and NVO in red against the right axis.

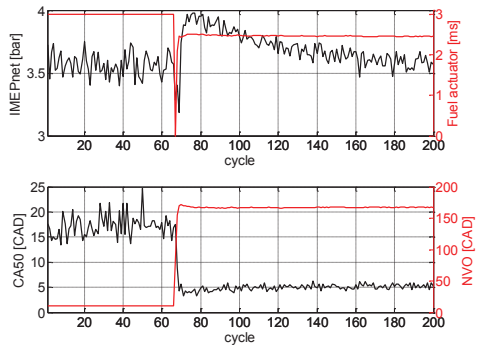

Figure 10. Mode switch using the model-based controller. The top plot shows IMEP in black against the left axis and fuel injection duration in red against the right axis. The bottom plot shows CA50 in black against the left axis and NVO in red against the right axis.

DISCUSSION

Using port injection in the EIVC mode created a need for disabling the fuel injection during the transition in order to burn the fuel trapped in the intake port. A possible future improvement would be to use direct injection since that should allow for a faster switch with no intermediate cycle. The model-based controller could also be improved by separating the observer into a time update and a measurement update as shown in (2). This would give a better state vector estimate and more accurate control.

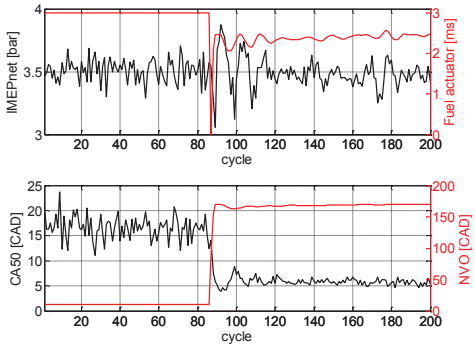

Figure 11. Mode switch using the PI controllers. The top plot shows IMEP in black against the left axis and fuel injection duration in red against the right axis. The bottom plot shows CA50 in black against the left axis and NVO in red against the right axis.

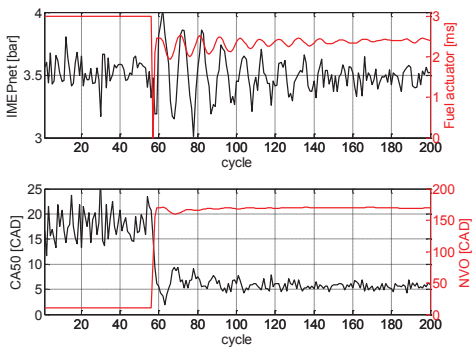

Figure12. Mode switch using the PI controllers. The top plot shows IMEP in black against the left axis and fuel injection duration in red against the right axis. The bottom plot shows CA50 in black against the left axis and NVO in red against the right axis.

Borgqvist et al. [6] made a comparison between SI and HCCI combustion using different valve strategies, on the same engine that was used in this study. One of the results was that the SI case with EIVC valve strategy suffers from high cycle-to-cycle variations of IMEPnet compared to the other SI cases investigated in the study (LIVC SI and throttled SI). High cyclic variation of combustion is a problem during mode switch because the cycles are linked through the trapped hot residual gases. Large variations of temperature of the residual gases from SI mode affect the outcome of the transition to HCCI mode. One alternative could be to use the LIVC strategy in SI mode. With this strategy, however, a fraction of the air fuel mixture is pushed back in to the intake manifold during the compression stroke. This introduces an additional complication which could be investigated further as future work.

In order to have an entirely automated transition it would be necessary to monitor the states of the combustion more thoroughly during SI combustion mode. This information could be fed to an intermediate model-based controller that would determine the valve and fuel parameter settings during the transition. To improve the HCCI combustion controller, the intermediate controller could provide the initial states to the HCCI combustion controller. The results in Figs. 9-12 show a decrease in IMEP during the first cycle of the transition followed by a recovery. The decrease occurs since the fueling during the transition was chosen conservatively to avoid high peak pressures and pressure rise rates.

Among the previously reported results, the majority focus on finding viable transition sequences. In [12], a model-based strategy for scheduling SI-HCCI transitions was presented. It was evaluated in simulation and provided fairly constant ignition timing and work output. A previous experimental study was reported in [8], also using port-injected fuel. The SI-HCCI transition was accomplished over three engine cycles and the variation in IMEP could be reduced to 0.3 bar during the transition. This compares well with the results in this study where the mode switch was accomplished over three engine cycles with a maximum deviation of 0.5 bar.

Two control strategies were evaluated in the experiments. The state-feedback controller was based on a third-order model obtained using system identification. The model order is comparable to physics-based modeling of HCCI were two states have been used to describe combustion phasing [9]. The third state then corresponds to the load dynamics. The model-based approach provided a smoother transient and could also be activated one cycle earlier than the PI approach as seen in Figs. 9-10 and 11-12. The PI controllers generated ringing in both outputs following the mode switch, particularly in IMEP.

The main benefit of the model-based controller is that interference between the control objectives could be avoided. By studying, e.g., the NVO signal in the experimental results in Figs. 9 and 10, it is seen that the model-based controller does a small peak to compensate for the change in fueling. The same transient using the PI controllers, shown in Figs. 11 and 12, exhibits a rather large peak with a longer duration which is rather in response to the effects of the load controller. Using NVO to control HCCI introduces the possibility of cycle-to-cycle control but demands careful tuning as the effect of a specific NVO depends on the burned gas temperature of the previous cycle. Model-based design is a useful tool for achieving this objective.

CONCLUSION

An experimental study of EIVC SI to NVO HCCI mode switch was performed. Particular care had to be taken to ensure that any fuel trapped in the intake port was burned as a first step of the mode switch. To avoid misfire or high pressure rise rates, a map of the effects of NVO and IVC during this cycle was put together. A model-based controller was implemented to stabilize the HCCI operation with the desired IMEP and CA50. For comparison, two PI controllers were implemented and evaluated. The advantage of the model-based controller was mainly evident in a smoother IMEP with no ringing.

ACKNOWLEDGEMENT

This research was supported by KCFP Closed-Loop Combustion Control, KCFP (Competence Center Combustion Processes)—Swedish Energy Adm. Ref. 22485-1

REFERENCES

1. J. Willand, R-G. Nieberding, G. Vent, C. Enderle, “The knocking Syndrome – Its Cure and its Potential”, SAE 982483
2. L. Koopmans, H. Ström, S. Lundgren, O. Backlund, I. Denbratt, ”Demonstrating a SI-HCCI-SI Mode Change on a Volvo 5-Cylinder Electronic Valve Control Engine”, SAE 2003-01-0753
3. N. Milovanovic, D. Blundell, S. Gedge, J. Turner, “SI-HCCI-SI Mode Transition at Different Engine Operating Conditions”, SAE 2005-01-0156
4. H. Kakuya, S. Yamaoka, K. Kumano, S. Sato, ”Investigation of a SI-HCCI Combustion Switching Control Method in a Multi-Cylinder Gasoline Engine”, SAE 2008-01-0792
5. T. Kitamura, J. Takanashi, Y. Urata, K. Ogawa, ”A Study on Ignition Timing and Combustion Switching Control of Gasoline HCCI Engine”, SAE 2009-01-1128
6. P. Borgqvist, P. Tunestål, B. Johansson: “Investigation and Comparison of Residual Gas Enhanced HCCI using Trapping (NVO HCCI) or Rebreathing of Residual Gases”, JSAE 20119058
7. S. Trajkovic, A. Milosavljevic, P. Tunestål, B. Johansson: “FPGA Controlled Pneumatic Variable Valve Actuation”, SAE Paper 2006-01-0041
8. Y. Zhang, H. Xie, H. Zhao: ”Investigation of SI-HCCI Hybrid Combustion and Control Strategies for Combustion Mode Switching in a Four-stroke Gasoline Engine”, Combustion Science and Technology, 181:5, 782-799
9. A. Widd, K. Ekholm, P. Tunestål, R. Johansson: ”Experimental Evaluation of Predictive Combustion Phasing Control in an HCCI Engine using Fast Thermal Management and VVA”, Proc. 2009 IEEE Multi-Conference on Systems and Control, St Petersburg, Russia, July 2009, pp. 334-339.
10. T. Tomoda, T. Ogawa, H. Ohki, T. Kogo, K. Nakatani, E. Hashimoto, ”Improvement of Diesel Engine Performance by Variable Valve Train System”, Int. J. Engine Research, 11:5, 2010, pp. 331-344.
11. R. Johansson, “System Modeling and Identification”, Prentice Hall, Englewood Cliffs, New Jersey, 1993.
12. M. Roelle, G. M. Shaver, J. C. Gerdes, ”Tackling the transition: a multi-mode combustion model of SI and HCCI for mode transition control”, IMECE2004-62188, Proc. IMECE’04, CA, USA, Nov 2004.
13. J. Bengtsson, P. Strandh, R. Johansson, P. Tunestål, and B. Johansson, “Hybrid Modelling of Homogeneous Charge Compression Ignition (HCCI) Engine Dynamics—A Survey”, Int. Journal of Control, Vol. 80, No. 11, pp. 1814-1848, 2007
14. J. Bengtsson, P. Strandh, R. Johansson, P. Tunestål and B. Johansson. Hybrid Control of Homogeneous Charge Compression Ignition (HCCI) Engine Dynamics, Int. Journal of Control, Vol. 79, No. 5, pp. 422–448, 2006.
15. D. Law, D. Kemp, J. Allen, G. Kirkpatrick, T. Copland: “Controlled Combustion in an IC-Engine with a Fully Variable Valve Train”, SAE 2000-01-0251.
16. H. Zhao, J. Li, T. Ma, N. Ladommatos: ”Performance and Analysis of a 4-Stroke Multi-Cylinder Gasoline Engine with CAI Combustion”, SAE 2002-01-0420.
17. P. Wolters, W. Salber, J. Geiger, M. Duesmann: “Controlled Auto Ignition Combustion Process with an Electromechanical Valve Train”, SAE 2003-01-0032.
18. A. Fuerhapter, W. F. Piock, G. K. Fraidl: “CSI – Controlled Auto Ignition – the Best Solution for the Fuel Consumption – Versus Emission Trade-Off?”, SAE 2003-01-0754.
19. L. Cao, H. Zhao, X. Jiang, N. Kalian: ”Effects of Intake Valve Timing on Premixed Gasoline Engine with CAI Combustion”, SAE 2004-01-2953.
20. R. Johansson: “Predictive and Adaptive Control”, Lecture Notes, Lund University, August 2010.

CONTACT

Corresponding author: Anders Widd, Department of Automatic Control, Lund University, Box 118, SE 221 00, Lund, Sweden, anders.widd@control.lth.se.

DEFINITIONS, ACRONYMS, ABBREVIATIONS

CA50: Crank angle of 50% fuel burned

CAD: Crank Angle Degree

EIVC: Early Intake Valve Closing

FPGA: Field Programmable Gate Array

HCCI: Homogeneous Charge Compression Ignition

IMEP: Indicated Mean Effective Pressure

NVO: Negative Valve Overlap

PI (control): Proportional Integral (control)

SI: Spark Ignition

VAF: Variance Accounted For

APPENDIX A

LabVIEW control system front panel.

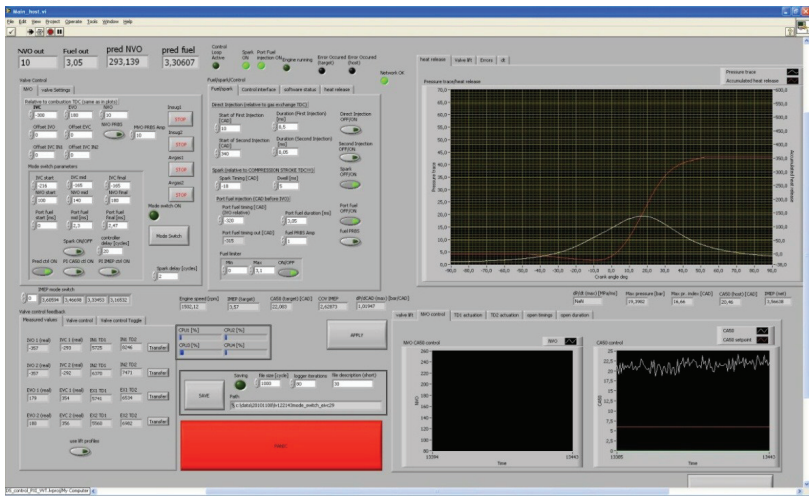

APPENDIX B

Mode switch sequence from EIVC SI to NVO HCCI. The blue and red curves are the intake and exhaust valve lift curves. The curves have been rescaled to fit in the same figure as the pressure trace. The maximum lift of both the intake and exhaust valves is 5 mm. The black curves are the pressure trace and the rescaled port fuel injector command signal from the control system.

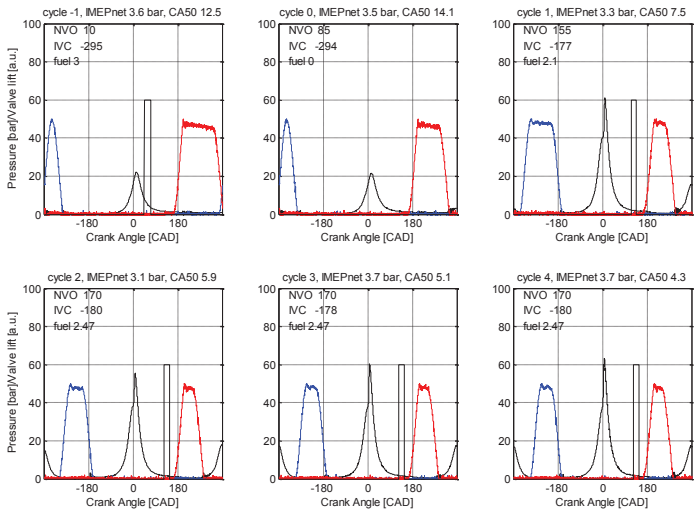

APPENDIX C

Mode switch sequence from EIVC SI to NVO HCCI. The sequence is an example of a mode switch transition with steep pressure rise rates. The accumulated fuel from the misfire in cycle 2 caused violent combustion with high peak pressures and pressure rise rates in subsequent cycles.

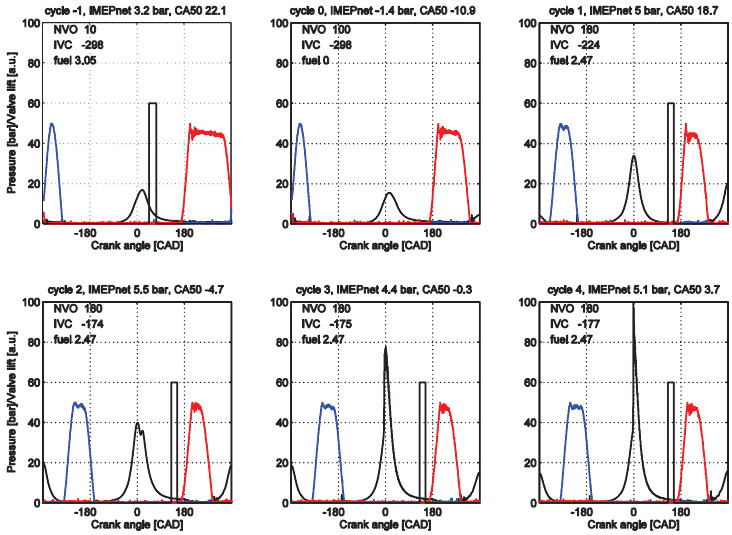

3

2012-01-0687

Gasoline Partially Premixed Combustion in a Light Duty Engine at Low Load and Idle Operating Conditions

Patrick Borgqvist, Per Tunestal, and Bengt Johansson
Lund University

ABSTRACT

Partially premixed combustion (PPC) has the potential of high efficiency and simultaneous low soot and NOx emissions. Running the engine in PPC mode with high octane number fuels has the advantage of a longer premix period of fuel and air which reduces soot emissions, even at higher loads. The problem is the ignitability at low load and idle operating conditions.

The objective of this study is investigation of the low load limitations with gasoline fuels with octane numbers RON 69 and 87. Measurements with diesel fuel were also taken as reference. The experimental engine is a light duty diesel engine equipped with a fully flexible valve train system. Trapped hot residual gases using negative valve overlap (NVO) is the main parameter of interest to potentially increase the attainable operating region of high octane number gasoline fuels.

Much lower soot is emitted with 69 and 87 RON gasoline compared to diesel at engine loads 1 bar IMEPgross to 3 bar IMEPgross but the combustion efficiency is significantly lower with gasoline at low load compared to diesel. Combustion efficiency increases with NVO for both diesel and gasoline. The 69 RON gasoline fuel can be run at idle (1 bar IMEPgross) operating conditions without a significant fraction of trapped hot residual gases. The 87 RON gasoline fuel could be run at 2 bar IMEPgross but with a high setting of NVO. There is a clear decrease of net indicated efficiency with NVO because of the decrease in gas-exchange efficiency. To achieve highest possible efficiency for a given fuel, at low load, as low as possible NVO should be used.

INTRODUCTION

Homogeneous charge compression ignition (HCCI) combustion has the potential of achieving high efficiency in combination with low NOx and soot emissions. The challenges with HCCI include combustion control, low power density and steep pressure rise rates. As a result, two branches of HCCI emerged, Spark assisted compression ignition (SACI), or controlled auto ignition (CAI), and partially premixed combustion (PPC). The idea with SACI is to operate, typically a SI-engine in HCCI mode at attainable operating conditions and in SI mode at high load operating conditions. SACI is the intermediate process between traditional SI flame propagation and HCCI auto ignition. HCCI mode is typically achieved through trapping of hot residual gases with early exhaust valve closing. The intake valve is opened symmetrically later after top dead center. The interval in crank angles from exhaust valve closing to intake valve opening is called negative valve overlap (NVO).

PPC combines traditional diesel combustion with HCCI. With PPC, fuel is injected earlier during the compression stroke and ideally mixes with air before the combustion starts to avoid soot formation. If a majority of the fuel is injected too early this will lead to too steep pressure rise rates as in the case with HCCI. One obvious benefit is also that the fuel injection timing can be used as control actuator to control combustion timing. In order to get enough separation from start of injection to start of combustion with diesel fuel a high fraction of EGR has to be used. This concept was used by Nissan [1] and is called Modulated Kinetics (MK) Combustion concept. Toyota investigated high EGR rate to suppress both soot and NOx with the smokeless rich diesel combustion concept [2]. In a different concept, as an alternative to using excessive EGR rates, Toyota used a double injection system with some of the fuel injected early to promote mixing with air. This concept is called UNIBUS [3, 4].

Kalghatgi introduced the concept of gasoline partially premixed combustion in 2006 [5, 6]. With a fuel that is harder to ignite, a longer mixing period from end of injection to start of combustion can be achieved without using high EGR fractions, too early injection timings or too low compression ratios. It was shown, in a heavy duty engine, that it is possible to achieve high efficiencies and low

emissions at low EGR fractions. In one case, with gasoline at IMEP 15.95 bar, smoke levels of 0.07 FSN, 0.58 g/kWh ISNOx and ISFC of 179 g/kWh was reported. Results in a light-duty engine are presented in [7, 8, 9]. Diesel was compared to gasoline up to 3000 rpm demonstrating low NOx emissions below 0.4 g/KWh with negligible smoke at 13 bar IMEP. Higher HC and CO emissions and higher heat-release rates at high loads compared to diesel is reported. It is argued that, because the higher the octane number the more problematic low load and high speed / high EGR operation becomes, the optimum fuels have octane numbers between 75 RON and 85 RON.

At Lund University, Manente et al. [10, 11] developed a gasoline PPC strategy running a variety of gasoline fuels with different octane numbers in a heavy duty engine. Gross indicated efficiencies up to 57 % with low NOx, HC and CO emissions and soot levels below of 0.5 FSN were demonstrated. Light duty engine experiments were performed in [12]. In this work an advanced injection strategy was developed where most of the fuel was injected very early during the compression stroke. In this work, diesel had 10 % higher gross indicated efficiency compared to gasoline, NOx was low for both diesel and gasoline but soot was much lower for gasoline, below 0.1 FSN compared to up to 9 FSN for the diesel fuel.

Figure 1 shows attainable operating region as a function of fuel octane number. The experiments were performed by Manente et al. [11] in a heavy duty engine. It is clearly seen that the attainable operating region decreases with fuel octane number. There are different ways to try to increase the attainable operating region, for example, using more advanced injection strategies, using negative valve overlap to trap hot residuals, or to use a glow plug.

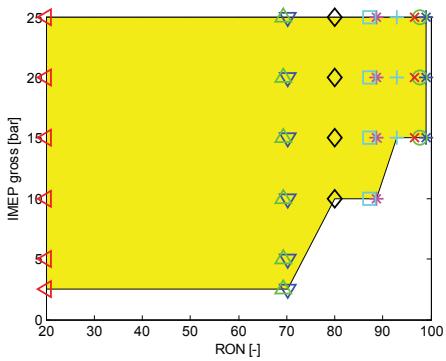

Figure 1 - PPC operating region from heavy duty engine experiments [11].

One alternative to the variable valve train system to be able to reach low load operating conditions with high octane number fuels is to use boosted inlet air. Solaka et al. [13] could run down to 2 bar IMEPgross at 1500 rpm but the combustion efficiency is low and the COV of IMEP is high at low load operating conditions. The variable valve train system is of practical interest because obtaining the required boost pressure with a standard turbo-charging system at low engine speed and load is expected to be challenging.

The main objective of this study is to investigate the low load limitations of different fuels with varying octane numbers and the effect of negative valve overlap. The experiments are performed at engine speed 800 rpm, and the goal is to reach idle operating condition (approximately 1 bar IMEPgross). The main tool is negative valve overlap to trap hot residual gases. Therefore, the effect of negative valve overlap is investigated in more detail.

First, gasoline PPC characteristics with two different combustion chambers are compared. The standard Volvo D5 combustion chamber is compared to a piston crown which has been used in a previous study to investigate different valve strategies on HCCI combustion [14, 15]. The objective of this initial investigation is to compare cases with low NVO settings since these cannot be used with the standard D5 piston. Second, a fuel comparison with diesel and gasoline at engine speed 800 rpm and varying engine loads from 1 bar IMEPgross up to 3 bar IMEPgross. The objective of this investigation is to get an estimate of the main differences at low engine speed and load between gasoline and diesel in terms of emissions and efficiency. Third, effects of NVO on diesel and gasoline fuels are investigated in more detail. Engine speed and load is constant 800 rpm and 2 bar IMEPgross.

After this investigation the problems associated with low load gasoline PPC should be better understood. And how utilization of NVO can improve low load operating condition performance of gasoline PPC operation and what the drawbacks are should also be better understood. Suggestions on how to proceed with this investigation are discussed in the Discussion section.

EXPERIMENTAL APPARATUS

The experimental engine is based on a Volvo D5 light duty diesel engine. The engine specifications can be seen in Table 1. It is run on only one of the five cylinders and is equipped with a fully flexible pneumatic valve train system supplied by Cargine Engineering. The Cargine valve train system was first demonstrated by Trajkovic et al. [16]. The valve actuators are placed on an elevated plate above the fuel injector and are connected to the valve stems with push-rods. Intake valve close timing is constant 180 CAD BTDC @ 1 mm valve lift and exhaust valve open timing is constant 180 CAD BTDC @ 1 mm valve lift. Maximum valve lift is approximately 5 mm. The fuel injection system is a common rail system with a with a 5 hole nozzle solenoid injector. The umbrella angle is 140 degrees and the nozzle hole diameters are 0.159 mm. The EGR is produced by pumping back the exhaust gases from the exhaust manifold to the inlet with a screw type compressor. The engine is run without boosted air. Intake gas (EGR and air) temperature is controlled with a heater in the intake manifold. For all the experiments in this study, Intake gas temperature is constant 40° C, and intake pressure is the same as the ambient pressure, approximately 1 bar.

Table 1 - Engine specifications.

Displacement (one cylinder)	0.48 Liters
Stroke	93.2 mm
Bore	81 mm
Compression ratio	16.5:1
Number of Valves	4
Valve train	Fully flexible

In-cylinder pressure is measured with a Kistler 6053C60 un-cooled piezo-electric pressure transducer fitted through a cooling channel between the intake and exhaust valves. HC, CO, CO2 and NOx emissions are measured with a Horiba Mexa 7500 analyzer system. Soot is measured with an AVL 415 smoke meter. EGR is calculated from measured CO2 in the intake manifold, which is measured with a Horiba MEXA-554JE system. EGR is calculated according to: $EGR = \frac{CO2_{intake}}{CO2_{exhaust}}$. The exhaust gases are cooled down before reaching the intake manifold.

The engine control system was developed by the author and was made with LabVIEW 2009 software. The control system is run from a separate target PC, NI PXI-8110, which is a dedicated real-time system. The target PC is equipped with an R series multifunctional data acquisition (DAQ) card with re-programmable FPGA hardware, NI PXI-7853R, and an M-series data acquisition card, NI PXI-6251. The user interface is run on a separate Windows based host PC. The host and target PCs communicates over TCP/IP.

In-cylinder pressure and valve lift curves are measured simultaneously with the FPGA DAQ card. The in-cylinder pressure and valve lift curve measurements are crank angle based with resolution 0.2 CAD/sample. Post-processing of the data is made in Matlab.

The valve lift curves are seen in Figure 2. The valve open speed is fast compared to conventional systems. In order to have valve clearance around top dead center, precautions have to be made. One alternative is to operate the valves with a minimum NVO setting to ensure that the valves are closed when the piston approaches top dead center. A second alternative is to modify the piston crown so that the valves can be opened with full flexibility.

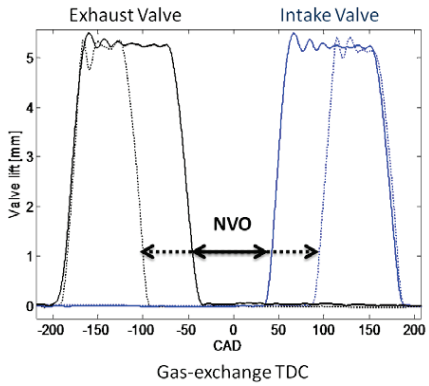

Figure 2 - Cargine valve train system valve lift curves with negative valve overlap (NVO).

In Figure 3, a photograph of the standard Volvo D5 piston is shown. With the standard Volvo D5 piston, the valve timings have to be set with a minimum NVO of 60 Crank Angle Degrees (CAD).

The piston crown in Figure 4 was inspired by a design by Tomoda et al. [17]. With this design it is possible to operate the Cargine valves with full flexibility. The piston has been used previously to evaluate different valve strategies on HCCI and SI combustion modes [14]. It was decided to use this piston also in an early stage of the PPC experiments. The reason is that this configuration enables investigation of differences between cases without NVO and 60 CAD NVO cases. Cases without NVO cannot be explored with the standard Volvo D5 piston. The compression ratios for both pistons are 16.5:1.

Figure 3 - Photograph of the standard Volvo D5 piston.

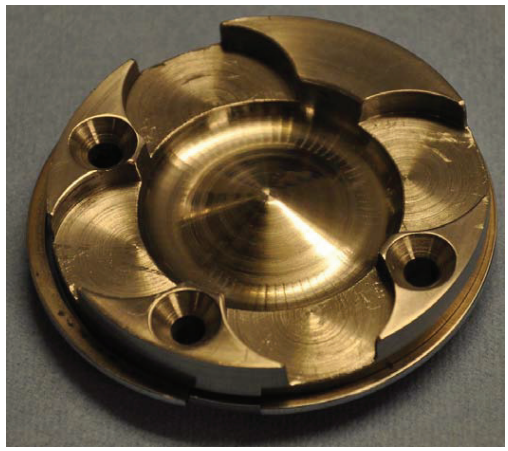

Figure 4 - Photograph of the modified piston with valve pockets.

The fuels used in this experiment are diesel and two different gasoline fuels. The gasoline fuels were supplied by Chevron and the diesel fuel is Swedish diesel MK1. The fuel specifications are shown in Table 2. These fuels were also used in previous study by Manente et al. [11].

Table 2 - Fuel specifications.

Fuel	RON	MON	LHV [MJ/kg]	A/F stoich
Diesel MK1	n.a.	20	43.15	14.9
Gasoline 69 RON	69	66	43.80	14.68
Gasoline 87 RON	87	81	43.50	14.60

RESULTS

MODIFIED PISTON COMPARISONS: NVO 10 VS NVO 60

The first experiment is an investigation of the effect of negative valve overlap using the modified piston, Figure 4. The objective is to investigate differences between the 60 CAD NVO case and 10 CAD NVO case. The reason is that the latter case cannot be explored with more conventional piston crowns and the Cargine valve train system. If it can be shown that there are no significant differences between the two NVO cases it will be assumed in future investigations that this limitation is of no significance of the results. Measurements are taken from NVO 10 CAD to NVO 140 CAD so that the differences between NVO 10 CAD and 60 CAD cases can be compared relatively to larger changes of NVO rather than comparing absolute values.

The engine load is 2 bar IMEPgross. A single fuel injection is used in all measurement points. CA50 is constant, approximately 7 CAD ATDC. Two different fuels, diesel and 69 RON gasoline, with and without EGR, are shown. The EGR fraction, in the cases it used, is shown in Figure 5. In the EGR cases, the EGR fraction is set to suppress NOx concentration to approximately 20 ppm at base NVO setting of 10 CAD. The EGR level is then gradually decreased with increased NVO to maintain a constant lambda, Figure 6.

There are a couple of reasons for showing both with and without EGR. Cases with EGR represent operating points that would have to be run to maintain reasonable engine out NOx emissions levels and is then of more practical value. But it is also interesting to see the effect of the increased fraction of trapped hot residual gases alone. Any effects seen (or not seen) are then influenced by (or not influenced by) the increase of trapped hot residual gas fraction and not the decrease of the EGR fraction.

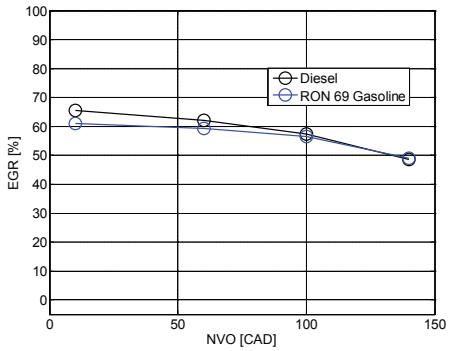

Figure 5 - EGR settings with the modified piston.

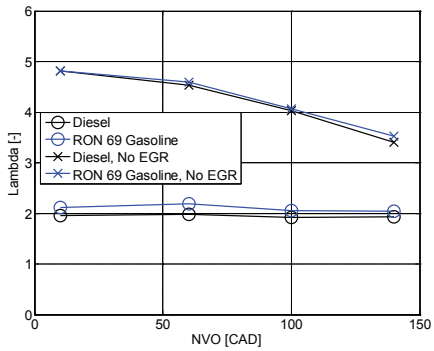

Figure 6 - Lambda.

The rate of heat-released for the diesel cases are shown in Figure 7. The NVO 10 and NVO 60 cases, with error bars are shown in Figure 8. There are no significant differences in heat-release rates from NVO 10 to NVO 60 either with EGR or without EGR.

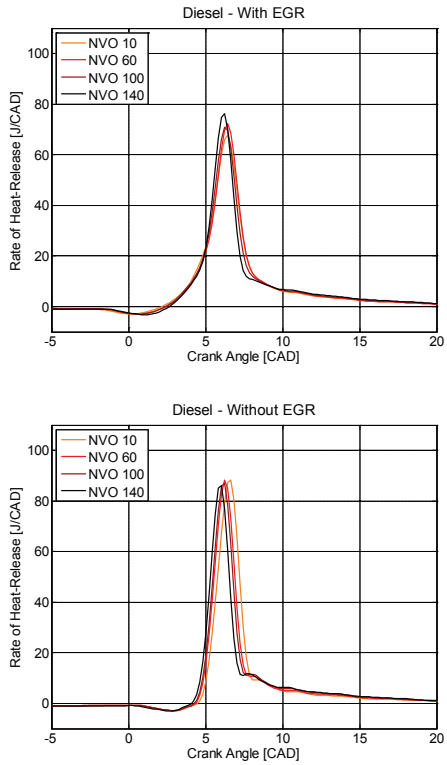

Figure 7 - Rate of heat-release curves from diesel experiments with NVO 10, 60, 100 and 140 CAD.

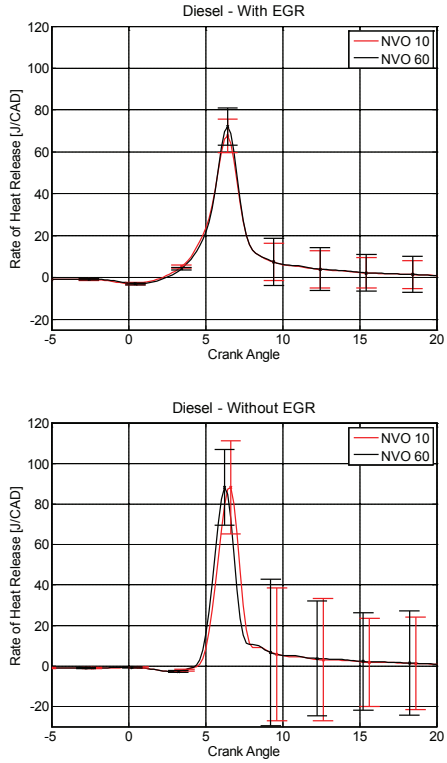

Figure 8 - Rate of heat-release curves from diesel experiments with NVO 10 and 60 CAD and with error bars showing plus minus one standard deviation.

The rate of heat-released cases for 69 RON gasoline cases are shown in Figure 9, and the NVO 10 and NVO 60 cases, with error bars, are shown in Figure 10. Again, same as in the diesel cases, the differences between NVO 10 and NVO 60 cases are small. The largest difference in these figures can be seen first when comparing NVO 100 with NVO 140, in the cases without EGR.

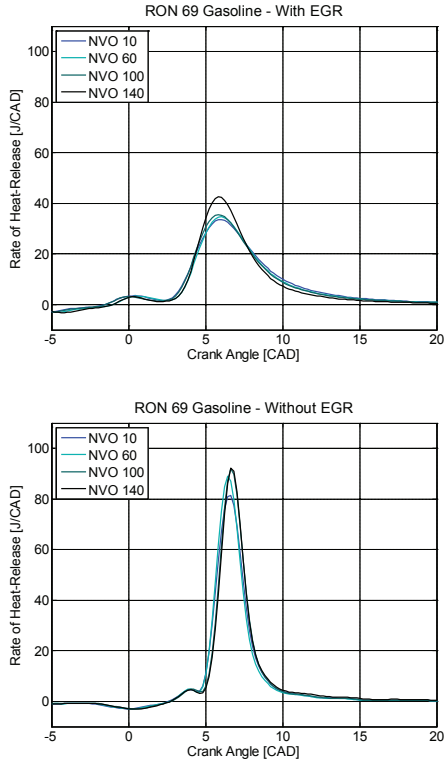

Figure 9 - Rate of heat-release curves from RON 69 gasoline experiments with NVO 10, 60, 100 and 140 CAD.

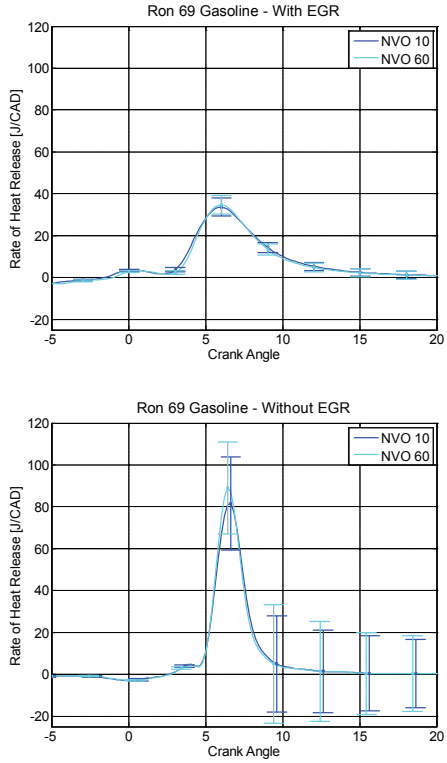

Figure 10 - Rate of heat-release curves from RON 69 gasoline experiments with NVO 10 and 60 CAD and with error bars showing plus minus one standard deviation.

The COV of IMEP is shown in Figure 11. COV of IMEP is a measure of cycle to cycle variations of combustion. It is seen that the difference between NVO 10 and NVO 60 on COV of IMEP is insignificant. It can also be seen that the cases without EGR have almost the same COV of IMEP compared to the cases with EGR. This means that the differences between the fuels in COV of IMEP are larger when EGR is used and that the gasoline cases will have larger COV of IMEP, or more unstable combustion, when EGR is used compared to diesel.

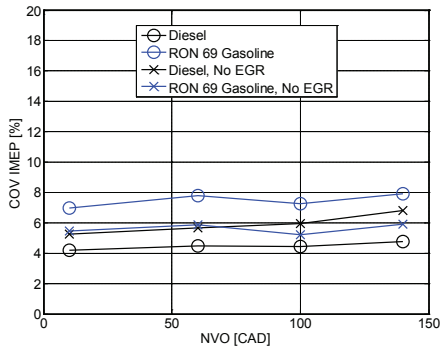

Figure 11 - COV IMEP of diesel and 69 RON gasoline, with and without EGR.

The ignition delay, defined as the difference in crank angles from start of injection (SOI) to CA10 (crank angle of 10 % accumulated heat-released), is shown in Figure 12. As expected, the ignition delay is longer with gasoline compared to diesel and with EGR compared to the cases without EGR. The differences between NVO 10 and NVO 60 cases on ignition delay are only small.

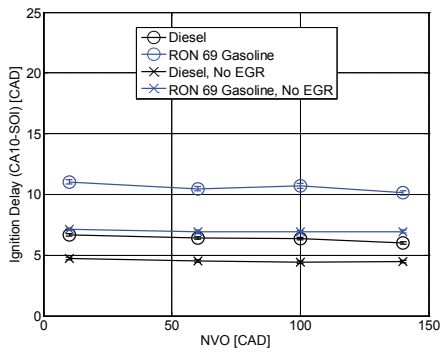

Figure 12 - Ignition delay, (CA10-SOI), of diesel and 69 RON gasoline, with and without EGR. The error bars show plus minus one standard deviation.

The negative effect of NVO on gas-exchange efficiency, Figure 13, is caused by heat-losses during the recompression of the residual gases. The gas-exchange efficiency is significantly decreased with increased NVO. The effect can be seen already from NVO10 CAD to NVO 60 CAD. But the relative difference is small compared to the differences from NVO 60 CAD to NVO 100 CAD, and from NVO 100 CAD to NVO 140 CAD. The conclusion is that there is a difference between NVO 10 CAD and NVO 60 CAD cases, but it is relatively small.

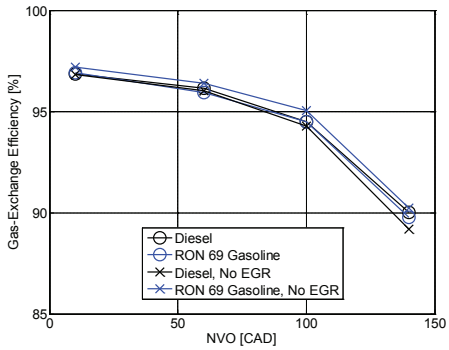

Figure 13 - Gas-exchange efficiency of diesel and 69 RON gasoline, with and without EGR.

Finally, the net indicated efficiency is shown in Figure 14. The net indicated efficiency is the product of the combustion efficiency, thermodynamic efficiency and gas-exchange efficiency. Since, the engine is operated on only one cylinder, and a sufficiently reliable friction model is unavailable, the net efficiency is the closest efficiency to the brake efficiency that can be achieved with this experimental setup. It is seen that the net indicated efficiency, up to NVO 100 CAD, is relatively unchanged.

Looking at all the results from this section, no significant differences between the NVO 10 and NVO 60 cases have been shown. In future work, the limitation of running with NVO 60 CAD will be assumed to be of no significance on the results when running the engine at low speeds and low load operating conditions.

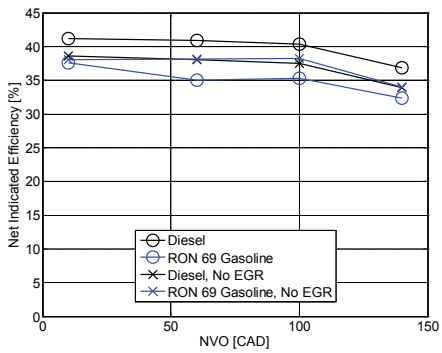

Figure 14 - Net indicated efficiency of diesel and 69 RON gasoline, with and without EGR.

FUEL COMPARISONS – EFFECT OF ENGINE LOAD

The differences in low load operation with gasoline compared to diesel are investigated. Initially, only two settings of NVO, 60 CAD NVO and 180 CAD NVO, are compared. A more detailed study on the effect of NVO is given in the next section. Some properties of the fuels that are used are shown in Table 2. The 69 RON gasoline fuel basically covers the same load range as the diesel fuel. The 87 RON gasoline fuel could only be run with the 180 CAD NVO setting and a minimum load limit at approximately 1.8 bar IMEPnet. The fuel injection strategy is single injection with common rail pressure 500 bar. Combustion timing, CA50, is constant 5 CAD for all

operating points with diesel and 69 RON gasoline fuels. In the case of 87 RON gasoline fuel, the fuel injection timing is constant -20 CAD ATDC. Setting the injection timing earlier would result in a significant increase of HC emissions because more fuel will get trapped in the squish volume. As a result, CA50 is retarded from 6 CAD ATDC at 1.8 bar IMEPnet to 8 CAD ATDC at 2.8 bar IMEPnet. The standard D5 piston, Figure 3, is used in all cases.

EGR is used to suppress NOx emissions to 20 ppm which corresponds to a NOx emission index of approximately 1 g/kg fuel. It would have been possible to run the engine with higher EGR fractions and thus lower NOx emissions. But the 20 ppm limit was chosen because it is a reasonable compromise between NOx suppression and combustion efficiency. Too low combustion efficiency results in high HC and CO emissions. The EGR settings are shown in Figure 15 and lambda is shown in Figure 16. In the cases with the diesel and RON 69 gasoline fuels, a lower EGR fraction is needed with increased load to suppress NOx emissions. Also, a lower EGR fraction is needed with 69 RON gasoline compared to diesel up to approximately 2 bar IMEPnet, regardless of NVO setting. In the case with 87 RON gasoline fuel, and constant injection timing, EGR is increased with load to suppress NOx emissions. A significantly lower EGR fraction is required compared to the diesel and 69 RON gasoline fuels 180 CAD NVO cases.

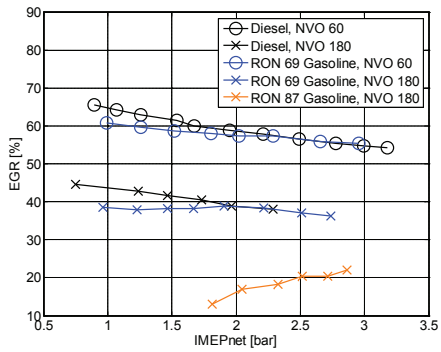

Figure 15 - The EGR settings used to suppress NOx emissions to 20 ppm.

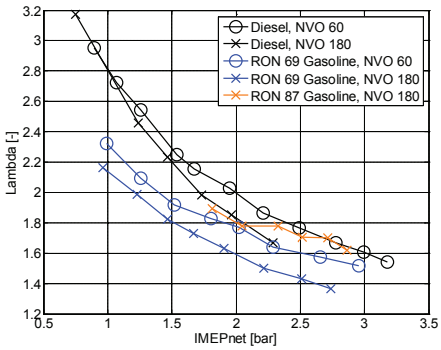

Figure 16 - Lambda plotted against IMEPgross.

The ignition delay is shown in Figure 17. As expected, the ignition delay is longer with gasoline compared to diesel. The ignition delay is longer with the 87 RON gasoline fuel compared to the 69 RON gasoline fuel. Also, the ignition delay of the NVO 180 CAD cases are to some extent shorter compared to the NVO 60 CAD cases. These differences can be understood by the differences in ignitability of the fuels. The elevated global in-cylinder temperature due an increased fraction of trapped hot residual gases explains the difference between the NVO 60 CAD and NVO 180 CAD cases.

The ignition delay is also longer with increased load. And the effect is more apparent on gasoline compared to diesel. This is an unexpected result. All cases are run lean and it is expected that an increased amount of fuel shortens the ignitions delay. The ignition delay increase is independent of trapped residual gas fraction. For the diesel and 69 RON gasoline cases, the EGR is decreased with load, which should decrease the ignition delay. In the 87 RON gasoline case, EGR is increased with load which partially explains the increase in ignition delay. In the diesel and 69 RON gasoline cases two different possibilities were considered. The first hypothesis is a lower global in-cylinder temperature at start of injection. This was considered because the injection timing is retarded with load in order to keep combustion timing constant. But analysis of the pressure-trace data did not reveal any significant temperature differences at start of injection at the varying engine loads. The second hypothesis is the amount of injected fuel. Injecting larger amount of fuel requires larger amount of energy for vaporizing the fuel which initially lowers the in-cylinder temperature resulting in longer ignition delays. This explanation is more reasonable. It also accounts for the difference in the amount of ignition delay increase from low to high load of the diesel cases compared to the RON 69 gasoline cases because the heat of vaporization is lower for diesel compared to gasoline.

The difference in EGR requirement for sufficient NOx reduction between the 87 RON gasoline fuel compared to the diesel and 69 RON gasoline fuels can be explained by the difference in ignition delay. A longer ignition delay gives more time for the fuel and air to mix before combustion. As a result, the NOx levels are reduced due to an increase of premixing [5]. In the cases with diesel compared to the 69 RON gasoline fuel, the differences in ignition delay do not result in any significant differences in EGR requirement for NOx reduction.

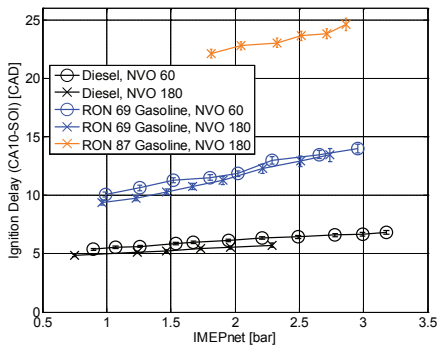

Figure 17 - Ignition delay plotted against engine load with error bars showing plus minus one standard deviation.

Figure 18 shows the standard deviation in IMEPnet calculated from 500 cycles each. The standard deviation in IMEPnet is shown as a measure of cycle-to-cycle variations and combustion stability in place of COV of IMEP. The reason is that the low load operating conditions result in peculiar trends originating from the COV of IMEP calculation itself. Looking at the standard deviation alone makes the interpretation of the results more clear.

The standard deviation of IMEPnet is higher for gasoline compared to diesel. The standard deviation of IMEPnet is also higher for the 180 CAD NVO cases compared to the 60 CAD NVO cases. This difference is smaller for the diesel case compared to the 69 RON gasoline case. The 87 RON gasoline case has lower standard deviation of IMEPnet compared to the 69 RON gasoline case. The running conditions for the 87 RON gasoline fuel is different compared to the other cases. For this fuel, the target CA50 could not be reached. SOI was constant and combustion timing occurred later compared to the other cases. One explanation for the higher standard deviation in the 69 RON gasoline cases compared to the diesel cases is the differences in ignition delay. A longer premixing period before combustion occurs increases the sensitivity of the in-cylinder conditions. The difference in standard deviation of IMEPnet between the 69 RON gasoline case and the diesel case is decreased with load up to approximately 2.5 bar IMEPnet. This could be explained by the decrease of lambda which makes the air-fuel mixture more reactive. A decreasing, slowly increasing, or approximately constant, standard deviation of IMEPnet results in a decreasing COV of IMEPnet. The latter can clearly be seen in Figure 18, for all fuel cases, after approximately 2.5 bar IMEPnet.

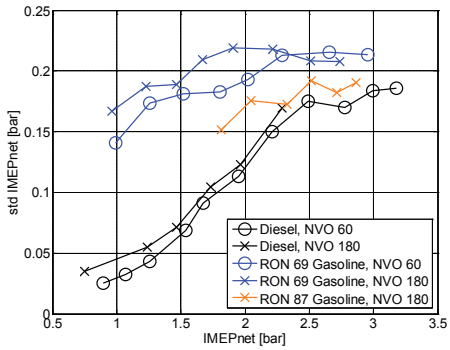

Figure 18 – Standard deviation in IMEPnet plotted against engine load.

The soot emissions are shown in Figure 19. The soot emissions of the gasoline fuels are low compared to diesel. This is explained by the longer ignition delay which increases the premixing of fuel and air before combustion [5]. There is a significant difference in soot emissions of the diesel case with 180 CAD NVO compared 60 CAD NVO. With a high fraction of trapped hot residual gases there is a more rapid increase of soot emissions starting at as low load as 1 bar IMEPnet. The corresponding increase of soot emissions for the 60 CAD NVO case does not occur until 2 bar IMEPnet. The difference in ignition delay is only small and does not explain the difference in soot emissions for the diesel cases. The lambda value at the soot emissions level of approximately 0.1 FSN is 2.2 at 1.5 bar IMEPnet for the 180 CAD NVO case and 1.7 for the 60 CAD NVO case at 2.8 bar IMEPnet. The global air fuel ratio that results in the same amount of soot is thus significantly higher for the case with a high fraction of trapped hot residual gases. High levels of retained exhaust gases lead to increased stratification of temperature and EGR distribution [18]. Increased level of stratification with more locally rich and hot zones is one reasonable explanation for the difference in soot with increased NVO.

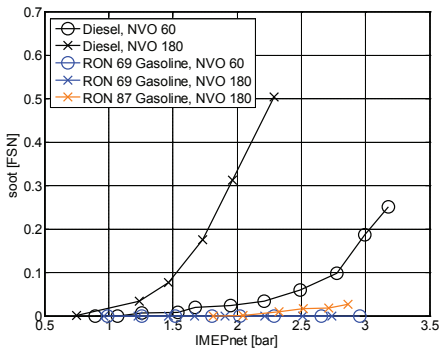

Figure 19 - Soot emissions plotted against engine load.

The combustion efficiency is shown is Figure 20. Combustion efficiency is higher for diesel compared to gasoline and higher for the 180 CAD NVO cases compared to the 60 CAD NVO cases. There is a significant improvement in combustion efficiency with load for the gasoline cases. In agreement with the results and discussions by Kalghatgi et al. [5, 6, 7], with increased ignition delay the local air fuel ratio approaches the lean global air fuel ratio and becomes less stratified. As a consequence, more HC and CO is produced with gasoline compared to diesel and with 87 RON gasoline fuel compared to 69 RON gasoline fuel, with the same setting of NVO. Also, as lambda is decreased with load, the combustion efficiency improves significantly for all gasoline cases. Increasing the fraction of trapped hot residual gases improves combustion efficiency for both gasoline and diesel. The increased fraction of trapped hot residual gas elevates the in-cylinder temperature and this also improves combustion efficiency.

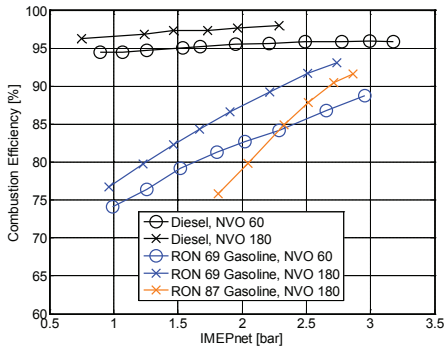

Figure 20 - Combustion efficiency plotted against engine load.

The thermodynamic efficiency is shown in Figure 21. The thermodynamic efficiency is defined as: $\eta_{thermodynamic} = \frac{IMEP_{gross}}{QhrMEP}$, where *IMEPgross* is the gross Indicated Mean Effective Pressure and *QhrMEP* is defined as $QhrMEP = \frac{Q_{HR}}{V_d}$. Q_{HR} [J] is the heat released during an engine cycle and V_d [m^3] is the engine displacement. In this work, *QhrMEP* is calculated from the combustion efficiency and the Fuel Mean Effective Pressure according to $QhrMEP = \eta_{combustion} \cdot FuelMEP$.

Finally, *FuelMEP* is defined as $FuelMEP = \frac{m_f \cdot Q_{LHV}}{V_d}$, where m_f [kg] is the mass of fuel supplied per cycle and Q_{LHV} [J/kg] is the lower heating value of the fuel.

The thermodynamic efficiency is the fraction of the heat released having resulted in mechanical work acting on the piston. The fraction of heat which is not converted to mechanical work is lost either through the cylinder walls or exhaust. The gasoline cases have higher thermodynamic efficiency compared to diesel. The thermodynamic efficiency of the diesels cases increase linearly with load and the differences compared to the gasoline cases becomes smaller with increased IMEPnet. The trend for the 87 RON gasoline fuel is different compare to the other cases. One possible explanation is the difference in injection timings, as already discussed.

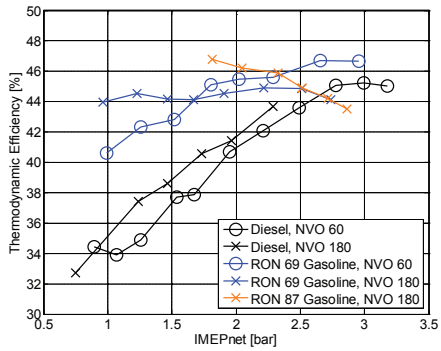

Figure 21 - Thermodynamic efficiency plotted against engine load.

The gross indicated efficiency is the product of the combustion efficiency and thermodynamic efficiency. For the same settings of NVO, the diesel cases have higher gross indicated efficiency compared to the gasoline cases. This means that the difference in combustion efficiency gives a higher gross indicated efficiency for the diesel cases compared to the gasoline cases despite the

difference in thermodynamic efficiency. The NVO 180 CAD cases compared to the NVO 60 cases have higher gross indicated efficiency for both diesel and gasoline which can be explained by the improvement in combustion efficiency.

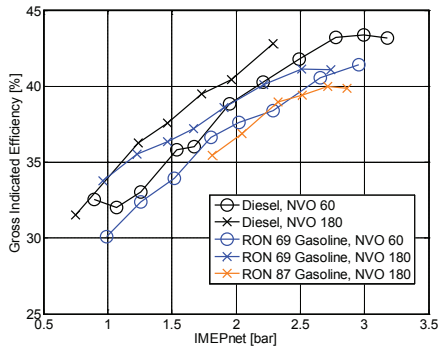

Figure 22 - Gross indicated efficiency plotted against engine load.

The gas-exchange efficiency is shown in Figure 23. As expected, there is a significant difference between the NVO 60 CAD and NVO 180 CAD cases. There is also an improvement in gas-exchange efficiency with engine load. This can be understood by the increase in gross indicated efficiency. Since the gas-exchange efficiency is defined as *IMEPnet* divided by *IMEPgross* which can be reformulated according to $\eta_{gas-exchange} = \frac{IMEP_{net}}{IMEP_{gross}} = \frac{IMEPgross-PMEP}{IMEP_{gross}} = 1 - \frac{PMEP}{IMEP_{gross}}$, where *PMEP* is the pumping losses. With increased load, *IMEPgross* increases but *PMEP* is approximately constant which results in an increase in gas-exchange efficiency.

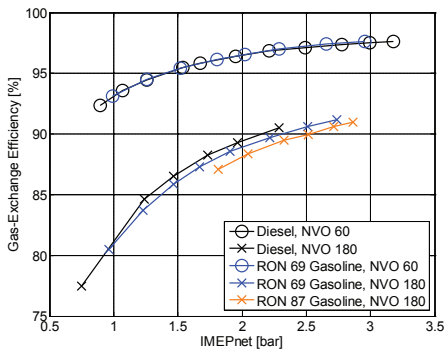

Figure 23 - Gas exchange efficiency plotted against engine load.

Finally, the net indicated efficiency, Figure 24, also takes the gas-exchange efficiency into account. It is seen that the diesel case with minimum NVO has the highest net indicated efficiency and the 87 RON gasoline case with 180 CAD NVO has the lowest indicated efficiency. The combustion efficiency is improved with increased NVO, but the penalty of reduced gas-exchange efficiency result in lower net indicated efficiency. But the main purpose of using NVO with gasoline PPC is not to get increased efficiency. The main purpose is to be able to run with higher octane number fuels also at low loads. And it is clear that NVO is necessary in order to run the 87 RON gasoline fuel at as low load as 2 bar IMEPnet without boosted air and with the same injection strategy as the other fuels.

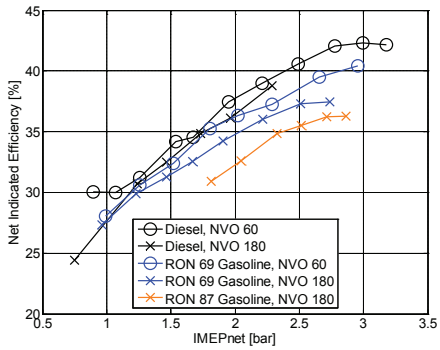

Figure 24 - Net indicated efficiency plotted against engine load.

FUEL COMPARISONS – EFFECT OF NVO

The objective of this investigation is comparison of the effect of negative valve overlap on diesel and gasoline with different octane numbers.

The standard D5 piston, Figure 3, is used in all experiment cases. The fuels are the same as was used in the previous section, Table 2. The fuel injection strategy is also the same as used previously. This is a single injection strategy with 500 bar common rail pressure and constant combustion timing, CA50, of 5 CAD for the diesel and 69 RON gasoline fuels. For the same reasons as discussed in the previous section, in the case of 87 RON gasoline fuel, the fuel injection timing, not CA50, is constant -20 CAD ATDC. The amount of injected fuel was determined for the diesel and 69 RON gasoline fuels at 60 CAD NVO to get the desired engine load of 2 bar IMEPgross. For the 87 RON gasoline fuel the injected fuel amount was set at 200 CAD NVO. The amount of injected fuel is not changed with NVO.

EGR is shown in Figure 25 and lambda is shown in Figure 26. For diesel and 69 RON gasoline cases, EGR was set to suppress NOx to approximately 20 ppm at the operating points with 60 CAD NVO. As NVO is increased, EGR is decreased to maintain constant lambda. Lambda is used as an indication of the total EGR fraction, internal and external. The objective is to replace the cold EGR with the internal (hot). In the 87 RON gasoline case, the EGR fraction was set at NVO 200 CAD to match the EGR fraction of the diesel and 69 RON gasoline cases. In Figure 26, a distinct decrease of lambda can be seen after 220 CAD NVO. 220 CAD NVO is the point where the EGR fraction has been reduced to 0 % and cannot be further reduced to maintain constant lambda.

It should be noted that the EGR condition for the effect of NVO investigation is different compared to the previous section, effect of load investigation. In this section, EGR is changed to maintain a constant lambda, but in the previous section EGR is changed to suppress NOx. This means that the operating condition 180 CAD NVO 1.75 bar IMEPnet of the previous section does not match the operating condition 180 CAD NVO 2 bar IMEPgross of this section. According to Figure 23, the gas-exchange efficiency at 1.75 bar IMEPnet approximately is approximately 87 % which then calculates to 2 bar IMEPgross.

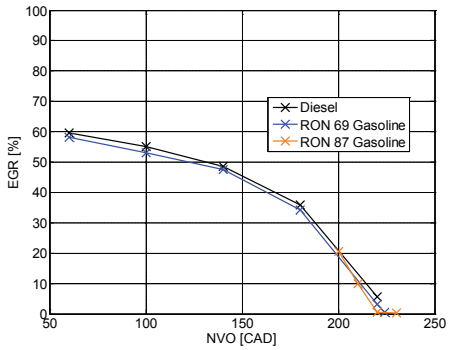

Figure 25 - EGR.

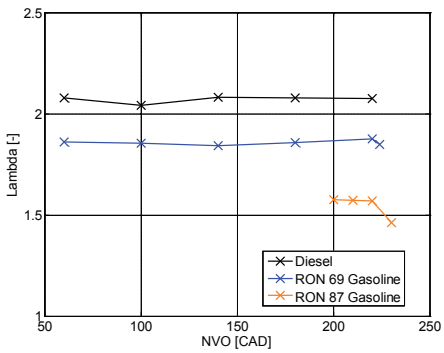

Figure 26 - Lambda.

Figure 27 shows the ignition delay. The ignition delay is longer with 69 RON gasoline compared to diesel, and longer with 87 RON gasoline compared to 69 RON gasoline. There is a small decrease in ignition delay with NVO up to 220 CAD NVO for all fuels. This is in agreement with the results of the previous section, Figure 17, with only a small difference with the 180 CAD NVO cases compared to the 60 CAD NVO cases.

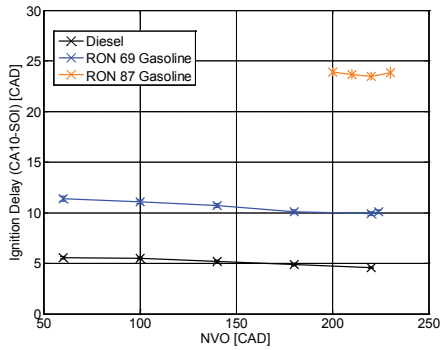

Figure 27 - Ignition delay with error bars showing plus minus one standard deviation.

The standard deviation in IMEPnet is seen in Figure 28. The standard deviation in IMEPnet is lower for diesel compared to gasoline and lower for the 69 RON gasoline case compared to the 87 RON gasoline case. The standard deviation in IMEPnet is relatively unchanged with NVO for the diesel and 69 RON gasoline fuel cases. For the 87 RON gasoline case, there is a significant decrease of standard deviation in IMEPnet with NVO. With the 87 RON gasoline case, combustion stability is clearly affected by NVO. The 87 RON fuel will not combust at all with a too low setting of NVO with the operating conditions in this investigation.

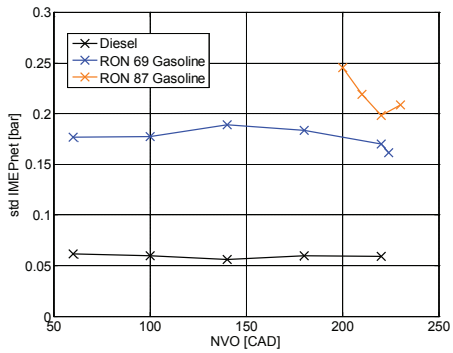

Figure 28 – Standard deviation in IMEPnet plotted against NVO.

The NOx emissions, Figure 29, are first suppressed with EGR at 60 CAD NVO to 20 ppm, as explained in the beginning of this section. EGR is adjusted to maintain constant lambda with increased NVO. For both the diesel and the 69 RON gasoline cases, an increase in NOx can clearly be seen after 140 CAD NVO. This is explained by the increased temperature from replacing EGR with trapped hot residual gases. In the case of the 87 RON gasoline fuel, EGR was set to match the EGR fraction of the diesel and 69 RON gasoline cases. It is clearly seen that the EGR requirement for the 87 RON gasoline fuel is lower compared to the other fuels. The same fraction of EGR as the diesel and 69 RON gasoline cases results in a significantly lower NOx level. Also for the 87 RON gasoline fuel, NOx emissions are increased as EGR is replaced by trapped hot residual gases. At 220 CAD NVO, EGR has been entirely replaced by trapped residual gases. With higher NVO than 220 CAD, NOx is decreased because of the higher EGR fraction.

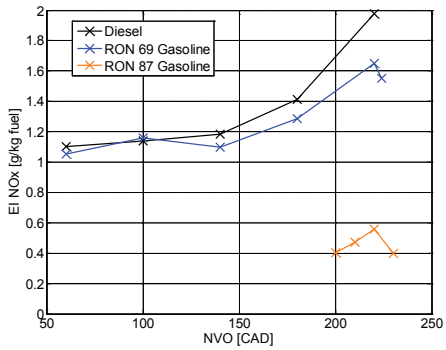

Figure 29 – NOx concentration.

The soot emissions are seen in Figure 30. Soot emissions are somewhat higher for diesel compared to the 69 RON gasoline fuel. The diesel case soot emissions are increased with NVO from 140 CAD. The higher soot emissions of the 87 RON gasoline case, compared to the other fuels, is an unexpected result. The longer ignition delay increases premixing of fuel and air before combustion which should result in lower soot emissions. The discussion on possible reasons for the higher soot emissions for the 87 RON gasoline fuel is postponed until the Discussion section.

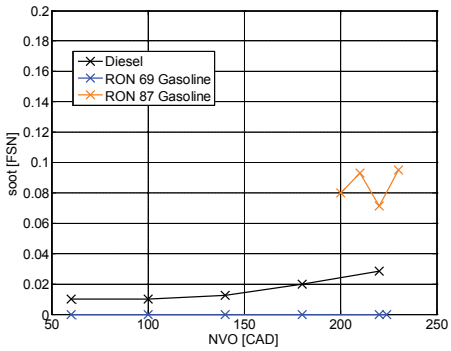

Figure 30 - Soot.

The combustion efficiency is seen in Figure 31. The combustion efficiency is higher for diesel compared to gasoline and higher for the 69 RON gasoline fuel compared to the 87 RON gasoline fuel. And there is a clear improvement in combustion efficiency with NVO for both gasoline and diesel. This is in agreement with the combustion efficiency results, Figure 20, from the Effect of Engine Load section. The improvement in combustion efficiency with NVO can be explained by the increased in-cylinder temperature from an increased fraction of trapped hot residual gases.

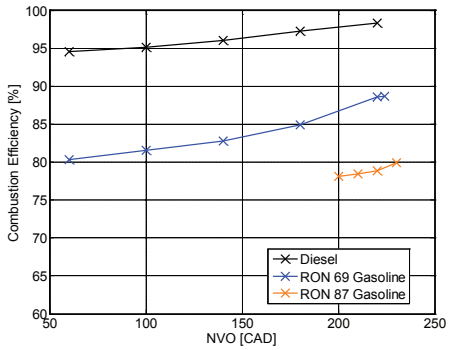

Figure 31 - Combustion efficiency.

The thermodynamic efficiency is seen in Figure 32. It is higher for gasoline compared to diesel in agreement with the results from Figure 21. There is also a decrease in thermodynamic efficiency with NVO after 180 CAD.

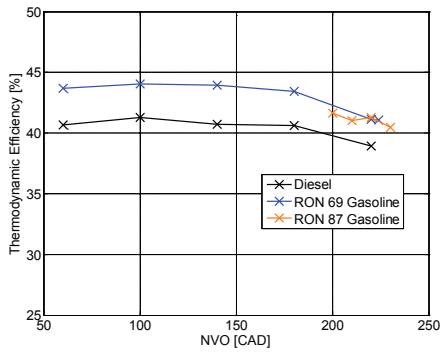

Figure 32 - Thermodynamic efficiency.

The gross indicated efficiency is seen in Figure 33. The gross indicated efficiency is higher for diesel compared to the gasoline cases. This is a result of the low combustion efficiency of the gasoline cases. A small increase in gross indicated efficiency with NVO can be seen up to 180 CAD NVO as a result of the increased combustion efficiency. After 180 CAD NVO a small decrease in gross indicated efficiency can be seen in the diesel case and the gasoline cases are relatively unchanged. This is explained by the decrease of thermodynamic efficiency after 180 CAD NVO.

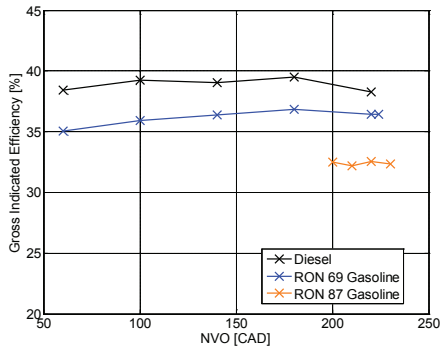

Figure 33 - Gross indicated efficiency.

The gas-exchange efficiency is seen in Figure 34. As expected, the gas-exchange efficiency is decreased with NVO.

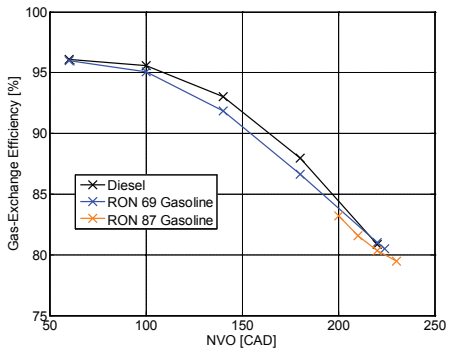

Figure 34 - Gas-exchange efficiency.

The net indicated efficiency is shown in Figure 35. The net indicated efficiency decreases with NVO because of the decrease in gas-exchange efficiency. In total, the low gas-exchange efficiency will cancel out the positive effects of NVO gained in increased combustion efficiency. For the higher octane number fuels there is a limit on minimum NVO that is required to be able to run the fuel at low load. But in terms of efficiency, it is better to have as low NVO as possible.

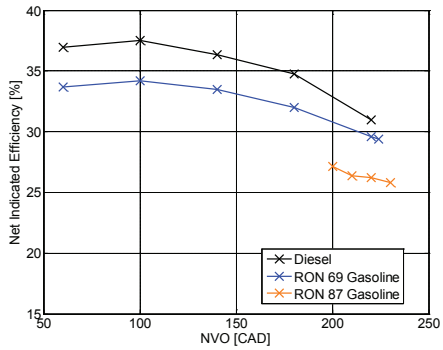

Figure 35 – Net indicated efficiency.

Effect of NVO on Combustion Efficiency

The combustion efficiency of the gasoline cases are significantly lower compared to diesel. One final question on this topic is how much the combustion efficiency would be improved without EGR, using NVO alone. EGR is used to lower the in-cylinder temperature to suppress NOx formation but at the same time this leads to an increase of HC and CO emission. Ignoring NOx limitations, how much would the combustion efficiency improve? The RON 69 gasoline fuel combustion efficiency, from Figure 31, is plotted with the combustion efficiency when no EGR is used in Figure 36. At this engine speed, engine load and with the simplest possible injection strategy, the maximum achievable combustion efficiency with this fuel is roughly 90 %, which is still lower than the diesel case. The combustion efficiency is then relatively unchanged with NVO up to 180 CAD NVO.

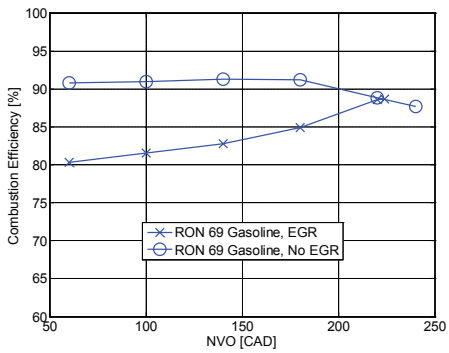

Figure 36 - Combustion efficiency of RON 69 gasoline cases with and without EGR.

DISCUSSION

The main objective of this study is to investigate the low load limitations of different fuels with varying octane numbers and the effect of negative valve overlap. It was shown that the 69 RON gasoline fuel could be run at as low load as 1 bar IMEPnet without a significant fraction of trapped hot residual gases. An increased fraction of NVO did not improve on combustion stability as the standard deviation in IMEPnet was relatively unaffected. The 87 RON gasoline fuel could only be run with a significant fraction of trapped hot residual gases. The NVO settings used was as high as 180 CAD NVO and the minimum attainable load was approximately 1.75 bar IMEPnet with the operating conditions used in this study. NVO had a significant effect on combustion stability as the standard deviation in IMEPnet clearly decreased.

The thermodynamic efficiency is higher for the gasoline cases compared to diesel but the combustion efficiency is significantly lower which result in a lower gross indicated efficiency for gasoline compared to diesel at low load operating conditions. NVO can be used to increase the combustion efficiency but the high penalty of reduced gas-exchange efficiency results in a lower net indicated efficiency. The main purpose of NVO is to increase the attainable operating region with high octane number fuels and as low NVO as possible should be used to get as high efficiency as possible. In terms of HC and CO emissions, increased NVO has a positive effect on combustion efficiency which results in lower HC and CO emissions. In most cases in this study, the soot emissions of the gasoline cases are low compared to the diesel case.

Running with even higher octane number gasoline fuels is expected to further decrease the attainable load operating region. The main purpose of NVO for gasoline PPC is to elevate the temperature of the sub-sequent cycle sufficiently to ignite the fuel. But the problem is that the potential temperature increase is limited by the exhaust temperature. A fuel with a high octane number will require a high temperature to ignite. This temperature requirement is possibly higher than what is possible to obtain if the load is too low. There is thus a need for additional strategies in order to increase the attainable low load limit further. Also, in terms of efficiency, it is beneficial to be able to use as low NVO as possible. Increased boost pressure is one method to increase the attainable operating region. But in practice the applicability of boosted air is limited at low engine speed and load. Urushihara et al. [20] showed that fuel injection during the negative valve overlap expanded the lean limit for HCCI combustion. It would be interesting to investigate the effect of NVO pilot injection on attainable low load and minimum NVO requirement for gasoline PPC. In this investigation a single injection strategy was used for all cases. It would also be interesting to investigate the effect of more advanced injection strategies using multiple injections, possibly in combination with a glow plug. A natural step to proceed on this investigation is to look into more advanced injection strategies.

The high soot emissions of the 87 RON gasoline fuel compared to the diesel and 69 RON gasoline fuel, Figure 30, is an unexpected result. Looking at lambda, Figure 26, it is seen that the air fuel ratio is significantly lower for the 87 RON gasoline fuel compared to diesel and the 69 RON gasoline fuel. The difference in lambda between the different fuels, even though approximately the same EGR fraction (Figure 25) is used for all fuels, is explained by the higher amount of fuel needed for the gasoline fuels to have the same engine load, 2 bar IMEPgross. This is seen in Figure 33, the gross indicated efficiency. The 87 RON gasoline fuel was run with the lowest air fuel ratio of all fuels. One explanation for the high soot emissions of the 87 RON gasoline case is the overall low air fuel ratio in combination with the increased stratification due to the high NVO setting. As seen in Figure 29, the NOx emissions of the 87 RON gasoline case is lower compared to the other cases. The temperature is sufficiently low to avoid the NOx formation zones in the well-known Φ-T diagram of NOx and soot formation [19]. But locally, the air fuel ratio is sufficiently low to get soot formation.

SUMMARY/CONCLUSIONS

For all experiments, engine speed was constant 800 rpm. And intake manifold temperature was controlled at 40° C, and intake pressure was the same as the ambient pressure, approximately 1 bar. The first experiment was an investigation of the effect of negative valve overlap using the modified piston crown with valve pockets. The objective was to investigate differences between the 60 CAD NVO case and 10 CAD NVO. The second experiment was a fuel comparison with diesel and 69 and 87 RON gasoline fuels at varying engine loads from 1 bar IMEPgross up to 3 bar IMEPgross. The third experiment investigated effects of NVO on the diesel and gasoline fuels in more detail. Engine load was constant 2 bar IMEPgross.

- No significant differences between the NVO 10 and NVO 60 cases have been shown with the modified piston with valve pockets running at low engine speed and load.
- The 69 RON gasoline could be run at 1 bar IMEPgross without a significant fraction of trapped hot residual gases. The minimum attainable load with the 87 RON gasoline fuel was approximately 2 bar IMEPgross with a significant fraction of trapped hot residual gases. The effect of NVO on combustion stability, measured as standard deviation in IMEPnet, was found to be most positive with the 87 RON gasoline fuel.
- The ignition delay is significantly longer with the 87 RON gasoline fuel. A longer ignition delay gives more time for the fuel and air to mix before combustion. As a result, the NOx levels are reduced due to increased mixing of fuel and air before combustion. This also has a positive effect on soot emissions which were lower for the gasoline fuels at the different engine load cases in this investigation compared to diesel.
- Combustion efficiency is significantly lower with gasoline compared to diesel. The combustion efficiency for the gasoline cases was shown to be as low as 75% compared to 95% combustion efficiency with the diesel fuel. Combustion efficiency increases with NVO for both diesel and gasoline. The gross indicated efficiency is lower with gasoline compared to diesel as a consequence of the low combustion efficiency.
- There is a clear decrease of net indicated efficiency with NVO because of the decrease in gas-exchange efficiency. To get as high efficiency as possible, for a given fuel, as low as possible NVO should be used.

REFERENCES

1. Kimura S., Aoki O., Ogawa H., Muranaka S., Enomoto Y., ”New Combustion Concept for Ultra-Clean and High-Efficiency Small DI Diesel Engines”, SAE 1999-01-3681
2. Akihama K., Takatori Y., Inagaki K., Sasaki S., Dean A., ”Mechanism of the Smokeless Rich Diesel Combustion by Reducing Temperature”, SAE 2001-01-0655
3. Yanigahara H., Sato Y., Minuta J., ”A simultaneous reduction in NOx and soot in diesel engines under a new combustion system (Uniform Bulky Combustion System – UNIBUS)”, 17th International Vienna Motor Symposium, pp 303-314, 1996
4. Hasegawa R., Yanigahara H., “HCCI Combustion in DI Diesel Engine”, SAE 2003-01-0745
5. Kalghatgi G. T., Risberg P., Ångström H., ”Advantages of Fuels with High Resistance to Auto-Ignition in Late-injection, Low-temperature, Compression Ignition Combustion”, SAE 2006-01-3385
6. Kalghatgi G. T., Risberg P., Ångström H., ”Partially Pre-Mixed Auto-Ignition of Gasoline to Attain Low Smoke and Low NOx at High Load in a Compression Ignition Engine and Comparison with a Diesel Fuel”, SAE 2007-01-0006
7. Kalghatgi G. T., Hildingsson L., Johansson B., “Low NOx and Low Smoke Operation of a Diesel Engine using Gasoline-like Fuels”, ICES2009-76034
8. Hildingsson L., Kalghatgi G., Tait N., Johansson B., Harrison A., “Fuel Octane Effects in the Partially Premixed Combustion Regime in Compression Ignition Engines”, SAE 2009-01-2648
9. Kalghatgi G.T., Hildingsson L., Harrison A., Johansson B., “Low- NOx, low-smoke operation of a diesel engine using “premixed enough" compression ignition – Effects of fuel autoignition quality, volatility and aromatic content”, THISEL 2010 Conference on Thermo- and Fluid Dynamic Processes in Diesel Engines
10. Manente V., Johansson B., Tunestal P., ”Effects of Different Type of Gasoline Fuels on Heavy Duty Partially Premixed Combustion”, SAE 2009-01-2668
11. Manente V., Johansson B., Tunestal P., Zander C., Cannella W., “An Advanced Internal Combustion Engine Concept for Low Emissions and High Efficiency from Idle to Max Load Using Gasoline Partially Premixed Combustion”, SAE 2010-01-2198
12. Manente V., Johansson B., Tunestal P., Sonder M., Serra S., ”Gasoline Partially Premixed Combustion: High Efficiency, Low NOx and Low Soot by using an Advanced Combustion Strategy and a Compression Ignition Engine”, FCE09, Istanbul Turkey
13. Solaka H., Tuner M., Johansson B., ”Investigation of Partially Premixed Combustion Characteristics in Low Load Range with Regards to Fuel Octane Number in a Light Duty Diesel Engine”, SAE 2012-01-0684
14. Borgqvist P., Tunestål P., Johansson B., ”Investigation and Comparison of Residual Gas Enhanced HCCI using Trapping (NVO HCCI) or Rebreathing of Residual Gases”, SAE 2011-01-1772, JSAE 20119058
15. Widd A., Johansson R., Borgqvist P., Tunestål P., Johansson, B., ”Investigating Mode Switch from SI to HCCI using Early Intake Valve Closing and Negative Valve Overlap”, SAE 2011-01-1775, JSAE 20110923
16. Trajkovic S., Milosavljevic A., Tunestål P., Johansson B., “FPGA Controlled Pneumatic Variable Valve Actuation”, SAE 2006-01-0041
17. Tomoda T., Ogawa T., Ohki H., Kogo T., Nakatani K., Hashimoto E., ”Improvement of Diesel Engine Performance by Variable Valve Train System”, 30. Internationales Wiener Motorensymposium 2009
18. Rothamer A., Snyder J., Hanson R., Steeper R., Fitzgerald R., ”Simultaneous imaging of exhaust gas residuals and temperature during HCCI combustion”, Proceedings of the Combustion Institute 32 (2009) 2869-2876
19. Akihama K., Takatori Y., Inagaki K., Sasaki S., Dean A. M., ”Mechanism of the Smokeless Rich Diesel Combustion by Reducing Temperature”, SAE 2001-01-0655
20. Urushihara T., Hiraya K., Kakuhou A., Itoh T., ”Expansion of HCCI Operating Region by the Combination of Direct Fuel Injection, Negative Valve Overlap and Internal Fuel Reformation”, SAE 2003-01-0749

CONTACT INFORMATION

Patrick Borgqvist

Lund University
Dept. of Energy Sciences
Div. of Combustion Engines
P.O. Box 118
221 00 Lund
Sweden

patrick.borgqvist@energy.lth.se

ACKNOWLEDGMENTS

The authors wish to show their appreciation to the Competence Centre Combustion Processes (KCFP), Swedish Energy Agency Grant number 22485-2, for their financial support. The authors would also like to acknowledge Cargine Engineering for supplying and helping with the valve train system. The authors would also like to expresses their gratitude to Bill Cannella from Chevron Corporation for supplying the gasoline fuels and to Håkan Persson from Volvo Car Corporation for hardware support and valuable discussions. The author would also like to acknowledge the work in the lab made by Master's Thesis students Hjalmar Arvidsson and Olivan Marku.

DEFINITIONS/ABBREVIATIONS

ATDC	After Top Dead Centre
CAD	Crank Angle Degree
CAI	Controlled Auto Ignition
DAQ	Data Acquisition
HCCI	Homogeneous Charge Compression Ignition
IMEP	Indicated Mean Effective Pressure
NVO	Negative Valve Overlap
PPC	Partially Premixed Combustion
SACI	Spark Assisted Compression Ignition
SI	Spark Ignition
SOI	Start of Injection

4

2012-01-1578

The Usefulness of Negative Valve Overlap for Gasoline Partially Premixed Combustion, PPC

Patrick Borgqvist, Martin Tuner, Augusto Mello, Per Tunestal and Bengt Johansson
Lund University

ABSTRACT

Partially premixed combustion has the potential of high efficiency and simultaneous low soot and NOx emissions. Running the engine in PPC mode with high octane number fuels has the advantage of a longer premix period of fuel and air which reduces soot emissions, even at higher loads. The problem is the ignitability at low load and idle operating conditions.

The objective is to investigate the usefulness of negative valve overlap on a light duty diesel engine running with gasoline partially premixed combustion at low load operating conditions. The idea is to use negative valve overlap to trap hot residual gases to elevate the global in-cylinder temperature to promote auto-ignition of the high octane number fuel. This is of practical interest at low engine speed and load operating conditions because it can be assumed that the available boost is limited. The problem with NVO at low load operating conditions is that the exhaust gas temperature is low. While an increase of NVO potentially increases the in-cylinder temperature at intake valve closing, increasing NVO also increases the EGR fraction which lowers the global in-cylinder temperature. The question is to what extent NVO can be used to extend the low load operating region. Investigations on the effect of the glow plug are also included.

The experimental engine is modeled with the engine simulation tool AVL Boost to retrieve information about trapped residual gas fraction and in-cylinder temperature with varying NVO and load at low engine speed and load operating conditions. Measured experimental data is used as input to the engine simulation model at all operating conditions. Measured model inputs include valve lift curves, in-cylinder pressure trace and calculated heat-release profiles.

INTRODUCTION

Homogeneous charge compression ignition (HCCI) combustion has the potential of achieving high efficiency in combination with low NOx and soot emissions. The challenges with HCCI include combustion control, low power density and steep pressure rise rates. As a result, two branches of HCCI emerged, spark assisted compression ignition (SACI), and partially premixed combustion (PPC). SACI is the intermediate process between SI flame propagation and HCCI auto ignition. HCCI mode is typically achieved through trapping of hot residual gases with early exhaust valve closing. The intake valve is usually opened symmetrically after top dead center. The interval in crank angles from exhaust valve closing to intake valve opening is called negative valve overlap (NVO). The idea to use negative valve overlap for HCCI was first proposed by Willand et al. [1] in 1998 and was demonstrated by Lavy et al. [2] in 2000.

PPC combines traditional diesel combustion with HCCI. With PPC, the fuel injection is completed before start of combustion to promote mixing of fuel and air, but the charge is not homogeneous. One benefit compared to traditional HCCI combustion is that the fuel injection timing can be used as control actuator for the combustion timing. In order to get enough separation from start of injection to start of combustion with diesel fuel, a high fraction of EGR has to be used. This concept was used by Nissan [3] and is called Modulated Kinetics (MK). Toyota used high EGR rates to suppress both soot and NOx with the smokeless rich diesel combustion concept [4]. In a different concept, as an alternative to using excessive EGR rates, Toyota used a double injection system with some of the fuel injected early to promote mixing with air. This concept is called UNIBUS [5, 6].

Kalghatgi introduced the concept of gasoline partially premixed combustion in 2006 [7, 8]. With a fuel that is harder to ignite, a longer mixing period from end of injection to start of combustion can be achieved without using high EGR fractions, too early injection timings or too low compression ratios. Results from a light-duty engine were published in [9-11].

At Lund University, Manente et al. [12, 13] developed a gasoline PPC strategy running a variety of gasoline fuels with different octane numbers in a heavy duty engine. Gross indicated efficiencies up to 57 % with low NOx, HC and CO emissions and soot levels below of 0.5 FSN were demonstrated. Light duty engine experiments were performed in [14].

As demonstrated in a heavy-duty engine, there is a clear decrease in attainable gasoline-PPC engine operating region with increased fuel octane number [13]. There are different tools that can be used to try to extend the attainable operating region, for example, using more advanced injection strategies, using NVO to trap hot residuals, and to use a glow plug. This work focuses on NVO.

Running gasoline PPC with higher octane number fuels at idle operating conditions is a challenge. At low load and engine speed operating conditions it can be assumed that the available boost is limited and that reaching auto-ignition conditions will be difficult with a standard turbo-charger. Application of NVO is usually associated with SACI and is used to achieve HCCI combustion in a spark ignition engine [15-18]. PPC is a diesel engine concept and it is not aimed at achieving traditional HCCI. The compression ratio is higher compared to what is usually seen with SACI and there is no spark plug (there is usually a glow plug). The objective of this work is to investigate if the potential of NVO application for gasoline PPC. The focus of this work is on idle operating conditions at low engine speed without boost. The reason is that NVO is expected to be most useful towards idle operating conditions. The focus of this work is on combustion stability and to see if it can be improved with NVO. The engine-out efficiency is not expected to be high at these operating conditions and it is not the focus of this work. In a previous work by Borgqvist et al. [19], it was found that it was possible to operate the light duty diesel engine with 87 RON gasoline fuel down to approximately 2 bar IMEPgross with a significant fraction of trapped hot residual gases. This work is a continued investigation with more emphasis on NVO.

The problem with NVO at low load operating conditions is that the exhaust gas temperature is low. While an increase of NVO potentially increases the in-cylinder temperature, increasing NVO also increases the EGR fraction which lowers the specific heat ratio and thus the global in-cylinder temperature. The question is to what extent NVO can be used to extend the low load operating region. Simulations are performed with a 1-D engine simulation tool, AVL BOOST, to determine the residual gas fraction and in-cylinder temperature.

EXPERIMENTAL APPARATUS AND SETUP

The experimental engine is based on a Volvo D5 light duty diesel engine. The engine properties can be seen in Table 1. It is run on only one of the five cylinders and is equipped with a fully flexible pneumatic valve train system supplied by Cargine Engineering. The Cargine valve train system was first demonstrated by Trajkovic et al. [20]. The valve actuators are placed on an elevated plate above the fuel injector and are connected to the valve stems with push-rods. Intake valve closing (IVC) timing is constant 180 CAD BTDC @ 1 mm valve lift and exhaust valve opening timing is constant 180 CAD BTDC @ 1 mm valve lift. Maximum valve lift is approximately 5 mm. The fuel injection system is a common rail system with a with a 5 hole nozzle solenoid injector. The umbrella angle is 140 degrees and the nozzle hole diameters are 0.159 mm.

Experimental data is collected with varying settings of NVO from 60 CAD to 220 CAD and at varying engine load from approximately 2 bar IMEPgross to 3.4 bar IMEPgross. The fuel that is used is 87 RON gasoline. The fuel injection strategy is a single injection with start of injection (SOI) at 22 CAD BTDC. At a few operating points with relatively high load, the start of injection have to be retarded in order to have combustion timing occur after top dead center. The common rail pressure is constant at 500 bar. Engine load is varied by increasing the fuel injection duration. The glow plug is continuously on. The engine is run without boosted air and without EGR. Intake air temperature is controlled with a heater in the intake manifold to 40° C. The engine speed is 800 rpm.

Lambda (the air fuel ratio divided with the stoichiometric air fuel ratio) varies with both engine load and NVO. Since the investigated load region is relatively small, the largest effect is from NVO. Lambda is approximately 3 at NVO 60 CAD and decreases with NVO down to approximately 1.3 at NVO 220 CAD.

Table 1 - Engine properties.

Displacement (one cylinder)	0.48 Liter
Stroke	93.2 mm
Bore	81 mm
Compression ratio	16.5:1
Number of Valves	4
Valve train	Fully flexible
Fuel	87 RON gasoline

The engine control system was developed by the author in LabVIEW 2009. The control system is run from a separate target PC, NI PXI-8110, which is a dedicated real-time system. The target PC is equipped with an R series multifunctional data acquisition (DAQ) card with re-programmable FPGA hardware, NI PXI-7853R, and an M-series data acquisition card, NI PXI-6251. The user interface is run on a separate Windows based host PC. The host and target PCs communicate over TCP/IP.

In-cylinder pressure and valve lift curves are measured simultaneously with the FPGA DAQ card. The in-cylinder pressure and valve lift curve measurements are crank angle based with resolution 0.2 CAD/sample. Post-processing of the data is made in Matlab.

The valve lift curves are seen in Figure 1. The valve open speed is fast compared to conventional systems. In order to ensure valve clearance around top dead center the minimum NVO that is tested is 60 CAD.

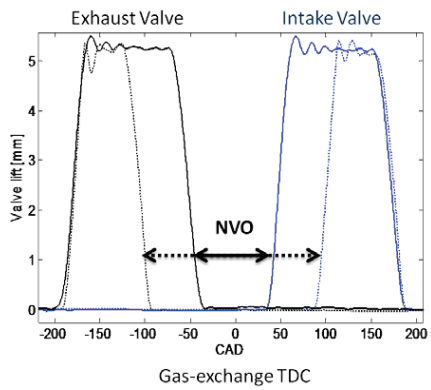

Figure 1 - The valve lift curves of the Cargine valves with negative valve overlap.

ENGINE SIMULATION MODEL IMPLEMENTATION

To determine the residual gas fractions and in-cylinder temperatures for the various operating points, a model of the experimental engine was implemented in the 1-D engine simulation tool AVL BOOST v2011.1, Figure 2. The model was calibrated by comparing calculated and measured motored cycles to achieve correct settings of for instance compression ratio and heat transfer parameters. For each operating point the experimental settings, for instance fuel mass, valve lift curves, heat release rates and evaporation rates etc, were applied to the simulation model. Small adjustments of heat transfer parameters and valve timings were done to achieve close agreement between calculated and measured cylinder pressures. An example is seen in Figure 3.

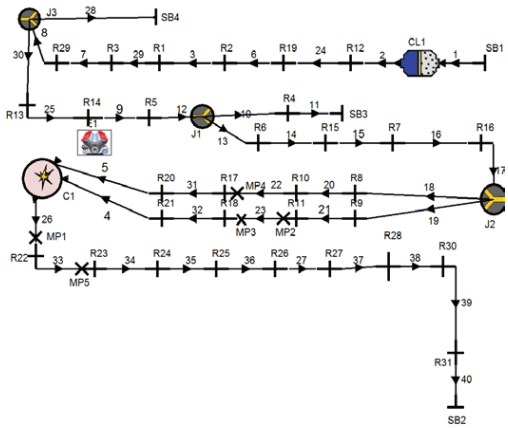

Figure 2 – The engine simulation model in BOOST.

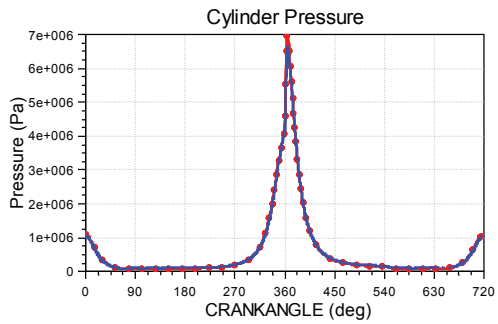

Figure 3 - Calculated cylinder pressure (red/dotted) versus experimental cylinder pressure (blue). The figure shows a typical agreement between the calculated and measured cases.

RESULTS AND DISCUSSION

ENGINE SIMULATION MODEL RESULTS

The residual gas mass fraction and in-cylinder temperature, which are obtained from the engine simulation model, are seen in Figure 4 and Figure 5, respectively. The circles with the color magenta that is seen in the figures show the locations of the experiment data. Due to time constraints it was not possible to simulate all of the measured operating points.

When NVO is increased, a larger fraction of hot residual gases are trapped in the cylinder, which increases the in-cylinder temperature at IVC timing. The in-cylinder temperature at IVC timing is affected by both the fraction and temperature of the trapped residual gases, as seen in Figure 6. It is obvious that the highest initial charge temperatures are reached with a high residual gas fraction and exhaust gas temperature. And, as expected, the effect of exhaust gas temperature on initial charge temperature is small when the residual gas fraction is low.

From the simulation model results, it is seen that NVO has a dominating influence on both residual gas mass fraction and in-cylinder temperature at IVC timing. As expected, the effect of engine load on in-cylinder temperature at IVC timing is noticeable only when the residual gas fraction is sufficiently high. This is not a surprising result but it is still useful to verify that the simulation model captures this expected behavior.

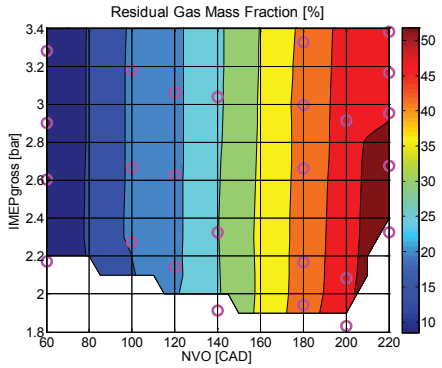

Figure 4 – The residual gas mass fraction from the AVL BOOST simulation.

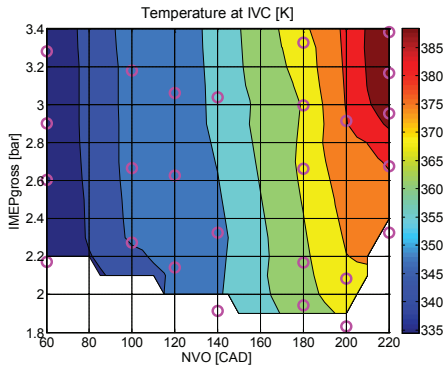

Figure 5 – The in-cylinder temperature at intake valve closing from the AVL BOOST simulation.

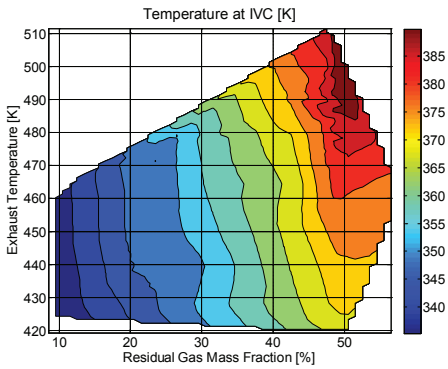

Figure 6 – Effects of residual gas mass fraction and the exhaust gas temperature on the in-cylinder temperature at intake valve closing

The first question is whether or not the global in-cylinder temperature after compression is counteracted by an increase of the residual gas fraction. Increasing the residual gas fraction increases the in-cylinder temperature at IVC timing. But increasing the fraction of residual gases also lowers the ratio of specific heats which lowers the temperature after compression. According to the AVL BOOST engine simulation model results, Figure 7, it is seen that the temperature after compressions is not significantly affected by the residual gas fraction. According to the simulation model, the dominating effect on the global in-cylinder temperature after compression is from the in-cylinder temperature at IVC timing. The in-cylinder temperature at SOI timing is continuously increased with NVO, at least up to 220 CAD NVO, which corresponds to a residual gas mass fraction of approximately 50%.

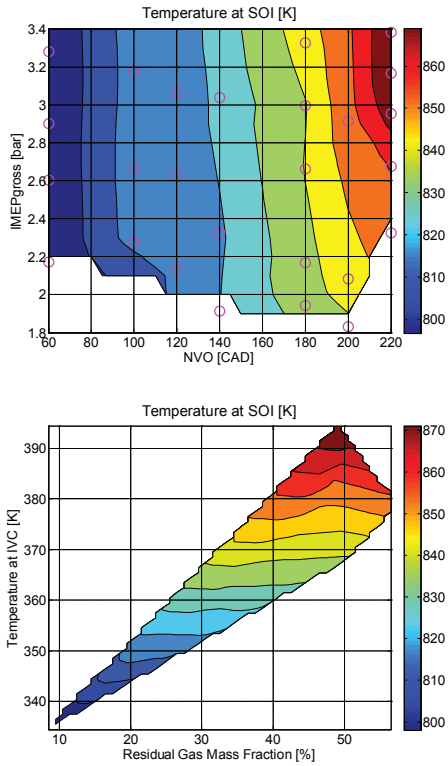

Figure 7 – In-cylinder temperature at start of fuel injection timing from the AVL BOOST simulation model.

The in-cylinder temperature at start of combustion (SOC) timing is seen in Figure 8. Between SOI and SOC the temperature is increased from the additional compression of the cylinder but there is also a decrease of in-cylinder temperature from fuel vaporization. The figure shows that the in-cylinder temperature at SOC timing is increased with increased residual gas fraction.

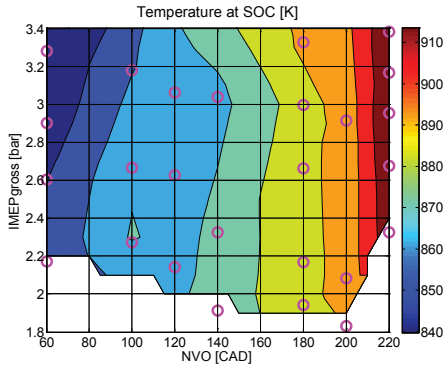

Figure 8 – In-cylinder temperature at start of combustion timing from the AVL BOOST simulation model.

EXPERIMENT RESULTS

In this section the influence of NVO on combustion parameters such as ignition delay, combustion efficiency and emissions are shown and discussed. Again, the magenta circles are shown in some figures to show the locations of the measured operating points. The parameters that are shown here are calculated from measured data, not simulated. An increased fraction of residual gases result in increased stratification in temperature and EGR distribution [21]. One of the main differences compared to traditional SACI with NVO is that also the fuel distribution is less homogeneous due to the relatively late fuel injection. It would be very interesting to perform optical diagnostics of the in-cylinder fuel, EGR and temperature distribution in order to get a deeper understanding of the auto-ignition and combustion. Initially, single cylinder experiments are useful to get a fundamental understanding of NVO on the combustion.

The rate of heat-released curves with varying NVO and constant fuel injection timing and duration are seen in Figure 9. Engine load is approximately 3 bar IMEPgross. It is seen that the peak rate of heat-release increases with increased NVO up to NVO 180 CAD. The combustion duration becomes significantly shorter when NVO is increased from NVO 60 CAD to NVO 120 CAD. When NVO is increased from 200 CAD to 220 CAD the ignition delay becomes significantly longer, the peak rate of heat-release is lower and the combustion duration becomes longer.

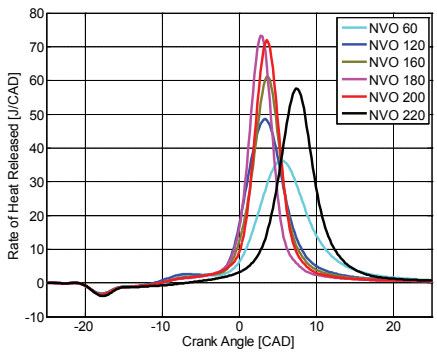

Figure 9 – Rate of heat released curves with NVO from 60 CAD to 220 CAD.

The ignition delay, defined as SOI-CA10, is shown against NVO and engine load in Figure 10. It is seen that the ignition delay is shorter at the higher engine load operating points and also that is shortest in the NVO region from approximately 120 CAD up to 200 CAD, which corresponds to a residual gas fraction from approximately 20-45 percent. This is not explained by the global in-cylinder temperature conditions alone since the highest temperatures are achieved with the highest settings of NVO. One possible explanation is that if the mixture is too diluted, either with air, or with trapped residual gases, the auto-ignition chemistry is slowed down and the fuel mixture becomes less reactive. Also, the fuel, EGR and temperature distribution could have a significant effect.

Another possible contributing factor is the low temperature reactions. Figure 11 shows the rate of heat released curves with varying NVO zoomed in over the region prior to the main combustion event where the low temperature reactions can be seen. The rate of heat released from the low temperature reactions can be distinguished with NVO up to 200 CAD. At 220 CAD NVO the in-cylinder temperature is the highest and no low temperature reactions can be seen. It is possible that the low temperature reactions assist in triggering the main combustion event. This would then partially explain the long ignition delay in the 220 CAD NVO cases where the in-cylinder temperature is the highest. The long ignition delays in the cases with low NVO settings, where the low temperature reactions are clearly seen, can be explained by the low in-cylinder temperature.

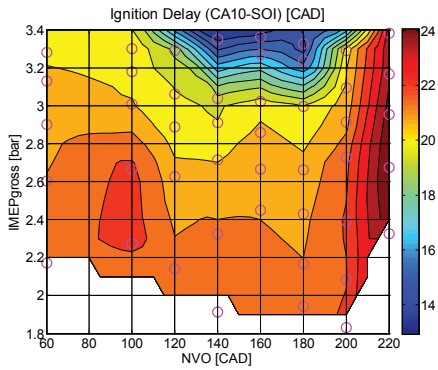

Figure 10 – Effects of the negative valve overlap setting and engine load on the ignition delay, defined as CA10-SOI

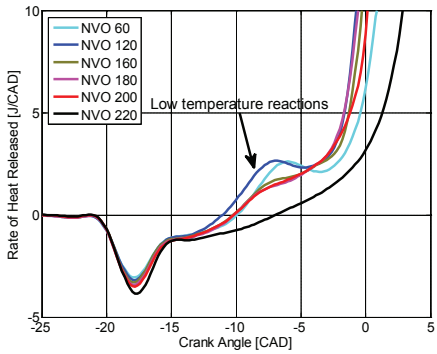

Figure 11 – Zoomed in rate of heat released curves from NVO 60 CAD to 220 CAD.

The combustion timing, defined as the crank angle of 50 % accumulated heat released, CA50, is shown against NVO and engine load in Figure 12. Since the injection timing was constant with a few exceptions, the combustion timing is reflected by the ignition delay.

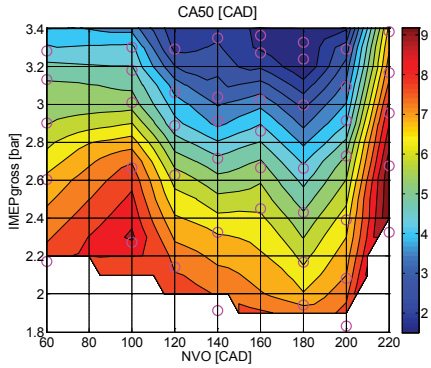

Figure 12 – Effects of the negative valve overlap setting and engine load on combustion timing.

The combustion duration, defined as CA90-CA10, is shown in Figure 13. The combustion duration is unaffected when NVO is increased from 60 CAD to 100 CAD and becomes shorter when NVO is increased from 100 CAD to 180 CAD. For a given engine load, the combustion duration is the shortest with NVO settings 180-200 CAD (40-45% residual gas fraction). Again, this is not explained by the global in-cylinder temperature alone, because, according to the engine simulation model, the highest in-cylinder temperature is reached with the highest possible NVO setting. The in-cylinder fuel, EGR and temperature distribution probably has a significant effect. The combustion duration also decreases with engine load, and this is explained by the temperature decrease.

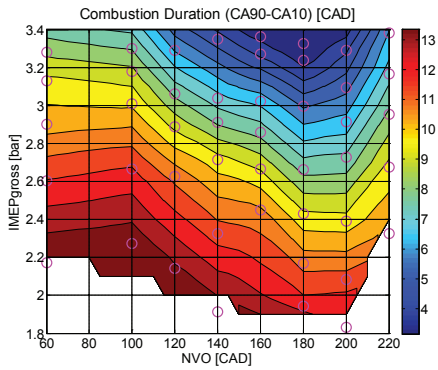

Figure 13 – Effects of the negative valve overlap setting and engine load on combustion duration (CA90-CA10).

The next question is if and how much the low load limit can be extended with NVO. The standard deviation in IMEPnet is shown against NVO and engine load in Figure 14. The standard deviation in IMEPnet is used instead of COV of IMEP, which is often seen as a measure of cycle-to-cycle variations and combustion instability. The lowest standard deviation in IMEPnet occurs with a NVO setting of 180 CAD which corresponds to a residual gas fraction from approximately 40-45 %. This is the NVO setting where the ignition delay and combustion duration are relatively short indicating that the mixture is prone to auto-ignite and that it burns rapidly.

If a limit is set to 0.2 bar in standard deviation in IMEPnet, the effect of low load limit expansion with NVO can be investigated. At the 60 CAD NVO setting, the low load limit would be reached already around 3.2 bar IMEPgross. At NVO 180 CAD, the low load limit can be extended down to 2.2 bar IMEPgross. In summary, an increase in NVO from 60 CAD to 180 CAD results in an increase in residual gas fraction from approximately 10 to 40 % and an approximately 30 K elevated initial charge temperature. The result is that the low load limit is extended from 3.2 bar IMEPgross down to 2.2 bar IMEPgross.

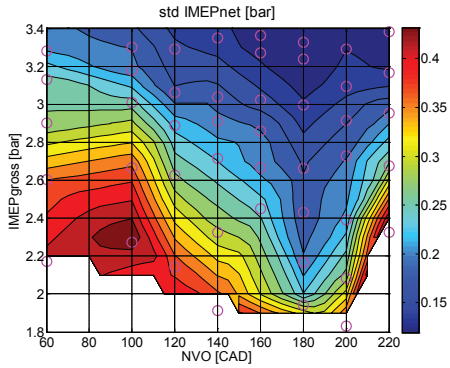

Figure 14 – Effects of the negative valve overlap setting and engine load on standard deviation in IMEPnet.

The next question is how the combustion efficiency is affected by NVO. The combustion efficiency is shown against NVO and engine load in Figure 15. Unfortunately the CO measurement instrument was saturated at the lowest engine load operating conditions. The measurement points where the instrument was saturated are shaded in grey in the figure. The combustion efficiency increases with NVO but decreased with load. This can be explained by the changes in in-cylinder temperature. The optimum combustion efficiency also peaks around NVO 180 CAD, which was also the optimum NVO for the standard deviation in IMEPnet. The decrease in combustion efficiency when going from NVO 180 CAD to 220 CAD is small.

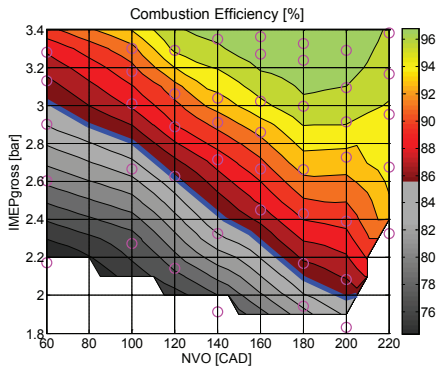

Figure 15 – Effects of the negative valve overlap setting and engine load on combustion efficiency. The grey-colored region below the thick blue line indicates that the CO measurement instrument was saturated.

The next investigation is the effect of NVO on NOx and soot emissions. Since no external EGR is used, the NOx emissions are expected to be significant. The reason for not using EGR is that the goal with the NVO application is to go down in load. Lowering the in-cylinder temperature further with EGR is expected to lower the combustion efficiency, which is already low at the low load operating conditions. This would limit the attainable low load operating region even further. When the engine load is sufficiently low, NOx emissions are expected to be low. The NOx emissions are shown against NVO and engine load in Figure 16. It is seen that NOx emissions are low when the engine load is low and when the residual gas fraction is high. The NOx emissions are high in the NVO region where combustion is the most stable and the ignition delay is the shortest.

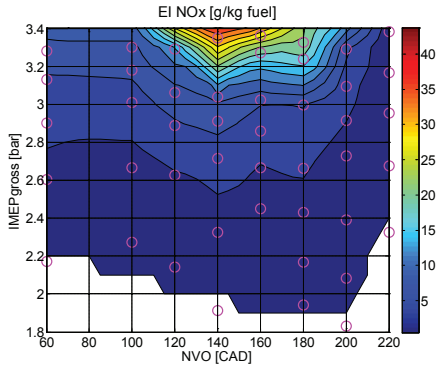

Figure 16 – Effects of the negative valve overlap setting and engine load on Nox emissions.

The soot emissions are shown against NVO and engine load in Figure 17. The soot emissions at low load gasoline PPC with NVO operating conditions do not correlate entirely with the ignition delay. A long ignition delay promotes mixing of fuel and air prior to combustion to suppress soot emissions. Soot emissions are detectable when the NVO setting is high, but where also the ignition delay is long. The soot formation under these operating conditions can be explained by the low global air fuel ratio.

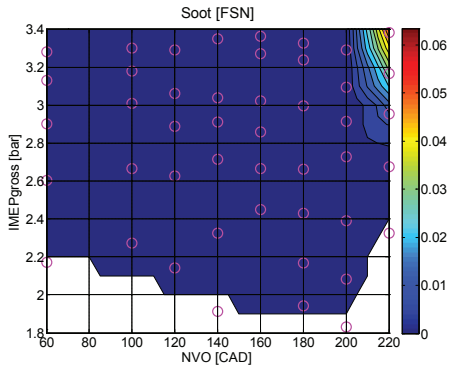

Figure 17 – Effects of and negative valve overlap setting and engine load on soot emissions.

Effect of Glow Plug

The final investigation is on the effect of glow plug in combination with NVO. The results presented up to here have been measured with the glow plug continuously on. The final investigation is on how the glow plug affects combustion. The rate of heat-released curves with varying NVO and constant fuel injection timing and duration are seen in Figure 18. The operating conditions are the same as presented in Figure 9, but the glow plug is turned off. In comparison with Figure 9, one observation is that the spread in crank-angle of peak rate of heat-released appears to be larger. A second observation is that the peak rate of heat-released in the cases with the lowest and highest setting of NVO are significantly higher when the glow plug is on. These observations are an indication that the glow plug has an effect on the combustion.

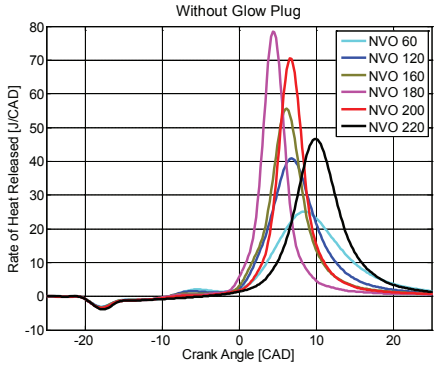

Figure 18 - Rate of heat released curves with NVO from 60 CAD to 220 CAD without the glow plug.

One question is how the glow plug affects the early phase of combustion, prior to the main combustion event. The rate of heat released curves zoomed in over the region where the low temperature reactions can be seen are shown in Figure 19. Cases with the glow plug turned on and off are shown in the same figure. It is observed that the rate of heat-release from the low temperature reactions is higher when the glow plug is on. The low temperature reactions are still distinguishable when the glow plug is off which shows that these are not initiated by the glow plug. In the 220 CAD NVO case, no temperature reactions are observed independent of the glow plug setting. This is explained by the high in-cylinder temperature, see Figure 20.

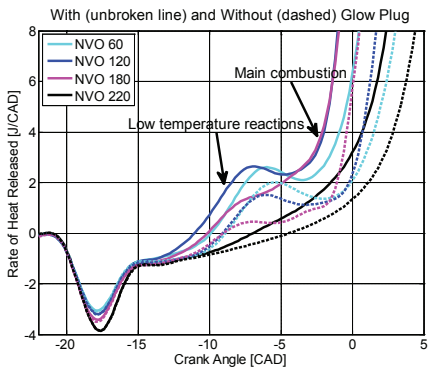

Figure 19 - Zoomed in rate of heat released curves from NVO 60 CAD to 220 CAD with and without the glow plug.

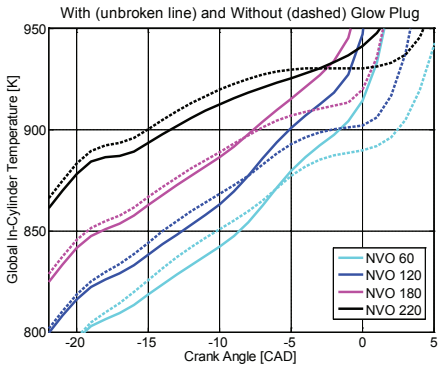

Figure 20 – Global in-cylinder temperature of different cases with varying NVO with and without the glow plug.

The ignition delay and combustion duration with and without the glow plug are shown in Figure 21. The operating points are the same as was shown in Figure 9 and Figure 18. The error bars show plus minus one standard deviation. The ignition delay is shorter when the glow plug is turned on independent of the residual gas fraction, but the standard deviation (the error bars) is higher. The combustion duration is shorter with the glow plug up to 180 CAD NVO. This is the NVO setting where combustion stability is the highest, and it can be seen that the glow plug has no effect on combustion duration in this case. If the residual gas fraction is increased further, the combustion duration is again shorter when the glow plug is on. According to these observations, the glow plug has an effect on both the early phase of combustion (CA10-SOI) and subsequent main combustion duration (CA90-CA10).

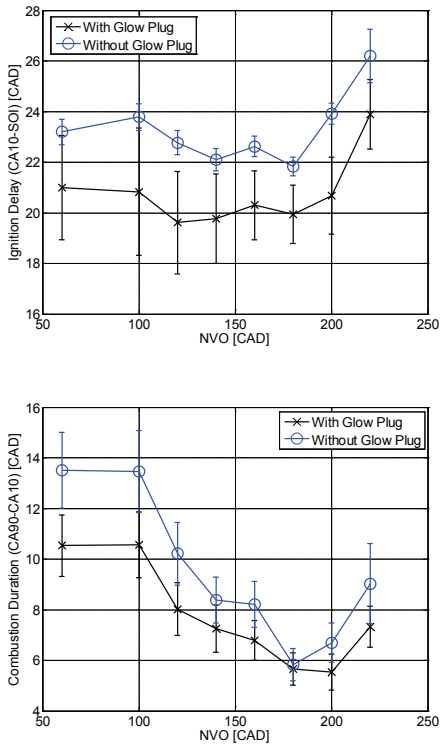

Figure 21 – The ignition delay and combustion duration with and without the glow plug. The error bars show plus minus one standard deviation.

The standard deviation of IMEPnet and combustion efficiency with and without the glow plug are shown in Figure 22. It is seen that the combustion stability and combustion efficiency is higher with the glow plug but that the improving effect decreases with NVO. At the 180 CAD NVO setting, the combustion stability and combustion efficiency is relatively high independent of the glow plug setting. The conclusion is that the glow plug has an observable effect on ignition delay and combustion duration and the effect on combustion stability and combustion efficiency is more prominent with low residual gas fractions. An optimum NVO exists that maximizes combustion stability and combustion efficiency and the glow plug has no additional improving effect in this case.

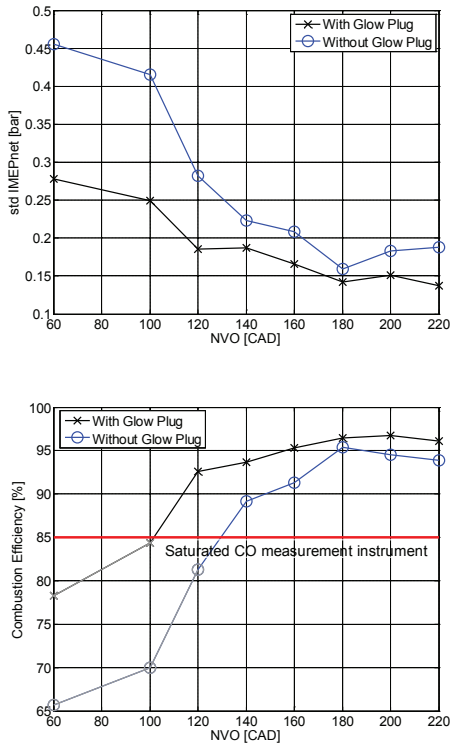

Figure 22 – Standard deviation of IMEPnet and combustion efficiency with and without the glow plug. Operating points below the red line in the combustion efficiency figure were measured with a saturated CO measurement instrument.

SUMMARY/CONCLUSIONS

The objective was to investigate the usefulness of negative valve overlap on a light duty diesel engine running with gasoline partially premixed combustion at low load operating conditions. The focus was on low engine speed and load since it is assumed that the available boost is limited and the utilization of negative valve overlap is expected to have a more important role in extending the low load limit. At higher engine speed and load the usefulness of negative valve overlap on gasoline PPC is expected to be limited.

The experimental light duty diesel engine was run with 87 RON gasoline at varying load and NVO settings at engine speed 800 rpm. A simulation model was implemented with AVL BOOST based on the experimental data. Residual gas mass fraction and in-cylinder temperature was calculated from the simulation model.

- The first question was whether or not the global in-cylinder temperature after compression is counteracted by an increase of the residual gas fraction. According to the simulation model, the dominating effect on the global in-cylinder temperature after compression is from the initial charge temperature and not the residual gas fraction
- The shortest ignition delay was measured from approximately 120 CAD up to 200 CAD, which corresponds to a residual gas fraction from approximately 20-45 percent. And the combustion duration is the shortest with NVO settings 180-200 CAD (40-45% residual gas fraction). This is not explained by the global in-cylinder temperature alone. Also, the fuel, EGR and temperature distribution could have a significant effect.

- If a limit is set on standard deviation on IMEPnet to be associated with the minimum attainable load, the low load limit could be extended from 3.2 bar IMEPgross down to 2.2 bar IMEPgross when NVO is increased from 60 CAD to 180 CAD. The combustion efficiency is also the highest around 180 CAD NVO.
- The NOx emissions are high in the NVO region where combustion is the most stable and the ignition delay is the shortest. And the soot emissions are high in the region where the residual gas fraction is this highest and the global air fuel ratio is the lowest.
- The glow plug has an observable effect on ignition delay and combustion duration and the effect on combustion stability and combustion efficiency is more prominent with low residual gas fractions. An optimum NVO exists that maximizes combustion stability and combustion efficiency and the glow plug has no additional improving effect in this case.

REFERENCES

1. Willand, J., Nieberding, R-G., Vent, G., Enderle, C., "The Knocking Syndrome – Its Cure and Its Potential", SAE 982483, 1998
2. Lavy, J., Dabadie, J-C., Angelberger, C., Duret, P., Willand, J., Juretzka, A., Schäflein, J., Ma, T., Lendresse, Y., Satre, A., Shulz, C., Krämer, H., Zhao, H., Damiano, L., "Innovative Ultra-low NOx Controlled Auto-Ignition Combustion Process for Gasoline Engines : the 4-SPACE Project", SAE 2000-01-1837, 2000
3. Kimura, S., Aoki, O., Ogawa, H., Muranaka, S., Enomoto Y., "New Combustion Concept for Ultra-Clean and High Efficiency Small DI Diesel Engines", SAE 1999-01-3681, 1999
4. Akihama K., Takatori Y., Inagaki K., Sasaki S., Dean A., "Mechanism of the Smokeless Rich Diesel Combustion by Reducing Temperature", SAE 2001-01-0655, 2001
5. Yanigahara H., Sato Y., Minuta J., "A simultaneous reduction in NOx and soot in diesel engines under a new combustion system (Uniform Bulky Combustion System – UNIBUS)", 17th International Vienna Motor Symposium, pp 303-314, 1996
6. Hasegawa R., Yanigahara H., "HCCI Combustion in DI Diesel Engine", SAE 2003-01-0745, 2003
7. Kalghatgi G. T., Risberg P., Ångström H., "Advantages of Fuels with High Resistance to Auto-Ignition in Late-injection, Low-temperature, Compression Ignition Combustion", SAE 2006-01-3385, 2006
8. Kalghatgi G. T., Risberg P., Ångström H., "Partially Pre-Mixed Auto-Ignition of Gasoline to Attain Low Smoke and Low NOx at High Load in a Compression Ignition Engine and Comparison with a Diesel Fuel", SAE 2007-01-0006, 2007
9. Kalghatgi G. T., Hildingsson L., Johansson B., "Low NOx and Low Smoke Operation of a Diesel Engine using Gasoline-like Fuels", ICES2009-76034, 2009
10. Hildingsson L., Kalghatgi G., Tait N., Johansson B., Harrison A., "Fuel Octane Effects in the Partially Premixed Combustion Regime in Compression Ignition Engines", SAE 2009-01-2648, 2009
11. Kalghatgi G.T., Hildingsson L., Harrison A., Johansson B., "Low- NOx, low-smoke operation of a diesel engine using "premixed enough" compression ignition – Effects of fuel autoignition quality, volatility and aromatic content", THISEL 2010 Conference on Thermo- and Fluid Dynamic Processes in Diesel Engines, 2010
12. Manente V., Johansson B., Tunestal P., "Effects of Different Type of Gasoline Fuels on Heavy Duty Partially Premixed Combustion", SAE 2009-01-2668, 2009
13. Manente V., Johansson B., Tunestal P., Zander C., Cannella W., "An Advanced Internal Combustion Engine Concept for Low Emissions and High Efficiency from Idle to Max Load Using Gasoline Partially Premixed Combustion", SAE 2010-01-2198, 2010
14. Manente V., Johansson B., Tunestal P., Sonder M., Serra S., "Gasoline Partially Premixed Combustion: High Efficiency, Low NOx and Low Soot by using an Advanced Combustion Strategy and a Compression Ignition Engine", FCE09, Istanbul Turkey, 2009
15. Law, D., Kemp, D., Allen, J., Kirkpatrick, G., Copland, T., "Controlled Combustion in an IC-Engine with a Fully Variable Valve Train", SAE 2000-01-0251, 2000
16. Koopmans, L., Denbratt, I., "A Four Stroke Camless Engine, Operated in Homogeneous Charge Compression Ignition Mode with Commercial Gasoline", SAE 2001-01-3610, 2001
17. Cao, L., Zhao, H., Jiang, X., Kalian, N., "Effects of Intake Valve Timing on Premixed Gasoline Engine with CAI Combustion", SAE 2004-01-2953, 2004
18. Johansson, T., Johansson, B., Tunestål, P., Aulin, H., "The Effect of Intake Temperature in a Turbocharged Multi Cylinder Engine operating in HCCI mode", SAE 2009-24-0060, 2009
19. Borgqvist, P., Tunestal, P., Johansson, B., "Gasoline Partially Premixed Combustion in a Light Duty Engine at Low Load and Idle Operating Conditions", SAE 2012-01-0687, 2012
20. Trajkovic, S., Milosavljevic, A., Tunestål, P., Johansson, B., "FPGA Controlled Pneumatic Variable Valve Actuation", SAE 2006-01-0041, 2006
21. Rothamer A., Snyder J., Hanson R., Steeper R., Fitzgerald R., "Simultaneous imaging of exhaust gas residuals and temperature during HCCI combustion", Proceedings of the Combustion Institute 32 (2009) 2869-2876

CONTACT INFORMATION

Patrick Borgqvist
Lund University
Dept. of Energy Sciences
Div. of Combustion Engines
P.O. Box 118
221 00 Lund
Sweden
patrick.borgqvist@energy.lth.se

ACKNOWLEDGMENTS

The authors wish to show their appreciation to the Competence Centre Combustion Processes (KCFP), Swedish Energy Agency Grant number 22485-2, for their financial support. The authors would also like to acknowledge Cargine Engineering for supplying and helping with the valve train system. The authors would also like to expresses their gratitude to Bill Cannella from Chevron Corporation for supplying the fuel and to Håkan Persson from Volvo Car Corporation for hardware support and valuable discussions.

DEFINITIONS/ABBREVIATIONS

BTDC	Before Top Dead Centre
CAD	Crank Angle Degree
DAQ	Data Acquisition
HCCI	Homogeneous Charge Compression Ignition
IMEP	Indicated Mean Effective Pressure
IVC	Intake Valve Close
NVO	Negative Valve Overlap
PPC	Partially Premixed Combustion
SACI	Spark Assisted Compression Ignition
SOC	Start of Combustion
SOI	Start of Injection

5

Proceedings of the ASME 2012 Internal Combustion Engine Division Fall Technical Conference
ICEF2012
September 23-26, 2012, Vancouver, BC, Canada

ICEF2012-92069

THE LOW LOAD LIMIT OF GASOLINE PARTIALLY PREMIXED COMBUSTION USING NEGATIVE VALVE OVERLAP

Patrick Borgqvist, Öivind Andersson,
Per Tunestål, Bengt Johansson
Department of Energy Sciences
Faculty of Engineering
Lund University
Lund, Sweden

ABSTRACT

Partially premixed combustion has the potential of high efficiency and simultaneous low soot and NOx emissions. Running the engine in PPC mode with high octane number fuels has the advantage of a longer premix period of fuel and air which reduces soot emissions, even at higher loads. The problem is the ignitability at low load and idle operating conditions.

The objective is to investigate different multiple-injection strategies in order to further expand the low load limit and reduce the dependency on negative valve overlap in order to increase efficiency. The question is, what is the minimum attainable load for a given setting of negative valve overlap and fuel injection strategy. The experimental engine is a light duty diesel engine equipped with a fully flexible valve train system. The engine is run without boost at engine speed 800 rpm. The fuel is 87 RON gasoline.

A turbocharger is typically used to increase the boost pressure, but at low engine speed and load the available boost is expected to be limited. The in-cylinder pressure and temperature around top-dead-center will then be too low to ignite high octane number fuels. A negative valve overlap can be used to extend the low engine speed and load operating region. But one of the problems with negative valve overlap is the decrease in gas-exchange efficiency due to heat-losses from recompression of the residual gases. Also, the potential temperature increase from the trapped hot residual gases is limited at low load due to the low exhaust gas temperature. In order to expand the low load operating region further, more advanced injection strategies are investigated.

INTRODUCTION

Homogeneous charge compression ignition (HCCI) combustion has the potential of achieving high efficiency in combination with low NOx and soot emissions. The challenges with HCCI include combustion control, low power density and steep pressure rise rates. As a result, two branches of HCCI emerged, spark assisted compression ignition (SACI), and partially premixed combustion (PPC). SACI is the intermediate process between SI flame propagation and HCCI auto ignition. HCCI mode is typically achieved through trapping of hot residual gases with early exhaust valve closing. The intake valve is opened symmetrically later after top dead center. The interval in crank angles from exhaust valve closing to intake valve opening is called negative valve overlap (NVO). The idea to use negative valve overlap for HCCI was first proposed by Willand et al. [1] in 1998 and demonstrated by Lavy et al. [2] in 2000.

PPC combines traditional diesel combustion with HCCI. With PPC, the fuel injection is completed before start of combustion to promote mixing of fuel and air, but the charge is not homogeneous. One benefit compared to traditional HCCI combustion is that the fuel injection timing can be used as control actuator for the combustion timing. In order to get enough separation from start of injection to start of combustion with diesel fuel a high fraction of EGR has to be used. This concept was used by Nissan [3] and is called Modulated Kinetics (MK). Toyota used high EGR rates to suppress both soot and NOx with the smokeless rich diesel combustion concept [4]. In a different concept, as an alternative to using excessive EGR rates, Toyota used a double injection strategy

with some of the fuel injected early to promote mixing with air. This concept is called UNIBUS [5, 6].

Kalghatgi introduced the concept of gasoline partially premixed combustion in 2006 [7, 8]. With a fuel that is less prone to auto-ignite, a longer mixing period from end of injection to start of combustion can be achieved without using high EGR fractions, too early injection timings or too low compression ratios. Results from a light-duty engine were published in [9-11].

At Lund University, Manente et al. [12, 13] developed a gasoline PPC strategy running a variety of gasoline fuels with different octane numbers in a heavy duty engine. Gross indicated efficiencies up to 57 % with low NOx, HC and CO emissions and soot levels below of 0.5 FSN were demonstrated. Light duty engine experiments were performed in [14].

As demonstrated in a heavy-duty engine, there is a clear decrease in attainable gasoline-PPC engine operating region with increased fuel octane number [13]. The challenge is to operate the engine with high octane number fuels at low engine speed and load where the available boost is expected to be limited. There are different ways to try to expand the attainable operating region, for example, using more advanced injection strategies, using negative valve overlap to trap hot residuals, and to use a glow plug. All of these are utilized in this work.

This work is inspired by an article where different fuel injection strategies for cold start performance in a conventional diesel engine were investigated [15]. It was found that stability was improved with an injection strategy with three pilot injections with increasing fuel mass and that the glow plug is essential because the mixture only ignites close to the glow plug.

In a previous work by Borgqvist et al. [16], it was found that it was possible to operate the light duty diesel engine with 87 RON gasoline fuel down to approximately 2 bar IMEPgross with a significant fraction of trapped hot residual gases. The residual gases were trapped using negative valve overlap. The problem with gasoline PPC at low load compared to diesel is the low combustion efficiency. In addition, utilization of negative valve overlap results in low gas-exchange efficiency due to heat-losses from recompression of the trapped residual gases. Why this affects the gas-exchange efficiency can be understood by studying a PV-diagram and the definition of the gas-exchange efficiency (net indicated work divided by gross indicated work). If there were no heat losses, the enclosed area in the PV-diagram from exhaust valve closing to intake valve opening would be zero. But in reality it is not zero and the result is lower net indicated work and lower gas-exchange efficiency. The dependency on negative valve overlap ultimately results in higher fuel consumption at low loads compared to running with a fuel with low octane number.

The objective of this work is to improve the gasoline PPC combustion stability and combustion efficiency at low load and engine speed by using a more advanced injection strategy. The goal is to reach idle operating conditions. First, a split main fuel injection strategy is optimized using Design of Experiments (DoE). Secondly, a pilot injection is added early during the compression stroke. The optimized combustion strategies are used as starting-points to go further down in load to investigate if the low load limit can be extended compared to the single injection strategy. The fuel injection strategies are evaluated both with a high and low setting of negative valve overlap to investigate if combustion stability and combustion efficiency become less dependent on negative valve overlap.

Also, the improving effect of the glow plug is tested to see if it has similar improvement on stability with gasoline PPC as it had with cold start in diesel engines [15].

The fuel consumption or indicted efficiency of the engine will not be presented in detail in this work. The indicated efficiency at idle operating conditions is not expected to be high. The general idea is that the efficiency at more stable operating conditions will compensate for the efficiency at low load and engine speed operating points.

NOMENCLATURE

The input energy is expressed as FuelMEP (Fuel Mean Effective Pressure), which is the energy content of the fuel normalized with the displacement volume. The output energy of the engine is expressed as IMEP (Indicated Mean Effective Pressure) which is the work output from the engine normalized with the displacement volume. The work output is calculated from the measured in-cylinder pressure over either the complete engine cycle to calculate IMEPnet or by excluding the gas-exchange strokes to calculate IMEPgross.

EXPERIMENTAL APPARATUS

The experimental engine is based on a Volvo D5 light duty diesel engine. The engine properties can be seen in Table 1. It is run on only one of the five cylinders while the other four are motored. The motored pistons were drilled through and do neither compression nor expansion work. The working piston is equipped with a fully flexible pneumatic valve train system supplied by Cargine Engineering. The Cargine valve train system was first demonstrated by Trajkovic et al. [17]. The valve actuators are placed on an elevated plate above the fuel injector and are connected to the valve stems with push-rods. Intake valve closing timing is constant 180 CAD BTDC @ 1 mm valve lift and exhaust valve opening timing is constant 180 CAD BTDC @ 1 mm valve lift. Maximum valve lift is approximately 5 mm. The fuel injection system is a common rail system with a 5 hole nozzle solenoid injector. The umbrella angle is 140 degrees and the nozzle hole diameters are 0.159 mm. The common rail pressure is constant at 400 bar for all experiment cases. The engine is run without boosted air and without EGR. Intake air temperature is controlled with a heater in the intake manifold to 40° C. The engine speed is 800 rpm in all the experiments. The reason is that the goal is to reach idle operating conditions.

Table 1. Engine properties.

Displacement (one cylinder)	0.48 Liters
Stroke	93.2 mm
Bore	81 mm
Compression ratio	16.5:1
Number of Valves	4
Valve train	Fully flexible

The engine control system was developed in LabVIEW 2009 by the first author. The control system is run from a separate target PC, NI PXI-8110, which is a dedicated real-time system. The target PC is equipped with an R series multifunctional data acquisition (DAQ) card with re-programmable FPGA hardware, NI PXI-7853R, and an M-series data acquisition card, NI PXI-6251. The user interface is run on a separate Windows based host PC. The host and target PCs communicate over TCP/IP.

In-cylinder pressure and valve lift curves are measured simultaneously with the FPGA DAQ card. The in-cylinder pressure and valve lift curve measurements are crank angle based with resolution 0.2 CAD/sample. Post-processing of the data is made in Matlab.

The valve lift curves are seen in Figure 1. The valve opening speed is fast compared to conventional systems. In order to ensure valve clearance around top dead center the minimum NVO tested is 60 CAD.

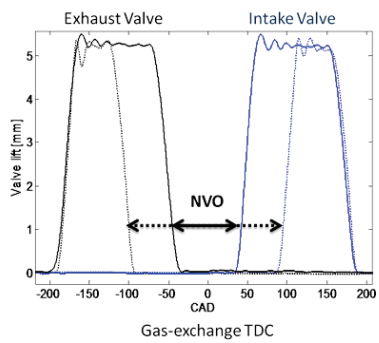

Figure 1. The valve lift curves of the Cargine valves with negative valve overlap.

SPLIT MAIN STRATEGY OPTIMIZATION

Design of Experiments

The setup and evaluation of the split main injection strategy optimization was done using DoE. A central composite design, based on a two-level full factorial design with superimposed axial and center points was chosen for the experiments. A more detailed description of this design and properties can be found in [18]. The graphical representation of the experimental factors can be seen in Figure 2. The experimental factors are the negative valve overlap, the fuel mass ratio between the two injections and the separation in crank angles between the start of injections. The level and coded value of each factor is seen in Table 2. All the experiment cases in the test matrix, Table 3, were run twice in randomized order. The replicate tests were mixed with the first tests. The injected fuel mass was constant for all test cases and corresponds to 7.5 bar FuelMEP. The selected amount of fuel mass was chosen so that all test cases could be run at a sufficiently stable operating point. The fuel injection timing of the first fuel injection event is constant –22 CAD BTDC. The duration of the second fuel injection controls FuelMEP.

The output variables, the standard deviation of IMEPnet and combustion efficiency were fitted to separate second order models:

$$y = Const. + x_1A + x_2B + x_3C + x_4AA + x_5BB + x_6CC + x_7AB + x_8AC + x_9BC \quad \text{(Eq. 1)}$$

A is the coded value for negative valve overlap, B is the mass fuel ratio between the first and second injection, and C is the separation in crank angles between the start of the two injections.

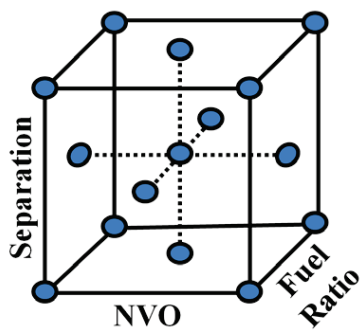

Figure 2. Graphical representation of the experimental factors and their levels.

Table 2. Engine control parameters.

	Low (-)	Base (0)	High (+)
NVO [CAD]	60	130	200
Fuel mass ratio (first/second injection) [%]	30/70	50/50	70/30
Fuel injection separation (SOI2-SOI1) [CAD]	7	9.5	12

Table 3. Test matrix in coded values.

Case	(A) NVO	(B) Fuel ratio	(C) Separation
1	-	-	-
2	+	-	-
3	-	+	-
4	+	+	-
5	-	-	+
6	+	-	+
7	-	+	+
8	+	+	+
9	0	0	0
10	-	0	0
11	+	0	0
12	0	-	0
13	0	+	0
14	0	0	-
15	0	0	+

Results and Discussion

The Pareto chart of the coefficients of the regression models of the standard deviation of IMEPnet, Figure 3, and combustion efficiency, Figure 4, shows the significance of each factor on the output. The blue line in the Pareto charts represents the cumulative sum of the coefficients which gives an idea of how much of the total behavior is captured when using a limited number of factors. This is however influenced by the scaling due to the choice of intervals for the factors in the DoE.

For the standard deviation of IMEPnet, which is a measure of combustion instability, the fuel mass ratio between the two injections (coded as B) is the most important factor. The negative valve overlap (coded as A) is the most important factor for combustion efficiency.

From analysis of the output of the regression models, the following conclusions can be made: 1) a large fraction of the fuel should be injected with the first injection. 2) A high setting of negative valve overlap results in improved combustion efficiency but the lowest standard deviation of IMEPnet was found for approximately 160 CAD NVO. 3) A too short or a too long separation between the fuel injections should be avoided. Conclusions 1 and 3 are independent of the residual gas fraction (NVO setting).

The first conclusion is somewhat different from what was concluded by Chartier et al. [15]. Even though the number of injections are different compared to this investigation, an increasing fuel mass for each fuel injection was found to be most beneficial for the case with cold-start with diesel fuel. But it appears to be the opposite in the case with low-load gasoline PPC.

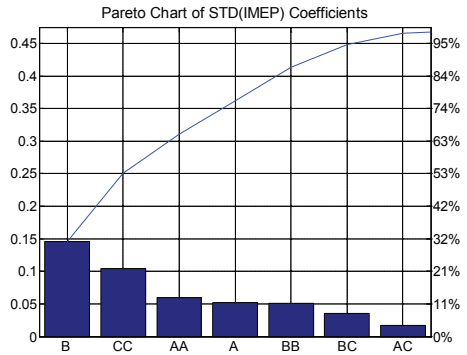

Figure 3. Pareto chart of the standard deviation of IMEPnet second order regression model coefficients, x_n, from Eq. 1. A is the coded letter for NVO, B is the coded letter for the fuel mass ratio between the injections, and C is the separation in crank angles between the start of the two injections.

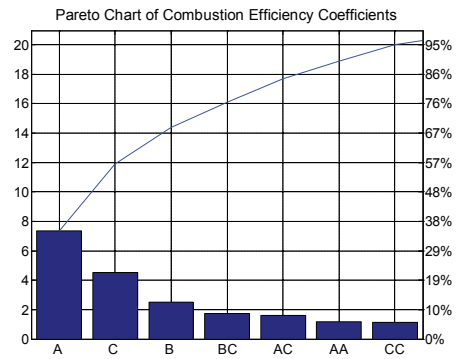

Figure 4. Pareto chart of the combustion efficiency second order regression model coefficients, x_n, from Eq. 1. A is the coded letter for NVO, B is the coded letter for the fuel mass ratio between the injections, and C is the separation in crank angles between the start of the two injections.

INJECTION STRATEGY COMPARISONS: RESULTS AND DISCUSSION

The optimized fuel injection strategy is now used to expand the low-load limit by reducing the injected amount of fuel in the second fuel injection event. One reason for preferring this approach is that it was concluded that a large fraction should be injected in the first fuel injection. A second alternative is to

reduce the common rail pressure which reduces the amount of fuel in both injections. A third alternative is to keep the common rail pressure constant and instead decrease the injection duration time of both fuel injections. The second alternative was initially tested but did not show any significant improvements compared to the preferred approach. The fuel injection strategy is tested both with a low (NVO 60) and high (NVO 200) fraction of residual gases. Only a high setting of NVO is used to get a reasonable trade-off between combustion stability and combustion efficiency. Test cases with a single fuel injection strategy are used as a reference.

Finally, initial tests with an additional pilot injection at -60 CAD are demonstrated. According to Collin et al. [19], an injection timing of -60 CAD BTDC is in the interval where the first signs of stratification of the fuel mixture around TDC can be seen. Also, according to Manente et al. [20], the optimum pilot injection timing for gasoline PPC was found to be at -60 CAD. The pilot injection is added to both the single injection strategy and the optimized split main injection strategy. A summary of all the injection strategies are seen in Figure 5.

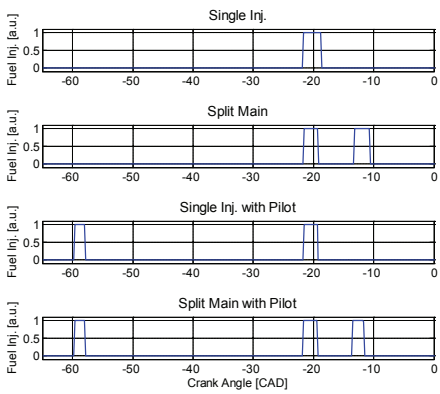

Figure 5. Representation of fuel injection signal from the engine control system over the different injection strategies.

Split Main Injection

The standard deviation of IMEPnet and combustion efficiency from engine load 1.7 bar IMEPgross up to 3.5 bar IMEPgross are seen in Figure 6 and Figure 7. It can be seen that the split main fuel injection strategy significantly improves the combustion stability for the NVO 60 CAD case compared to the single injection strategy. But when engine load is reduced to 2.5 bar IMEPgross the difference between the two strategies is small. The NVO 200 CAD cases have significantly lower standard deviation of IMEPnet compared to the NVO 60 cases, and the improvement of the split main injection strategy is less apparent.

In the combustion efficiency figures throughout this article, the CO measurement instrument was saturated at the lower load operating conditions. The saturated CO operating points are marked in the figures. The continued decrease in combustion efficiency past the first saturated operating condition is from hydrocarbon emissions.

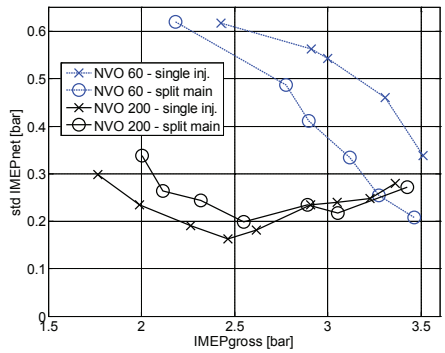

Figure 6. Standard deviation of IMEPnet of the single injection strategy compared to the optimized split main injection strategy.

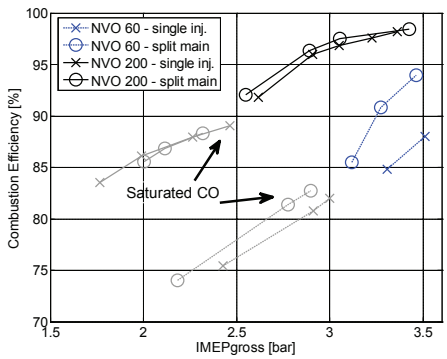

Figure 7. Combustion efficiency of the single injection strategy compared to the optimized split main injection strategy.

The combustion efficiency is also improved with the split main injection strategy for the NVO 60 cases. For the NVO 200 cases there is no apparent improvement in combustion efficiency from the single injection strategy to the split main injection strategy. There is a significant improvement in combustion efficiency with increased NVO. This is in

agreement with the regression model output (Eq.1) and with previous investigations of NVO effects [16]. When the fraction of trapped hot residual gases is increased, the in-cylinder temperature is higher and the air fuel ratio is decreased. With a higher in-cylinder temperature and possibly a lower air fuel ratio the effect of fuel injection strategy is less apparent.

Pilot Injection Strategy

A pilot injection at -60 CAD is added to both the single injection strategy and the split main injection strategy. The fuel amount in the pilot is kept constant and is the same that was used in the first fuel injection at the low setting from the DoE experiments, Table 2. The fuel injection timings are constant. The amount in the first split main injections is the same as used previously. Engine load is reduced by decreasing the amount of fuel in the second injection of the split main injections. When a portion of the fuel is shifted from the second split main fuel injection to the pilot, the duration of the second injection reaches zero at approximately 2.5 bar IMEPgross. The consequence is that the operating points from 2.5 bar IMEPgross and below of the split main with pilot strategy are replicates of the single injection with pilot strategy.

The standard deviation of IMEPnet of the single injection strategy compared to the single injection with pilot strategy is seen in Figure 8.

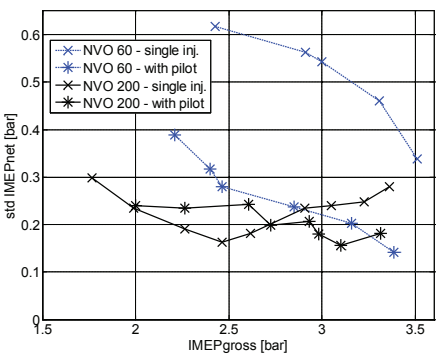

Figure 8. Standard deviation of IMEPnet of the single injection strategy compared to the single injection with pilot strategy.

The standard deviation of IMEPnet with lowest possible residual gas fraction (NVO 60) is significantly lower when the pilot injection is added. If the improvement is compared to the split main combustion strategy it appears as if the improvement is larger with the pilot injection compared to the split main injection strategy. Down to approximately 2.5 bar IMEPgross the standard deviation in IMEPnet is comparable to the NVO 200 CAD cases. In the case with a high fraction of trapped residual gases (NVO 200), no significant overall improvement can be observed in standard deviation of IMEPnet when the pilot injection is added.

The combustion efficiency of the single injection strategy compared to the single injection with pilot strategy is seen in Figure 9. The combustion efficiency is also improved when a pilot injection is added and the residual gas fraction is low. But the combustion efficiency of the 200 CAD NVO case is lower when the pilot injection is added.

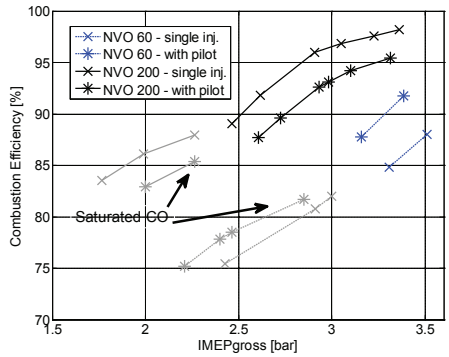

Figure 9. Combustion Efficiency of the single injection strategy compared to the single injection with pilot strategy.

Why is the combustion efficiency improved in the case with low residual gas fraction but reduced in the case with a high residual gas fraction when a pilot injection is added?

One possible reason could be wall impingement and also trapped fuel in the squish volume which results in increased hydrocarbon emissions and consequently lowers the combustion efficiency. This could be one explanation for the lower combustion efficiency when the pilot injection is added in the 200 CAD NVO case. But the combustion efficiency is improved when the same amount of fuel is added at the same injection timing in the 60 CAD NVO case. The explanation would then be that the positive effects on combustion compensate for the additional source of hydrocarbon emissions and the result is higher combustion efficiency.

The improving effect on combustion stability (cycle-to-cycle variations) in the 60 CAD NVO case has already been shown in Figure 8. The hydrocarbon emissions are seen in Figure 10. The hydrocarbon emissions in the 200 CAD NVO cases are approximately 200-300 ppm higher when the pilot injection is added. In the 60 CAD NVO case the measured hydrocarbon emissions at the highest engine load operating conditions, at approximately 3.5 IMEPgross, are the same with and without pilot injection. The improvement on combustion efficiency is then from lower CO emissions when the pilot is added.

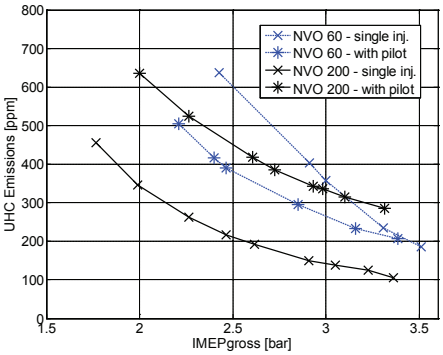

Figure 10. Unburned hydrocarbon (UHC) emissions of the single injection strategy compared to the single injection with pilot strategy.

The combustion timing, defined as the crank angle of 50 % accumulated heat-released, and combustion duration are seen in Figure 11 and Figure 12. It is clear that there is a significant impact on the combustion in the 60 CAD NVO case when the pilot injection is added. The combustion timing is significantly advanced and the combustion duration is shorter. In the 200 CAD NVO case, both combustion timing and combustion duration are unaffected when the pilot injection is added. It is likely that the increased in-cylinder temperature from the large fraction of trapped hot residuals is sufficiently high to promote combustion so that no additional improvements are gained from the pilot injection. Instead the addition of a pilot injection results in increased hydrocarbon emissions but no additional improvements on combustion.

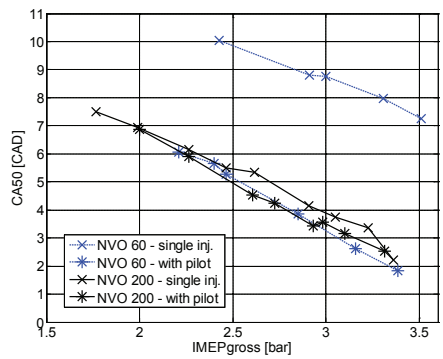

Figure 11. Combustion timing of the single injection strategy compared to the single injection with pilot strategy.

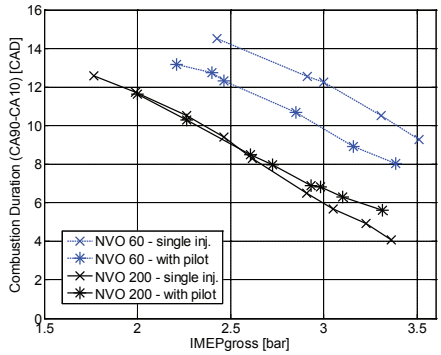

Figure 12. Combustion Duration of the single injection strategy compared to the single injection with pilot strategy.

Similar to the single injection cases, the standard deviation of IMEPnet and combustion efficiency of the split main injection strategy are compared to the split main injection with pilot strategy. The results are seen in Figure 13 and Figure 14. As already mentioned, the fuel injection duration of the second split main injection reached zero at approximately engine load 2.5 bar IMEPgross. This means that the operating points of the split main injection with pilot strategy below approximately 2.5 bar IMEPgross are replicates of the single injection with pilot strategy.

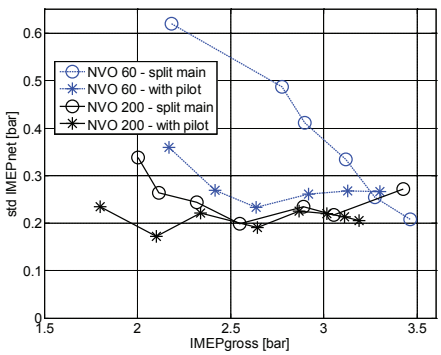

Figure 13. Standard deviation of IMEPnet of the split main strategy compared to the split main injection with pilot strategy.

Similar improvements can be seen for the NVO 60 CAD case in combustion stability (standard deviation of IMEPnet) when a pilot injection is added to the split main injection strategy. Another similarity is the decrease of combustion

efficiency in the 200 CAD NVO case with pilot injection. The major difference compared to the single injection with pilot strategy is that the combustion efficiency appears to be unaffected in the 60 CAD NVO case when a pilot injection is added. An improvement in combustion efficiency when going from a single injection strategy to the split main injection strategy was shown in Figure 7 and adding a pilot injection to the split main injection does not appear to improve combustion efficiency further.

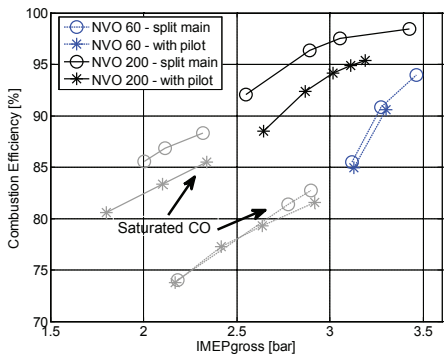

Figure 14. Combustion Efficiency of the split main strategy compared to the split main injection with pilot strategy.

From these experiments it is seen that it is possible to get comparably low standard deviation of IMEPnet (increased stability) without using a large fraction of trapped residual gases for an extended load range when a pilot injection is used. But the problem is still the low combustion efficiency which is significantly higher when a large fraction of trapped hot residuals is used.

Effect of Glow Plug

Finally, the effect of the glow plug is investigated. Chartier et al. [15] showed that the glow plug had an important role in the fuel injection strategy optimization applied to the cold-start performance in diesel engines. To investigate the importance of the glow plug in the cases with fuel injection optimization for low load gasoline PPC, the optimum split main injection case, in terms of minimum standard deviation, from the DoE test matrix, Table 3, is evaluated with and without glow plug at varying NVO settings.

From Figure 15 and Figure 16 it is seen that the glow plug has an improving effect on combustion stability and combustion efficiency. At the 100 CAD NVO operating point, the combustion stability is too low to see any effect from the glow plug on combustion stability. But after 120 CAD NVO there is a clear improvement on combustion stability when the glow plug is on. The improving effect appears to decrease with increasing NVO. This indicates that the glow plug has an important role but that it becomes less important depending on the fraction of trapped residuals.

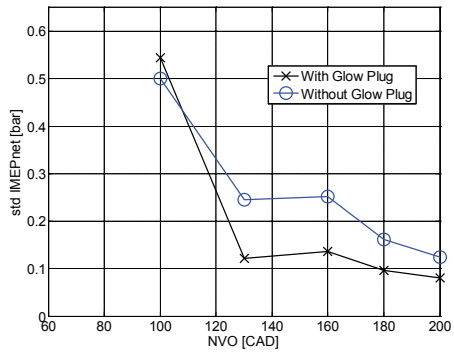

Figure 15. Standard deviation of IMEPnet for a split main injection test case with and without the glow plug.

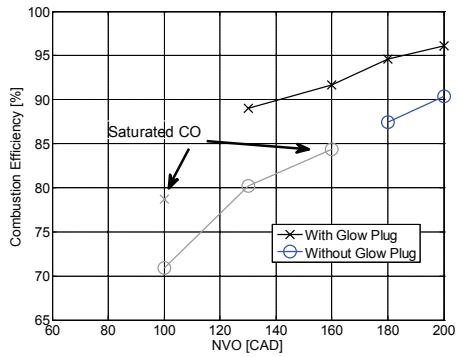

Figure 16. Combustion efficiency for a split main injection test case with and without the glow plug.

CONCLUSIONS

The objective was to investigate different injection strategies, with multiple injections, in order to further increase the low load limit and reduce the dependency on negative valve overlap in order to increase efficiency. A split main fuel injection strategy has been optimized from a second order regression model of combustion stability, measured as standard deviation in IMEPnet, and combustion efficiency using Design of Experiments. Also an additional pilot injection around -60 CAD was added. A single fuel injection strategy was used as reference.

- From the analysis of the output of the regression models it was concluded that a large fraction of the

fuel should be injected with the first injection. And a too short or a too long separation between the fuel injections should be avoided. A high setting of negative valve overlap results in improved combustion efficiency.

- In terms of combustion stability, a single injection with a pilot strategy has comparably low standard deviation of IMEPnet without using a large fraction of trapped hot residual gases over an extended operating region compared to a single injection strategy.
- The combustion efficiency is significantly improved with a large fraction of trapped hot residual gases and could not be substituted for a more advanced fuel injection strategy.

ACKNOWLEDGMENTS

The authors wish to show their appreciation to the Competence Centre Combustion Processes (KCFP), Swedish Energy Agency Grant number 22485-2, for their financial support. The authors would also like to acknowledge Cargine Engineering for supplying and helping with the valve train system. The authors would also like to expresses their gratitude to Bill Cannella from Chevron Corporation for supplying the fuel and to Håkan Persson from Volvo Car Corporation for hardware support and valuable discussions.

REFERENCES

[1] Willand, J., Nieberding, R-G., Vent, G., Enderle, C., “The Knocking Syndrome – Its Cure and Its Potential”, SAE 982483

[2] Lavy, J., Dabadie, J-C., Angelberger, C., Duret, P., Willand, J., Juretzka, A., Schäflein, J., Ma, T., Lendresse, Y., Satre, A., Shulz, C., Krämer, H., Zhao, H., Damiano, L., “Innovative Ultra-low NOx Controlled Auto-Ignition Combustion Process for Gasoline Engines : the 4-SPACE Project”, SAE 2000-01-1837

[3] Kimura, S., Aoki, O., Ogawa, H., Muranaka, S., Enomoto Y., ”New Combustion Concept for Ultra-Clean and High Efficiency Small DI Diesel Engines”, SAE 1999-01-3681

[4] Akihama K., Takatori Y., Inagaki K., Sasaki S., Dean A., ”Mechanism of the Smokeless Rich Diesel Combustion by Reducing Temperature”, SAE 2001-01-0655

[5] Yanigahara H., Sato Y., Minuta J., ”A simultaneous reduction in NOx and soot in diesel engines under a new combustion system (Uniform Bulky Combustion System – UNIBUS)”, 17th International Vienna Motor Symposium, pp 303-314, 1996

[6] Hasegawa R., Yanigahara H., “HCCI Combustion in DI Diesel Engine”, SAE 2003-01-0745

[7] Kalghatgi G. T., Risberg P., Ångström H., ”Advantages of Fuels with High Resistance to Auto-Ignition in Late-injection, Low-temperature, Compression Ignition Combustion”, SAE 2006-01-3385

[8] Kalghatgi G. T., Risberg P., Ångström H., ”Partially Pre-Mixed Auto-Ignition of Gasoline to Attain Low Smoke and Low NOx at High Load in a Compression Ignition Engine and Comparison with a Diesel Fuel”, SAE 2007-01-0006

[9] Kalghatgi G. T., Hildingsson L., Johansson B., “Low NOx and Low Smoke Operation of a Diesel Engine using Gasoline-like Fuels”, ICES2009-76034

[10] Hildingsson L., Kalghatgi G., Tait N., Johansson B., Harrison A., “Fuel Octane Effects in the Partially Premixed Combustion Regime in Compression Ignition Engines”, SAE 2009-01-2648

[11] Kalghatgi G.T., Hildingsson L., Harrison A., Johansson B., “Low- NOx, low-smoke operation of a diesel engine using “premixed enough" compression ignition – Effects of fuel autoignition quality, volatility and aromatic content”, THISEL 2010 Conference on Thermo- and Fluid Dynamic Processes in Diesel Engines

[12] Manente V., Johansson B., Tunestal P., ”Effects of Different Type of Gasoline Fuels on Heavy Duty Partially Premixed Combustion”, SAE 2009-01-2668

[13] Manente V., Johansson B., Tunestal P., Zander C., Cannella W., “An Advanced Internal Combustion Engine Concept for Low Emissions and High Efficiency from Idle to Max Load Using Gasoline Partially Premixed Combustion”, SAE 2010-01-2198

[14] Manente V., Johansson B., Tunestal P., Sonder M., Serra S., ”Gasoline Partially Premixed Combustion: High Efficiency, Low NOx and Low Soot by using an Advanced Combustion Strategy and a Compression Ignition Engine”, FCE09, Istanbul Turkey

[15] Chartier, C., Aronsson, U., Andersson, Ö., Egnell, R., ”Effect of Injection Strategy on Cold Start Performance in an Optical Light-Duty DI Diesel Engine”, SAE 2009-24-0045

[16] Borgqvist, P., Tunestal, P., Johansson, B., ”Gasoline Partially Premixed Combustion in a Light Duty Engine at Low Load and Idle Operating Conditions”, SAE 2012-01-0687

[17] Trajkovic, S., Milosavljevic, A., Tunestål, P., Johansson, B., “FPGA Controlled Pneumatic Variable Valve Actuation”, SAE 2006-01-0041

[18] Box, B. E. P., Hunter, J. S., W. G., “Statistics for Experimenters: Design, Innovation, and Discovery”, Second Edition, Wiley-Interscience, ISBN-13: 978-0471718130, New York, US, 2005

[19] Collin, R., Nygren, J., Richter, M., Aldén, M., Hildingsson, L., Johansson, B., “Studies of the Combustion Process with Simultaneous Formaldehyde and OH PLIF in a Direct-Injected HCCI Engine”, Proceedings of The Sixth International Symposium on Diagnostics and Modeling of Combustion in Internal Combustion Engines, Yokohama, Japan, pp. 311-317, 2004

[20] Manente, V., Johansson, B., Tunestal, P., ”Characterization of Partially Premixed Combustion with Ethanol: EGR Sweeps, Low and Maximum Loads”, ASME, ICES2009-76165, 2009

6

2013-01-0902

Comparison of Negative Valve Overlap (NVO) and Rebreathing Valve Strategies on a Gasoline PPC Engine at Low Load and Idle Operating Conditions

Patrick Borgqvist, Per Tunestål and Bengt Johansson
Lund University

ABSTRACT

Gasoline partially premixed combustion (PPC) has the potential of high efficiency and simultaneous low soot and NOx emissions. Running the engine in PPC mode with high octane number fuels has the advantage of a longer premix period of fuel and air which reduces soot emissions. The problem is the ignitability at low load and idle operating conditions.

In a previous study it was shown that it is possible to use NVO to improve combustion stability and combustion efficiency at operating conditions where available boosted air is assumed to be limited. NVO has the disadvantage of low net indicated efficiency due to heat losses from recompressions of the hot residual gases. An alternative to NVO is the rebreathing valve strategy where the exhaust valves are reopened during the intake stroke. The net indicated efficiency is expected to be higher with the rebreathing strategy but the question is if similar improvements in combustion stability can be achieved with rebreathing as with NVO.

The results show that the rebreathing valve strategy has similar improvements on combustion stability as NVO when the same fuel injection strategy is used. This work also includes results with the NVO valve strategy where a fuel injection is added during the NVO. When a fuel injection is added during the NVO, an additional improvement on combustion stability can be seen which is unmatched by the rebreathing valve strategy.

INTRODUCTION

Homogeneous charge compression ignition (HCCI) combustion has the potential of achieving high efficiency in combination with low NOx and soot emissions. The challenges with HCCI include combustion control, low power density and steep pressure rise rates. As a result, two branches of HCCI emerged, spark assisted compression ignition (SACI), and partially premixed combustion (PPC). SACI is the intermediate process between SI flame propagation and HCCI auto ignition. HCCI mode is typically achieved through trapping of hot residual gases with early exhaust valve closing. The intake valve is usually opened symmetrically after top dead center. The interval in crank angles from exhaust valve closing to intake valve opening is called negative valve overlap (NVO). The idea to use negative valve overlap for HCCI was first proposed by Willand et al. [1] in 1998 and was demonstrated by Lavy et al. [2] in 2000.

PPC combines traditional diesel combustion with HCCI. With PPC, the fuel injection is completed before start of combustion to promote mixing of fuel and air, but the charge is not homogeneous. One benefit compared to traditional HCCI combustion is that the fuel injection timing can be used as control actuator for the combustion timing. In order to get enough separation from start of injection to start of combustion with diesel fuel, a high fraction of EGR has to be used. This concept was used by Nissan [3] and is called Modulated Kinetics (MK). Toyota used high EGR rates to suppress both soot and NOx with the smokeless rich diesel combustion concept [4]. In a different concept, as an alternative to using excessive EGR rates, Toyota used a double injection system with some of the fuel injected early to promote mixing with air. This concept is called UNIBUS [5, 6].

Kalghatgi introduced the concept of gasoline partially premixed combustion in 2006 [7, 8], and something similar was shown by Johansson in 2005 [9]. With a fuel that is harder to ignite, a longer mixing period from end of injection to start of combustion can be achieved without using high EGR fraction, very early injection timing or very low compression ratio. Results from a light-duty engine were published in [10-12]. At Lund University, Manente et al. [13, 14] developed a gasoline PPC strategy running a variety of gasoline fuels with different octane numbers in a heavy duty engine. Gross indicated efficiencies up to 57 % with low NOx, HC and CO emissions as well as soot levels below of 0.5 FSN were reported. Light duty engine experiments were reported in [15].

At Delphi Corporation, Sellnau et al. [16, 17] achieved higher efficiency with gasoline compared to diesel in a single cylinder light duty Hydra engine with a gasoline direct injection compression ignition (GDCI) strategy using an optimized triple injection strategy. At low load operating condition, a rebreathing valve strategy was used to expand the low load limit.

As demonstrated in a heavy-duty engine, there is a clear decrease in attainable gasoline PPC operating region with increased fuel octane number [14]. One alternative strategy is to use two fuels with different auto-ignition properties. At University of Wisconsin - Madison, the reactivity controlled compression ignition (RCCI) strategy has been investigated [18-22]. The low cetane number fuel, for example gasoline, is typically port injected and the high cetane number fuel is direct injected. The idea is to adjust the auto-ignition properties of the fuel depending on engine speed and load.

The focus of this work is gasoline PPC. Only the gasoline fuel is used and it is direct injected. Running gasoline PPC with higher octane number fuels at low load and idle operating conditions is a challenge. At low load and engine speed operating conditions it can be assumed that the available boost is limited and that reaching auto-ignition conditions will be difficult with a standard turbo-charger. There are different tools that can be used to extend the attainable operating region, for example, using more advanced injection strategies, using for example NVO or rebreathing valve strategies to trap hot residuals, and to use a glow plug. The focus of this work is on the valve strategies. Application of NVO is usually associated with SACI and is used to achieve HCCI combustion in a spark ignition engine [23-26]. PPC is a diesel engine concept and it is not aimed at achieving traditional HCCI. The compression ratio is higher compared to what is usually seen with SACI and there is no spark plug (there is usually a glow plug).

In previous work by Borgqvist et al. [27-29] it was found that it was possible to operate the light duty diesel engine with 87 RON gasoline fuel down to approximately 2 bar IMEPgross with a significant fraction of trapped hot residual gases. The low load limit could be extended from approximately 3.2 bar IMEPgross to down to 2.2 bar IMEPgross by increasing NVO. The penalty with NVO is the decrease in gas-exchange efficiency due to increased heat losses from recompression of the residual gases. More advanced injection strategies have been investigated as an alternative to NVO. The conclusion was that a more advanced injection strategy could match combustion stability of the high NVO case but the combustion efficiency is higher with NVO regardless of injection strategy. A second approach is to use a different valve strategy. In this work a rebreathing strategy is used where the exhaust valves are reopened during the intake stroke. If the residual gases are first exhausted and then re-inducted during the intake stroke, recompression of the residual gases is avoided. But the question is if similar improvements of combustion stability and efficiency can be achieved with rebreathing as with NVO. According to Lang et al. [30] the charge mixture is more stratified and the temperature is higher with the NVO strategy compared to the rebreathing strategy. But this comparison was made for the CAI combustion concept. With PPC it can also be expected that the temperature is lower with the rebreathing strategy due to an expected lower residual gas temperature after re-induction. But the charge mixture stratification is expected to be high because of the relatively late fuel injection timing. In this work, results with a rebreathing strategy at low engine load and engine speed in comparison with the NVO strategy is presented.

In this first comparative investigation, a single fuel injection strategy is used. But an opportunity that is available with the NVO valve strategy is fuel injection during the NVO to promote fuel reformation. Urushihara et al. [31] were able to extend the lean limit of HCCI by injecting a portion of the fuel in the NVO. An investigation with a NVO injection strategy for low load gasoline PPC is presented after the NVO and rebreathing comparisons. And these results are finally compared to the rebreathing and NVO results with a single injection with emphasis on the possibility of low load limit extension of gasoline PPC in a light duty engine.

EXPERIMENTAL APPARATUS AND SETUP

The experimental engine is based on a Volvo D5 light duty diesel engine. The engine properties can be seen in Table 1. It is run on only one of the five cylinders and is equipped with a fully flexible pneumatic valve train system supplied by Cargine Engineering. The Cargine valve train system was first demonstrated by Trajkovic et al. [32]. The valve actuators are placed on an elevated plate above the fuel injector and are connected to the valve stems with push-rods. Intake valve closing (IVC) timing is constant, 180 CAD BTDC @ 1 mm valve lift, and exhaust valve opening timing is constant, 180 CAD BTDC @ 1 mm valve lift. Maximum valve lift is approximately 5 mm. The fuel injection system is a common rail system with a 5 hole nozzle solenoid injector. The umbrella angle is 140 degrees and the nozzle hole diameters are 0.159 mm.

Table 1. Engine Properties.

Displacement (one cyl.)	0.48 Liters
Stroke	93.2 mm
Bore	81 mm
Compression ratio	16.5:1
Number of Valves	4
Valve train	Fully flexible
Fuel	87 RON gasoline

The engine control system was developed by the author in LabVIEW 2009. The control system is run from a separate

target PC, NI PXI-8110, which is a dedicated real-time system. The target PC is equipped with an R series multifunctional data acquisition (DAQ) card with re-programmable FPGA hardware, NI PXI-7853R, and an M-series data acquisition card, NI PXI-6251. The user interface is run on a separate Windows based host PC. The host and target PCs communicate over TCP/IP. In-cylinder pressure and valve lift curves are measured simultaneously with the FPGA DAQ card. The in-cylinder pressure and valve lift curve measurements are crank angle based with resolution 0.2 CAD/sample. For each operating point 500 cycles are collected. Post-processing of the data is made in Matlab.

Experimental data is collected with varying settings of NVO from 60 CAD to 220 CAD and with varying settings of rebreathing with a second exhaust valve opening duration from 0 to 110 CAD. The NVO and rebreathing valve lift curves are seen in Figure 1 and Figure 2, respectively. The valve open speed is fast compared to conventional systems. In order to ensure valve clearance around top dead center a minimum NVO of 60 CAD is used. The same minimum NVO is used also for the rebreathing valve strategy. The consequence is that the 0 CAD rebreathing case is the same as the 60 CAD NVO case. With the current setup of the valve control system there is also a limit on the shortest possible valve open duration that can be used. For this reason, the shortest rebreathing setting that is used is 50 CAD.

The contour plots were generated in Matlab with the commands *contourf* and *TriScatteredInterp* using linear interpolation. The measurement points are indicated with magenta colored circles in the contour plots.

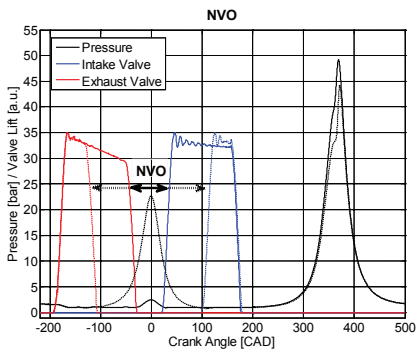

Figure 1. NVO valve strategy valve lift curves.

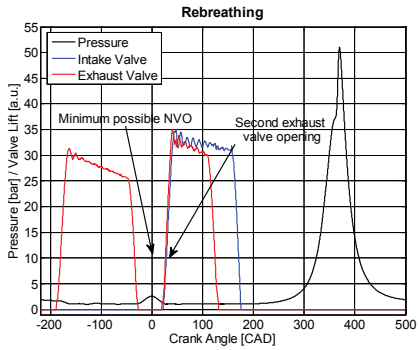

Figure 2. Rebreathing valve strategy valve lift curves.

Engine load is varied by increasing the fuel injection duration. The glow plug is continuously on. The engine is run without boosted air and without external EGR. Intake air temperature is controlled with a heater in the intake manifold to 40° C. The engine speed is 800 rpm. Lambda is calculated from air and fuel flow measurements. The air flow is measured with a Bronkhorst F-106AI-AGD-02-V air flow meter and the fuel flow is calculated from a Sartorius CP 8201 precision balance. The fuel balance is sampled for approximately 8 minutes after reaching stable operating conditions at selected operating points. The injector was calibrated assuming a linear correlation between fuel injector opening durations and the calculated fuel flows. Different fuel injection strategies were calibrated separately. At least four measurement points were sampled for each fuel injection strategy. Soot is measured with an AVL 415 smoke meter. HC, CO, CO2 and NOx emissions are measured with a Horiba Mexa 7500 analyzer system. The CO measurements were saturated for the most operating points presented in this work and are therefore not presented. The saturation limit of the CO measurement instrument is 10000 ppm.

RESULTS AND DISCUSSION

Valve Strategy Comparison

The NVO against rebreathing results are presented in this section. The outline of this section is to first identify similarities and differences in combustion characteristics, ignition delay, and combustion duration. And then compare combustion stability, unburned hydrocarbon emissions and finally net-indicated efficiency. The question is whether or not the rebreathing valve strategy has similar improving effects on combustion as NVO and what the gain is on efficiency. The results with the NVO strategy are discussed also in a previous work by Borgqvist et al. [28].

The engine load is varied from approximately 1.9 bar IMEPgross to 3.4 bar IMEPgross. The fuel that is used is an

87 RON gasoline. The fuel injection strategy is a single injection with start of injection (SOI) at 22 CAD BTDC. At a few operating points with relatively high load, the start of injection has to be retarded in order to have combustion timing after top dead center. The common rail pressure is constant at 500 bar.

The relative air fuel ratio (lambda) of the NVO and rebreathing strategy is shown in Figure 3. As expected, since there is no external EGR or boosted air, increasing NVO or rebreathing results in a larger fraction of trapped residual gases and a lower fraction of inducted air. An increase of rebreathing from 0 to 100 CAD results in approximately the same decrease in lambda as is achieved from increasing NVO from 60 to 200 CAD. At the 110 CAD rebreathing case, lambda is higher compared to the highest setting of NVO which can possibly be explained by a limited capability to re-induct the exhaust gases after a certain limit. There is no back-pressure valve to control the maximum possible amount of re-inducted residuals.

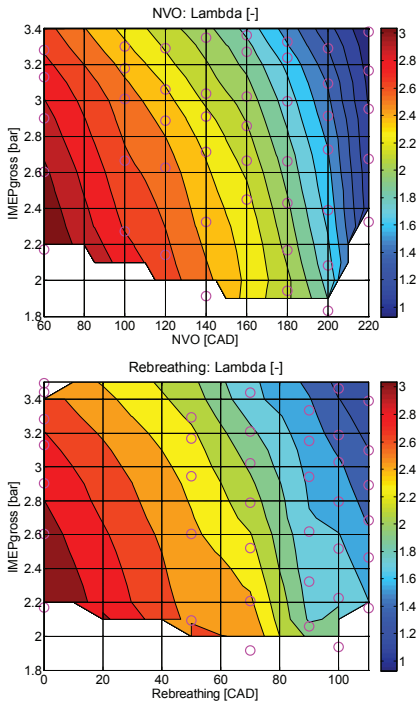

Figure 3. Relative air/fuel ratio (Lambda) with the NVO strategy compared to the rebreathing strategy.

The ignition delay, defined as the difference in crank angles from the crank angle of 10% accumulated heat release and start of fuel injection timing, is shown in Figure 4. Similar trends are observed with rebreathing compared to NVO. There is an intermediate setting of NVO at relatively high engine load from 120 to 200 CAD and 50 to 70 CAD rebreathing where the ignition delay is the shortest. As already mentioned, it was not possible to collect data with a rebreathing setting below 50 CAD. The ignition delay is long with both the highest setting of NVO and rebreathing. The ignition delay of the NVO case was discussed in a previous work by Borgqvist et al. [28]. Here it is interesting to observe that similar trends are seen regardless of valve strategy.

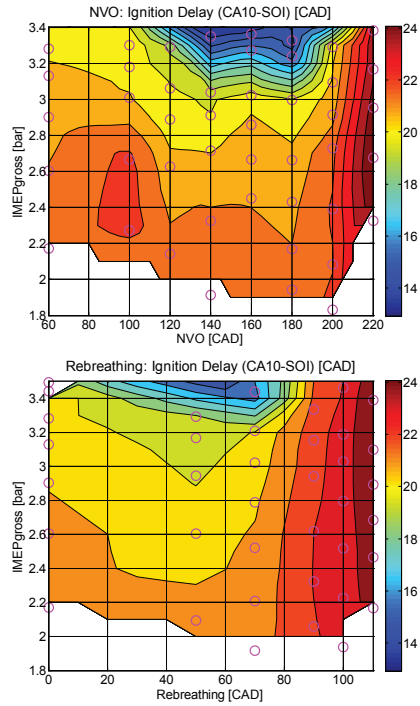

Figure 4.The ignition delay in crank angles with the NVO strategy [28] compared to the rebreathing strategy.

The combustion duration, defined as the difference in crank angles from crank angle of 90% accumulated heat release to crank angle of 10% accumulated heat release, is shown in Figure 5. Similar trends are observed also in combustion duration with rebreathing compared to NVO. The combustion duration becomes shorter with increased NVO up to 180 CAD and rebreathing up to 70 CAD. If even higher settings of NVO and rebreathing are used, the combustion duration becomes longer again. Globally, when the residual gas concentration is changed, the auto-ignition and combustion of the fuel is expected to be affected by the changes in in-cylinder

temperature and oxygen concentration. If the global in-cylinder temperature is low, it takes more time for the fuel to auto-ignite and the burn duration is longer. When the residual gas fraction is increased, the in-cylinder temperature is increased but the available oxygen concentration is also decreased. The auto-ignition process and combustion duration becomes shorter with increased residual gas fraction because of the temperature increase but is eventually slowed down because of the low oxygen concentration and high fraction of internal EGR.

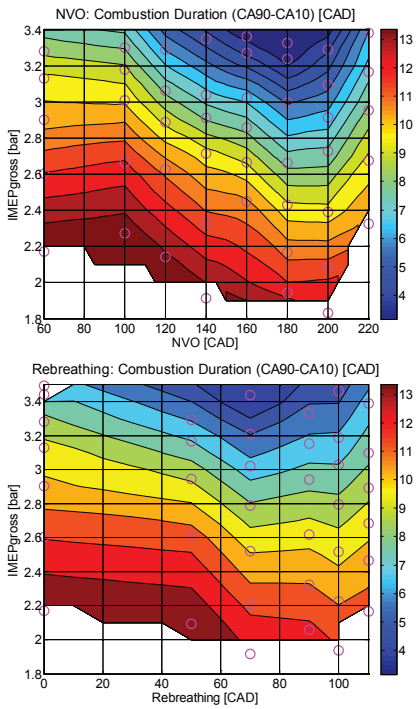

Figure 5. Combustion duration in crank angles with the NVO strategy [28] compared to the rebreathing strategy.

When comparing the two different valve strategies it would be interesting to compare the effect of differences in in-cylinder internal EGR and temperature distribution on combustion. It is difficult to make any quantitative statements about the effect of charge mixture stratification from the different valve strategies without optical measurements to support them. Rothamer et al. [33] showed that combustion strategies with a high fraction of trapped residuals, using NVO, results in significantly more stratification in temperature and EGR distribution compared to traditional HCCI with a low level of retained in-cylinder EGR. But the fuel was injected relatively early compared to this investigation with gasoline PPC where the fuel mixture stratification is assumed to be high because of the late injection timing. It would be expected that the charge mixture is more stratified and the temperature is higher with the NVO strategy compared to the rebreathing strategy [30]. But given the similarities in ignition delay and combustion duration, the dominating effect appears to be from the fuel mixture stratification due to the late fuel injection.

The combustion stability, measured as the standard deviation in IMEPnet is shown in Figure 6. It is interesting to see that the combustion stability has the same overall trend in improvement with rebreathing compared to NVO. This was not necessarily expected given the potentially lower residual gas temperature after re-induction compared to NVO. The combustion is the most stable where the fuel mixture is prone to auto-ignite and the burn duration is the shortest.

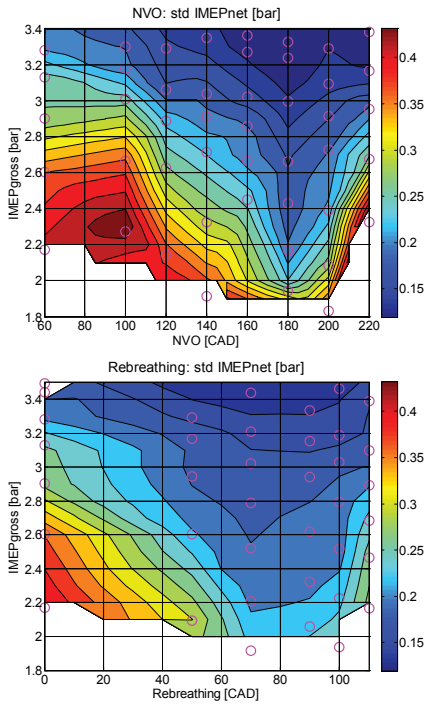

Figure 6. Combustion stability measured in standard deviation in IMEPnet with the NVO strategy [28] compared to the rebreathing strategy.

The unburned hydrocarbon emissions are shown in Figure 7. Again, similar trends are seen with rebreathing in comparison with NVO. One difference is that the unburned hydrocarbon emissions are lower with the highest setting of rebreathing compared to the highest setting of NVO. One possible

explanation is the lower amount of available oxygen in the NVO case as was seen from lambda, Figure 3.

It is interesting to note the similarities in trends and shape of the contour plots between the ignition delay, Figure 4, and unburned hydrocarbon emissions, especially for the NVO strategy. Since the fuel injection timing is constant, a longer ignition delay results in more retarded combustion phasing. At later combustion timings there is less time to fully oxidize the fuel. Also the peak combustion temperature is lower. Both time and temperature are needed to fully oxidize the fuel and intermediate species, for example CO. The oxygen concentration is also reduced when the residual gas fraction is increased. The longest ignition delays are observed where the residual gas fraction is the highest. The CO emissions are not reported in this investigation due to saturation of the CO measurement instrument at most of the lowest load operating conditions. High amounts of CO are produced because of insufficient temperature and time to be fully converted to CO2.

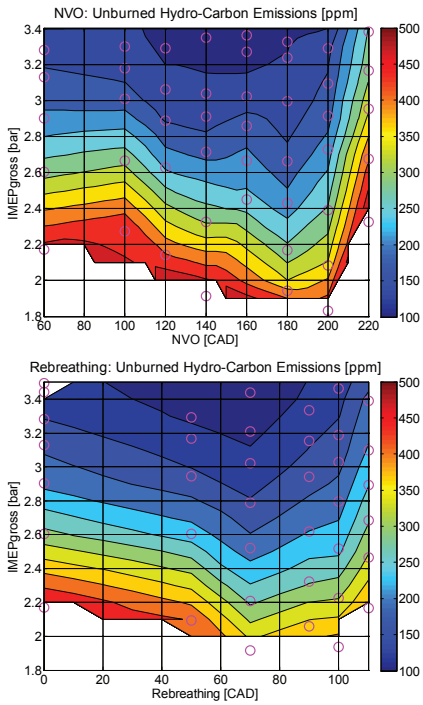

Figure 7. Unburned hydrocarbon emissions with the NVO strategy compared to the rebreathing strategy.

Another possible contributing effect to the unburned hydrocarbon emissions is from the effect of over-mixing. A longer ignition delay gives more time for mixing of the fuel and possibly a more homogeneous mixture with fewer zones with favorable conditions in temperature, fuel and oxygen concentration to promote auto-ignition. Again, there is a need to quantify this with optical diagnostics to quantify the effects of stratification on, for example, unburned hydrocarbon emissions and combustion stability.

The gas-exchange efficiency, defined as the ratio of IMEPnet to IMEPgross, is shown in Figure 8. As expected, the gas-exchange efficiency is higher with the rebreathing strategy compared to the NVO strategy. The gas-exchange efficiency decreases significantly with NVO due to increased heat losses from recompression of the residual gases which in turn results in a lower IMEPnet.

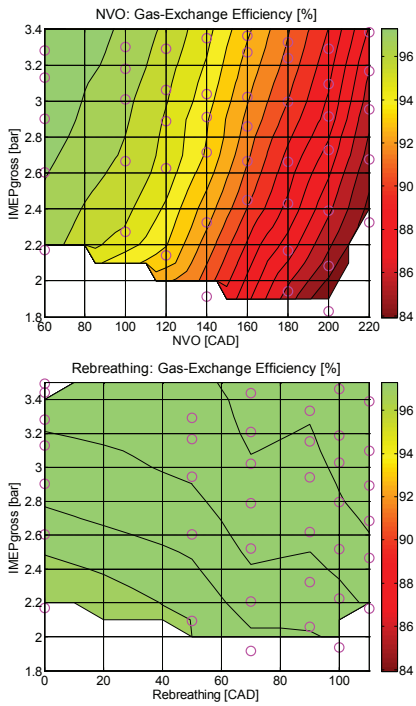

Figure 8. Gas-exchange efficiency with the NVO strategy compared to the rebreathing strategy.

The net indicated efficiency is shown in Figure 9. The net indicated efficiency is shown in favor of the gross indicated efficiency because this is closer to the break efficiency. Since the experiments were run on a single cylinder engine, reliable torque measurements are unavailable. The net indicated efficiency is shown against IMEPnet rather than IMEPgross because it more clearly shows the effect of the gas-exchange

efficiency with varying NVO. When shown against IMEPgross, the decrease in net indicated efficiency due to the decrease in gas-exchange efficiency is not as clearly seen.

The net indicated efficiency is generally higher with rebreathing compared to NVO. This is due to the higher gas-exchange efficiency with the rebreathing strategy. But the net indicated efficiency with the NVO strategy is not completely dominated by the decrease in gas-exchange efficiency. With increasing NVO there is also an increase in combustion efficiency, as indicated by the decrease of unburned hydrocarbon emissions, Figure 7, as was reported in [28]. The decrease in gas-exchange efficiency is to some extent compensated by an increase in combustion efficiency with increasing NVO.

To summarize, the rebreathing strategy has similar improving effects on combustion as the NVO strategy with the advantage of a higher net-indicated efficiency.

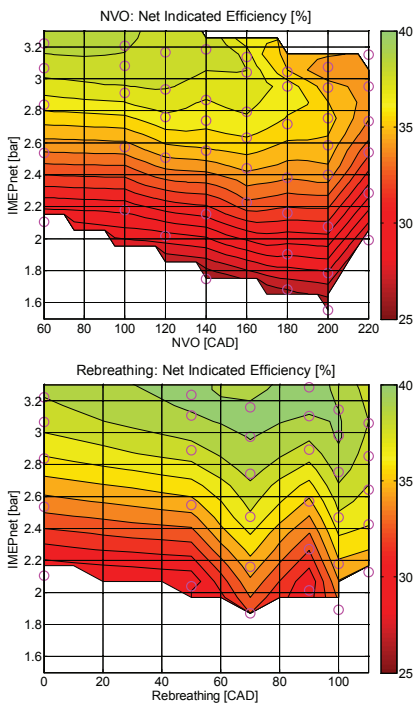

Figure 9. Net indicated efficiency with the NVO strategy compared to the rebreathing strategy.

NVO Fuel Injection

The focus of this section is on the NVO valve strategy. In the previous section a single fuel injection strategy was used to be able to compare both valve strategies. One injection strategy that has been used successfully with HCCI/CAI to extend the low load limit is to inject fuel during the NVO. In this section, a portion of the fuel is shifted from the main fuel injection to the NVO. The fuel injection profile, valve profile and pressure trace is shown in Figure 10. A constant fuel amount is injected during the NVO, and for the limited load range that is investigated in this work, the proportion between the two fuel injections are on average approximately 50/50. The main fuel injection timing was kept constant at 22 CAD BTDC when possible. The exception was with the higher setting of NVO where the fuel injection had to be retarded in order to have combustion timing after TDC.

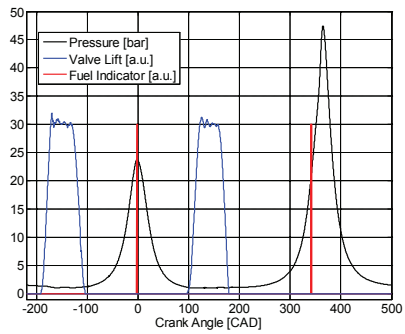

Figure 10. NVO fuel injection strategy.

According to Urushihara et al. [31] the injection timing during NVO is an important parameter that affects the width of the HCCI region. First, an investigation on the effect of fuel injection timing during NVO on the main combustion event is presented. The injected fuel amount is constant and the fuel ratio between the two injections is 50/50. The fuel injection timing of the NVO injection is varied from -22 to 0 CAD ATDC and NVO is constant at 220 CAD.

The rate of heat release during NVO and the rate of heat release of the subsequent main combustion event with varying NVO fuel injection timings are seen in Figure 11. It can be seen that earlier injection timing results in a higher rate of heat release during NVO but a lower peak rate of heat release during the main combustion. The rate of heat release during the main combustion with the -22 and -15 CAD ATDC fuel injections is nearly split in two parts. It is more apparent with the -15 CAD setting where two peaks are clearly distinguishable. In these cases there is a more distinct separation of the combustion of the more reactive fuel from

the NVO injection compared to the fuel that is injected during compression.

The largest effect on ignition delay is seen when the fuel is injected at 0 CAD. There is no apparent heat release during the NVO in this case and the subsequent main combustion rate of heat release curve is significantly retarded compared to the other cases.

An interesting side effect is the impact on the relative air fuel ratio, lambda, which is 1.08 with the -22 CAD fuel injection timing and 1.42 with fuel injection at 0 CAD. This means that there is a decrease in the amount of inducted fresh air when fuel is injected earlier during NVO which is perhaps not intuitive. This is most likely explained by the increased temperature from the heat release during NVO.

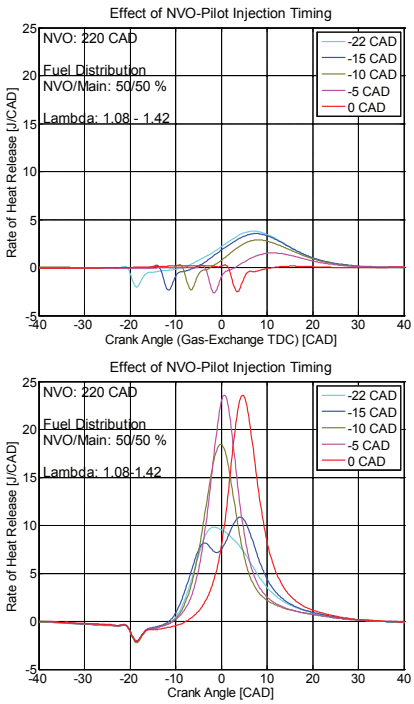

Figure 11. Rate of heat release during NVO (top figure) and subsequent main combustion with varying NVO injection timings.

The combustion stability and unburned hydrocarbon emissions are plotted in Figure 12. An optimum NVO fuel injection timing region that minimizes unburned hydrocarbon emissions and maximizes combustion stability (minimizes the standard deviation in IMEPnet) is found from -10 to -5 CAD ATDC.

The gas-exchange, gross- and net- indicated efficiencies are shown in Figure 13. The gas-exchange efficiency is above 100% when fuel is injected in the NVO with the earliest fuel injection timings. The reason is that IMEPnet is higher than IMEPgross since heat is released also during the NVO. But the net indicated efficiency is not the highest where the gas-exchange efficiency is the highest. With these fuel injection settings, the unburned hydrocarbon emissions are higher which indicates that the combustion efficiency is low. Additionally, there are probably also more heat losses when heat is released also during the NVO. The highest net indicated efficiency is achieved with NVO fuel injection timing -5 CAD ATDC.

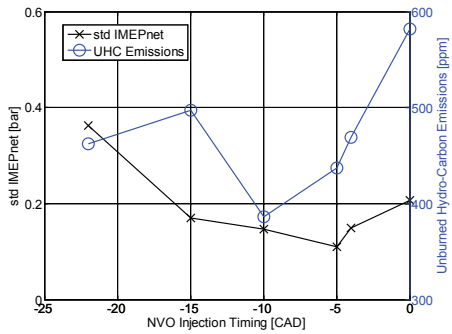

Figure 12. Combustion stability and unburned hydrocarbon emissions against NVO injection timing.

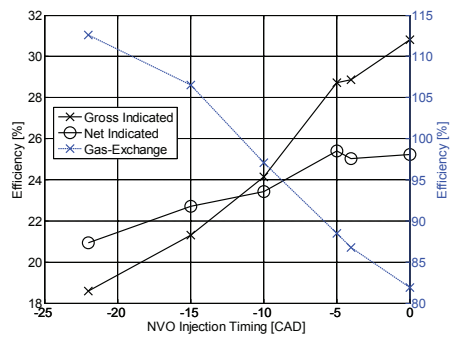

Figure 13. Gas-exchange, gross and net indicated efficiencies.

Taking into account both unburned hydrocarbon emissions, combustion stability and net indicated efficiency, the optimum NVO fuel injection timing is at -5 CAD ATDC. This is obviously not a universal NVO fuel injection timing for all engines and operating points. The point from this investigation

is that the NVO fuel injection timing is an important parameter to consider when this strategy is used also for gasoline PPC.

The second investigation is on the effect of engine load and NVO when the NVO fuel injection strategy is used. It is interesting to see if the low load limit of gasoline PPC can be extended when a NVO pilot injection is used. The NVO injection timing and fuel amount is constant and the control variables are NVO and fuel amount in the main injection. The NVO injection timing was set to -5 CAD ATDC and approximately 50% of the fuel is injected during NVO. The engine load operating region is even narrower than in the previous section. The relative air fuel ratio, lambda, is shown in Figure 14. According to the air and fuel flow calculations, the combustion is close to stoichiometric with the highest NVO setting, 220 CAD.

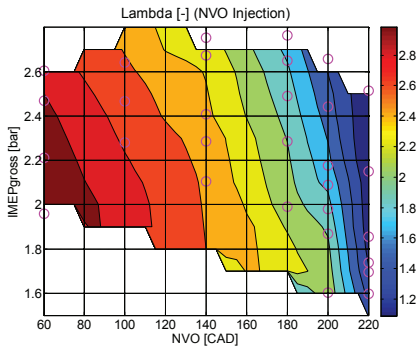

Figure 14. Relative air fuel ratio with the NVO injection strategy.

The ignition delay, Figure 15, is significantly shorter with the NVO injection and with the higher settings of NVO with gasoline PPC. There is relatively low effect from the NVO injection on the main combustion at the low NVO operating conditions but the effect is significant once NVO is increased beyond the threshold of 180 CAD NVO. The ignition delay becomes significantly shorter, from approximately 18 CAD to 8 CAD, when NVO is increased above the threshold of 180 CAD. If the temperature is too low and the mixture is too lean during NVO, there is almost no apparent effect on the main combustion.

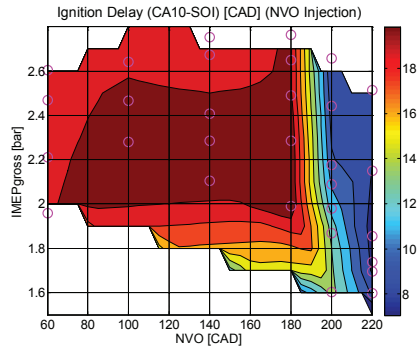

Figure 15. Ignition delay with the NVO injection strategy.

The combustion stability, Figure 16, is significantly improved with the NVO fuel injection when NVO is sufficiently high. The unburned hydrocarbon emissions, Figure 17, decrease with the NVO injection timing at the highest setting of NVO. This is different from previously shown results, with a single injection strategy, where the unburned hydrocarbon emissions decreased with NVO up to 180 CAD and then increased again with higher NVO settings. The same was true also for the combustion stability. The conditions during the NVO are obviously more important for the end result with the NVO injection strategy.

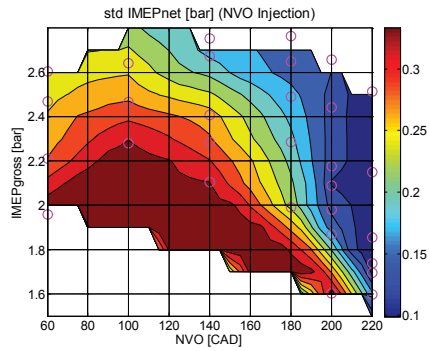

Figure 16. Combustion stability with the NVO injection strategy.

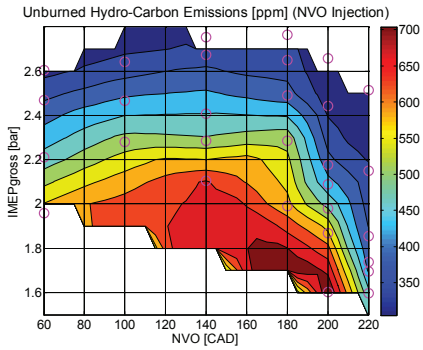

Figure 17. Unburned hydrocarbon emissions with the NVO injection strategy.

The NOx emissions are shown in Figure 18, and the soot emissions are shown in Figure 19. The NOx emissions are high with the 200 CAD NVO setting which is just above the NVO threshold where the ignition delay becomes significantly shorter but there is still an excess of oxygen. The soot emissions are high with the highest setting of NVO, 220 CAD, where the ignition delay is short and the air fuel ratio is low.

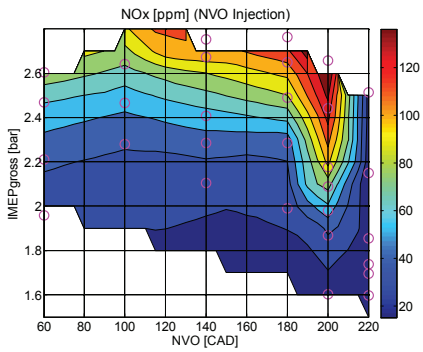

Figure 18. NOx emissions with the NVO injection strategy.

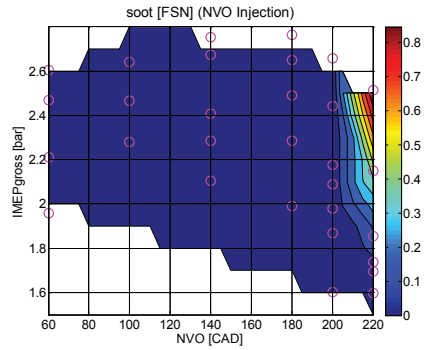

Figure 19. Soot emissions with the NVO injection strategy.

The net indicated efficiency is shown in Figure 20. Note that the net indicated efficiency is plotted against IMEPnet to be consistent with the previously shown net indicated efficiency results. The trend is the same as was seen with the NVO case and the single injection strategy, Figure 9. The combustion stability is improved and the unburned hydrocarbon emissions are reduced with the NVO injection strategy and high setting of NVO, but the efficiency is still lower with the highest settings of NVO where the positive effects were seen.

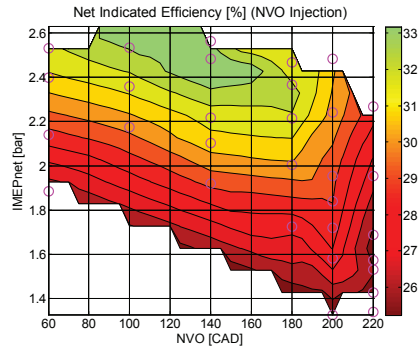

Figure 20. The net indicated efficiency with the NVO injection strategy.

The Low Load Limit

The results are summarized in this section with an emphasis on extending the low load limit using gasoline PPC. The optimal setting of NVO and rebreathing are used and compared with the optimal settings of the NVO injection strategy. The settings that resulted in the highest combustion stability are chosen in the comparison. The combustion stability is shown in Figure 21. The combustion stability is significantly improved with the NVO injection strategy

compared to the single injection cases with NVO and rebreathing. The difference between NVO and rebreathing is relatively small.

Two NVO settings are shown with the NVO injection strategy, 200 CAD and 220 CAD. Even though the combustion stability is the highest with the 220 CAD setting the soot emissions, Figure 22, are significantly higher already at relatively low engine load setting. The combustion stability with the 200 CAD NVO setting is also high compared to NVO and rebreathing strategies with single injection, but is without the penalty in soot emissions. It is also seen that an increase from 200 CAD NVO to 220 CAD is necessary in order to maintain combustion stability below engine load 1.8 bar IMEPgross but the additional extension of the low load limit is limited.

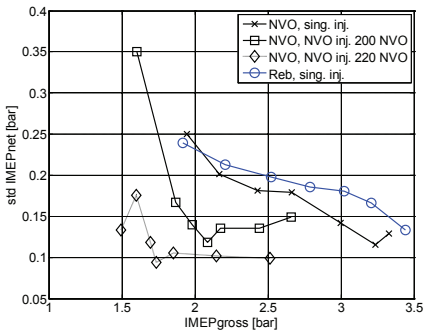

Figure 21. Combustion stability of the two different injection strategies with NVO compared to the rebreathing strategy with single injection.

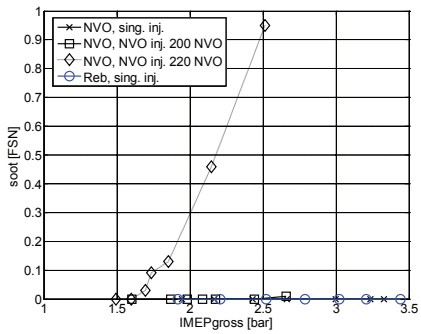

Figure 22. Soot emissions of the two different injection strategies with NVO compared to the rebreathing strategy with single injection.

The unburned hydrocarbon emissions are shown in Figure 23. There is a clear increase of unburned hydrocarbon emissions with decreased engine load regardless of valve and injection strategy. There is an improvement with the 220 NVO setting compared to the 200 NVO setting with the NVO injection strategy but the problem is then the soot emissions. Even though the combustion stability is improved with the NVO injection strategy there is no additional improvement on the hydrocarbon emissions at low engine load operating conditions. The reason is probably the low in-cylinder temperature.

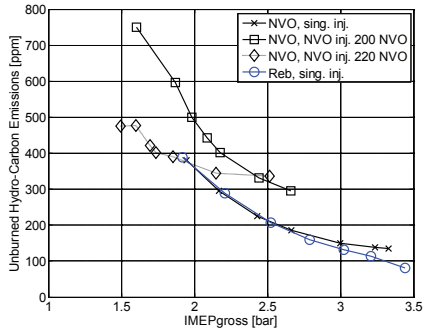

Figure 23. Unburned hydrocarbon emissions of the two different injection strategies with NVO compared to the rebreathing strategy with single injection.

In order to reduce the hydrocarbon and CO emissions at low engine load, after-treatment will most likely be necessary. In order to use an oxidation-type catalytic converter the exhaust gas temperature is of interest. The exhaust gas temperature is shown in Figure 24 for the NVO strategy. The exhaust gas temperature is below 200 °C for the lowest engine load operating points investigated here, which is below the 300 °C light-off temperature of a three-way catalytic converter [34].

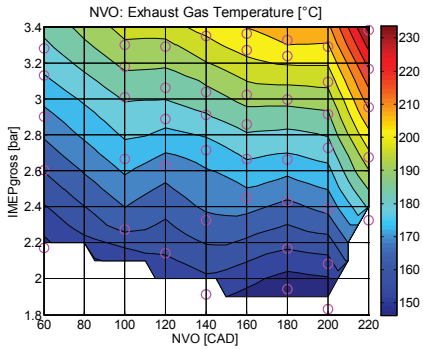

Figure 24. Exhaust gas temperature with the NVO strategy.

The NOx emissions are shown in Figure 25. The NOx emissions are low when the engine load is sufficiently low. No external EGR has been used in this investigation but it is expected to be required at the higher engine load operating conditions. External EGR was used in a previous work by Borgqvist et al. [27] in combination with NVO.

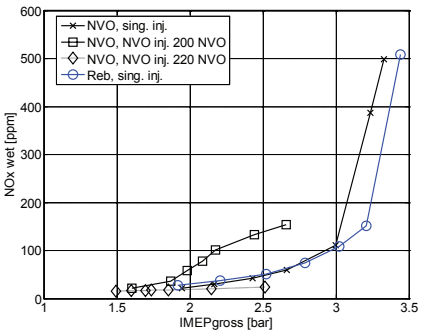

Figure 25. NOx emissions of the two different injection strategies with NVO compared to the rebreathing strategy with single injection.

The net indicated efficiency is shown in Figure 26. As expected, the rebreathing valve strategy has the highest efficiency compared to the NVO strategies. There is a significant decrease in efficiency with lower engine load which is explained by the decrease in combustion efficiency (indicated by an increase in unburned hydrocarbon emissions).

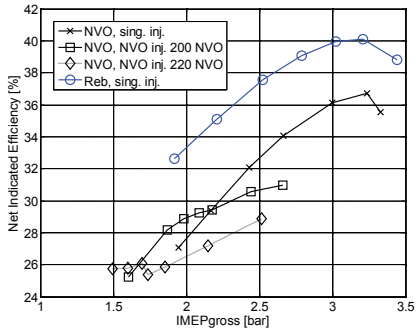

Figure 26. Net indicated efficiency of the two different injection strategies with NVO compared to the rebreathing strategy with single injection.

Suggested Operating Strategy

In order to minimize fuel consumption (maximize net indicated efficiency) while maintaining combustion stability, the suggestion is to use the rebreathing operating strategy at higher engine load from 2-2.5 bar IMEPgross and then change to NVO with NVO pilot injection at the lower engine load operating conditions. In order to make a more seamless transition between the different strategies the NVO strategy could be used as an intermediate strategy so that the residual gases are gradually replaced from being re-inducted to becoming trapped. The NVO injection is turned on once a sufficiently high NVO setting has been reached.

The unburned hydrocarbon emissions remain a problem regardless of valve or fuel injection strategy and after-treatment using an oxidation catalyst will be necessary.

SUMMARY/CONCLUSIONS

Results from a comparison of NVO with a rebreathing valve strategy have been shown on a single cylinder gasoline PPC light duty diesel engine with a glow plug. The conclusion was that the rebreathing strategy has similar improving effects on combustion as the NVO strategy with the advantage of a higher net-indicated efficiency.

A fuel injection was added during the NVO in combination with the NVO valve strategy only to investigate the potential of additional extension of the gasoline PPC low load limit. The NVO fuel injection timing was found to have a significant effect on both the rate of heat release during NVO and the subsequent main combustion. An optimum injection timing that maximized net indicated efficiency and combustion stability was found.

There is a significant improvement on combustion stability with the NVO fuel injection which is unmatched by the rebreathing valve strategy. The improvements with the NVO injection strategy are seen only with a sufficiently high NVO. But the soot emissions are high already at a relatively low engine load if NVO is too high.

There is a potential improvement on unburned hydrocarbon emissions with NVO or rebreathing. But there is a strong trend with increased unburned hydrocarbon emissions with decreased engine load regardless of valve strategy and NVO pilot injection.

A low load gasoline PPC operating strategy with a transition from rebreathing at high engine load to NVO with NVO injection at low engine load is suggested.

REFERENCES

1. Willand, J., Nieberding, R., Vent, G., and Enderle, C., "The Knocking Syndrome - Its Cure and Its Potential," SAE Technical Paper 982483, 1998, doi:10.4271/982483
2. Lavy, J., Dabadie, J., Angelberger, C., Duret, P. et al., "Innovative Ultra-low NOx Controlled Auto-Ignition Combustion Process for Gasoline Engines: the 4-SPACE Project," SAE Technical Paper 2000-01-1837, 2000, doi:10.4271/2000-01-1837
3. Kimura, S., Aoki, O., Ogawa, H., Muranaka, S. et al., "New Combustion Concept for Ultra-Clean and High-Efficiency Small DI Diesel Engines," SAE Technical Paper 1999-01-3681, 1999, doi:10.4271/1999-01-3681
4. Akihama, K., Takatori, Y., Inagaki, K., Sasaki, S. et al., "Mechanism of the Smokeless Rich Diesel Combustion by Reducing Temperature," SAE Technical Paper 2001-01-0655, 2001, doi:10.4271/2001-01-0655
5. Yanigahara, H., Sato, Y., Minuta, J., "A simultaneous reduction in NOx and soot in diesel engines under a new combustion system (Uniform Bulky Combustion System – UNIBUS)", 17th International Vienna Motor Symposium, pp 303-314, 1996
6. Hasegawa, R. and Yanagihara, H., "HCCI Combustion in DI Diesel Engine ," SAE Technical Paper 2003-01-0745, 2003, doi:10.4271/2003-01-0745
7. Kalghatgi, G., Risberg, P., and Ångström, H., "Advantages of Fuels with High Resistance to Auto-ignition in Late-injection, Low-temperature, Compression Ignition Combustion," SAE Technical Paper 2006-01-3385, 2006, doi:10.4271/2006-01-3385
8. Kalghatgi, G., Risberg, P., and Ångström, H., "Partially Pre-Mixed Auto-Ignition of Gasoline to Attain Low Smoke and Low NOx at High Load in a Compression Ignition Engine and Comparison with a Diesel Fuel," SAE Technical Paper 2007-01-0006, 2007, doi:10.4271/2007-01-0006
9. Johansson, B., "High-Load Partially Premixed Combustion in a Heavy-Duty Diesel Engine", 2005 Diesel Engine Emissions Reduction (DEER) Conference Presentations August 21-25, 2005 Chicago, Illinois
10. Kalghatgi, G., T., Hildingsson, L., Johansson, B., "Low NOx and Low Smoke Operation of a Diesel Engine using Gasoline-like Fuels", ICES2009-76034, 2009
11. Hildingsson, L., Kalghatgi, G., Tait, N., Johansson, B. et al., "Fuel Octane Effects in the Partially Premixed Combustion Regime in Compression Ignition Engines," SAE Technical Paper 2009-01-2648, 2009, doi:10.4271/2009-01-2648
12. Kalghatgi, G.,T., Hildingsson, L., Harrison, A., Johansson, B., "Low- NOx, low-smoke operation of a diesel engine using "premixed enough" compression ignition – Effects of fuel autoignition quality, volatility and aromatic content", THISEL 2010 Conference on Thermo- and Fluid Dynamic Processes in Diesel Engines, 2010
13. Manente, V., Johansson, B., Tunestal, P., and Cannella, W., "Effects of Different Type of Gasoline Fuels on Heavy Duty Partially Premixed Combustion," *SAE Int. J. Engines* 2(2):71-88, 2010, doi:10.4271/2009-01-2668
14. Manente, V., Zander, C., Johansson, B., Tunestal, P. et al., "An Advanced Internal Combustion Engine Concept for Low Emissions and High Efficiency from Idle to Max Load Using Gasoline Partially Premixed Combustion," SAE Technical Paper 2010-01-2198, 2010, doi:10.4271/2010-01-2198
15. Manente, V., Johansson, B., Tunestal, P., Sonder, M., Serra, S., "Gasoline Partially Premixed Combustion: High Efficiency, Low NOx and Low Soot by using an Advanced Combustion Strategy and a Compression Ignition Engine", FCE09, Istanbul Turkey, 2009
16. Sellnau, M., Sinnamon, J., Hoyer, K., and Husted, H., "Gasoline Direct Injection Compression Ignition (GDCI) - Diesel-like Efficiency with Low CO2 Emissions," *SAE Int. J. Engines* 4(1):2010-2022, 2011, doi:10.4271/2011-01-1386
17. Sellnau, M., Sinnamon, J., Hoyer, K., and Husted, H., "Full-Time Gasoline Direct-Injection Compression Ignition (GDCI) for High Efficiency and Low NOx and PM," *SAE Int. J. Engines* 5(2):300-314, 2012, doi:10.4271/2012-01-0384
18. Kokjohn, S., Hanson, R., Splitter, D., and Reitz, R., "Experiments and Modeling of Dual-Fuel HCCI and PCCI Combustion Using In-Cylinder Fuel Blending," *SAE Int. J. Engines* 2(2):24-39, 2010, doi:10.4271/2009-01-2647
19. Hanson, R., Kokjohn, S., Splitter, D., and Reitz, R., "An Experimental Investigation of Fuel Reactivity Controlled PCCI Combustion in a Heavy-Duty Engine," *SAE Int. J. Engines* 3(1):700-716, 2010, doi:10.4271/2010-01-0864
20. Kokjohn, S., Hanson, R., Splitter, D., Kaddatz, J. et al., "Fuel Reactivity Controlled Compression Ignition (RCCI) Combustion in Light- and Heavy-Duty Engines," *SAE Int. J. Engines* 4(1):360-374, 2011, doi:10.4271/2011-01-0357
21. Hanson, R., Kokjohn, S., Splitter, D., and Reitz, R., "Fuel Effects on Reactivity Controlled Compression Ignition

(RCCI) Combustion at Low Load," *SAE Int. J. Engines* 4(1):394-411, 2011, doi:10.4271/2011-01-0361
22. Hanson, R., Curran, S., Wagner, R., Kokjohn, S. et al., "Piston Bowl Optimization for RCCI Combustion in a Light-Duty Multi-Cylinder Engine," *SAE Int. J. Engines* 5(2):286-299, 2012, doi:10.4271/2012-01-0380
23. Law, D., Kemp, D., Allen, J., Kirkpatrick, G. et al., "Controlled Combustion in an IC-Engine with a Fully Variable Valve Train," SAE Technical Paper 2001-01-0251, 2001, doi:10.4271/2001-01-0251
24. Koopmans, L. and Denbratt, I., "A Four Stroke Camless Engine, Operated in Homogeneous Charge Compression Ignition Mode with Commercial Gasoline," SAE Technical Paper 2001-01-3610, 2001, doi:10.4271/2001-01-3610
25. Cao, L., Zhao, H., Jiang, X., and Kalian, N., "Effects of Intake Valve Timing on Premixed Gasoline Engine with CAI Combustion," SAE Technical Paper 2004-01-2953, 2004, doi:10.4271/2004-01-2953
26. Johansson, T., Johansson, B., Tunestål, P., and Aulin, H., "The Effect of Intake Temperature in a Turbocharged Multi Cylinder Engine operating in HCCI mode," *SAE Int. J. Engines* 2(2):452-466, 2010, doi:10.4271/2009-24-0060
27. Borgqvist, P., Tunestal, P., and Johansson, B., "Gasoline Partially Premixed Combustion in a Light Duty Engine at Low Load and Idle Operating Conditions," SAE Technical Paper 2012-01-0687, 2012, doi:10.4271/2012-01-0687
28. Borgqvist, P., Tuner, M., Mello, A., Tunestal, P. et al., "The Usefulness of Negative Valve Overlap for Gasoline Partially Premixed Combustion, PPC," SAE Technical Paper 2012-01-1578, 2012, doi:10.4271/2012-01-1578
29. Borgqvist, P., Andersson, Ö., Tunestål, P., Johansson, B., "The Low Load Limit of Gasoline Partially Premixed Combustion using Negative Valve Overlap," ASME, ICEF2012-92069, 2012
30. Lang, O., Salber, W., Hahn, J., Pischinger, S. et al., "Thermodynamical and Mechanical Approach Towards a Variable Valve Train for the Controlled Auto Ignition Combustion Process," SAE Technical Paper 2005-01-0762, 2005, doi:10.4271/2005-01-0762
31. Urushihara, T., Hiraya, K., Kakuhou, A., and Itoh, T., "Expansion of HCCI Operating Region by the Combination of Direct Fuel Injection, Negative Valve Overlap and Internal Fuel Reformation," SAE Technical Paper 2003-01-0749, 2003, doi:10.4271/2003-01-0749
32. Trajkovic, S., Milosavljevic, A., Tunestål, P., and Johansson, B., "FPGA Controlled Pneumatic Variable Valve Actuation," SAE Technical Paper 2006-01-0041, 2006, doi:10.4271/2006-01-0041
33. Rothamer, A., Snyder, J., Hanson, R., Steeper, R., Fitzgerald, R., "Simultaneous imaging of exhaust gas residuals and temperature during HCCI combustion", Proceedings of the Combustion Institute 32 (2009) 2869-2876
34. BOSCH Automotive Handbook, 6th edition, page 663, ISBN 1-86058-474-8, 2004

CONTACT INFORMATION

Patrick Borgqvist
Lund University
Dept. of Energy Sciences
Div. of Combustion Engines
P.O. Box 118
221 00 Lund
Sweden

patrick.borgqvist@energy.lth.se

ACKNOWLEDGMENTS

The authors wish to show their appreciation to the Competence Centre Combustion Processes (KCFP), Swedish Energy Agency Grant number 22485-2, for their financial support. The authors would also like to acknowledge Cargine Engineering for supplying and helping with the valve train system. The authors would also like to expresses their gratitude to Bill Cannella from Chevron Corporation for supplying the fuel and to Håkan Persson from Volvo Car Corporation for hardware support and valuable discussions.

DEFINITIONS/ABBREVIATIONS

ATDC	After Top Dead Centre
BTDC	Before Top Dead Centre
CAD	Crank Angle Degree
DAQ	Data Acquisition
GDCI	Gasoline Direct Injection Compression
HCCI	Homogeneous Charge Compression Ignition
IMEP	Indicated Mean Effective Pressure
IVC	Intake Valve Close
NVO	Negative Valve Overlap
PPC	Partially Premixed Combustion
RCCI	Reactivity Controlled Compression Ignition
SACI	Spark Assisted Compression Ignition
SOC	Start of Combustion
SOI	Start of Injection